The Design and Synthesis of Inhibitors of the Enzyme Poly(Adenosine Diphosphate Ribose)polymerase and the Investigation of the Mechanism of Action of the Suspected Ultimate Carcinogen Chloroacetaldehyde

D Rhodes BSc MPhil

University of Newcastle upon Tyne

June 1995

Acknowledgements

The work presented in this thesis was carried out in the Department of Chemistry at the University of Newcastle upon Tyne between January 1990 and September 1992.

I would like to express my gratitude to my supervisors Professor B T Golding, Dr C Bleasdale and Dr R J Griffin for their constant guidance and encouragement during my research at Newcastle.

I would like to thank Professor W McFarlane for his suggestions and help regarding the nuclear magnetic resonance experiments reported in this thesis.

I should also like to express my thanks to:-

Dr M N S Hill, Mr I McKeag and Ms L Cook for their help with NMR spectra determination; Mr D Dunbar for elemental analyses and infra red spectra and Mr S Addison for mass spectra.

The technical staff in the Department of Chemistry especially T Johnstone, E R Hart, J Marshall, R Anderson and A Wright.

I am also grateful for the support given to me by my colleagues in the laboratory including Oonah, Joe, Keith, Jane, Frank, Leslie and Orrock.

A maintenance grant from the Northern Cancer Research Campaign is also acknowledged.

Abstract

This thesis describes the preparation of inhibitors of the enzyme poly(adenosine diphosphate ribose)polymerase (PARP) and the mechanism of action of the carcinogen vinyl chloride. Initially the enzyme's function, purification and its known inhibitors are discussed. The enzyme's cofactor, nicotinamide adenine diphosphate (NAD^+), is described in terms of its function in PARP and other enzymes, and its crystal structure and solution conformation(s). The high field proton and carbon-13 NMR spectra of this compound are fully assigned using two dimensional NMR experiments (COSY and ROESY) and selective spin decoupling. Using similar techniques the high field proton and carbon-13 NMR spectra of the reduced analogue, NADH, are assigned. This NMR data showed that the conformation of the 1,4-dihydropyridine ring of this molecule was a dynamic equilibrium mixture of two boats. However, it was discovered that these boat conformations were unequally populated and a rationale for this phenomenon is given.

The rationale of enzyme inhibitor design with respect to PARP is described and the subsequent preparation and potencies of PARP inhibitors are both described and discussed. These included the preparation of 3-methoxycyclohexane carboxamide which was synthesised to test a hypothesis of the nature of PARP inhibitors. Partially saturated substituted benzamide systems were synthesised to determine the degree of unsaturation necessary for inhibition while similar compounds were synthesised by reducing *N*-alkylnicotinamides. Direct NAD^+ analogues were prepared in which an adenine unit was separated by a methylene chain from a 3-oxy substituted benzamide. By varying the length of the methylene chain 3-(9-(12-dodecyloxy)adenine)benzamide was shown to inhibit the enzyme. Amongst these inhibitors were the unique compounds benzoxazole-4-carboxamides which were found to be the most potent inhibitors to be synthesised during this period. A

correlation of the physical properties of literature compounds with their activity is discussed along with the applicability of this technique to PARP and its inhibitors.

The metabolic activation and carcinogenesis of vinyl chloride are described. The reaction of chloroacetaldehyde (a metabolite of vinyl chloride) is discussed with a detailed description of its reaction with nucleosides to form the fluorescent etheno compounds, with particular emphasis on the adenine system. A detailed investigation of the reaction mechanism of chloroacetaldehyde with adenosine was undertaken by determining the intermediates and products of the acid catalysed decomposition of N^6-(2,2-dimethoxyethyl)adenosine. An ethenoadenine deuteriation experiment along with the previous experiment gave evidence toward the reaction mechanism of chloroacetaldehyde with adenosine.

In summary, the cofactor of PARP NAD^+ has been fully characterised by proton and carbon-13 NMR spectroscopy; a unique conformational property of NADH has been characterised; a new and novel class of potent inhibitors of PARP has been discovered and the reaction mechanism of chloroacetaldehyde with adenosine has been determined.

Contents

Chapter 3

Chapter 4

Abbreviations

NMR	**Nuclear Magnetic Resonance**
COSY	**Correlation Spectroscopy**
ROESY	**Rotating Frame Overhauser Correlation Spectroscopy**
HSC	**Heteronuclear Shift Correlation**
HETCOR	**Heteronuclear Shift Correlation**
FID	**Free Induction Decay**
od	**Outer Diameter**
PARP	**Poly(Adenosine Diphosphate Ribose)polymerase**
poly(ADPR)	**poly(Adenosine Diphosphate Ribose)**
NAD^+	**Nicotinamide Adenosine Diphosphate**
NADH	**Nicotinamide Adenine Dinucleotide Hydride**
RNA	**Ribonucleic Acid**
DNA	**Deoxyribonucleic Acid**
TFIIIA	***Xenopus* Transcription Factor III A**
DTIC	**5-(3,3-Dimethyl-1-triazeno)-4-imidazole Carboxamide**
MIC	**5-(3-Methyl-1-triazeno)-4-imidazole Carboxamide**
AICA	**5-Amino-4-imidazole Carboxamide**
BCNU	**1,3-*bis*(2-Chloroethyl)-1-nitroso Urea**
DMS	**Dimethyl Sulphate**
PVC	**Polyvinyl Chloride**
TLC	**Thin Layer Chromatogram**
SET	**Single Electron Transfer**

Chapter 1

1.1 The Chromosomal Structure of DNA

Carcinogenesis, cell differentiation, DNA repair and replication seem to have the common link that they are dependent upon the chromatin structure of DNA. Within an organism all the different cell types (*eg* skin, hair, muscle *etc*...) contain the same DNA molecules. It is, however, changes of chromatin structure about specific sets of genes from one cell type to another that are responsible for cell differentiation (*ie* what makes a skin cell a skin cell, a hair cell a hair cell *etc*...). Chromatin structure participates in both the initiation of DNA replication and DNA repair processes at specific sites that have been damaged by carcinogens. It is for these reasons that an understanding of the chromatin structure of DNA is warranted.

About 1.8 metres of DNA containing approximately five billion base pairs is packed into a single mammalian nucleus of 8 μmetres diameter. The DNA's double helix is organised around twenty five million nucleosomes - protein structures consisting of eight individual basic proteins called histones - which in turn form partially understood secondary, tertiary and quaternary structures. The condensed chromatin thus formed contains about fifty thousand loops or domains with each domain containing five to two hundred kilo bases of DNA. These domains can either be transcriptionally active or inactive depending upon the presence or absence of various proteins such as histone H1 and high mobility group nonhistones, as well as variant or modified histones.[1,2,3,4]

1.2 The Function of Poly(Adenosine Diphosphate Ribose)

The necessary processes of DNA transcription, replication and repair are all dependent upon poly(adenosine diphosphate ribose) or poly(ADPR). Before any of these processes can occur two events have to take place: a specific alteration in the three dimensional chromatin structure (to make the DNA accessible) and the binding

of requisite enzymes and proteins to the exposed DNA. The first of these two events occurs when poly(ADPR) is formed upon one of the chromatin histones. When this happens a large build up of localized negative charge occurs which alters the three dimensional structure of chromatin. In a similar manner poly(ADPR) can modify the structure (and hence function) of other enzymes and other proteins. Thus, changes in chromatin structure inevitably lead to alterations in gene expression, replication and repair.

1.3 The Structure and Synthesis of Poly(Adenosine Diphosphate Ribose)

Poly(ADPR) is the third most abundant naturally occurring nucleic acid after DNA and RNA and consists of repeating units of adenosine diphosphate ribose (**1**, see Figure 1). Initially a protein displaces nicotinamide from nicotinamide adenosine diphosphate (**2**, NAD^+) with a carboxylate (in the case of histones H1 and H2B) to form an α bond to the sugar. Then units repeat *via* bonds from the 2'-hydroxyl of the ribose attached to adenine and the anomeric carbon (in an α manner), of another monomer, of the ribose that is not attached to adenine. Along these polymeric chains branch points can occur when the 2'-hydroxyl of the ribose which is not attached to adenine forms a bond with the anomeric carbon (again, in an α manner) of another monomeric non-adenine attached ribose (see Figure 1).

1.4 Poly(Adenosine Diphosphate Ribose)Polymerase

The chromatin structural modifier, poly(ADPR), is formed from the cofactor NAD^+ (see Section 1.3) by the enzyme poly(adenosine diphosphate ribose)polymerase (PARP). In addition to catalysing the synthesis of poly(ADPR), PARP catalyses the transfer of poly(ADPR) onto various proteins modifying their structures and hence

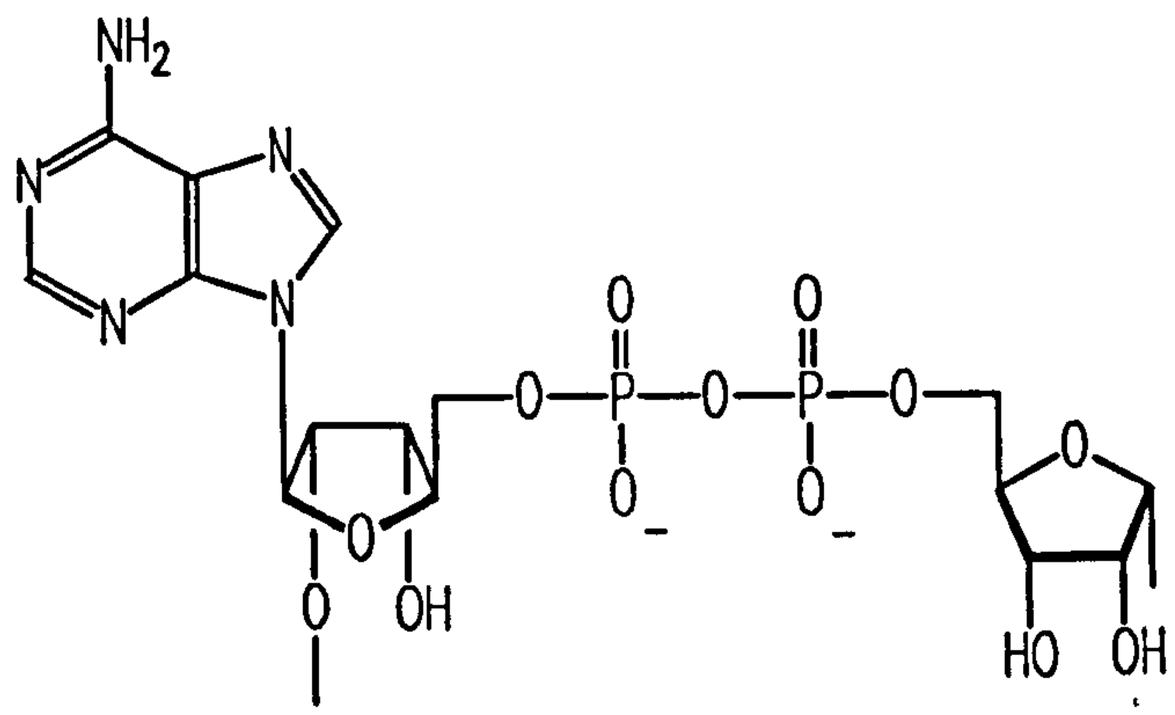

Adenosine Diphosphate Ribose 1

Ade = Adenine

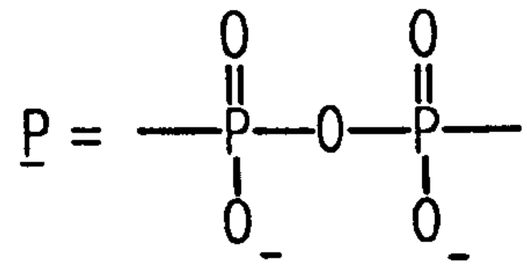

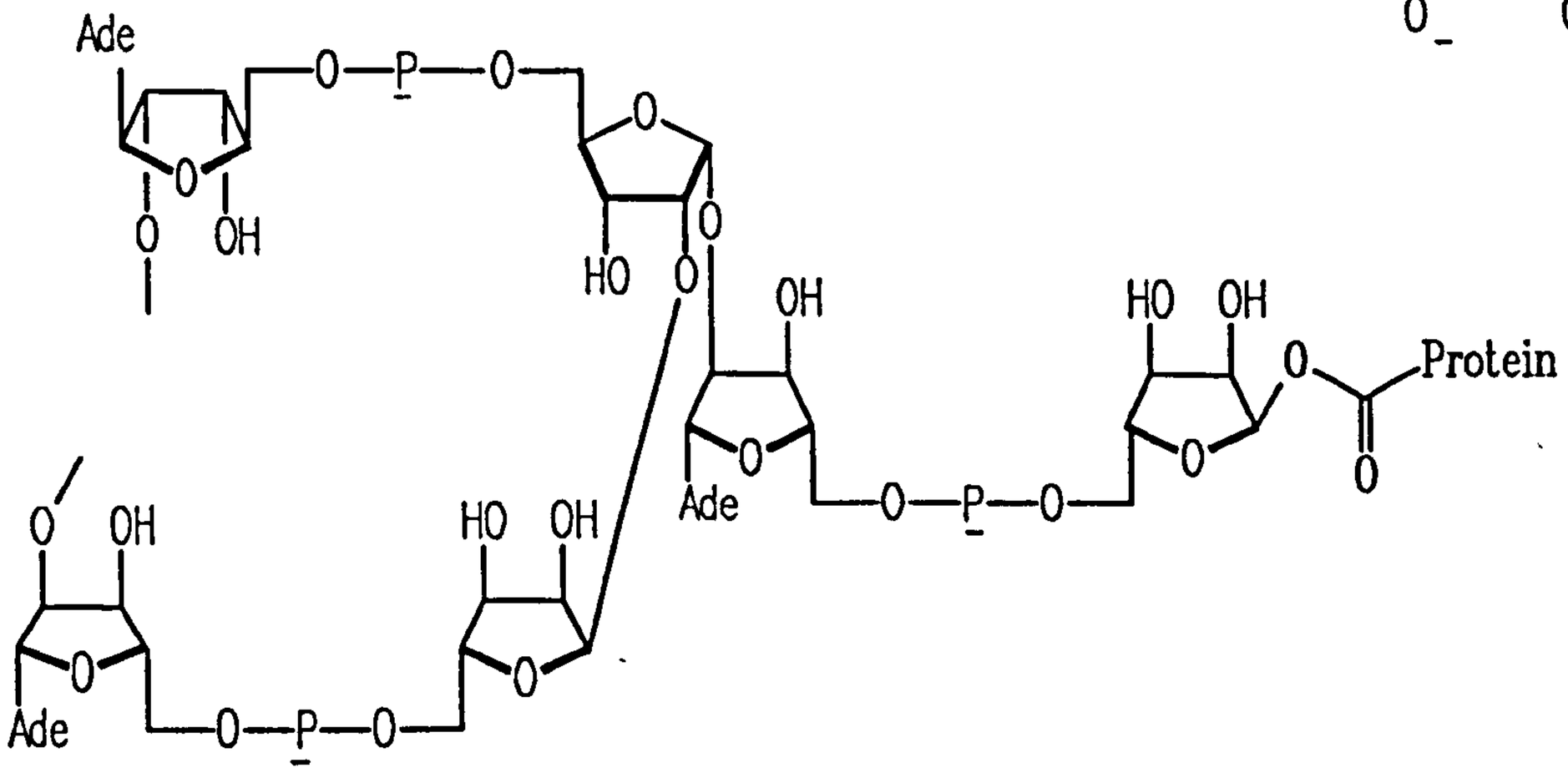

Poly(Adenosine Diphosphate Ribose)

The Structure of Poly(Adenosine Diphosphate Ribose)

Figure 1

their function. Examples of the proteins the enzyme regulates include histones (see Section 1.3), it is automodifying, and various other DNA dependent enzymes. Thus, enzymes involved in the breaking and joining of DNA strands, ligase II and topoisomerase I and II, are regulated by this enzyme. PARP is involved in the modification of proteins involved in gene expression and DNA replication (such as acetylated histones) and further, it modifies nuclear matrix proteins.

The effect of PARP, the formation of poly(ADPR), was first demonstrated in 1963 (and further in 1966) when it was observed in liver extracts.[5,6] Since then PARP has been found in a large variety of cells from vertebrate to invertebrate animals and has also been found in single celled organisms and plants. It is now thought to be ubiquitous within the plant and animal kingdoms. PARP can be described as a zinc binding nuclear DNA dependent enzyme.

1.5 Zinc Finger Proteins[7,8]

A necessary part of the function of many cellular enzymes is to bind to DNA (or RNA). An example of such a protein is *Xenopus* transcription factor III A (TF III A). It was discovered that this enzyme contained repeated amino acid units along its length which were characterized by two cysteines and two histidines. The two cysteines were usually separated by one or two amino acids. Several amino acids separated the second cysteine from the first histidine, which was separated from the second histidine by one or two amino acids. This enzyme was found to contain seven to eleven mole equivalents of zinc which were crucial to its activity. *X*-ray absorption experiments showed that the zinc atoms reside in a similar environment. This environment was thought to be that of a tetracoordinated atom with two sulphur ligands and two nitrogen ligands. The effect of this phenomenon was to produce a tertiary structure of 'fingers' within the protein held in place by the zinc. These

fingers were found to be rich in basic and polar amino acids suggesting that binding to DNA (or RNA) could occur about these regions.

It was found that this arrangement was not peculiar to TF III A. A number of zinc containing DNA (RNA) binding proteins were found to have this cysteine/histidine arrangement indicating that zinc fingers are an evolutionary mechanism for the binding of protein to DNA or RNA.

1.5.1 PARP: A Zinc Finger Protein[9]

PARP is a DNA binding enzyme which was found to contain zinc fingers for this purpose. However, these zinc fingers are different from the zinc fingers found in the class of proteins described earlier. The zinc within PARP is bound by three cysteines and one histidine rather than by two cysteines and two histidines. Another difference is in the size of PARP's fingers; they have more amino acids between the inner zinc binding cysteines and are thus much longer. A further feature of PARP's zinc fingers is that they are different from each other.

The binding of PARP to DNA was investigated by obtaining PARP molecules that had been mutated in such a manner that the integrity of one of the fingers was corrupted. In this way it was observed that one of the fingers binds much more tightly to DNA than the other one. The results of this mutation study indicate that the tighter binding finger may be responsible for both DNA binding and DNA strand break recognition, whilst the other finger may not bind to DNA but may have the rôle of interacting with another PARP molecule. Therefore, a dimer of PARP binds to DNA. This rationalisation is consistent with the observations that when PARP binds to a single strand break DNA molecule, a symmetrical footprint of seven nucleotides on each side of the nick is observed. Thus, both the size and symmetry of the PARP bound DNA region suggest that PARP binds to DNA as a dimer.

1.6 Purification of PARP

The isolation and purification of PARP has become increasingly efficient over a relatively short period of time. Initially PARP was extracted from cells by classical wet techniques and purified by column chromatography. The purification steps of this technique were further improved using affinity chromatography. Genetic engineering has subsequently been used to give a good supply of PARP.

1.6.1 Classical Techniques

PARP has been previously obtained from many sources including calf thymus which is briefly described below.[10] The procedure began with the homogenisation of frozen calf thymus in a buffered solution. Centrifugation produced a supernatant which was treated with salmon protamine sulphate (to precipitate DNA) and centrifuged again. The supernatant obtained from this process was purified by column chromatography:

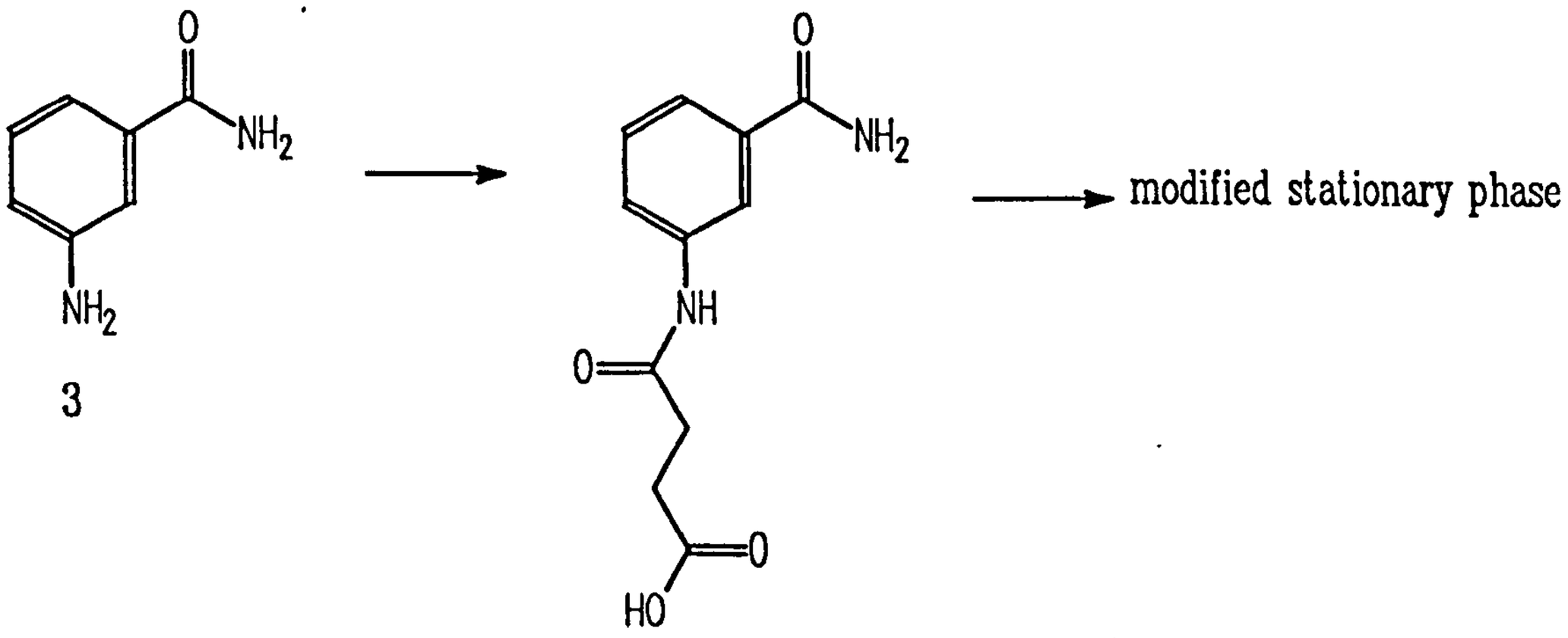

The Coupling of 3-Aminobenzamide to Sepharose 4B

Figure 2

firstly, with DNA-agarose as stationary phase and secondly, with hydroxylapatite as the stationary phase. The proteinaceous fraction obtained was then gel filtered on a Sephadex G-150 column to give the enzyme.

1.6.2 Affinity Chromatography

Purification of the enzyme was improved by the use of affinity chromatography. The stationary phase of a column was modified in such a manner as to incorporate molecules that bind to the enzyme. In this example[11] 3-aminobenzamide (**3**) was coupled (*via* a succinyl linker) to Sepharose 4B (see Figure 2). A supernatant obtained by classical techniques was passed through the modified column to leave the enzyme adsorbed upon it. The enzyme was then eluted from the column using a buffer that contained another compound (3-methoxybenzamide (**4**)) that binds to the enzyme. A further column removed the 3-methoxybenzamide and the pure enzyme was obtained. Using this technique the pure enzyme could be prepared within a few hours. The procedure was shown to be effective in preparing the enzyme from a number of different sources, such as human placenta and horse, rat and chicken liver.

1.6.3 Genetic Engineering

In this technique the nucleus of a cell was transfected with a piece of complementary DNA that codes for PARP. The cell was then multiplied by cultivation and the enzyme obtained by the methods described earlier. *Escherichia coli* was initially used for this process but the enzyme obtained from this cultivation was found to be incomplete. It was only when insect cells were used[12] that pure PARP was obtained.

The classical technique produced 3.2 mg of enzyme from 29,800 mg of crude extract; the affinity chromatography technique gave 0.3 mg of enzyme from 20,000 mg of

crude extract whilst the genetically engineered cells produced 20 mg of enzyme from 365 mg of crude extract.

For 1 kg of crude extract the amount of enzyme produced is:

classical technique	107 mg
affinity chromatography	15 mg
genetic engineering	55,000 mg

1.6.4 Enzyme Characteristics

PARP can be characterised in terms of its mass and its Michaelis constant for NAD^+. The values for the three techniques, classical, affinity chromatography and genetic engineering are: 110 kDa, 55 μM; 115 kDa, 52 μM and 116 kDa, 50 μM, respectively.

1.7 DNA Repair and PARP

When DNA is attacked by electrophiles a number of repair mechanisms become operational.[13] The repair mechanism in which PARP is involved occurs when DNA strand breaks appear: this phenomenon 'switches on' PARP. This has been shown when DNA strand breaks are produced by nucleases - the result is the rapid synthesis of poly(ADPR) upon histones. As described earlier, this has the effect of making the damaged DNA accessible to repair enzymes. The exposed DNA is then repaired by a multi - enzymic process and PARP is poly(ADP-ribosylated); this has results in the inactivation of PARP, thus the DNA is repaired and is then allowed to supercoil and the metabolism of the cell carries on as before.

The electrophiles that attack DNA are usually the metabolites of chemicals that the body has ingested (Scheme 1). A chemical that the body has no use for is usually oxidised which has the effect of increasing its water solubility making it easier for the body to excrete. This oxidising process, however, sometimes has the detrimental effect of creating an electrophile. Therefore, if the body ingests benzene (**5**), which is found in car exhaust fumes, it can be oxidized to (z,z) muconaldehyde (**6**) which may subsequently react with DNA.[14] Other examples of these chemicals include urethane or *O*-ethyl carbamate (**7**),[15,16,17] which is found in food and beverages: this compound may be oxidised to *O*-epoxyethyl carbamate (**8**), which may react with DNA. A further example is the industrial chemical vinyl chloride (**9**),[17] the monomer of polyvinylchoride (PVC), which is thought to be metabolically oxidised

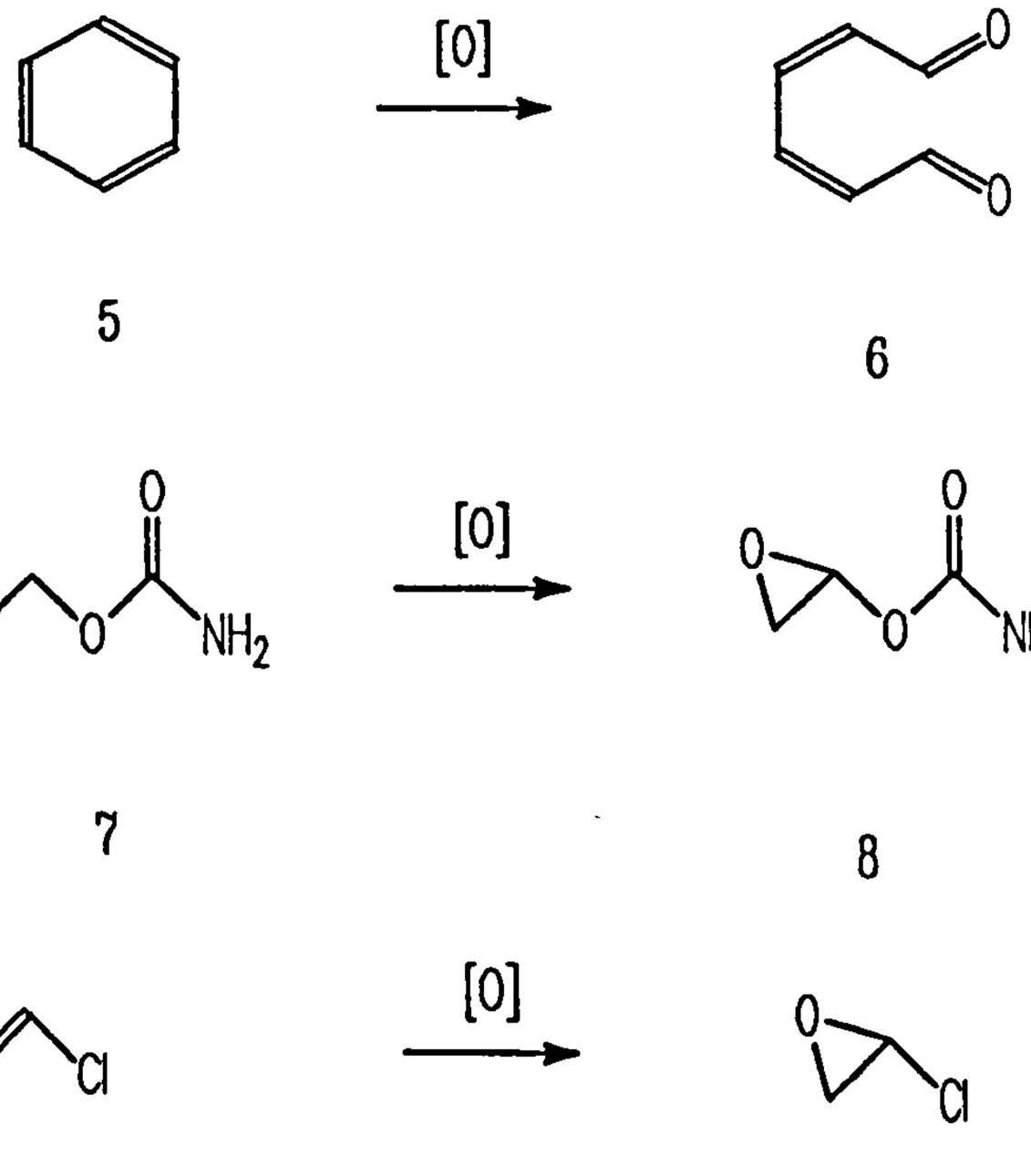

Examples of Suspected Carcinogen Metabolites

Scheme 1

to chlorooxirane (**10**). Subsequent rearrangement of **10** forms the bifunctional electrophile chloroacetaldehyde (**11** , see Chapter 6) which is thought to form adducts with DNA (see Scheme 1).

It is thus apparent that if it were not for the many repair processes mentioned earlier carcinogenesis would be much more prevalent.

The effect of DNA alkylation, apart from DNA repair or carcinogenesis, is cell death. (This was first observed in soldiers who survived the effects of mustard gas (bis(2-chloroethane)sulphide **12**).[18] If healthy cells could be killed by DNA alkylation then cancerous cells could be killed in a similar manner and furthermore, since cancerous cells tend to have a higher metabolic rate than healthy cells, there should be discrimination in alkylating agent (*i.e.* drug) uptake between healthy and cancerous cells. Chemotherapy is therefore the treatment of cancer patients with cytotoxic drugs that preferentially kill cancerous cells due to their higher metabolic rate.

For example, one treatment of melanoma utilises the drug Dacarbazine, which has, as its active constituent, 5-(3,3-dimethyl-1-triazeno)-4-imidazole carboxamide (DTIC, **13**).[19] After ingestion of this compound it is metabolized to 5-(3-methyl-1-triazeno)-4-imidazole carboxamide (MIC, **14**) which forms, after tautomerisation and cleavage, 5-amino-4-imidazole carboxamide (AICA, **15**) and the methylating agent, methyl diazonium ion (**16**, see Scheme 2).

A further example of a cytotoxic alkylating agent is 1,3-bis(2-chloroethyl)-1-nitrosourea (BCNU, **17**) which is used to treat acute lymphocytic leukeamia.[20] Decomposition of this compound gives the chloroisocyanate (**18**) and 2-chloro-1-nitrosoethylamine (**19a**) which can tautomerise to the diazotic acid **19b**. This compound can then go on to form the diazonium compound (**20**) shown in Scheme 3.

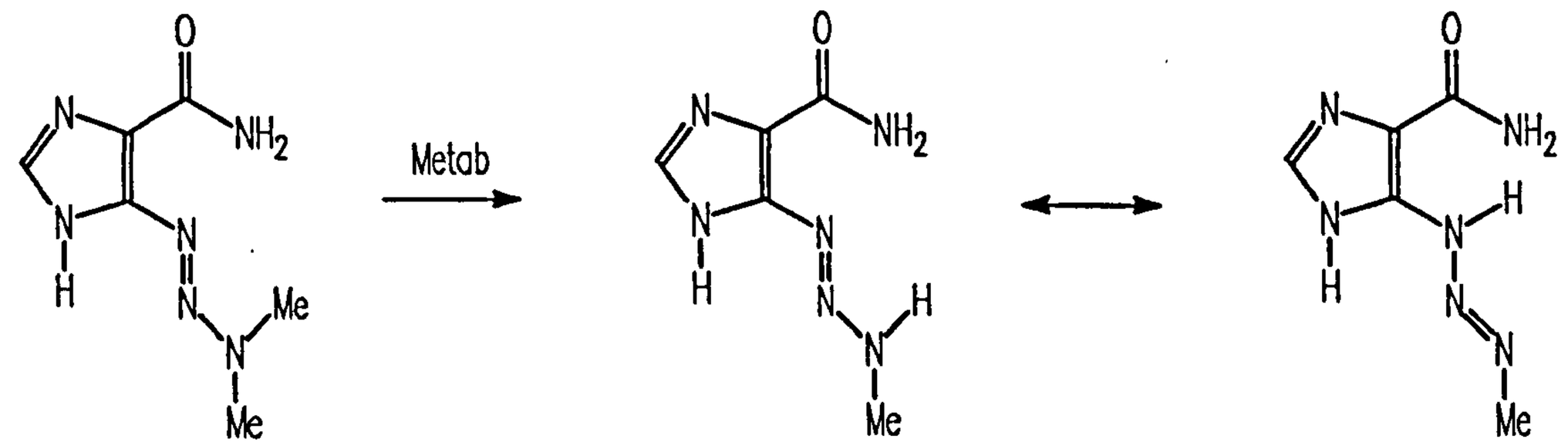

The Metabolic Activation of 5-(3,3-Dimethyl-1-Triazeno)-4-imidazole Carboxamide

Scheme 2

Unfortunately the same repair mechanism that protects healthy cells from electrophilic metabolites also protects cancerous cells from chemotherapeutic drugs. Thus, tumors do not always respond to chemotherapy.

Therefore, the effectiveness of anticancer drugs will be increased by inhibiting the DNA repair enzyme PARP.

This central premise is supported by a large amount of evidence showing that inhibitors of PARP inhibit DNA repair and potentiate the cell killing capacity of alkylating agents. When cells were exposed to dimethyl sulphate (DMS, **21**), a potent alkylating agent, the NAD^+ concentration of these cells was found to decrease. When

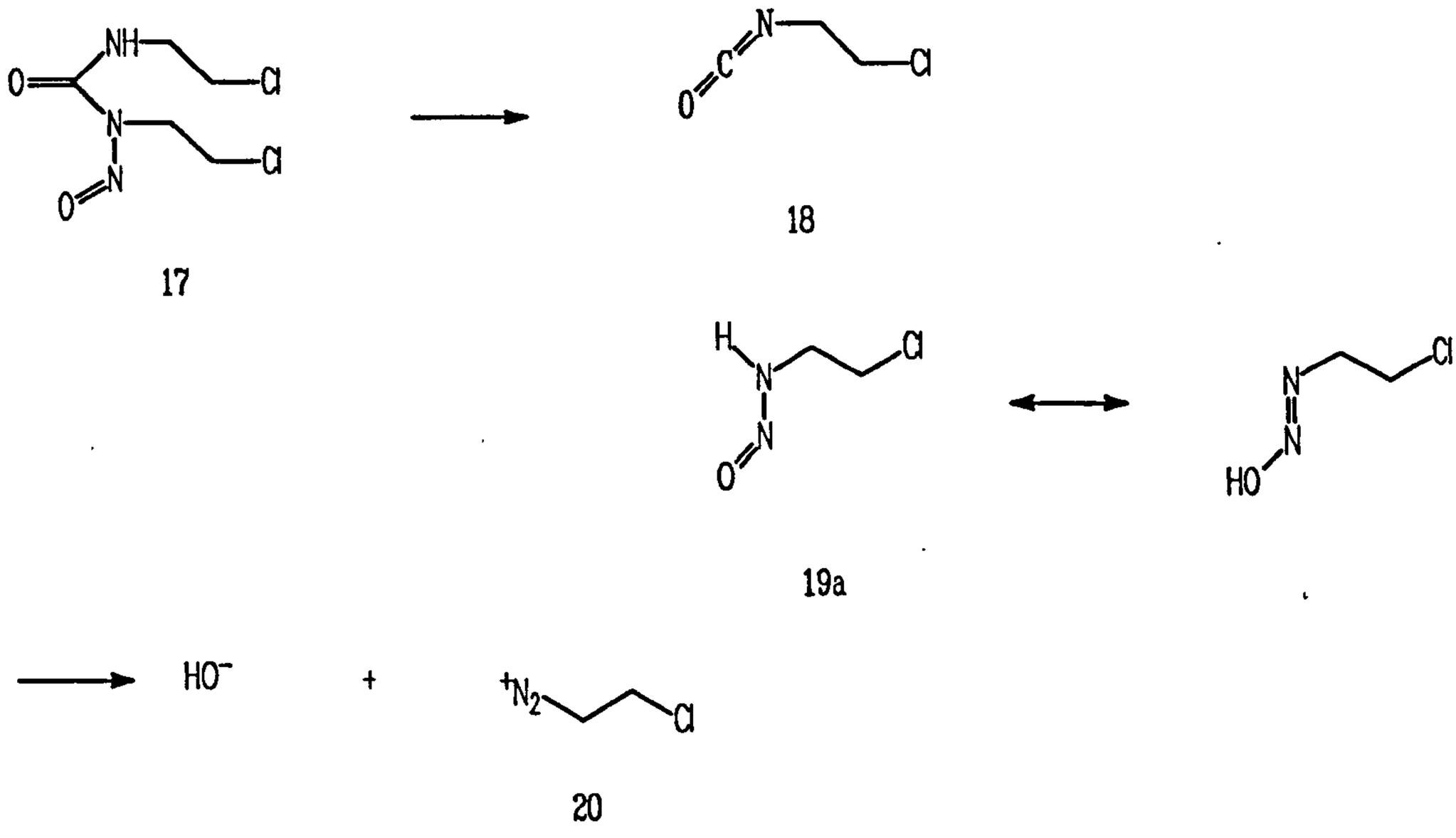

The Activation of 1,3-Bis(2-Chloroethyl)-1-Nitrosourea

Scheme 3

DMS was applied to cells in the presence of a PARP inhibitor (3-aminobenzamide, **3** or 3-methoxybenzamide, **4**) there was no decrease in NAD^+ concentration observed.

During this experiment the strand length of the DNA of the cells was determined by sedimentation studies. Immediately after incubation with DMS the cellular DNA was found to appear in the middle of a sedimentation gradient. Forty minutes after the removal of DMS, sedimentation studies showed that the DNA had increased significantly in size and after eighty minutes the DNA appeared at the same place as undamaged DNA. When this sedimentation study was repeated, with the application of a PARP inhibitor immediately after removal of DMS, it showed that there was no appreciable increase in the size of DNA after forty minutes. That is, the DNA was not repairing itself. Eighty minutes later the DNA showed only a slight increase in size, whilst after five hours the bulk of the DNA had not yet returned to its original size. This same study also showed the increase in cytotoxicity of cells towards DMS in the presence of PARP inhibitors.[21] Other studies have shown similar results using

other DNA-damaging agents (eg *N*-methyl-*N*-nitrosourea (**22**) and γ-radiation) and other PARP inhibitors.[22]

These experiments have progressed by studying the effects of antitumour drugs in the presence of inhibitors of PARP. Thus, the active metabolite 5-(3-methyl-1-triazeno)-4-imidazole carboxamide (MIC, **14**) of the drug 5-(3,3-dimethyl-1-triazeno)-4-imidazole carboxamide (DTIC, **13**, see earlier) has been shown to increase cell death in the presence of PARP inhibitors.[23] Another antitumour drug, bleomycin, which is thought to cleave DNA strands has also been shown to have an increased potency in the presence of PARP inhibitors.[24]

Chapter 2

2.1 Inhibitors of PARP

Inhibitors of PARP have been sought since its discovery. They were required as molecular mechanistic probes of the enzyme: if an inhibitor of PARP was given *in vivo*, then any cellular dysfunction observed meant that PARP played a role in that cellular function. Throughout the course of PARP's history many compounds have been discovered which inhibit this enzyme. A large proportion of these inhibitors also participate in other known metabolic pathways and so would be useless for PARP *in vivo* dysfunction studies. However, this complication is overshadowed by the lack of inhibitors that have both potency and aqueous solubility. The latter two points must be overcome in order to obtain suitable inhibitors of PARP.

2.1.1 3-Substituted Benzamides

Benzamide (**23**) has been known to be an inhibitor of PARP since 1975. It is a close analogue of nicotinamide (**24**) but does not have a ring nitrogen, which means that it cannot be metabolised by NAD^+ biosynthetic enzymes. However, benzamide has

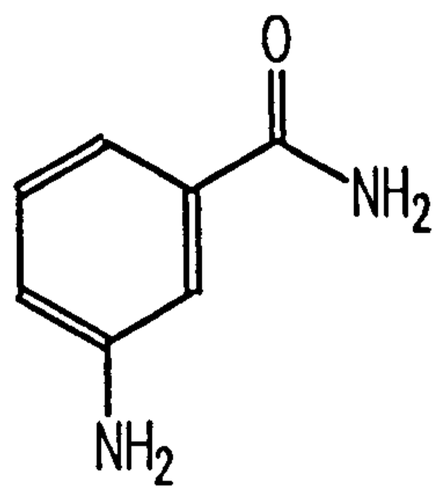

3-Aminobenzamide 3

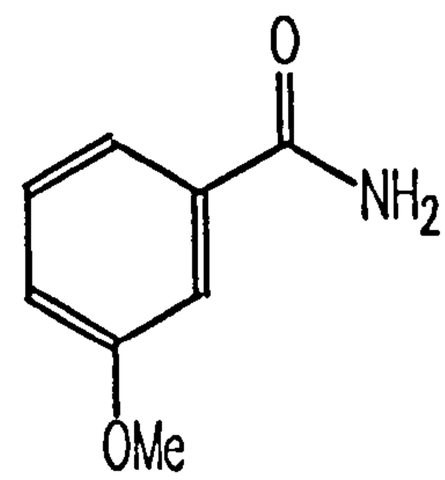

3-Methoxybenzamide 4

Inhibitors of PARP

Figure 3

low aqueous solubility and is very hydrophobic making it unsuitable for physiological studies.

3-Substituted benzamides, such as 3-methoxybenzamide and 3-aminobenzamide (**4** and **3**, Figure 3), were shown to be strong inhibitors of PARP and have good solubility properties, which meant that they could be used in physiological studies.[25]

2.1.2 Dihydroisoquinolines[26]

It was realised that inhibition of PARP would increase the effectiveness of chemotherapy and radiotherapy. With this in mind certain dihydroisoquinolines were tested. These compounds were chosen because of their similarity to 3-substituted benzamides. They were designed so that they had a rigid amide orientation: it was thought that this particular orientation was optimal for inhibition. This hypothesis was proved by synthesizing and testing 2-alkyl-3-substituted benzamides. These compounds have the opposite preferred amide orientation to that of the dihydroisoquinolines. The 2-alkyl-3-substituted benzamides were found to be inactive whilst the dihydroisoquinolines were found to be inhibitors (Figure 4). Substitution of the dihydroisoquinolines at the 5 position gave extremely potent inhibitors of PARP (with the exception of the 5-nitro substituent). Substituted dihydroisoquinolines were also tested but were shown to be less potent than the corresponding 5-substituted compounds.

This work suggests that both a fixed amide orientation and a *meta* substituent are both necessary for potent inhibition. It is interesting to note that a *para* substituent, which can directly donate electron density to the amide carbonyl, shows less inhibition than the corresponding *meta* compound (Figure 5).

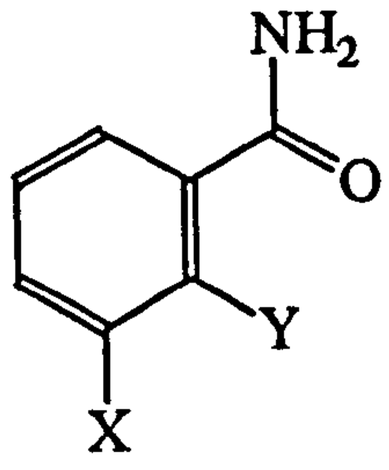

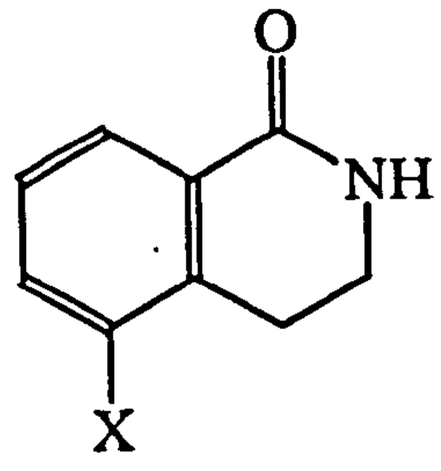

X = OMe, NH_2

Y = Me, Et

Structural Comparison of the 2-Alkyl-3-Substitutedbenzamides
and the Dihydroisoquinolines

Figure 4

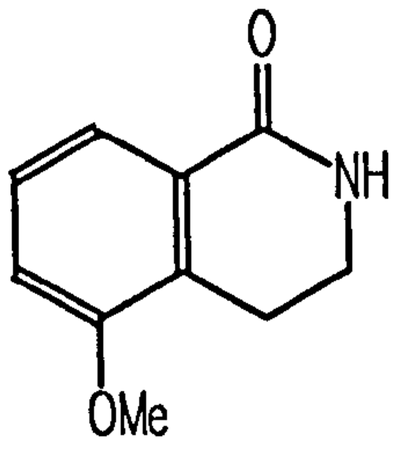

IC_{50} (uM) = 0.42

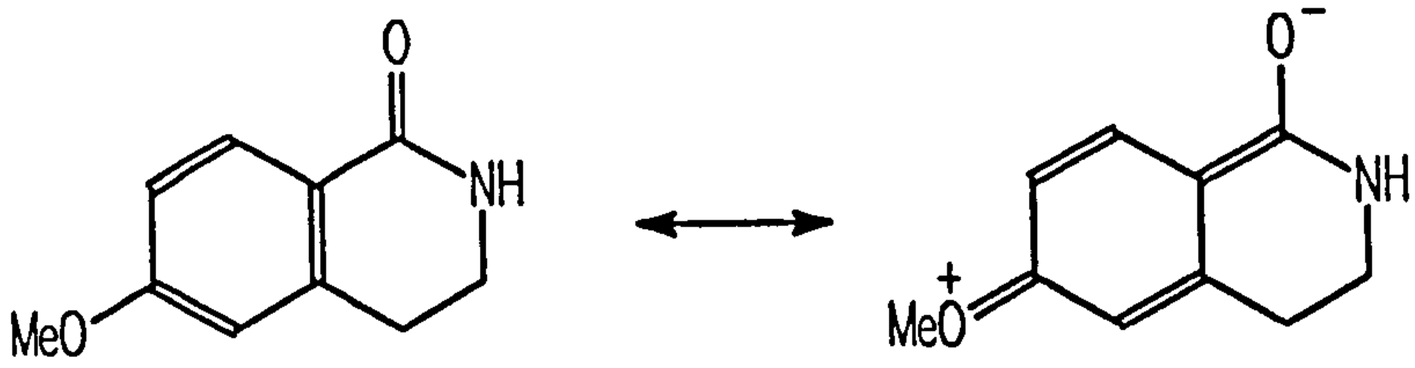

IC_{50} (uM) = 39

Potencies of'meta' and 'para' Substituted Dihydroisoquinolines

Figure 5

2.1.3 Other Inhibitors of PARP[27]

The most potent inhibitor found by Banasik *et al* was 4-amino-1,8-naphthalimide (25). This compound has a rigid amide and can be viewed in two ways with respect to the amide substituent. It can be regarded as a compound that has a *para* amine and a *meta* sp^2 carbon or simply as an amide that has an electron rich *meta* sp^2 carbon. In the former case, even though direct *para* electron donation from the amine is seen, the magnitude of this electron donation is tempered by the other canonical forms of the

25

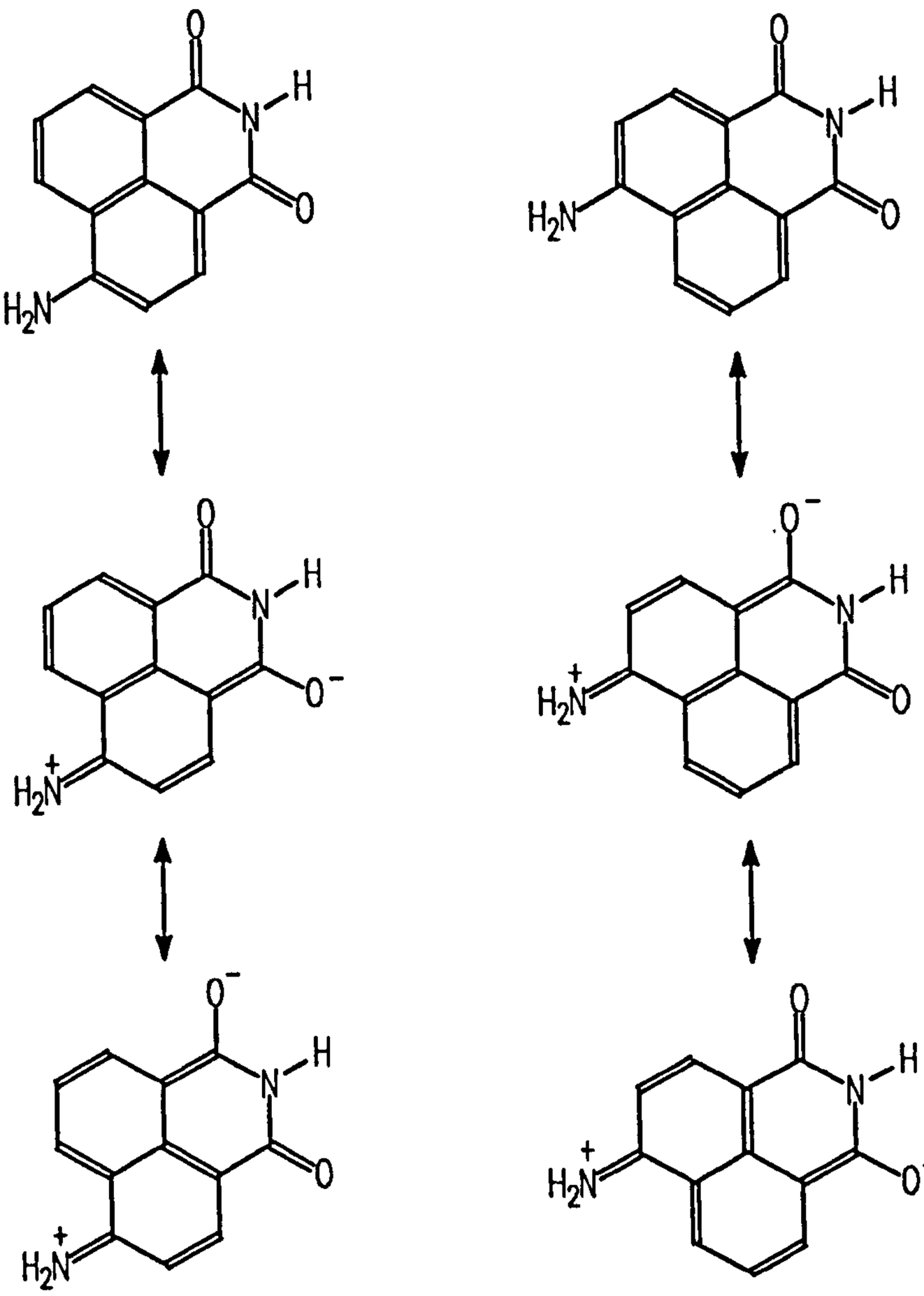

The Canonical Forms of 4-Amino-1,8-Naphthalimide

Figure 6

molecule. For this reason this molecule cannot be regarded as a simple analogue of a *para* substituted benzamide (Figure 6).

2.1.4 The Design of PARP Inhibitors Based Upon Literature Precedent

A study of the literature of PARP inhibitors indicates that three requirements are necessary for these compounds to be effective:

(i) A 6-membered ring.

(ii) An amide functional group.

(iii) A substituent at the three position relative to the amide.

The extent that the literature has explored these three aspects will now be discussed (Figure 7).

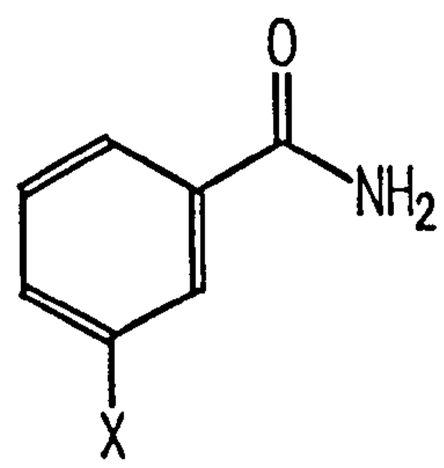

Proposed Molecular Template for Inhibitors of PARP

Figure 7

(i) 6-membered ring

Literature inhibitors generally have the molecular skeleton depicted above (Figure 7). It is thought that an unsaturated ring is necessary for activity, however, partially unsaturated ring systems have not been investigated.

Heterocyclic systems, such as nicotinamide (3), have shown activity but not to as great an extent as non-heterocyclic systems. In addition nicotinamide systems decrease in potency when they are substituted at the three position. This is thought to be a consequence of starving the carbonyl group of electrons. A method of incorporating an alkyl substituted nicotinamide without incurring loss of electron density from the carbonyl group is through the formation of *N*-alkyldihydronicotinamides (see Section 4.3.2).

(ii) Amide functionality

The orientation of the amide function necessary for inhibition has been shown to be that depicted above by the workers who designed the dihydroisoquinoline class of inhibitors[26] (Figure 4, Section 2.1.2).

Another aspect of the amide function is the extent of substitution upon the nitrogen atom. Potent inhibitors have been discovered which have one nitrogen proton substituted for an alkyl group[27] but it is not known if both protons can be substituted. That is, does the enzymic site have a hydrogen bond accepting group that accommodates an amide nitrogen proton?

A third aspect to the amide functionality is its carbonyl group. It could be envisaged that within the enzyme the inhibitor binds by forming a 'hydrogen bond' at the carbonyl oxygen. If this were the case then a correlation between inhibition and carbonyl electron donation would be expected to be seen. The extent of carbonyl electron donation can be quantitatively determined spectroscopically: either by IR carbonyl stretching frequencies or carbon-13 NMR chemical shifts. In this way it should be possible to show a correlation between carbonyl electron donation and inhibitory potency (see Section 5.1.1).

(iii) 3-Substituent

Inhibition has been observed within compounds that do not have a 3-substituent, however it seems that potency is increased with an electron - donating substituent (*eg* amino) at the three position. Further work is required to determine the nature and function of the 3-substituent.

2.2 Assay of PARP Inhibitor Potency

The activity of PARP, with or without the presence of an inhibitor, was determined by incubating permeabilized cells with radioactively labelled NAD^+ in the presence of double stranded oligonucleotide. The amount of poly(ADPR) produced, determined by the amount of material obtained after work up, was a measure of the activity of PARP (see Materials and Methods).

Nucleotides, such as NAD^+ and the oligonucleotides mentioned above, do not permeate intact living cells. The cells used in the assay were made permeable to nucleotides by suspending in hypotonic buffer. After suspension in this buffer the cells were suspended in an isotonic buffer where the assay was carried out. It was originally thought that it was possible to do the assay using isolated nuclei, however, it has been shown that this procedure gave misleading results. PARP activity was shown to depend upon the number of DNA strand breaks, which in isolated nuclei are comparatively high and thus the activity of PARP was comparatively high. The DNA structure of permeabilized cells is very nearly the same as that of intact cells and so the activity of PARP is comparable to that in the cell.[28]

The enzyme in the permeabilized cells was activated by the presence of double stranded oligonucleotides.[29,30] It is possible to activate indirectly cellular PARP by inducing DNA lesions with carcinogens or DNase I, both of which cause strand

breaks in the chromosomal DNA. The addition of double stranded oligonucleotides however, directly activates the enzyme within the cell. Thus, using this method the percentage inhibition of a potential inhibitor can be determined at various concentrations and by making a plot of percentage inhibition against concentration of inhibitor an IC_{50} can be determined.

Chapter 3

3.1 The Cofactor NAD+

3.1.1 The Design of Enzyme Inhibitors

A number of approaches are available for the rational design of enzyme inhibitors.

The two approaches we used were the synthesis of molecules based upon the structures of:

(a) the enzyme's cofactor.

(b) known inhibitors found in the literature.

Thus, a prerequisite of molecule design based on (a) above is the full characterisation of the cofactor with particular emphasis upon its crystal structure(s), enzyme bound crystal structure(s) and solution conformation(s).

The cofactor of PARP and of a large number of other enzymes is nicotinamide adenosine diphosphate (NAD^+ **2**, Figure 8).

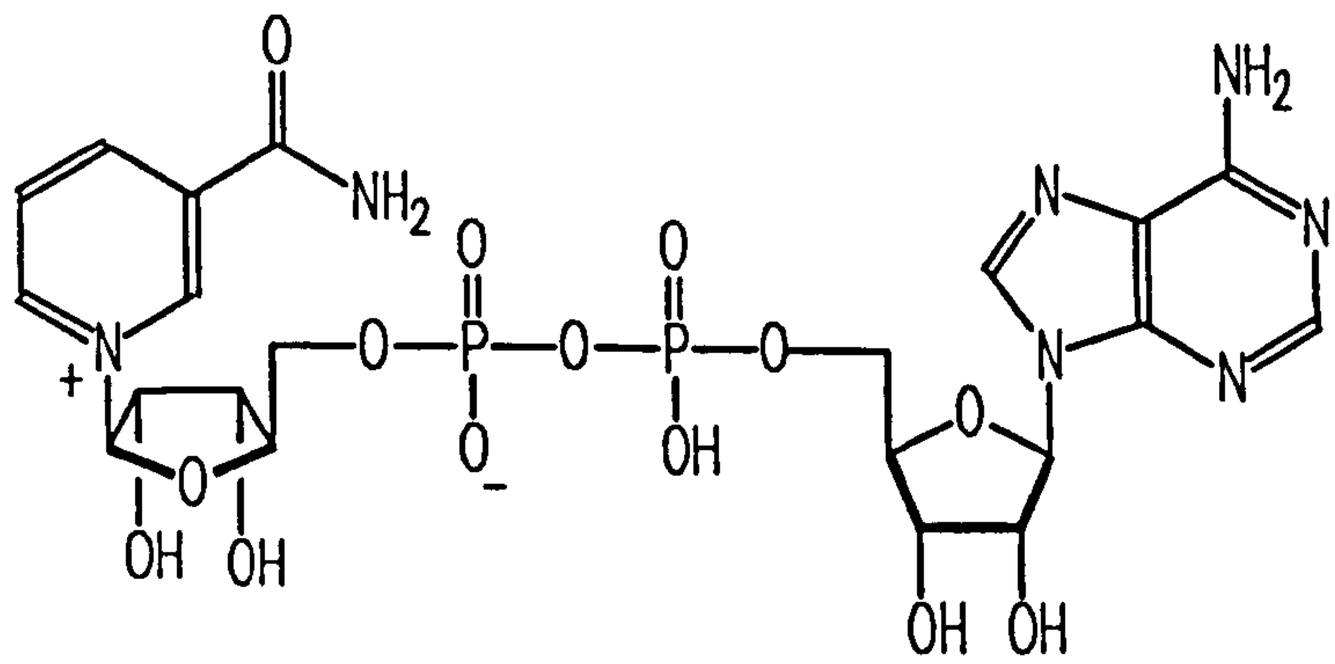

Nicotinamide Adenosine Diphosphate

Figure 8

As can be seen from Figure 8 a pyridinium cation (a good nucleofuge) is attached *via* an *N*-glycosidic bond to the C-1 of D-ribose in a β - manner (α forms have also been observed but are usually enzymically inactive). This nicotinamide - ribose moiety is linked to adenosine *via* a pyrophosphate group making the molecule a dinucleotide (*cf* Section 1.3). Usually NAD^+ is involved in enzymic redox reactions where, as cofactor, it acts as a hydride acceptor. The hydride anion is accepted at C-4 of the nicotinamide ring (the aromaticity of which is lost) forming a quinoid type structure. The reduced form of NAD^+ is represented as NADH (**26**, see Figure 9).

Ethanol alcohol dehydrogenase is an example of an enzyme which has NAD^+ as a cofactor and which effects a redox reaction. This enzyme oxidises ethanol (**27**) to ethanal (**28**), in the manner shown in Figure 10, with NAD^+ accepting the hydride anion produced (the proton which is also produced goes into solution).

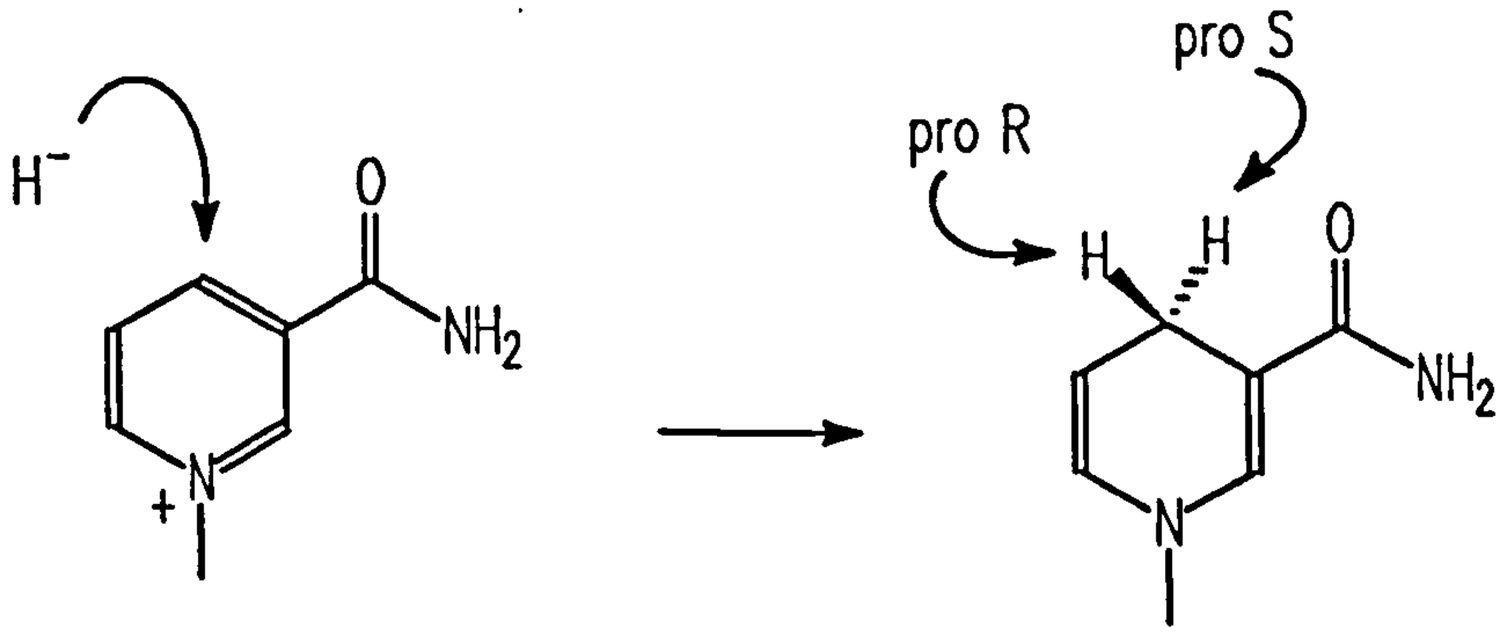

NAD^+ 2 NADH 26

NAD^+ as a Hydride Acceptor

Figure 9

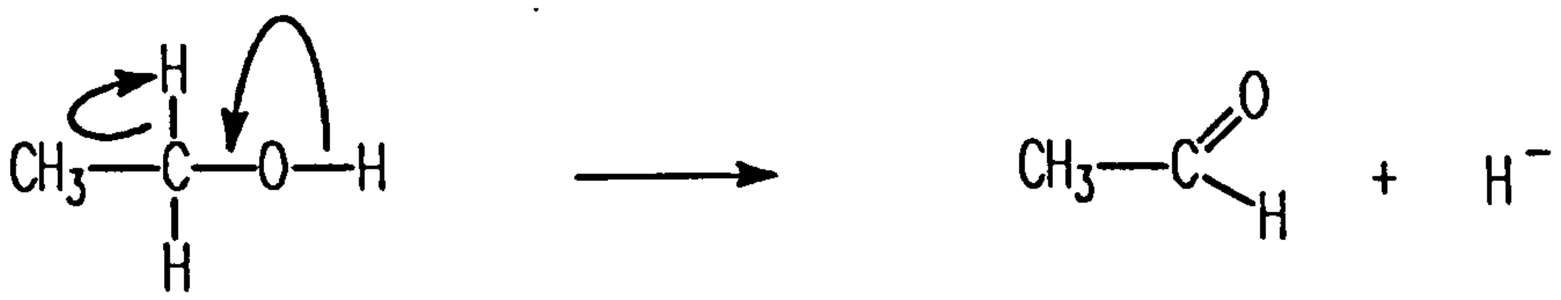

27 28

The Oxidation of Ethanol to Ethanal

Figure 10

When NAD^+ accepts a hydride ion in this manner, a prochiral centre is produced (at C-4 of the dihydronicotinamide ring) within the resulting NADH. That is, hydride transfer is stereospecific. Thus, ethanol, lactate and malate dehydrogenases transfer the *pro*-R hydride, whilst 3-phosphoglyceraldehyde and glucose dehydrogenases are *pro*-S specific (see Figure 9).

A large number of enzymic redox reactions which have NAD^+ as a cofactor have been studied and described in the literature. However, care must be taken if we are to take any of the results - such as enzyme bound crystal structures of NAD^+ - as premises for the design of our molecules. This is because PARP is not a redox enzyme but an ADP-ribosylating enzyme. The crystal structure of NAD^+ (which was determined by Saenger *et al*[31]) can be used as a premise for our work. The description of this crystal structure will help explain some of our ideas for drug design and introduce all the nomenclature necessary for an explanation of the results of a two dimensional NMR spectroscopic solution conformation study of NAD^+ (see Section 3.4).

3.2 The Crystal Structure of NAD^+

The crystal structure of the dihydrate of the lithium salt of NAD^+ - Li^+NAD^+, $C_{21}H_{26}N_7O_{14}P_2Li.2H_2O$ - is detailed below and is reproduced in Diagram 1.

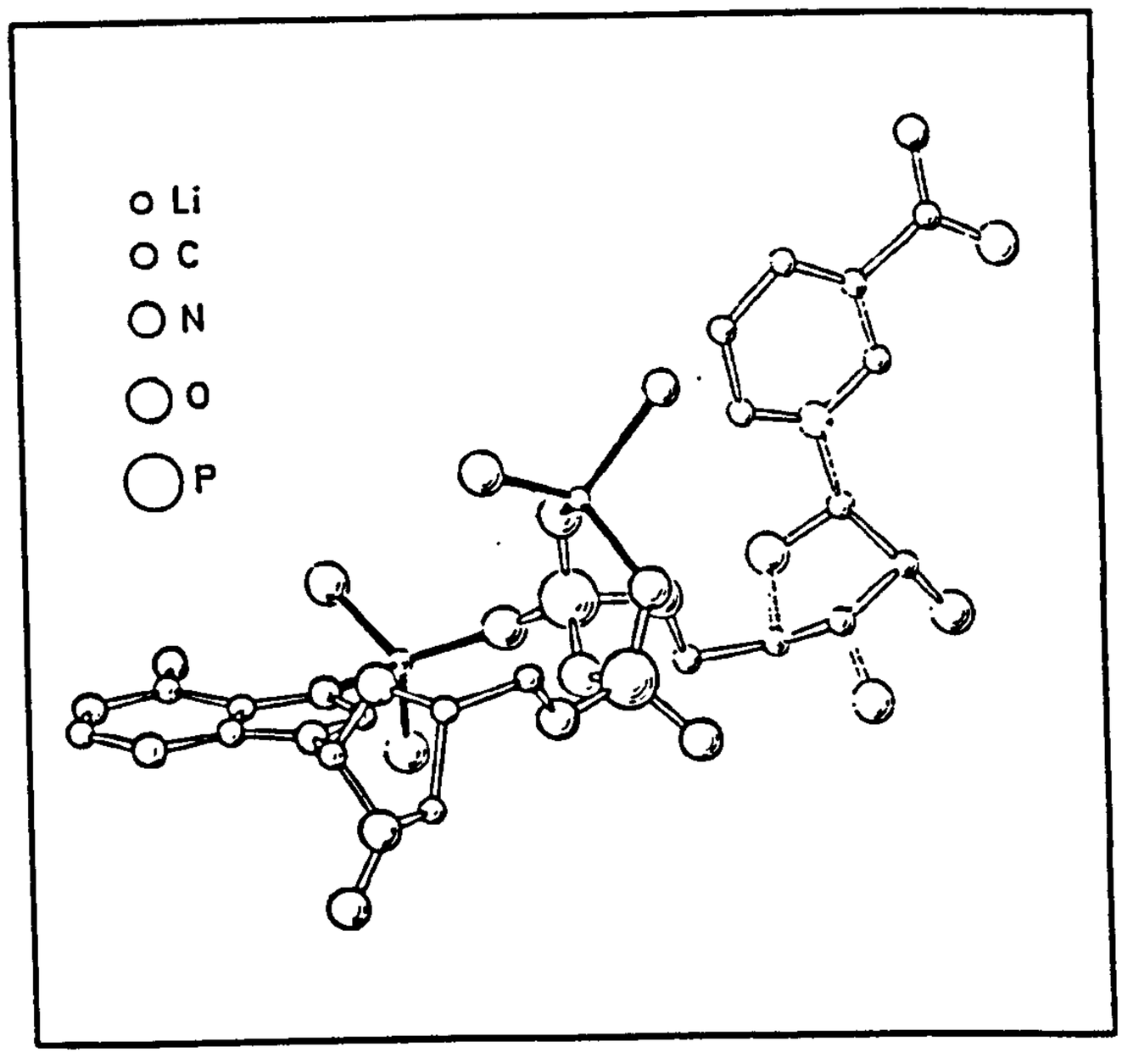

The Crystal Structure of NAD^+

Diagram 1

Furthermore, it is described by a consideration of various components and bonds, such as: the two sugars; the sugar base bonds; the C4'-C5' bonds and the pyrophosphate linkage.

Nomenclature[32]

Within a system of four atoms designated ABCD, the three atoms ABC can describe a plane as can the three atoms BCD. The angle at which these planes intersect is called the dihedral angle. Angles formed by a clockwise rotation of the rear bond are designated positive, whilst anticlockwise rotations are negative. If the dihedral angle is 0° the system is synperiplanar (*cis*), if the dihedral angle is 180° the system is antiperiplanar (*trans*). The region between 0° and 90° is the synclinal or gauche

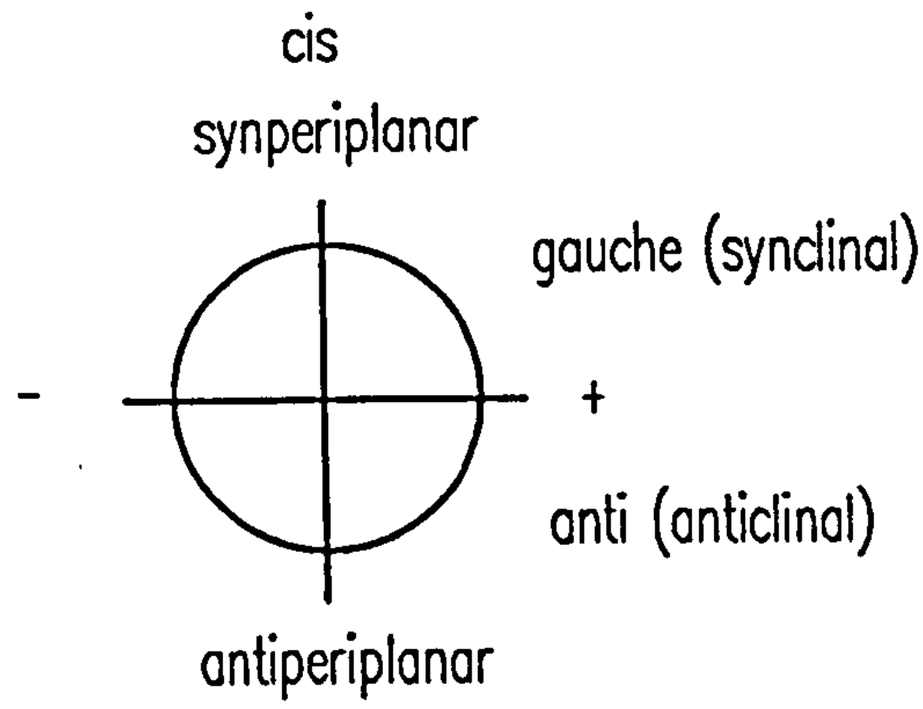

Illustration of the Nomenclature of the Dihedral Angle

Figure 11

region and the region between 90° and 180° is the anti or anticlinal region (see Figure 11).

3.2.1 The Sugar Conformations

The conformations of the furanose sugars are succinctly described by the pseudorotation concept.[33] Briefly, the sugar's C1', C4' and O atoms describe a plane; any atoms above that plane (*ie* on the same side as the C5' atom) are called *endo* whilst the atoms below it are said to be *exo*. This gives rise to two conformations: envelope (E) and twist (T). An envelope occurs when one atom does not deviate or only slightly deviates from the plane, whilst the other atom shows a large deviation; a twist conformation occurs when both atoms display similar (but opposite) deviations from the plane. In Figure 12 the arrows show the direction of deviation from the plane defined by the remaining atoms indicated by '•'. The adenosine ribose has a C(2')-*endo* (^{2}E) envelope whilst the nicotinamide ribose has a C(3')-*endo* C(2')-*exo* ($^3T_2$) twist conformation, both of which are also represented in Figure 12.

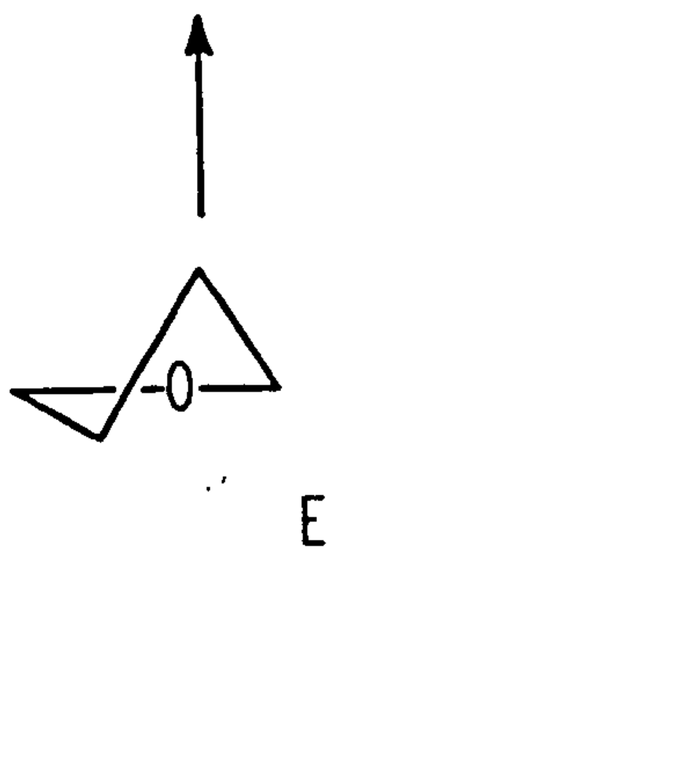

The Envelope and Twist Conformations of NAD^+ Ribofuranoses

Figure 12

3.2.2 The Glycosidic Bonds

The relative orientation of the bases with respect to the sugars is described by the torsional angle about the glycosidic bonds. The angles for adenosine (O(1')-C(1')-N(9)-C(8)) and nicotinamide ribose (O(1')-C(1')-N(1)-C(6)) show that both bases adopt an *anti* conformation: *ie* the bases are directed away from the sugars. This is represented in Figure 13 where the bold lines represent the bonds which form the torsion angle. In the crystal structure the value for the adenosine moiety is 52° and for the nicotinamide the value is 15°.

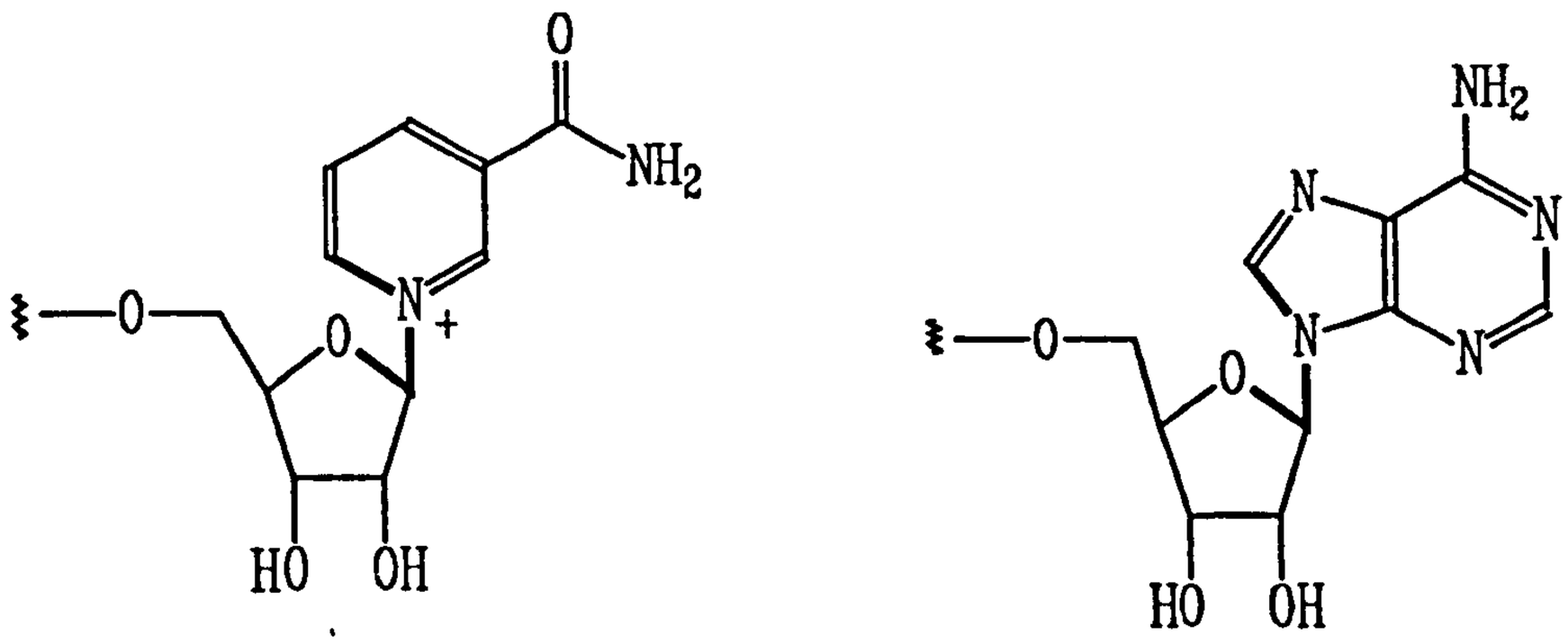

The Relative Base/Sugar Orientations of NAD^+

Figure 13

3.2.3 The C4'-C5' Orientation

The orientation observed for (O(5')-C(5')-C(4')-C(3')) in NAD^+ is the preferred conformation for other nucleotides. In both cases within NAD^+ the orientation can be described as + gauche. Thus, the O5' atoms are above the ribose ring, which is depicted in Figure 14. The torsion angles (described by the bold bonds) for the two sugars are 48° and 47° for the adenosine and nicotinamide riboses, respectively.

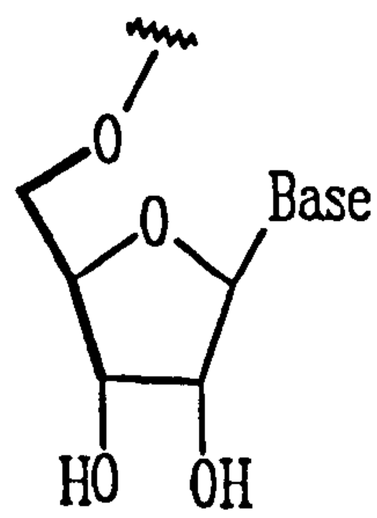

The C4'-C5' Orientation of Ribose

Figure 14

3.2.4 The Pyrophosphate Linkage

Many crystal structures of compounds containing the pyrophosphate linkage have been determined making comparisons between them and NAD^+ possible. The P-O bond distances in the P-O-P group tend to differ by about 0.1 Å for molecules such as CDP and ADP (depending upon their counterions), whilst the P-O bond distances are similar for symmetrical molecules such as di-β-naphtholpyrophosphate. Since the pyrophosphate group within NAD^+ is symmetrically substituted by ribose units connected in the same way (*via* O5') then the P-O bond distances should be very similar. However, the bond distances were found to be disymmetrical, one bond was about 0.1 Å longer than the other. The P_N-O_{PP} bound was found to be longer than the P_A-O_{PP} bond. This was thought to be a consequence of the lithium cation coordination (see Diagram 2).

Another feature of the pyrophosphate group was its POP bond angle of 130°. This was consistent with the values observed for this angle in other nucleotides, but not with phosphoesters where the bond angle about POC is usually 120°. This phenomenon has important consequences for the dihedral angles of the pyrophosphate group and can allow it to occupy a synperiplanar (*cis*) orientation.

The O5'-P_N torsion angle was found to be + gauche (79°) whilst the O5'-P_A torsion angle was - anticlinal (-125°). The latter result, again, was thought to be a consequence of lithium cation coordination. However, in solutions without any cations, greater flexibility can be envisioned.

3.2.5 The Bases and Li^+ Cation Coordination

Both bases are almost planar and orientated nearly perpendicular to one another. The Li^+ cation is tetrahedrally coordinated to adenine N7 and a pyrophosphate oxygen of

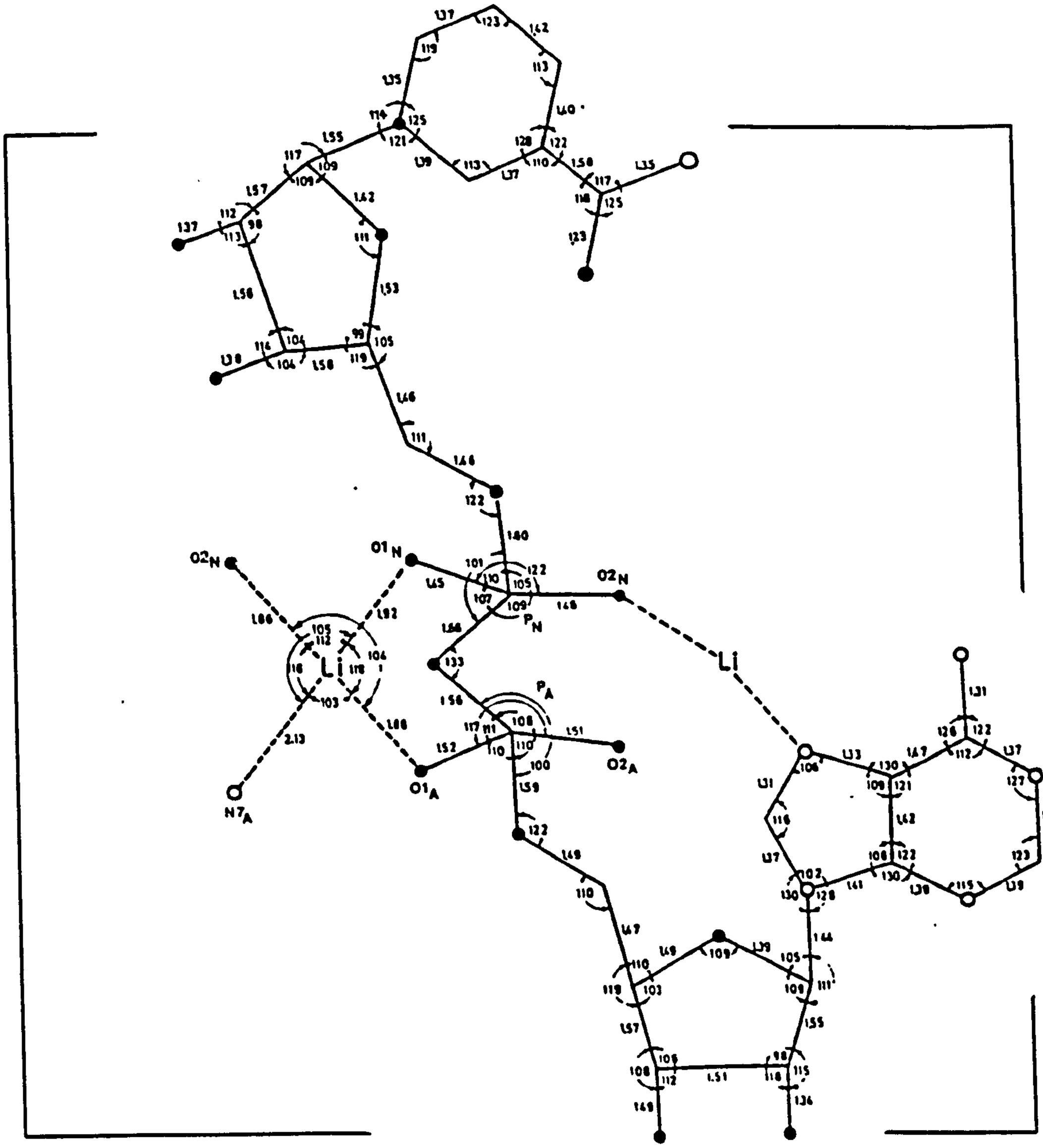

The Crystal Structure of NAD^+ Showing Lithium Coordination

Diagram 2

the nicotinamide part of the pyrophosphate group. The Li^+ cation is further coordinated to the pyrophosphate oxygens of another NAD^+ molecule (see Diagram 2).

3.3 Solution conformation of NAD^+

The proposed solution conformation of NAD^+ was determined from the analysis of NMR spectroscopic data of various reduced and oxidized pyridine dinucleotides. This research began in the late 1960's and early 1970's and initially no useful data was won due to the low field strengths (60 MHz) used to determine the spectra. In 1970 Sarma and Kaplan[34] obtained higher field (220 MHz) spectra of some reduced and deuterio labelled pyridine dinucleotides. They observed an AB splitting pattern which was assigned to the H4' and H4" protons of a 1,4-dihydropyridine dinucleotide. That is, the two protons (H4' and H4") were seen to have different chemical shifts. This difference in chemical shift was rationalized by employing the idea of a folded dinucleotide: the nucleotide was thought to be folded in such a manner that the adenine half of the molecule resided over the reduced pyridine half of the molecule. In this way one of the protons at position four would exist in a different chemical environment to the other proton and a chemical shift difference, induced by the adenine ring current, would be seen between them. From this premise and using specifically deuteriated (D4' or D4") 1,4-dihydropyridine dinucleotides they proposed the proportions of dinucleotide conformer (right or left handed helix) in solution.

This paper and other similar papers were later appraised by Jacobus.[35] Before turning to the previous paper he presented various stereochemical definitions and related these definitions to the NMR properties of the reduced pyridine dinucleotides. In particular the reduced pyridine protons H4' and H4" within the previous example were diastereotopic and as such were anisochronous. That is, they have different chemical shifts whatever their environment. Thus, the results described by Sarma and Kaplan could be rationalized without the need to invoke a helical model. It was concluded that the NMR results so far could only define the topography of these molecules with ambiguity.

This observation however, does not preclude the existence of helical conformers. In a dynamic system with a pyrophosphate linkage that possesses the capacity for the degree of flexibility described earlier (see above), then NAD^+ (NADH etc...) most probably exists in three forms: an extended one similar to its crystal structure and two stereochemically distinct helical or folded conformations. Furthermore, this hypothesis could be tested by nOe NMR experiments and perhaps even the proportions of the folded species could be determined by expeditious use of deuterio-labelled dihydropyridine dinucleotides (see Future Work).

In summary NAD^+ adopts the expected conformations derived from comparison with other nucleotides. The peculiarities of the crystal structure seem to be a consequence of the lithium cation coordination.

3.4 Further Investigations of The Solution Conformation of NAD^+

The design of some of our inhibitors of PARP was to be based upon the structure of PARP's cofactor NAD^+. The 500 MHz ^1H and 125 MHz ^{13}C NMR spectra of NAD^+ were determined with a view to discovering some empirical data that would help to describe its solution conformation.

3.4.1 The NMR Spectra of Adenosine 5'-(Trihydrogen Diphosphate)5'→ 5' ester with 3-(Aminocarbonyl-1-B-D-Ribofuranosyl-Pyridinium, hydroxide, inner salt (NAD^+)

Notation: A position about the nicotinamide ring will be designated N_n where n is a number. A position about the sugar ring attached to the nicotinamide ring will be designated $N_{n'}$. In the adenosine system the letter N will be replaced by A. This numbering system is illustrated in Figure 15.

NAD^+: This compound consists of two parts joined by a diphosphate linkage: one part consists of adenosine which is attached to the diphosphate group *via* the 5' (A5') hydroxyl group; the other part consists of nicotinamide attached to ribofuranose from the N1 nitrogen to the anomeric N1' carbon in a β manner with the N5' hydroxyl joined to the diphosphate linkage (see Figure 15).

3.4.2 NMR Spectrum of NAD^+

When considering the NMR (^1H or ^{13}C) spectra of NAD^+ we expect to see a problem with the differentiation of the two ribose units. This problem has been

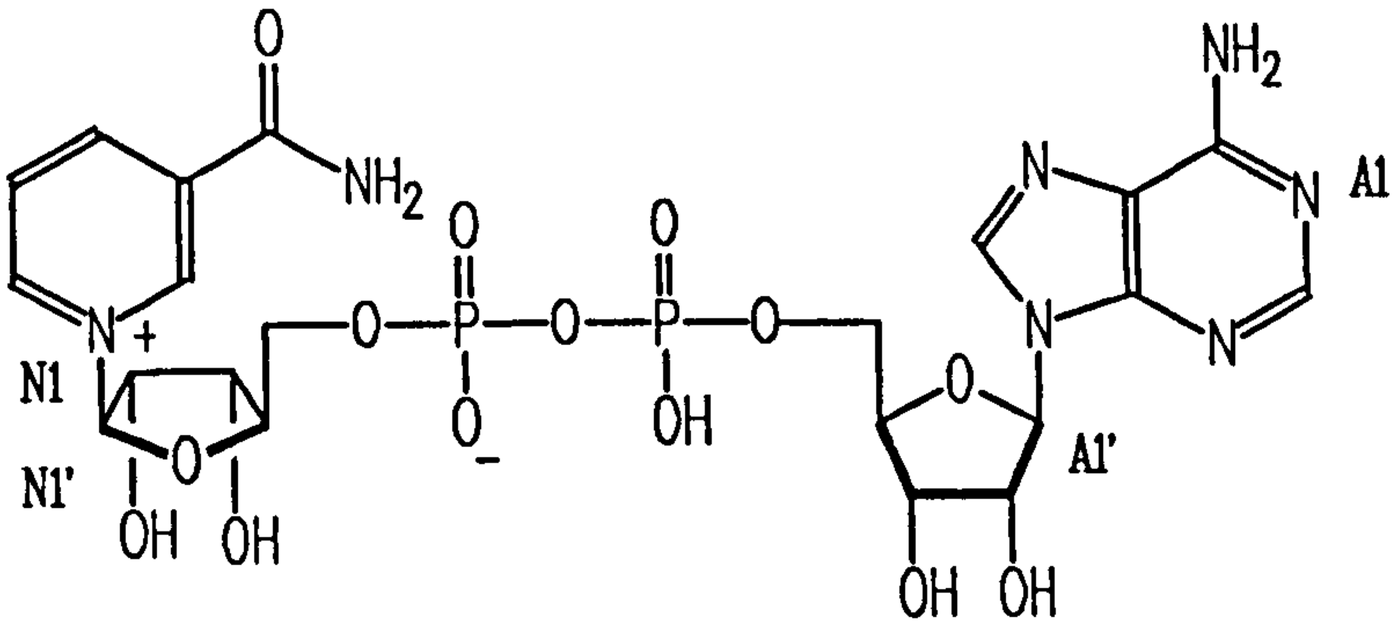

The Numbering of NAD^+

Figure 15

overcome for the ^1H NMR spectrum of this compound by using a high field spectrometer (500 MHz) and correlation spectroscopy (COSY) to assign coupled peaks. Our assignments have been further confirmed by rotating frame Overhauser effect spectroscopy (ROESY).

The ^{13}C spectrum of NAD^+ has been assigned by using heteronuclear shift correlation spectroscopy and selective spin decoupling. Carbon-phosphorus coupling indicating the conformation of the molecule about the phosphodiester linkage is also observed and discussed.

3.4.3 The 500 MHz ^1H NMR Spectrum of NAD^+

This spectrum (spectrum 1) has three distinct regions: the first, between δ 9.6 and δ 8.2, contains the aromatic protons; the second, between δ 6.4 and δ 6.0, contains the two anomeric protons; and lastly the sugar protons are between δ 5.0 and δ 4.0. This is in accord with the ^1H NMR spectra of *N*-alkyl nicotinamide salts[36] and adenosine.[37]

The ^{1}H NMR Spectrum of NAD^{+}

Spectrum 1

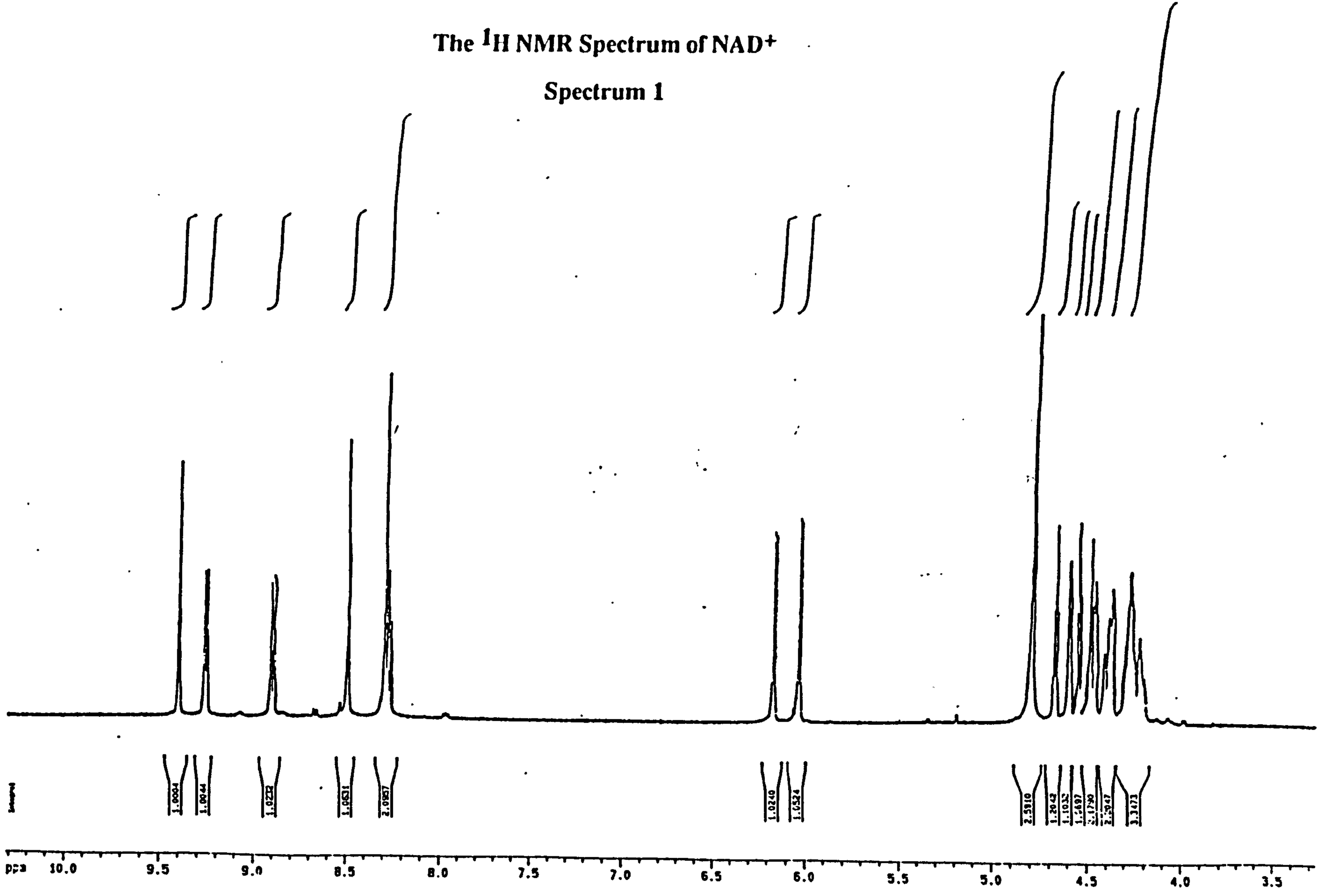

The ^{1}H NMR Spectrum of NAD^{+}

Spectrum 1

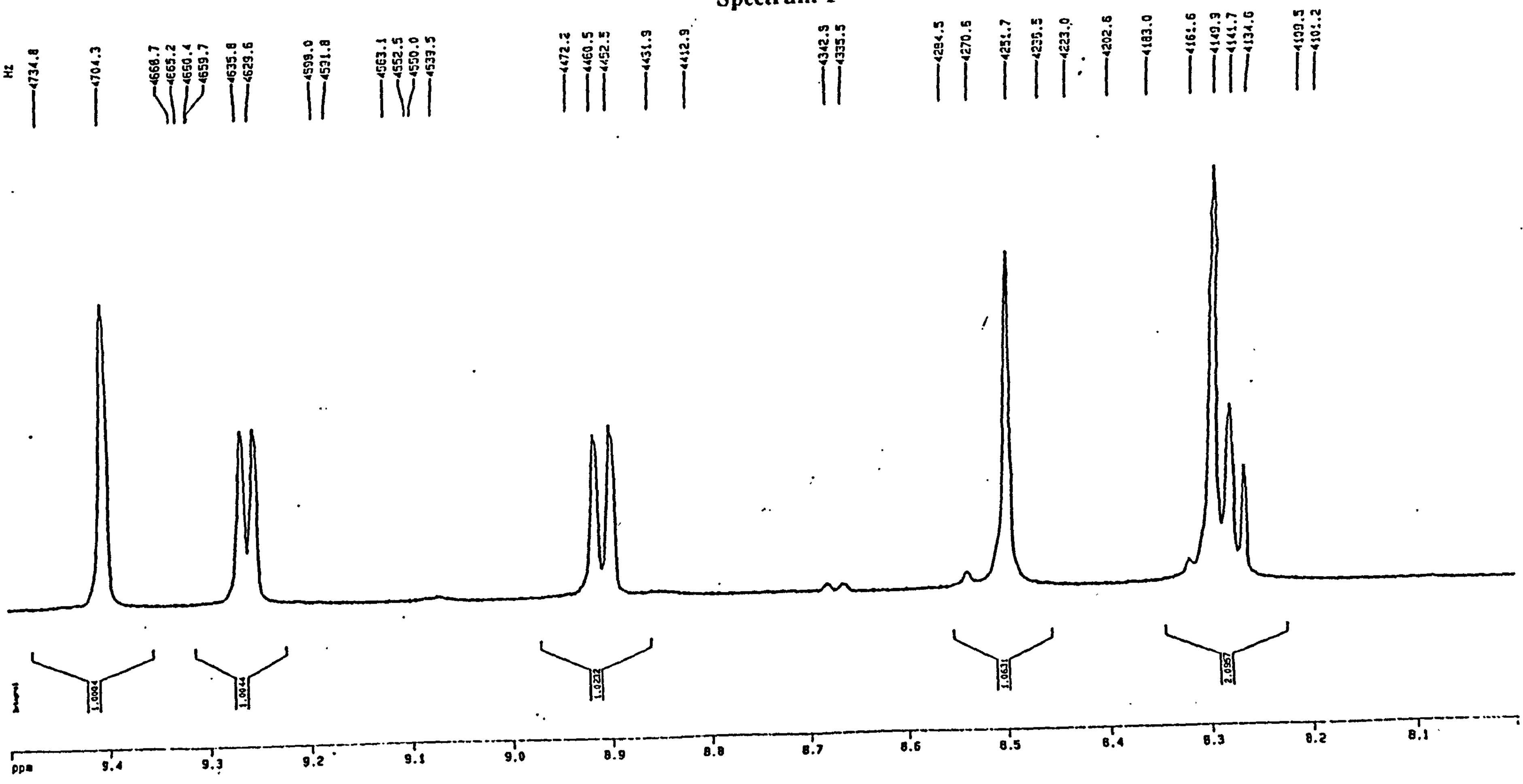

The ^{1}H NMR Spectrum of NAD^{+}

Spectrum 1

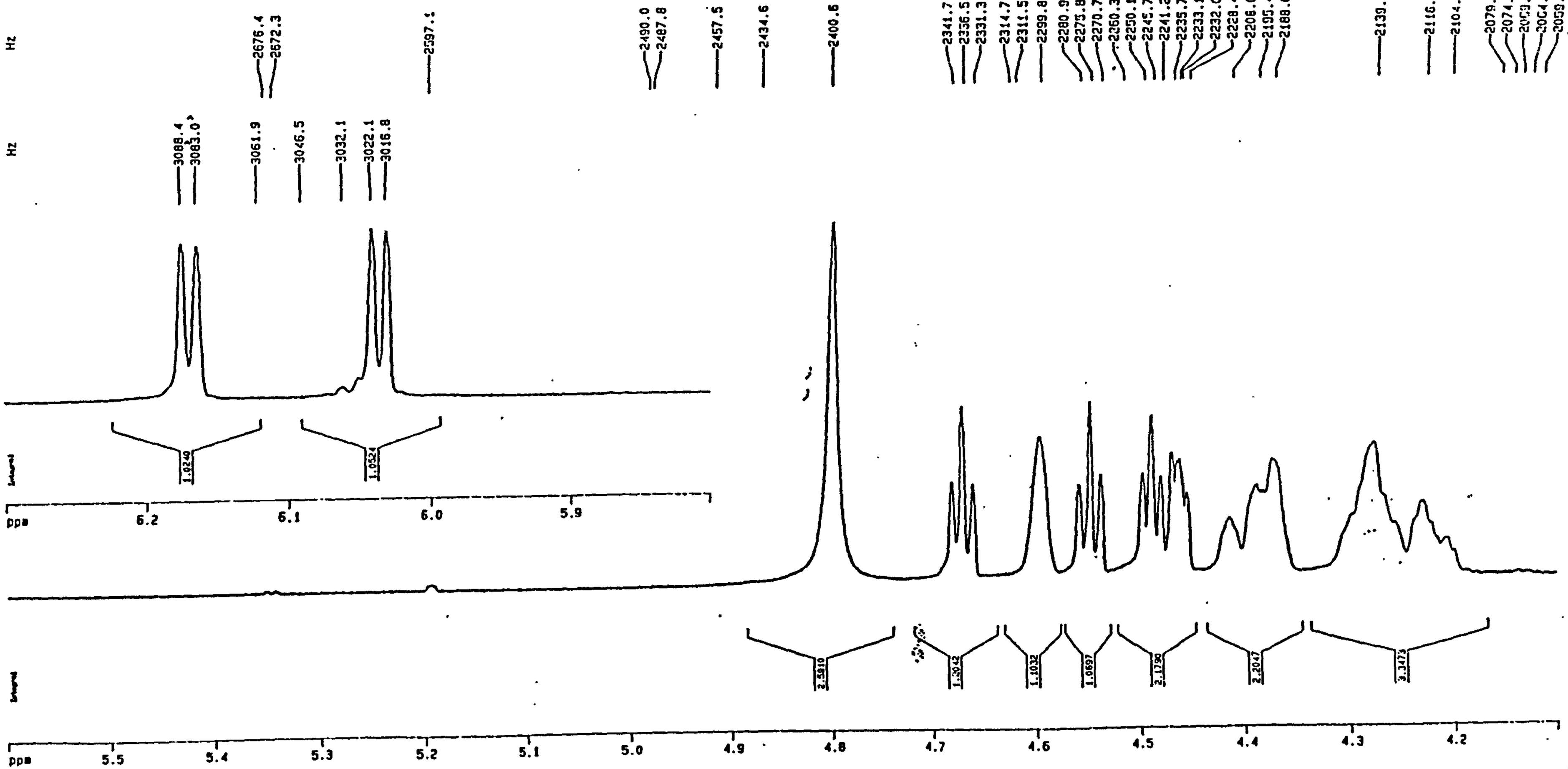

The signal furthest downfield is a singlet at δ 9.41, which arises from N2. The protons N6 and N4, both doublets, have chemical shifts of δ 9.28 and δ 8.91, respectively. The adenine protons appear next, with A8 further downfield (δ 8.50) than A2 (δ 8.30). The signal at δ 8.30 merges with what should be a triplet centred at δ 8.28: this corresponds to N5. At other concentrations these two signals separate.

Of the two anomeric protons, the one alpha to the positive nitrogen is confirmed to be the furthest downfield by ROESY experiments. So we have a doublet at δ 6.18 representing N1' and another doublet at δ 6.05 (A1').

The sugar protons in spectrum 1 were assigned with the help of COSY spectra of NAD^+. The COSY spectra 2 and 3 show which protons are coupled to each other within the NAD^+ molecule. Coupling between the anomeric protons N1' and A1' is seen with N2' and A2' (spectrum 2). The A2' proton appears at δ 4.67 whilst the N2' proton appears at δ 4.55; these two signals are seen as triplets in the one dimensional spectrum of NAD^+ (spectrum 1). Spectrum 3 shows details of the sugar region. It shows correlation between A2' and A3' (δ 4.49), whilst N2' correlates with N3' (δ 4.47): these are seen to be a triplet (A3') and a poorly resolved double-doublet in spectrum 1. A3' correlates with A4' (δ 4.38) and this signal is seen to correlate with the A5' and A5" protons, which are in the region δ 4.3 - δ 4.2. In spectrum 1, A4' appears as a broad singlet whilst the A5' and A5" protons appear as a broad multiplet. At N3' a correlation is seen to N4' (δ 4.59) which appears as a broad singlet downfield of N3' in spectrum 1. The N4' signal is coupled to N5' (δ 4.39) and N5" (δ 4.27); these two signals occupy two widely spaced multiplets in spectrum 1.

The adenine sugar rings protons appear at higher field with increasing distance from the anomeric position. The nicotinamide sugar ring does not have this property: the proton N4' is downfield to N3'. Another difference in the two sugars is that the

COSY Spectrum of NAD^+

Spectrum 2

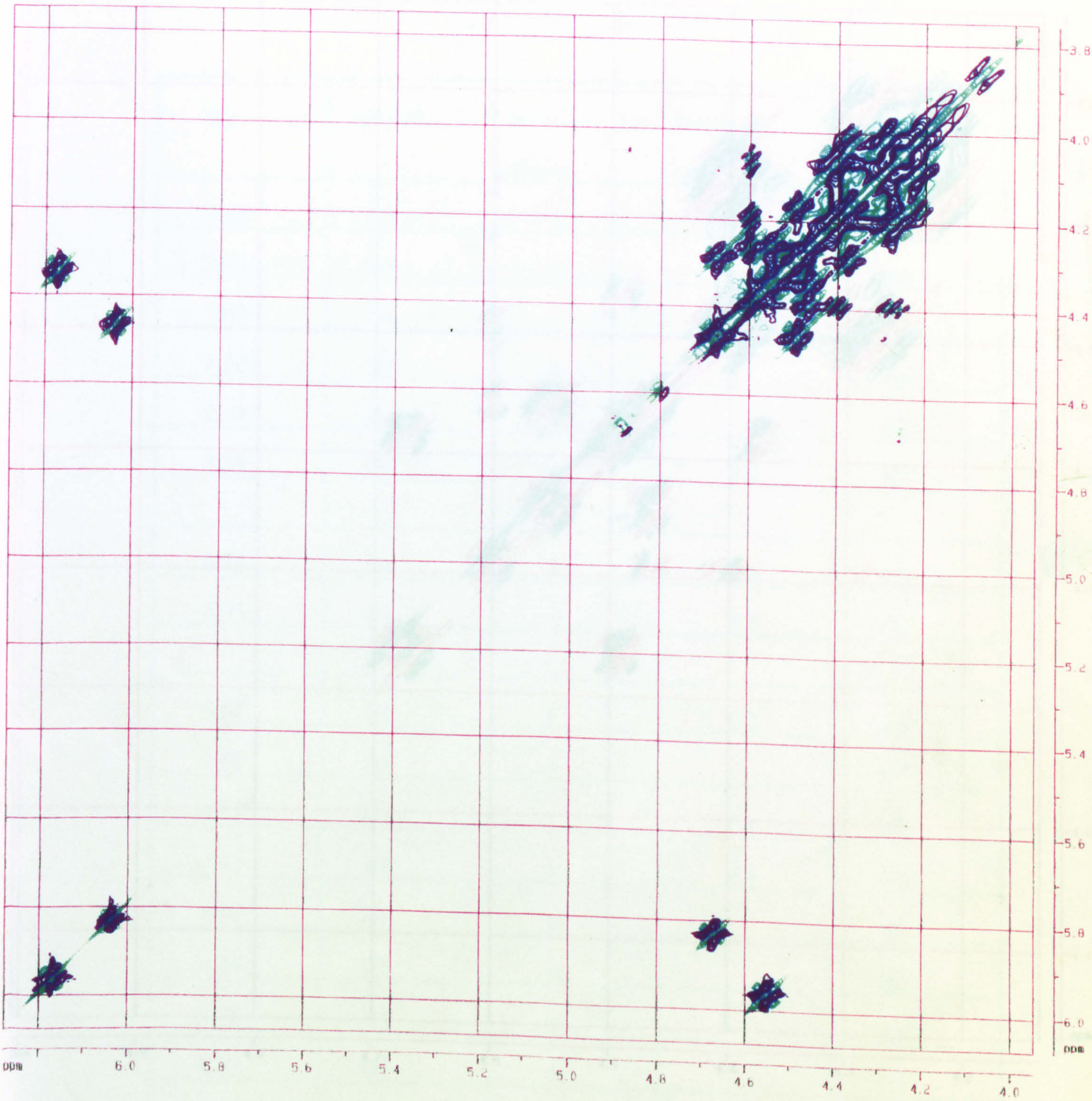

COSY Spectrum of NAD^+

Spectrum 3

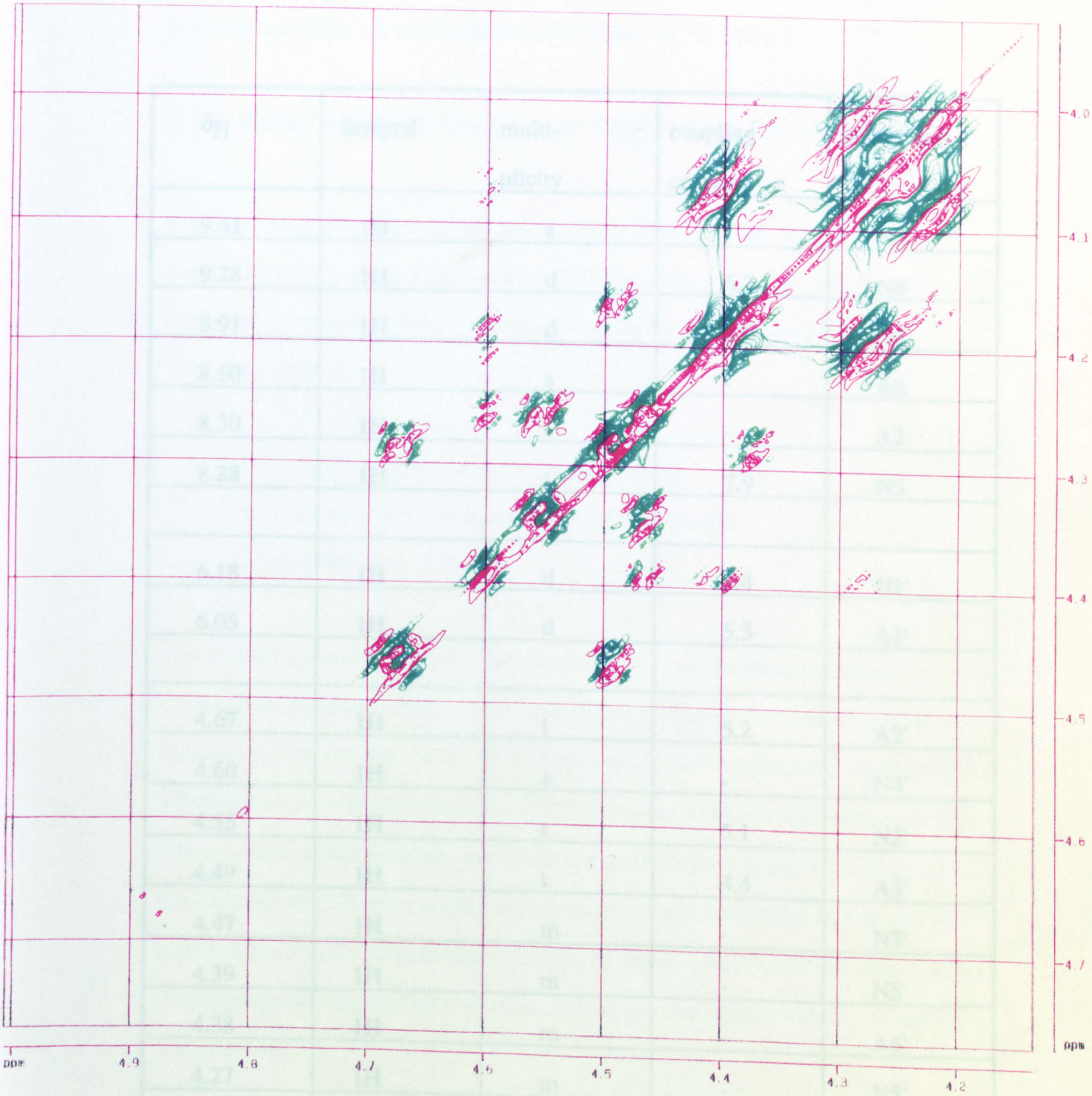

chemical shifts of the protons N5' and N5" are dissimilar, whilst the corresponding A5' and A5" protons are similar.

δ_H	Integral	multi-plicity	coupling constant	assignment
9.41	1H	s	-	N2
9.28	1H	d	6.2	N6
8.91	1H	d	8.0	N4
8.50	1H	s	-	A8
8.30	1H	s	-	A2
8.28	1H	t	7.9	N5
6.18	1H	d	5.4	N1'
6.05	1H	d	5.3	A1'
4.67	1H	t	5.2	A2'
4.60	1H	s	-	N4'
4.55	1H	t	5.1	N2'
4.49	1H	t	4.4	A3'
4.47	1H	m	-	N3'
4.39	1H	m	-	N5'
4.38	1H	m	-	A4'
4.27	1H	m	-	N5'
4.2 - 4.3	2H	m	-	A5', A5"

Table 1

The conformations of the two sugars seem to be very similar because their coupling constants, between corresponding protons, are similar. For instance the anomeric doublets both have a 5 Hz coupling to the triplets of N2' and A2'.

3.4.4 Rotating Frame Overhauser Effect Spectroscopy of NAD^+

Rotating frame Overhauser effect spectroscopy (ROESY) can be used to estimate distances between the protons (usually) within a molecule. When this technique was applied to a solution of NAD^+ in D_2O it was hoped that two pieces of information would be obtained:

a. It would confirm our previous assignments.
b. It would give a strong indication of the solution conformation of NAD^+.

The ROESY spectrum of NAD^+ (spectrum 4a) is a two dimensional spectrum which shows contours along a diagonal, the colour and density of the contours giving an indication of the strength of the signal represented. Off this diagonal, signals are seen which represent nuclear Overhauser effect interactions between the protons of the different parts of the molecule but which are spatially proximate. It is obvious that these signals should occur when the protons are alpha to one another, but weaker interactions can also occur between protons of larger separations even when it is not immediately obvious that such protons are close to one another. This is shown in Spectrum 4b.

As well as the qualitative interpretation of these spectra it is also possible to give a quantitative interpretation of the spectra by obtaining the relative intensities of the off diagonal signals. These are actually proportional to the volume integrals of the peaks

The ROESY Spectrum of NAD⁺

Spectrum 4a

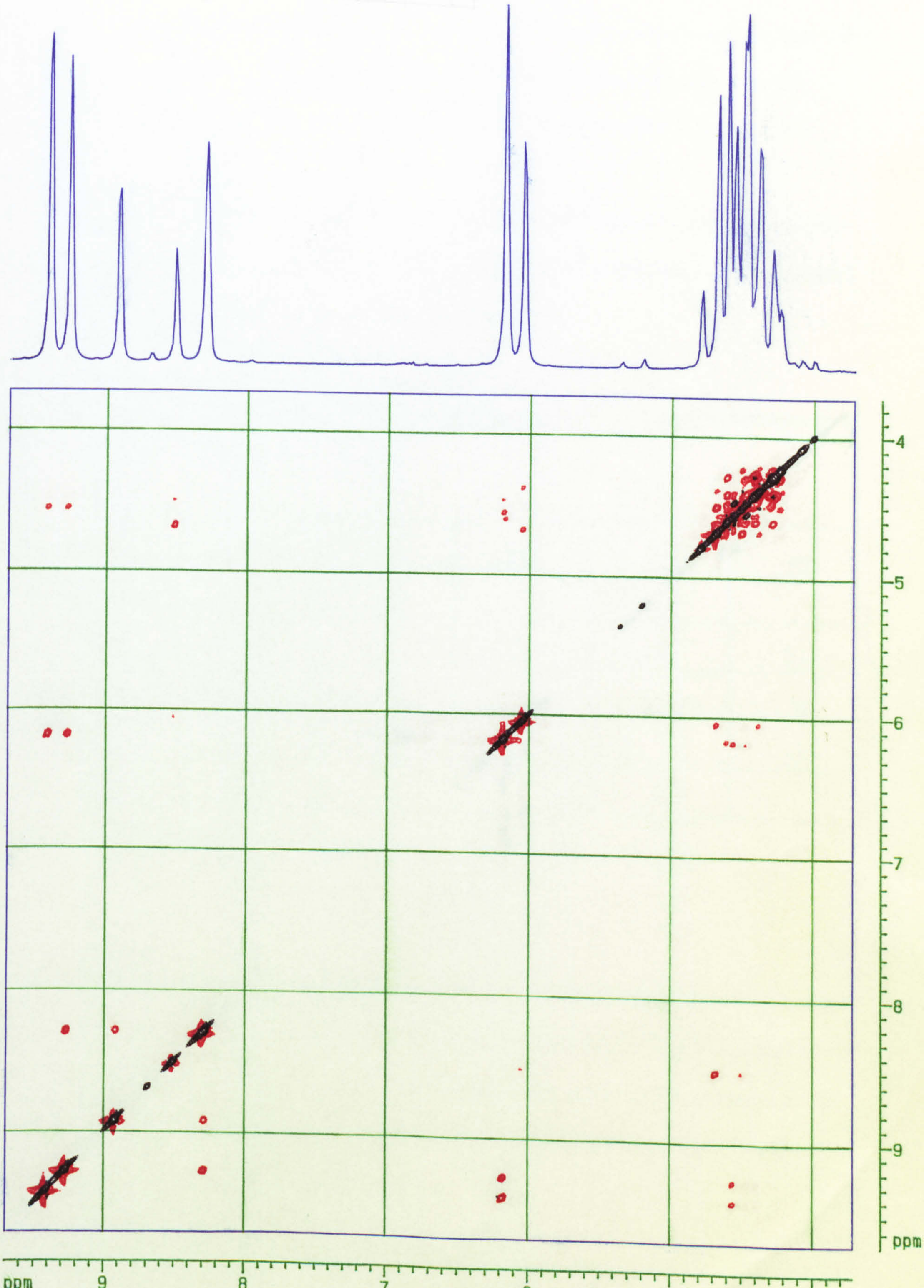

The ROESY Spectrum of NAD^+

Spectrum 4b

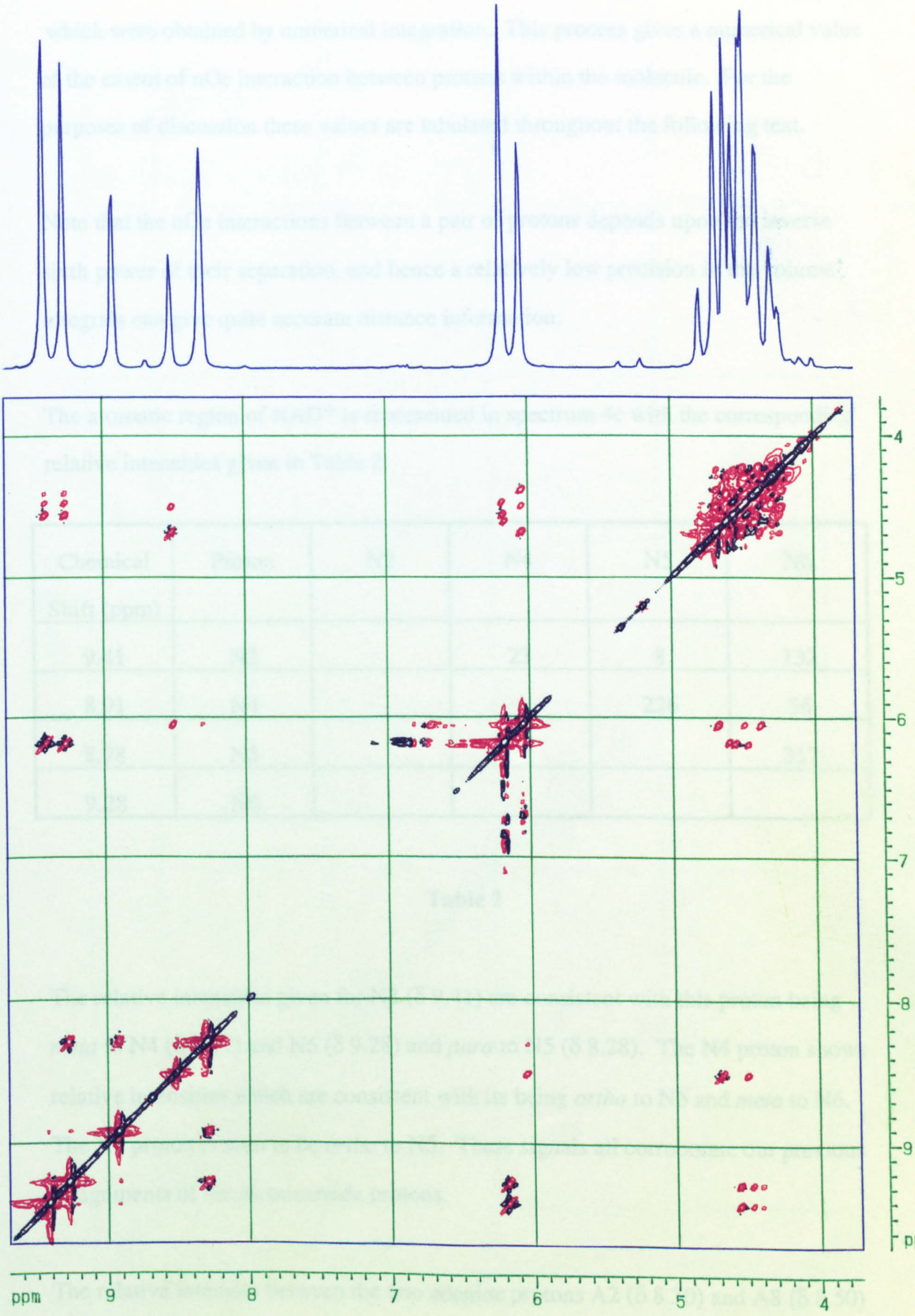

which were obtained by numerical integration. This process gives a numerical value of the extent of nOe interaction between protons within the molecule. For the purposes of discussion these values are tabulated throughout the following text.

Note that the nOe interactions between a pair of protons depends upon the inverse sixth power of their separation, and hence a relatively low precision in the volume integrals can give quite accurate distance information.

The aromatic region of NAD^+ is represented in spectrum 4c with the corresponding relative intensities given in Table 2.

Chemical Shift (ppm)	Proton	N2	N4	N5	N6
9.41	N2		23	8	132
8.91	N4			226	36
8.28	N5				317
9.28	N6				

Table 2

The relative intensities given for N2 (δ 9.41) are consistent with this proton being *meta* to N4 (δ 8.91) and N6 (δ 9.28) and *para* to N5 (δ 8.28). The N4 proton shows relative intensities which are consistent with its being *ortho* to N5 and *meta* to N6. The N6 proton is seen to be *ortho* to N5. These signals all corroborate our previous assignments of the nicotinamide protons.

The relative intensity between the two adenine protons A2 (δ 8.30) and A8 (δ 8.50) has a value of 46 (and is not tabulated). This value is larger than what would be

The ROESY Spectrum of NAD^+

Spectrum 4c

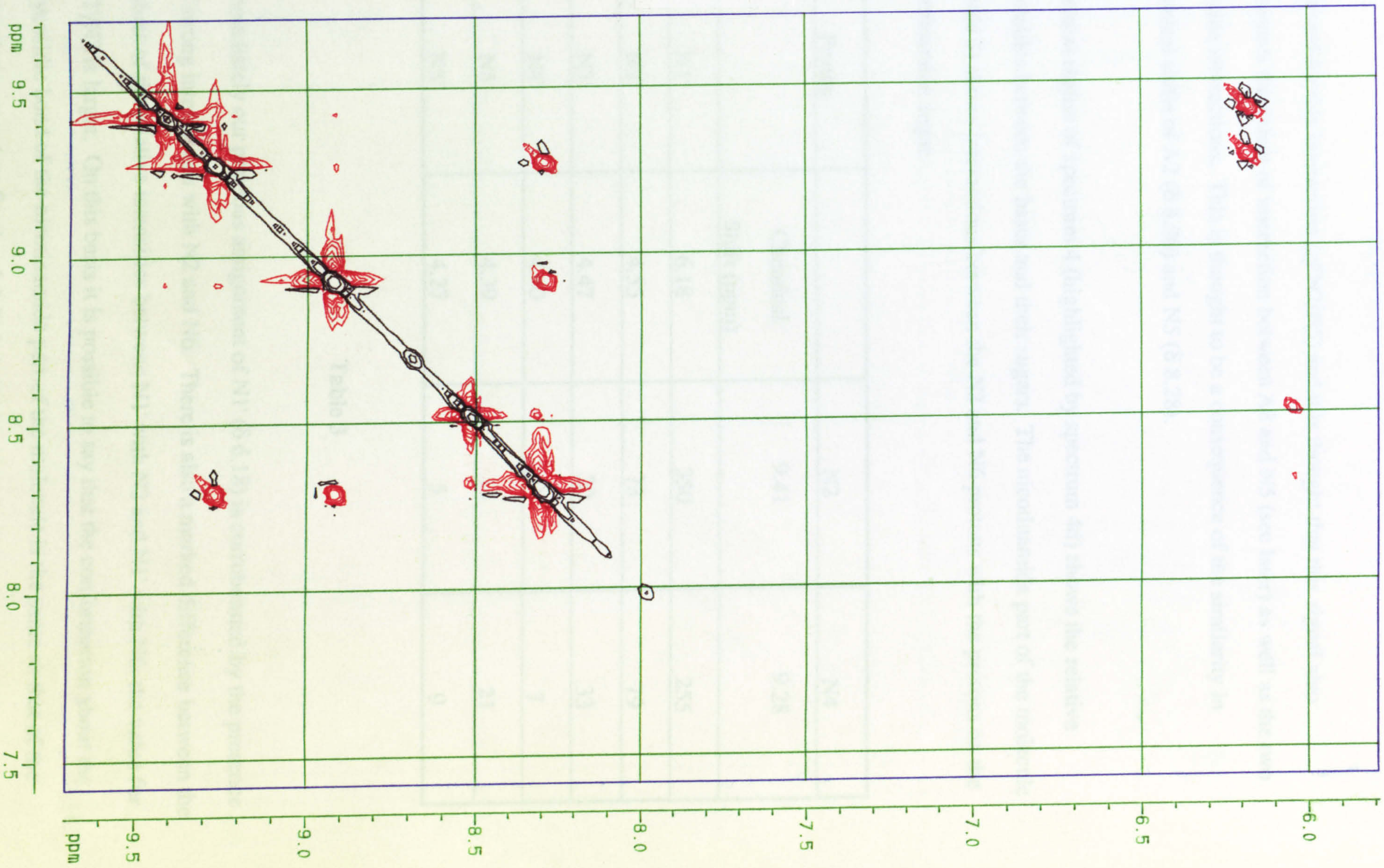

expected for this interaction (*cf* N2/N5) and it is thought that this signal also represents the extent of interaction between A8 and N5 (see later) as well as the two adenine interactions. This is thought to be a consequence of the similarity in chemical shifts of A2 (δ 8.30) and N5 (δ 8.28).

The next region of spectrum 4 (highlighted by spectrum 4d) shows the relative intensities between the bases and their sugars. The nicotinamide part of the molecule (Table 3) shows interactions between the N2 and N6 protons with the protons on the nicotinamide sugar.

Proton		N2	N4
	Chemical Shift (ppm)	9.41	9.28
N1'	6.18	350	255
N2'	4.55	73	79
N3'	4.47	20	33
N4'	4.60	9	7
N5'	4.39	14	21
N5"	4.27	5	9

Table 3

Immediately our previous assignment of N1' (δ 6.18) is corroborated by the presence of strong interactions with N2 and N6. There is also a marked difference between the values of the relative intensities between N1' with N2 and N1' with N6: the value for N1'/N2 is larger. On this basis it is possible to say that the conformation about the glycosidic bond of the nicotinamide part of the molecule is the same as that of the crystal structure (see Section 3.2.2) *ie* it has an *anti* conformation. Interactions are

The ROESY Spectrum of NAD$^+$ Showing the Relative Intensities of the Bases and their Sugars

Spectrum 4d

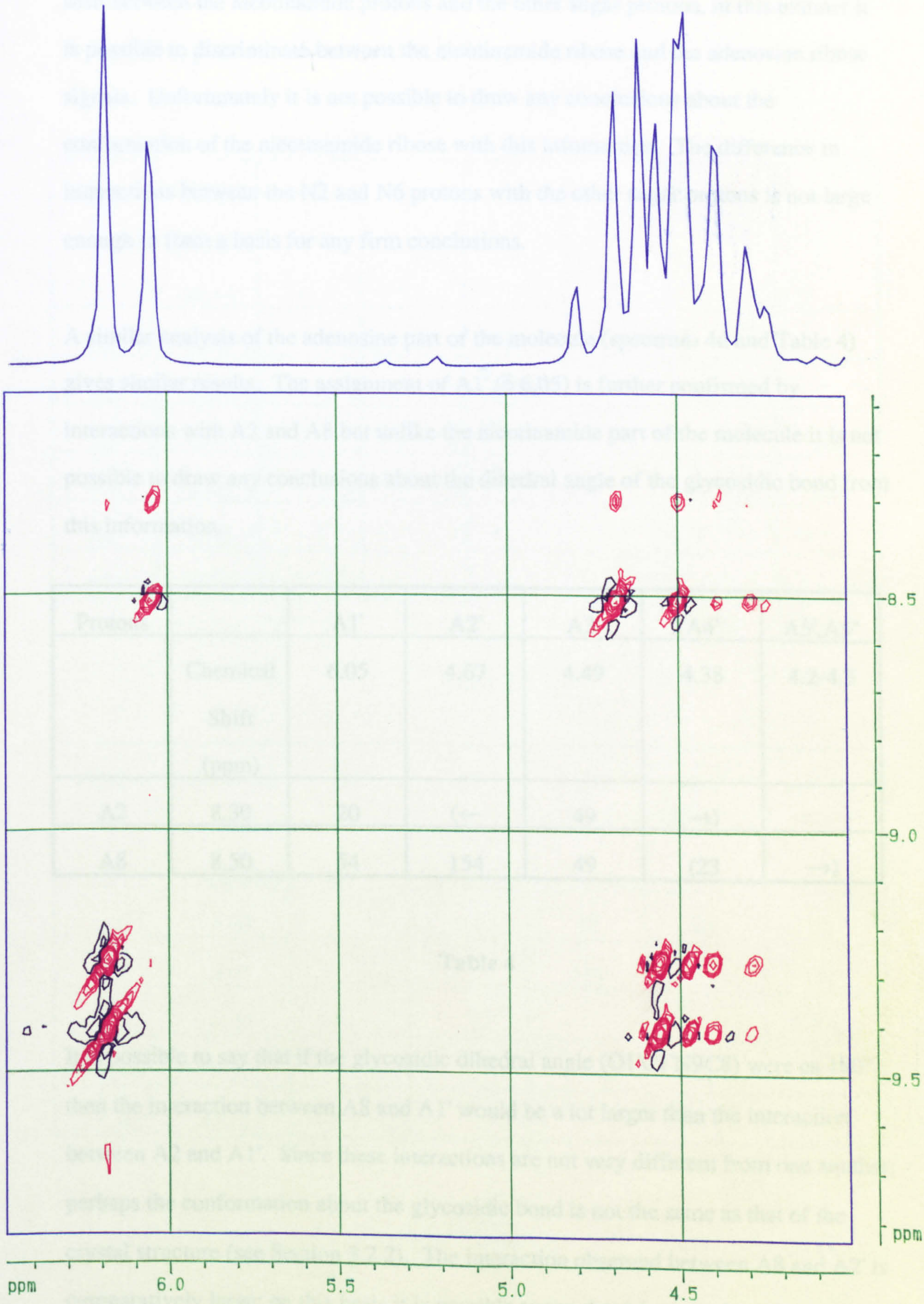

seen between the nicotinamide protons and the other sugar protons, in this manner it is possible to discriminate between the nicotinamide ribose and the adenosine ribose signals. Unfortunately it is not possible to draw any conclusions about the conformation of the nicotinamide ribose with this information. The difference in interactions between the N2 and N6 protons with the other sugar protons is not large enough to form a basis for any firm conclusions.

A similar analysis of the adenosine part of the molecule (spectrum 4d and Table 4) gives similar results. The assignment of A1' (δ 6.05) is further confirmed by interactions with A2 and A8 but unlike the nicotinamide part of the molecule it is not possible to draw any conclusions about the dihedral angle of the glycosidic bond from this information.

Protons		A1'	A2'	A3'	A4'	A5',A5"
	Chemical Shift (ppm)	6.05	4.67	4.49	4.38	4.2-4.3
A2	8.30	20	(←	49	→)	
A8	8.50	54	154	49	(23	→)

Table 4

It is possible to say that if the glycosidic dihedral angle (O1'C1'N9C8) were ca 180° then the interaction between A8 and A1' would be a lot larger than the interaction between A2 and A1'. Since these interactions are not very different from one another, perhaps the conformation about the glycosidic bond is not the same as that of the crystal structure (see Section 3.2.2). The interaction observed between A8 and A2' is comparatively large: on this basis it is possible to say that adenine adopts an *anti*

conformation with its sugar in NAD^+. A further interaction is seen between A8 and A3' which is of the same value as the total value of the interactions between A2 and A2', A3' and A4'.

Protons	Chemi-cal Shift (ppm)	N1'	N2'	N3'	N4'	N5'	N5"
N1'	6.18		69	35	57		
N2'	4.55			(120)		(120)	
N3'	4.47				159		206
N4'	4.60					(186)	201
N5'	4.39						
N5"	4.27						

Table 5

Protons	Chemical shift (ppm)	A1'	A2'	A3'	A4'	A5',A5"
A1'	6.05		94	32	64	3
A2'	4.67			255	82	15_{17}
A3'	4.49					206_{104}
A4'	4.38					53
A5',A5"	4.2-4.3					

Table 6

The extent with which the anomeric sugar protons (N1' and A1') interact with the other sugar protons is highlighted by spectrum 4e. This information further corroborates the assignments of the sugar protons. Thus, N1' interacts with the protons: N2', N3' and N4' (see Table 5) while A1' interacts with A2', A3', A4' and slightly with A5', A5" (see Table 6).

The extent with which the sugar protons interact with each other is depicted in Spectrum 4f. Here we can see that N2' interacts with N3' and N5' (Table 5), the interaction is most probably greater with N3' than N5' but because of the complicated nature of this region of the spectrum, it was not possible to differentiate between these two signals. Similarly, no interaction between N2' and N4' is indicated: this does not mean that that there is no interaction; rather, it was not possible to determine a 'meaningful' relative intensity. A large relative intensity was observed between N3' and N4' while an even larger interaction was seen between N3' and N5'. This phenomenon can be explained by supposing that the conformation of this ribose is such that N3' is *endo*. (Whether this is a twist or envelope conformation is not apparent). An unequal interaction is seen between N4' and the N5' and N5" protons which simply means that the N4' proton is not equidistant to the N5' and N5" protons.

The adenine ribose system (Table 6) appears to adopt a similar conformation to that of the nicotinamide ribose. Based upon the large value of the relative intensity observed for the interaction between A3' and the A5' and A5" protons it can be supposed that this ring is A3' *endo*. This result corroborates the earlier assertion that the two rings had similar conformations (this was based upon them having similar anomeric coupling constants; see earlier, Section 3.4.3).

An aspect of conformation that this technique allows us to explore is the proximity of the two bases to each other. It is seen that interactions occur between the adenine and

The ROESY Spectrum of NAD+ Showing the Anomeric Proton Interactions with the Other Sugar Protons

Spectrum 4e

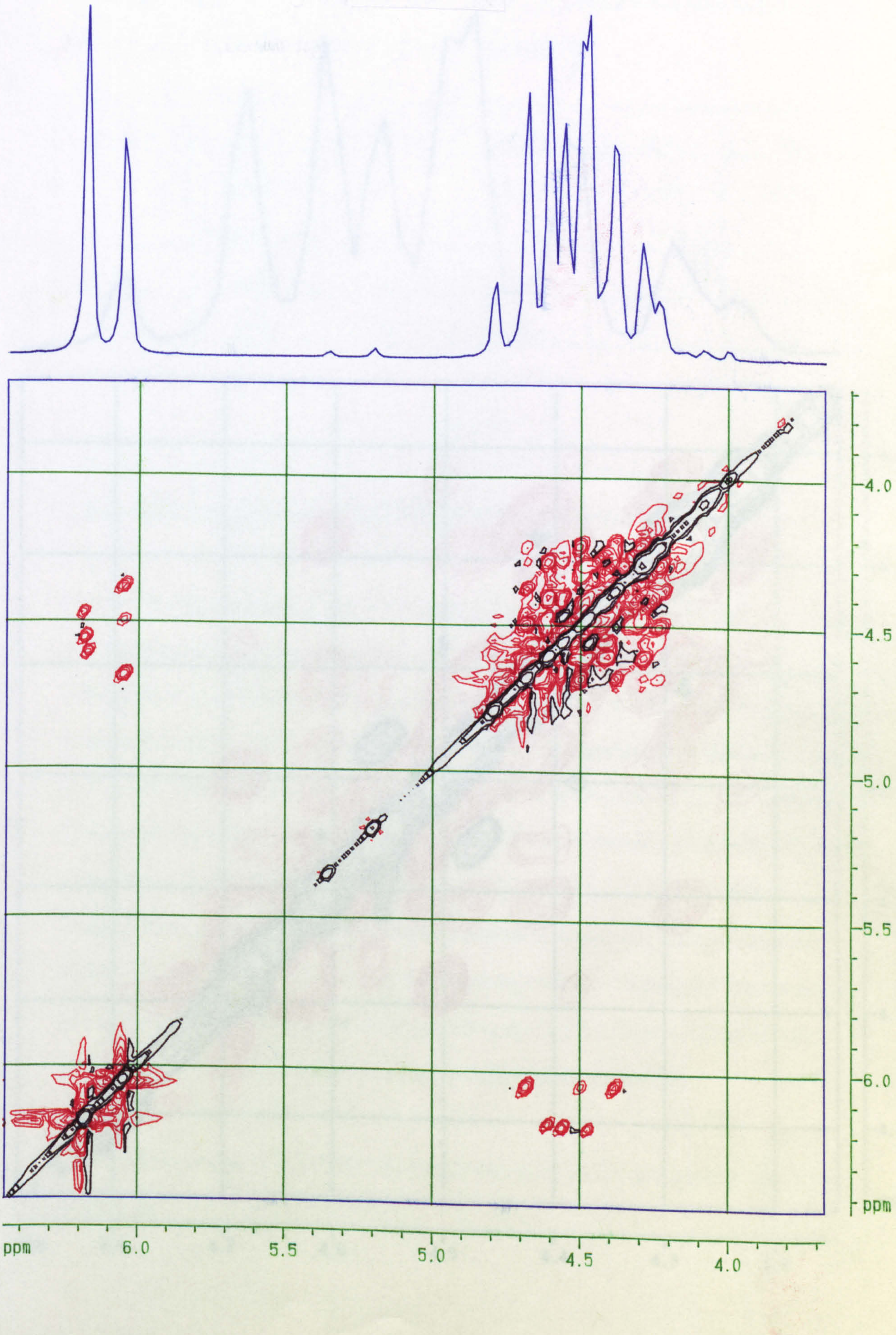

The ROESY Spectrum of NAD$^+$ Showing the Sugar Proton Interactions

Spectrum 4f

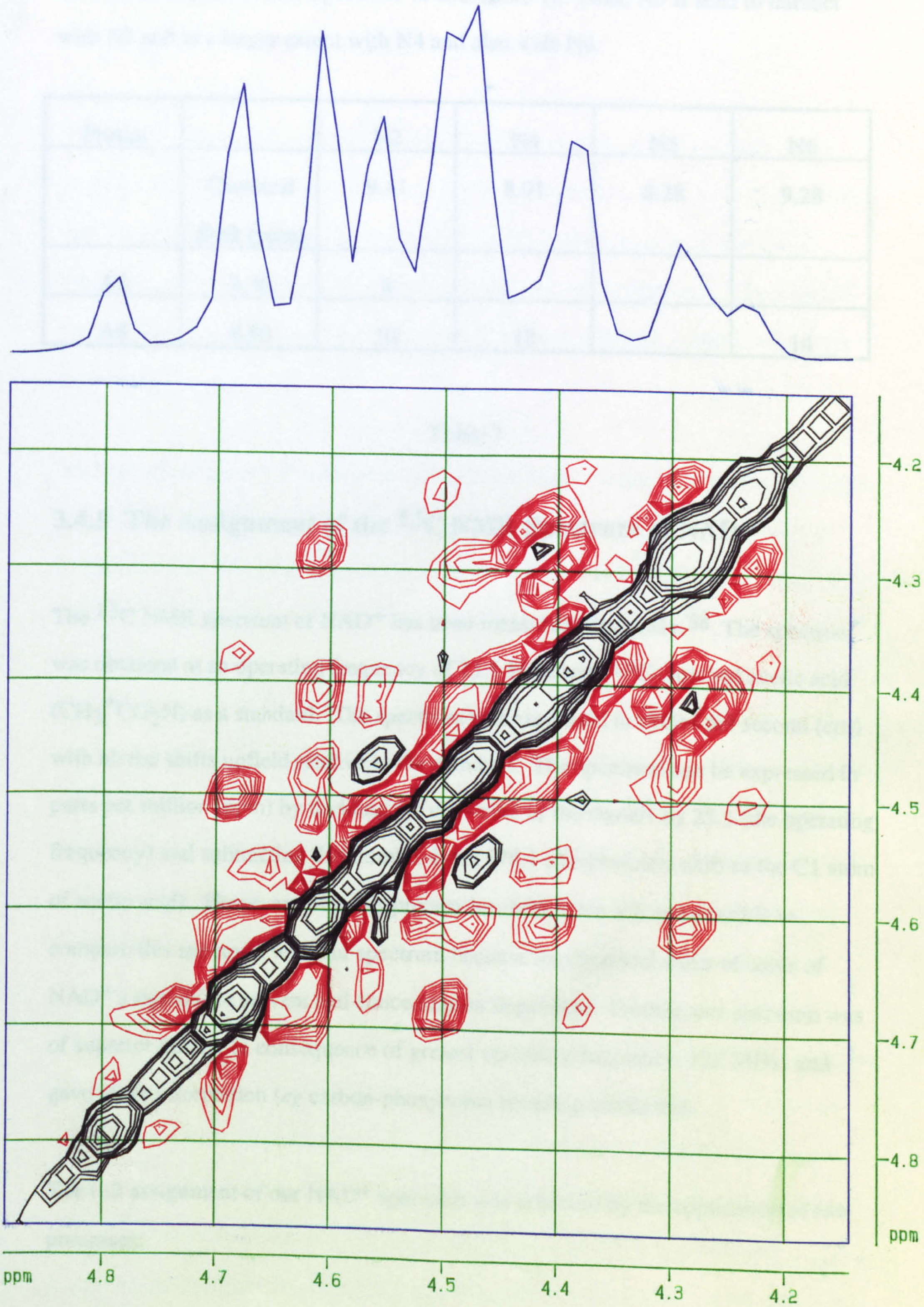

nicotinamide protons (see Spectrum 4b and Table 7). Thus, A8 is seen to interact with N2 and to a larger extent with N4 and also with N6.

Proton		N2	N4	N5	N6
	Chemical Shift (ppm)	9.41	8.91	8.28	9.28
A2	8.30	8			
A8	8.50	10	18		14

Table 7

3.4.5 The Assignment of the ^{13}C NMR Spectrum of NAD^+

The ^{13}C NMR spectrum of NAD^+ has been measured previously.[38] The spectrum was obtained at an operating frequency of 25.1 MHz with ^{13}C-enriched acetic acid ($CH_3{}^*CO_2H$) as a standard. The spectrum was expressed in cycles per second (cps) with all the shifts upfield relative to the standard. The spectrum can be expressed in parts per million (ppm) by dividing the cps value of the signals by 25.1 (the operating frequency) and subtracting this number from 178.1 (the chemical shift of the C1 atom of acetic acid). However, after this process has been done it is not possible to compare this spectrum with our spectrum because the chemical shifts of some of NAD^+'s signals are solvent and concentration dependent. Further, our spectrum was of superior quality (a consequence of greater operating frequency, 125 MHz) and gave more information (*eg* carbon-phosphorus coupling constants).

The full assignment of our NAD^+ spectrum was achieved by the application of two processes:

(i) Heteronuclear Shift Correlation (HSC)

(ii) Heteronuclear Selective Spin Decoupling

The carbon atoms of NAD^+ can be classified into two types: carbons with one or more protons attached to them and carbons with no protons attached to them. The HSC experiment correlates the chemical shift of a carbon atom with that of its attached proton(s). Since the ^1H NMR spectrum of NAD^+ has been fully assigned (see earlier) then any carbon with a proton attached to it can be assigned using this technique.

An HSC spectrum is a two dimensional spectrum with the one dimensional ^1H NMR spectrum of NAD^+ along one axis and the one dimensional ^{13}C NMR spectrum along the other. A coupling between a carbon and its attached proton is indicated by a peak at the intersection of the chemical shifts of the two signals.

The ^1H NMR signal that appears furthest downfield is N2 (δ 9.41) and is seen to correlate with the ^{13}C NMR signal at δ 142.41 (see Spectrum 5). In this manner the ^{13}C NMR signal at δ 142.41 is assigned to the N2 carbon. The next signal assigned was the one that correlated to the ^1H NMR signal of N6 (δ 9.28), this appeared at δ 145.08 and so was ascribed to the N6 carbon. In this manner all of the hydrogen-bearing carbons of NAD^+ were assigned (see Table 8).

All of the carbons thus described have a coupling constant, $^1J_{C\text{-}H}$, of between 140 to 220 Hz and appear as doublets in the ^1H coupled ^{13}C NMR spectrum. They may also have a larger range (normally $^2J_{C\text{-}H}$ or $^3J_{C\text{-}H}$) coupling which makes these signals appear as double multiplets. In this spectrum a feature of the carbon atoms that do not have an attached hydrogen is that they usually have a three bond coupling to at least one proton. It is therefore possible to determine exactly which proton is associated with which multiplet by the technique of selective spin decoupling.

The ^{13}C NMR Spectrum of NAD+

Spectrum 5

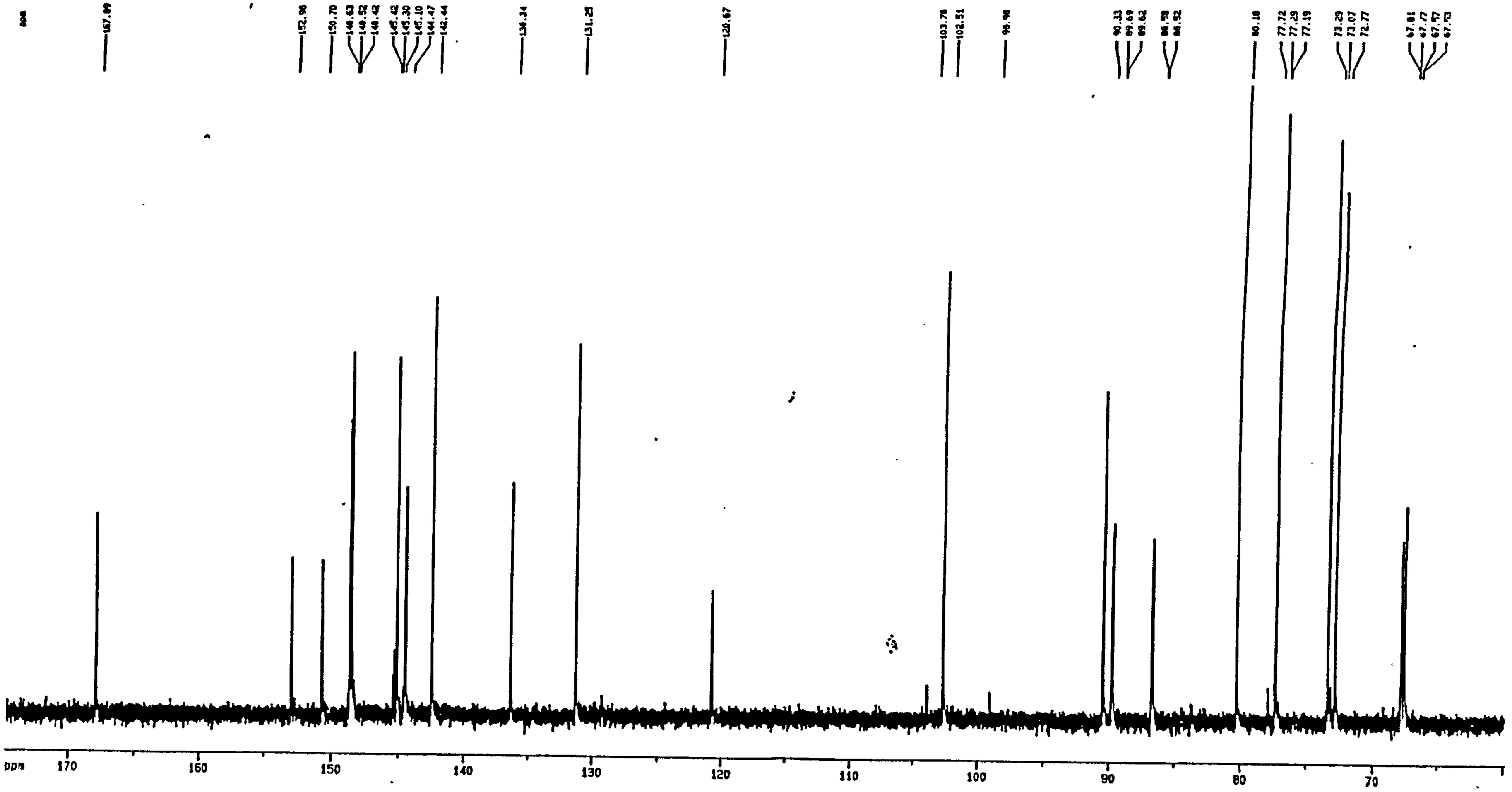

Normally ^{13}C NMR spectra are obtained under conditions of complete (broad band) proton decoupling and then consist of a set of singlets. In the absence of such decoupling these singlets appear as multiplets showing large splittings (^{1}J) and also smaller splittings (^{2}J or ^{3}J) which may not always be resolved. By the use of selective decoupling at appropriate power levels it is possible to remove the fine structure arising from coupling to a chosen proton, only providing that this has a sufficient chemical shift difference from other protons in the same molecule. This technique is of special value for assigning the longer range C-H couplings - particularly those of non-protonated carbons. In this manner it is possible to assign the remaining carbons.

The signal furthest downfield (δ 167.83) is almost certainly the carbonyl carbon of NAD^{+}. This appears as a triplet - or more correctly, a poorly resolved double doublet - in the proton-coupled ^{13}C NMR spectrum. When the proton-coupled ^{13}C NMR spectrum is recorded with simultaneous low power irradiation of the N2 proton the carbonyl carbon multiplet signal collapses to a doublet. Irradiation at other proton frequencies have no effect. Similarly, when this process is repeated with irradiation of the N4 proton, the signal appears as a doublet. In this manner the assignment of this signal to the carbonyl carbon was confirmed (see Table 8).

Irradiation of the A2 proton (δ 8.30) causes the doublet centred at δ 152.18 to collapse to a singlet. This signal was assigned to the A6 carbon. Although the A4 carbon has a $^{3}J_{C\text{-}H}$ coupling to A2 this carbon is discounted since it also has the potential to couple to the A8 and A1' protons which would lead to a much more complicated signal than a doublet.

The signal at δ 150.18 was assigned to the carbon at A4. In the proton-coupled ^{13}C NMR spectrum this signal appeared as a double double doublet. When the A2 proton

was selectively spin decoupled from this signal the largest coupling disappeared to leave a double doublet. The mid coupling disappeared when the A8 proton was irradiated, while the decoupling of the A1' proton removed the smallest coupling from this multiplet.

The remaining carbons to be assigned are N3 and A5. The N3 carbon (δ 136.30) was found to have a $^{3}J_{C\text{-}H}$ coupling to the N5 proton whilst the A5 carbon (δ 120.62) was found to be coupled to the A8 proton.

A feature of our spectrum, that was not apparent from the earlier workers determination, was the presence of doublets due to carbon-phosphorus coupling. A value of 9 Hz is seen for the vicinal coupling between each of the C4'-P nuclei; the values of the geminal coupling constants are 4.4 Hz for the A5'-P nuclei and 4.7 Hz for the N5'-P nuclei. (A larger vicinal than geminal coupling constant is consistent with observations on other nucleotides).[39]

The geminal coupling constant is consistent with values obtained for other nucleotides and alkyl phosphate esters.[40] The vicinal coupling constant is consistent with a *trans* arrangement within the POC5'C4' parts of the molecule.[41,42,43]

The dihedral angle can be calculated approximately within the POC5'C4' if the parameters A, B and C of the Karplus equation (Equation 1), for these elements in this type of system, are known.

$$J = A.\cos^2\theta + B.\cos\theta + C \qquad \text{Equation 1}$$

From studies of the angle POC3'C4' in selected cyclic 3',5' mononucleotides these parameters have been determined to be A = 6.4, B = -1.3 and C = 1.2 and these parameters have been used to determine this angle in other similar 3',5'

mononucleotides and 3' → 5' oligonucleotides. An extension of this approach to the angle POC3'C2' required an adjustment of parameter C to zero owing to the electronegativity of the base.[44] The angle POC5'C4' has apparently not been studied in this way but a similar Karplus equation with essentially similar parameters will apply. Aplication of this equation to our system yields θ close to 0° or 180°. The solution with θ = 0 for each dihedral angle is not considered to be a reasonable reflection of the conformation of NAD^+, since there would be too many steric interactions between atoms within the molecule. It is much more plausible to have θ = 180° which means that the steric interactions would be minimized, if not totally negated.

This NMR spectroscopic work suggest that in solution NAD^+:

(i) has its bases *anti*

(ii) has C3' *endo* sugars

(iii) has a phosphate group fully extended from the O5' atoms

(iv) exists in a small proportion in a folded conformation

δ_C ppm	Assignment	$^1J_{C-H}$ /Hz	$^3J_{C-H}$ /Hz
167.83	C=O		CO/N2 = CO/N4; 3.6, 3.6
152.18	A6		A6/A2; 7.6
150.58	A4		A2/A4, A4/A8, A4/A1'; 12.8, 5.5, 2.1
148.49	N4	172	N4/N2 = N4/N6; 5.8
147.59	A2	215	
145.08	N6	199	multiplet
144.76	A8	221	A8/A1'; 4.3
142.41	N2	193	multiplet
136.30	N3		N3/N5; 7.3
131.22	N5	178	N4/N6; 3.6
120.62	A5		A5/A8; 11.9
102.45	N1'	177	multiplet
90.44	A1'	168	"
89.59	N4'	144	"
86.53	A4'	170	"
80.15	N2'	152	"
77.26	A2'	150	"
73.24	N3'	154.5	"
72.70	A3'	152	"
67.76	A5'	146.8, 148.3	"
67.56	N5'	152.4, 146.6	"

Table 8

3.5 The Assignment of the 500 MHz ^{1}H and 125 MHz ^{13}C NMR Spectra of NADH

The complete assignment of the ^{1}H and ^{13}C NMR spectra of NAD^{+} led to the expectation that, by using similar techniques, the full assignment of nicotinamide adenine dinucleotide hydride (NADH) would be feasible. As well as using the techniques that were employed to assign NAD^{+}, an additional NMR experiment was used to assign the reduced NADH. This experiment is a two dimensional heteronuclear shift correlation (HSC or HETCOR, see earlier) process known as a C-H/HOHAHA experiment. This is essentially an extension of the normal HETCOR experiment in which a given carbon is correlated not only with its directly bound proton(s), but also with those protons that are themselves coupled to the directly bound one. Thus, if the chemical shift of a proton is known, the chemical shift of the carbon it is attached to can be determined from the HETCOR experiment. Using this chemical shift it is then possible to determine, from the C-H/HOHAHA spectrum, the chemical shift of the proton it is attached to and any chemical shifts of protons coupled to the previous proton. This process can be repeated using the new proton

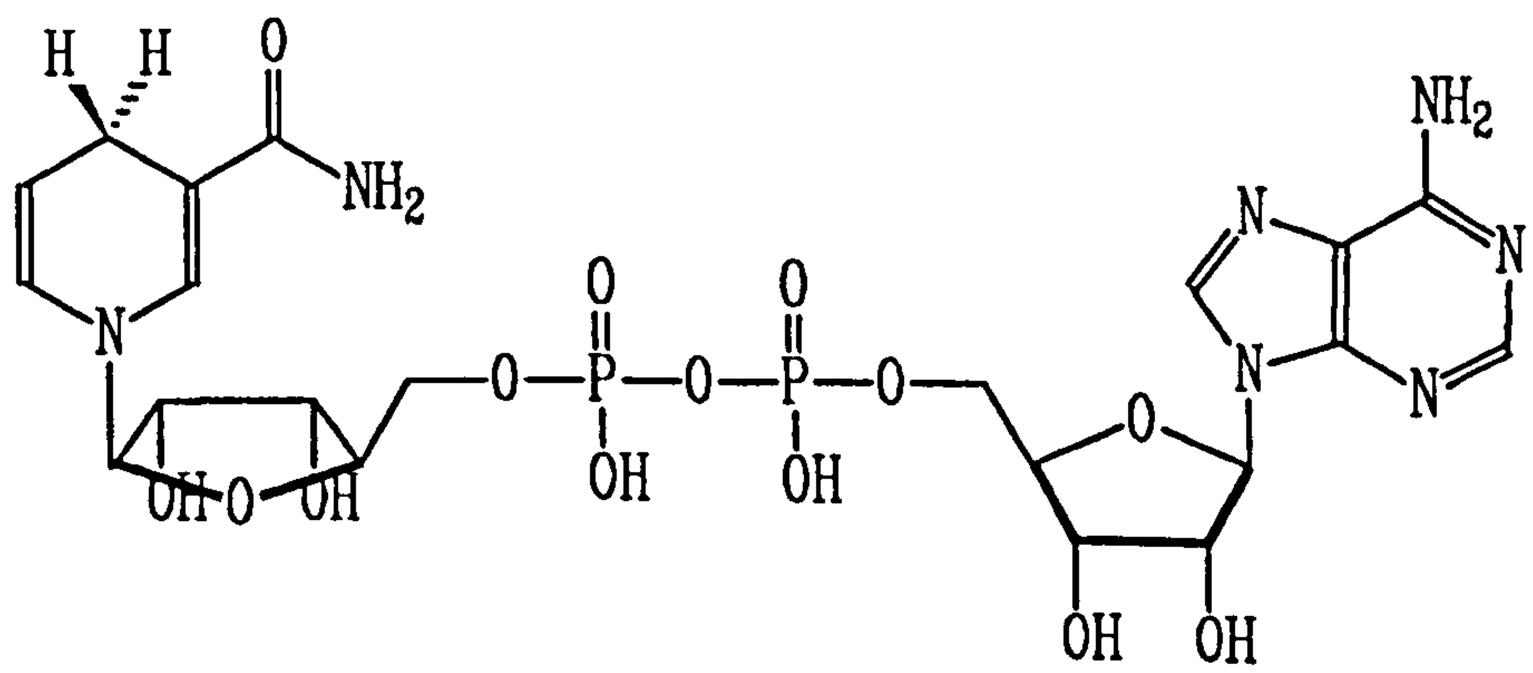

Nicotinamide Adenine Dinucleotide Hydride (NADH)

Figure 15a

chemical shifts to assign the chemical shifts of the carbons they are attached to and hence the chemical shifts of any coupled protons. It effectively provides a means of tracing out the carbon skeleton in a sequential manner without recourse to doubly labelled species.

NADH consists of two nucleotides (see Figure 15a) which can be considered as individual entities in order to assign the proton spectrum. The assignment began by comparing the spectra of similar molecules *eg* NAD^+ (see Spectrum 1), adenosine, *N*-benzyl-1,4-dihydronicotinamide (63) and *N*-methyl-1,4-dihydronicotinamide (64, see Spectrum 7). On this basis assignments of A8, A2 and A1' were made (see Table 8a for proton chemical shifts) and confirmed by a ROESY spectrum which showed correlations of A8 with A1' and of A8 with resonances in the sugar region (δ 4 - 5). The chemical shift of A2' was obtained from a COSY spectrum of NADH, since it was coupled to A1'. The chemical shift of the carbon attached to the proton at A2' was obtained from the HETCOR spectrum (Spectrum 5b, see Table 8b for carbon-13 chemical shifts). Using this chemical shift, from the C-H/HOHAHA spectrum (Spectrum 5c) the chemical shift of the proton A3' was obtained. This process was repeated to give the chemical shift of A4' and an indication of where the A5',5" signals were to be found.

The chemical shifts of the nicotinamide-hydride part of the molecule were also initially assigned by comparison with previously assigned spectra (see earlier). Thus, N2, Nic4',4", N5 and N6 were assigned (Nic4',4" represent the two diastereotopic protons at N4; N is now referred to as Nic in order to avoid confusion with the sugar position N4'). A ROESY spectrum placed N1' at δ 4.20 but the other protons about this part of the molecule were more difficult to assign. It was found that the carbon-13 chemical shifts (see Spectrum 5d) of N4',A4' and N5',A5' appeared in similar positions (and this was further confirmed by their phosphorus-31 coupling). Since the adenosine half of the molecule had been assigned the N4' and N5' carbons were

The ^{1}H NMR Spectrum of NADH Spectrum 5a

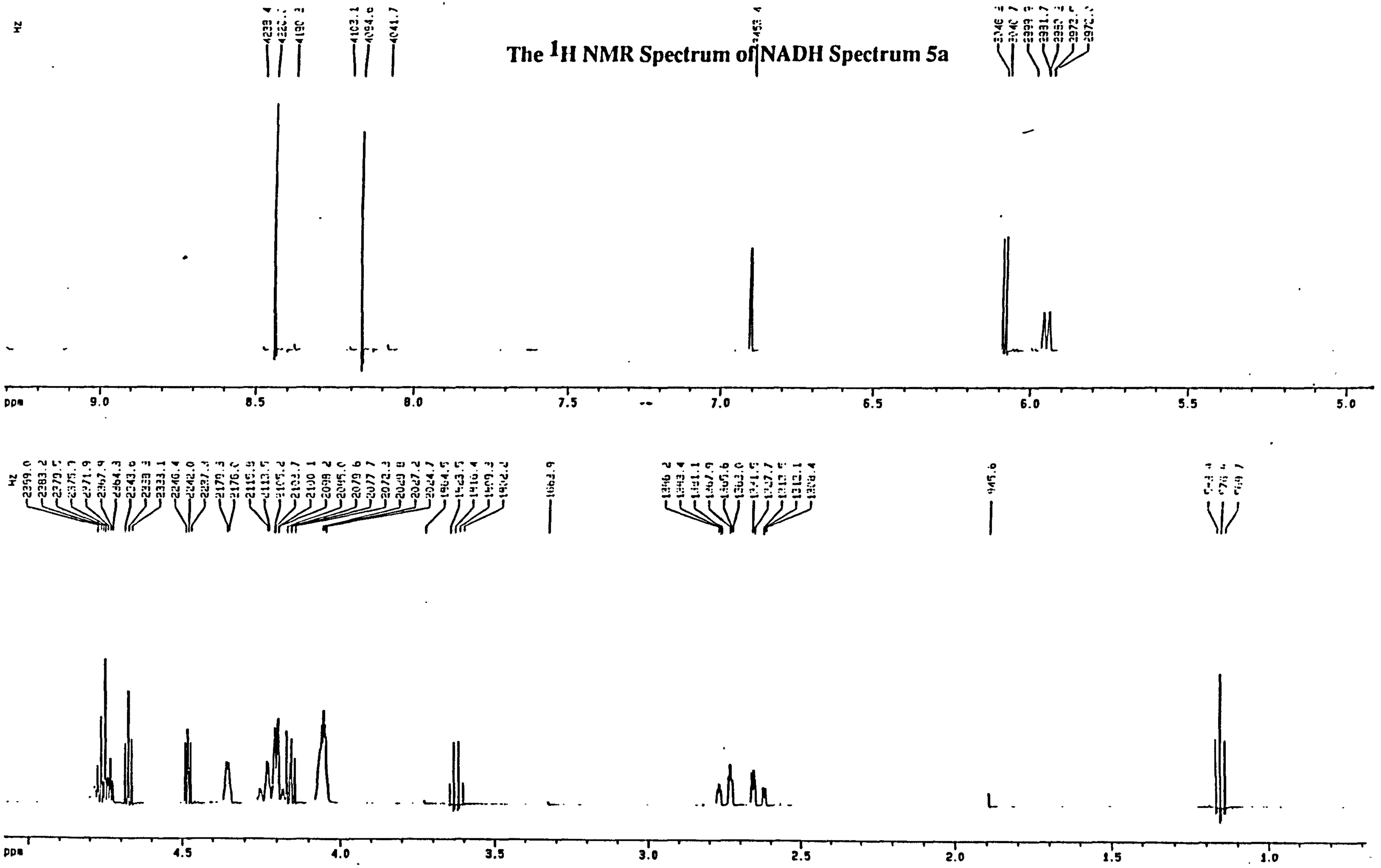

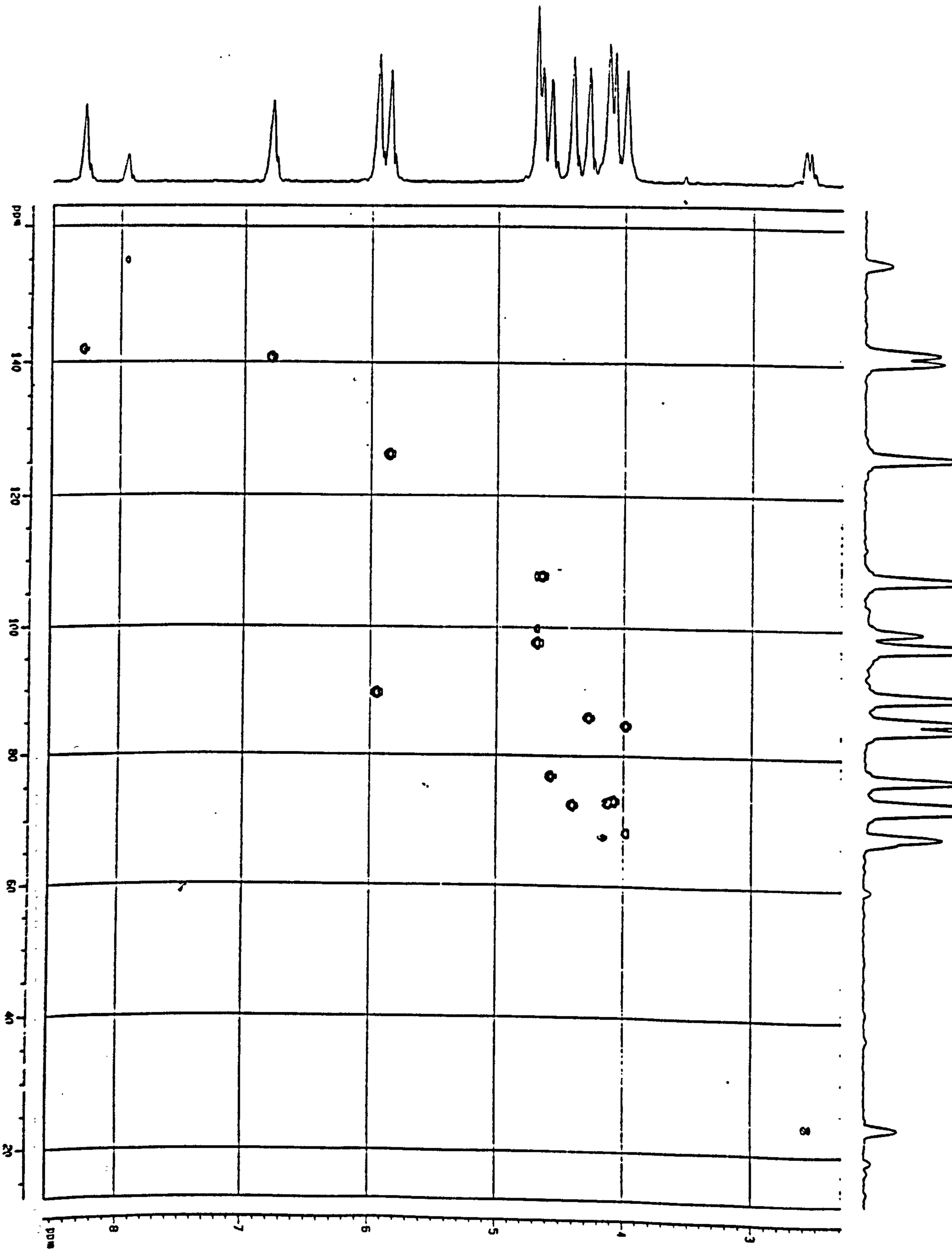

The HETCOR Spectrum of NADH

Spectrum 5b

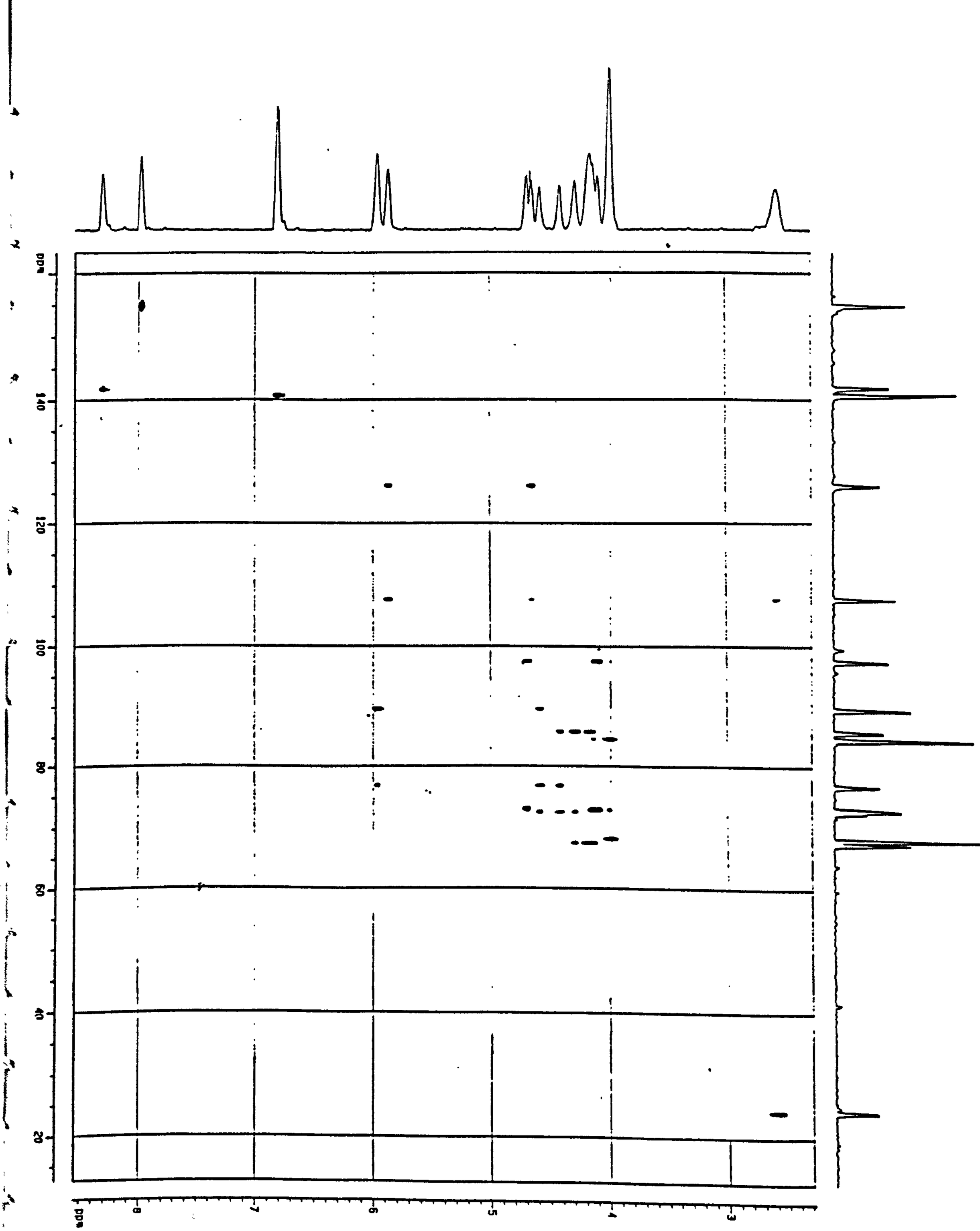

The C-H/HOHAHA Spectrum of NADH

Spectrum 5c

assigned by default. Inspection of the HETCOR spectrum gave the chemical shifts of the N4' and N5',5" protons which were found to have very similar chemical shifts and small coupling constants. These latter factors meant that the asssignment of N3' and N2' by the techniques described earlier was not possible. Thus, of the remaining protons it is possible to say in which region they may be found but not to give their exact chemical shifts. For example, A5',5", N3' and N2' appear in the region δ 4.10 - 4.30, with one of these protons appearing at the same position as N5.

Important features of the ^1H NMR spectrum of NADH are the chemical shifts and

δ_H	Integral	Multiplicity	Coupling Constant	Assignment
8.45	1H	s	-	A8
8.19	1H	s	-	A2
6.91	1H	s	-	N2
6.09	1H	d	5.5	A1'
5.92	1H	dd	1.5, 8.2	N6
4.7 - 4.8	2.5H	m	-	N5*
4.68	1H	t	5.2	A2'
4.49	1H	t	4.4	A3'
4.45	1H	m	-	A4'
4.12 - 4.30	4H	m	-	A5',5",N3',N2',N1'
4.00 - 4.10	3H	m	-	N4',N5',5"
2.75	1H	dd	17.8, 2.9, 2.4	Nic4'
2.65	1H	dd	17.8, 3.8, 1.3	Nic4"

Table 8a

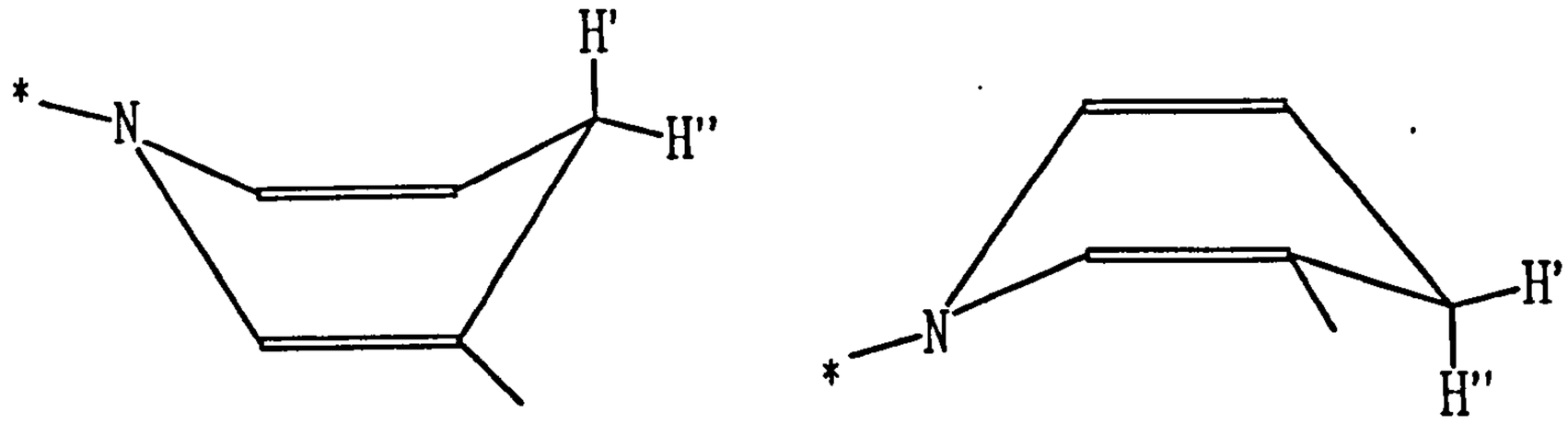

A B

The Conformations of NADH

Figure 15b

coupling constants of the protons Nic4',4". Since NADH is a chiral molecule, Nic4' and Nic4" are diastereotopic and hence are expected to have different chemical shifts. If the reduced nicotinamide ring is not planar, two boat like conformations are possible in which the sp^3 carbon N4 can be regarded as being "above" the plane of the carbons 2, 3, 5 and 6 in one form and "below" it in the other (Forms A and B, see Figure 15b) with a dynamic equilibrium existing between the two forms. In one conformation Nic4' occupies a pseudoaxial position and Nic4" occupies a pseudoequatorial position, while in the other conformation the situation is reversed. Suppose that when Nic4' occupies a pseudoaxial position (Form A) it has a chemical shift of δ_a and when in the pseudoequatorial position (Form B) it has a chemical shift of $\delta_{e'}$ and so the chemical shift of Nic4' ($\delta_{H'}$) is given in equation 2.

$$\delta_{H'} = 1/2(\delta_a + \delta_{e'}) \qquad \text{equation 2}$$

$$\delta_{H''} = 1/2(\delta_e + \delta_{a'}) \qquad \text{equation 3}$$

Since the reverse is true for Nic4" its chemical shift ($\delta_{H"}$) will be given by equation 3. The protons Nic4' and Nic4" are coupled to the proton N5 by a coupling constant (^3J) whose value will be dependent upon whether the protons (Nic4',4") were in a pseudoaxial ($^3J_{ax}$) or pseudoequatorial ($^3J_{eq}$) position.

Thus, assuming $^3J_{ax}(A) = {}^3J_{ax}(B)$

and $^3J_{eq}(A) = {}^3J_{eq}(B)$

For equal populations of the two forms A and B, equations 4 and 5 would apply.

$$^3J(H') = 1/2(J_{ax} + J_{eq}) \qquad \text{equation 4}$$

$$^3J(H") = 1/2(J_{ax} + J_{eq}) \qquad \text{equation 5}$$

However, in fact $^3J(H') \neq {}^3J(H")$ and so it follows that the populations of A and B are not equal. The ^3J coupling constants of the protons are: δ 2.65, $^3J = 3.8$, and δ 2.75, $^3J = 2.9$, Hz (with ^4J couplings of 1.3 and 2.4 Hz, respectively). The average of the two ^3J coupling constants (3.35 Hz) was found to be the same as the ^3J coupling constant in *N*-benzyl-1,4-dihydronicotinamide, while the average of the ^4J coupling constants is the same as the ^4J coupling constant in *N*-benzyl-1,4-dihydronicotinamide.

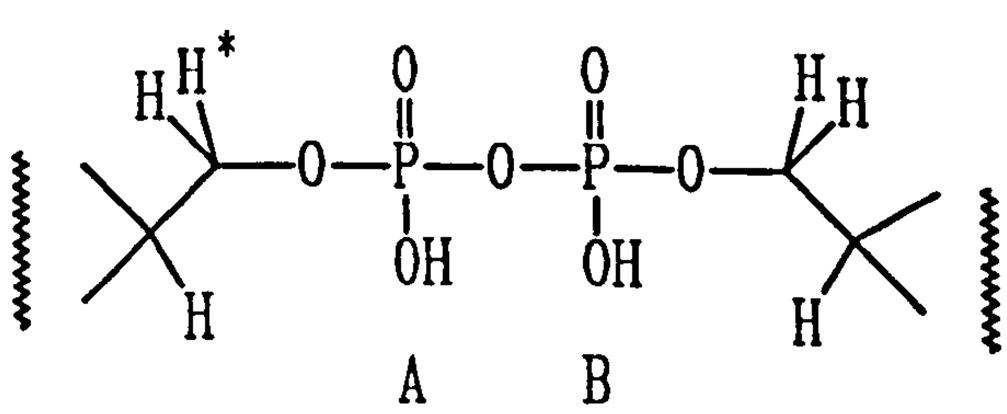

The Dinucleotide Bridge of NADH

Figure 15c

A consequence of the reduced nicotinamide ring 'flipping' is that this part of the molecule becomes chiral. Since the sugar part of the molecule is already chiral the boat conformations A and B are diastereoisomers. As diastereoisomers have different physical properties from one another, it is expected that one of the diastereoisomers A or B is more stable than the other. This phenomenon may explain the difference in populations described earlier. Recent studies have described crystal structures of simple *N*-alkyl-1,4-dihydronicotinamides which show that their dihydropyridine rings are planar.[45] However, the solution conformation may be different and in any case a planar dihydropyridine ring for NADH would not explain the NMR data. As discussed on page 68 a planar dihydropyridine ring would lead to identical multiplicities for the two C4 protons hence the NMR data presented gives conclusive evidence for the predominance of one diastereotopic conformation of NADH.

The protons in NADH 'associated' with phosphorus (*ie* the ones close to the dinucleotide bridge N4',5'5" and A4',5',5", see Figure 15c) exhibit a special coupling phenomenon. For example, for the proton marked '*' in Figure 15c, a doublet would naïvely be expected due to the coupling $J(P_AH)$ since presumably $J(P_BH) \approx 0$. The coupling between the two phosphorus atoms is expected to be approximately 10 Hz and their chemical shifts are (fortuitously) equal. Therefore, the system must be regarded as AXX' where H = A, P_A = X and P_B = X'. If the chemical shift difference between X and X' is zero then instead of a doublet, a triplet is seen which has its outer lines separated by $J(HP_A) + J(HP_B)$ [= $J(HP_A)$ in this case]. This effect is sometimes 'called' the virtual coupling[46] of P_B to H.

The ^{13}C NMR spectrum (Spectrum 5d) was partially assigned (see Table 8b) using similar techniques to the assignment of NAD^+.

δ_C	Multiplicity	Assignment
174.83	q	C=O
157.53	q	
154.93	d	A2
150.93	q	A
141.80	d	A8
140.67	d	N
126.22	d	N6
120.71	q	A
107.69	d	N5
102.30	q	
97.53	d	
89.58	d	A1'
85.89	d	A4'
84.64	d	N4'
76.92	d	A2'
73.19	d	
72.91	d	
72.58	d	A3'
24.28	t	N4

Table 8b

The ^{13}C NMR Spectrum of NADH

Spectrum 5d

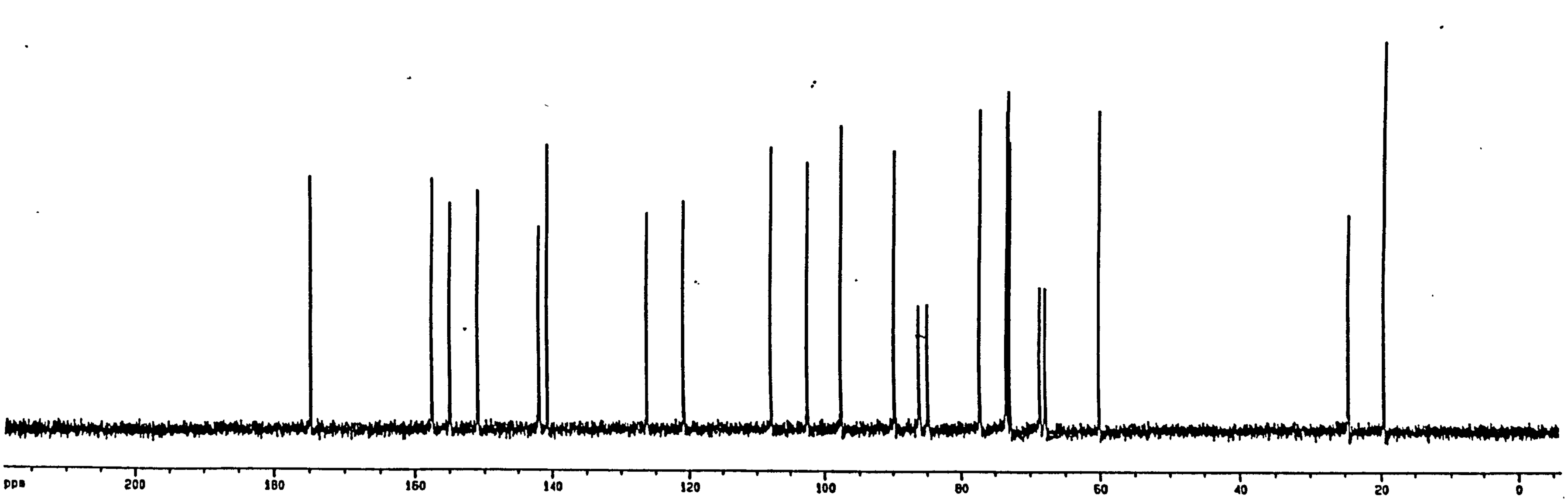

Chapter 4

4.1 Inhibitors at Newcastle

Below are described two classes of inhibitor: those based upon the cofactor NAD^+ and those based upon literature inhibitors.

Inhibitors based upon the cofactor NAD^+.

4.1.1 Adenine Alkyl Benzamides

These compounds were direct analogues of NAD^+. The differences incorporated were that benzamide replaced nicotinamide and an alkyl chain (whose length was varied) replaced the dinucleotide linkage with adenine.

These compounds were prepared by converting 3-hydroxy benzamide (29) into 3-(bromoalkoxy)benzamides which were further transformed to 3-(purinealkoxy)benzamides. From the latter compounds the 3-(adeninealkoxy)benzamides were produced (see Scheme 6).

4.1.2 The Preparation of 3-Hydroxybenzamide (29)

The title compound was prepared from commercially available 3-hydroxybenzoic acid (30). Our strategy was to protect the hydroxyl group and then activate the acid part of the molecule toward nucleophilic attack. This was followed by the formation of the amide and finally the removal of the protecting group to form the title compound.

4.1.2.1 The Mixed Anhydride Method[47,48]

In this preparation 3-hydroxybenzoic acid (**30**) was treated with ethyl chloroformate (**31**), which serves the dual purpose of protecting (deactivating) the hydroxyl group and activating the acidic part of the molecule by forming a mixed acid anhydride intermediate (**32**). This was isolated in 64 % yield. The ^{1}H NMR spectrum of this molecule showed two ethyl groups of slightly differing chemical shift (200 MHz d_6-DMSO; δ 1.30 (3H, t, C*H*$_3$), 1.34 (3H, t, C*H*$_3$), 4.32 (2H, q, C*H*$_2$), 4.39 (2H, q, C*H*$_2$)) and the aromatic signals of a *meta* substituted benzene ring (δ 7.50 (1H, d,*H*4), 7.57 (1H, dd, *H*5), 7.90 (1H, s, *H*2), 7.98 (1H, d, *H*6)). This intermediate (**32**) was treated with liquid ammonia to form the amide and remove the protecting group from the hydroxyl part of the molecule (see Scheme 4)

Unfortunately 3-hydroxybenzamide (**29**) was isolated in only 5 % yield. Another problem with this procedure was the formation (and removal) of *O*-ethyl carbamate (**7**) a suspected carcinogen.[49,50]

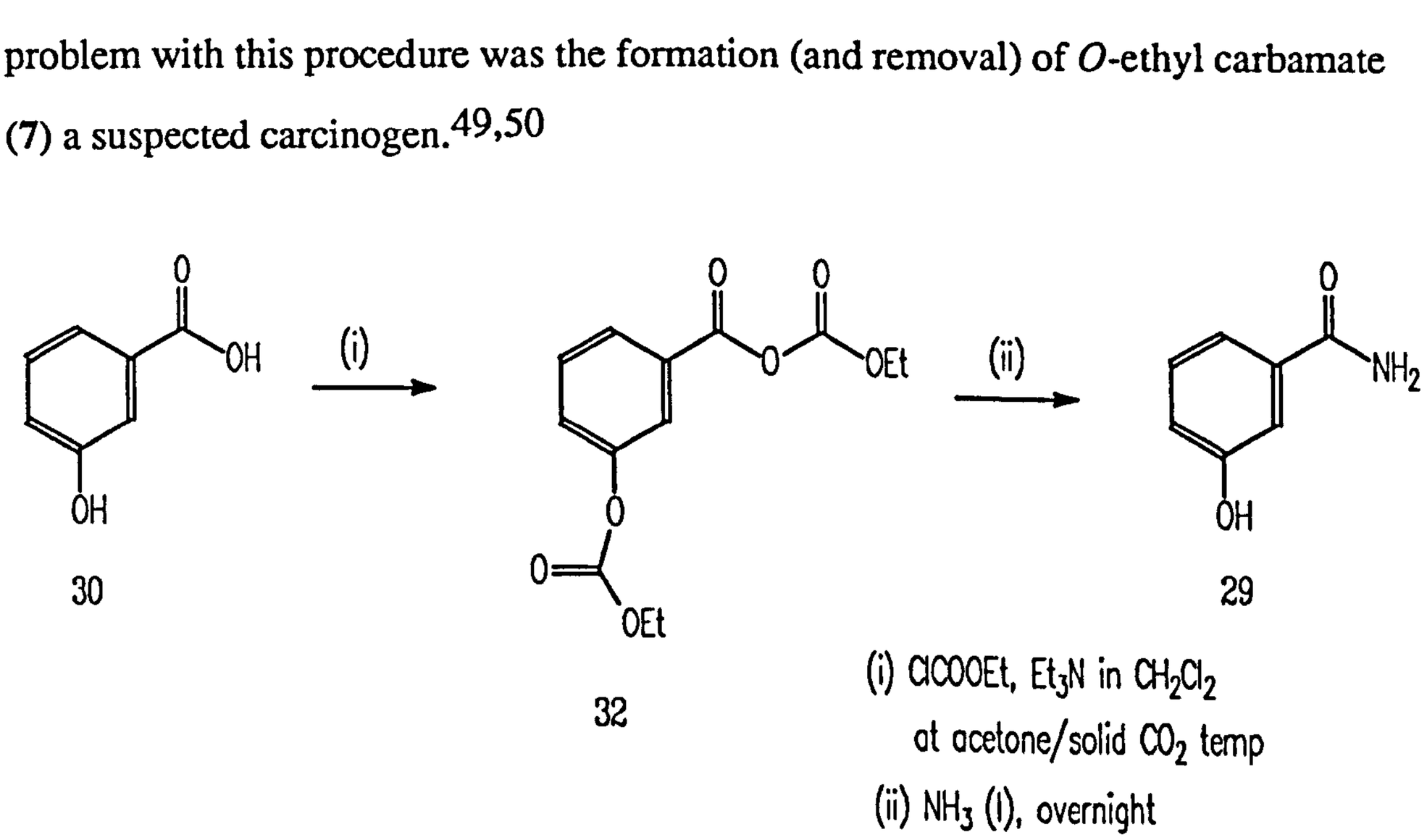

The Mixed Anhydride Preparation of 3-Hydroxybenzamide

Scheme 4

4.1.2.2 The Acetate/Acid Chloride Method[51]

In this technique the hydroxyl of 3-hydroxybenzoic acid (**30**) was protected (deactivated) as its acetate (**33**) which was formed in 92 % yield (the ^{1}H NMR of this compound showed the presence of the acetate signal at δ 2.39). The acid functional group was converted into the acid chloride (**34**) by heating with thionyl chloride under refluxing conditions. The amide was formed by reaction of the isolated acid chloride with aqueous ammonia solution, which also removed the acetate protecting group. This procedure conveniently produced 3-hydroxybenzamide (**29**) in *ca* 70 % overall yield (see Scheme 5).

4.1.3 The Preparation of 3-(Bromoalkyloxy)benzamides

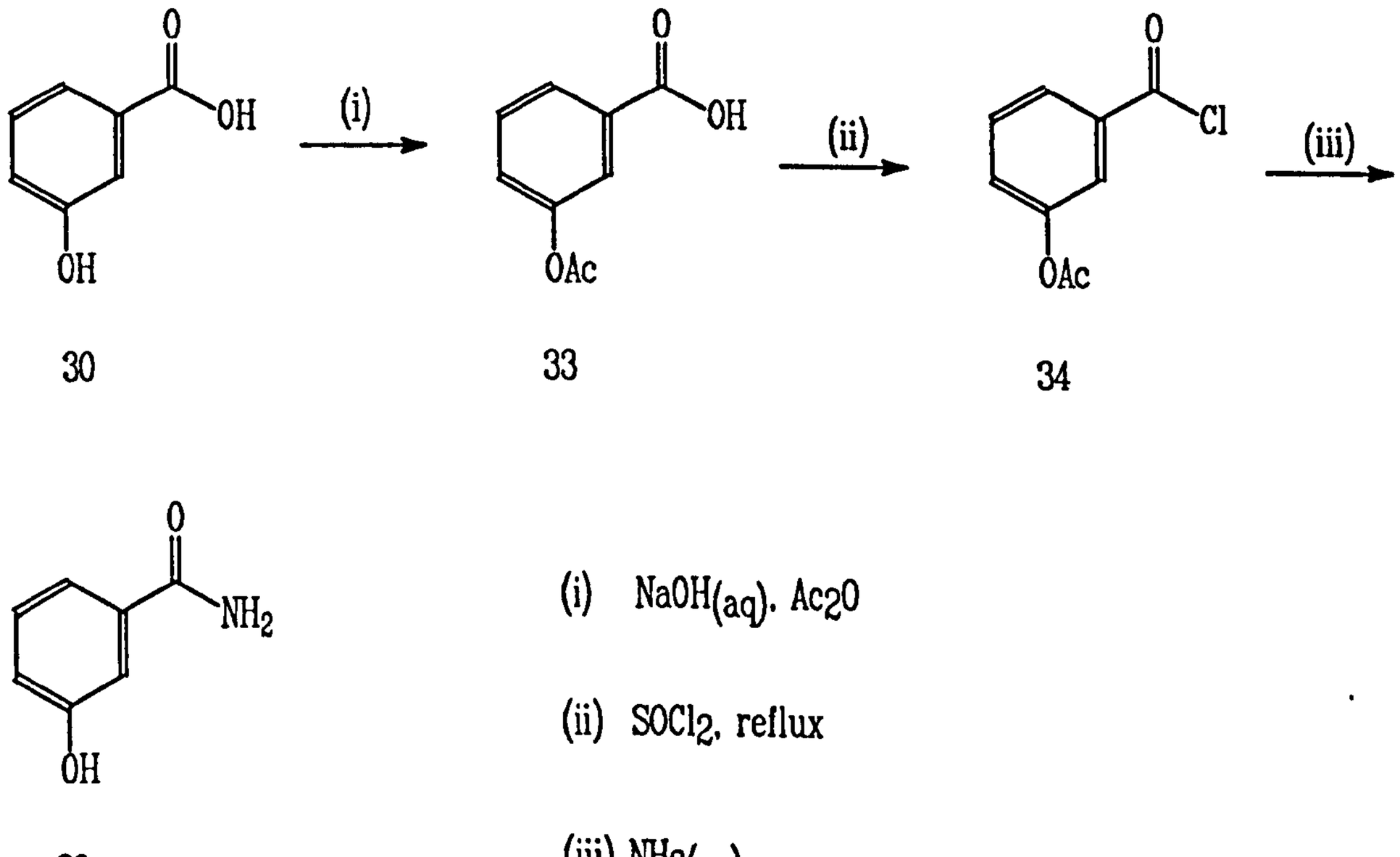

29

The Acetate/Acid Chloride Preparation of 3-Hydroxybenzamide

Scheme 5

The 3-(bromoalkyloxy)benzamides were prepared by refluxing a dibromo alkane with 3-hydroxybenzamide (**29**) in the presence of potassium carbonate. The reactions were followed by TLC and work up consisted of evaporation of acetonitrile, flash chromatography and recrystallisation. To suppress reaction at both ends of the alkyl chain, the dibromoalkane was used in excess (two to one mole ratio).

The ^{1}H NMR spectra of these compounds corroborated their proposed structures. Generally, the spectra had a region that was similar to the spectrum of 3-hydroxybenzamide (**29**), displaying the amide protons and a pattern of signals in the aromatic region indicative of a 1,3-disubstituted benzene. The bromoalkyl proton signals appeared, as expected, in the upfield region of the spectrum. Common to all the spectra were two triplets which were indicative of the methylene signals α to the electronegative substituents oxygen and bromine. The signal furthest downfield represented the methylene protons α to the oxygen (δ 4.15) whilst the α bromomethylene triplet appeared slightly further upfield (δ 3.64). The methylene protons β to the electronegative substituents were represented by a broad multiplet (δ 1.90 ppm) which was common to all the spectra. The remaining signals in the alkyl chain of 3-(5-bromopentyloxy)benzamide (**35**) appeared as a multiplet (δ 1.60) which was slightly downfield with respect to the alkyl envelope of the 8-bromo (**36**) and 12-bromo (**37**) compounds (δ 1.40).

The ^{13}C NMR spectra become increasingly difficult to assign as the number of signals increases in the upfield region. However, they all have the common signals of the carbonyl carbon, the aromatic signals and the signals which represent carbons α to the electronegative atoms oxygen and bromine in the alkyl chain.

4.1.3.1 Potency of the 3-(Bromoalkyloxy)benzamides

Although these compounds were synthesised with a view to using them to prepare the 3-(adenine-9-alkyloxy)benzamides and were not expected to show any inhibition against PARP, their potency was assessed. A serendipitous result was not expected rather, empirical data that could be rationalised was sought.

Compound No	Chain Length n	% Inhibition 10 μM	30 μM	100 μM
35	5	ND	57, 52	90, 72
36	8	0, 5	ND	Insoluble
37	12	0,0	0,4	Insoluble

Table 9

3-(5-Bromopentyloxy)benzamide (**35**) did exhibit some inhibition against PARP, whilst the 8-bromo and 12-bromo compounds (**36** and **37**) were found to be inactive. The lack of potency of the latter two compounds was largely due to their aqueous insolubility but even at low concentrations there was very little, if any, inhibition against PARP. It could be rationalised that the 5-bromo compound (**35**) behaves in a similar manner to inhibitors such as 3-methoxybenzamide (**4**). In this case the 5-bromoalkyl chain is not long enough to interfere any binding sites within the enzyme. If this is true, then the 8-bromo and 12-bromo compounds (**36** and **37**), as well as being sparingly soluble, may have their enzyme-substrate binding capacity disrupted by their bromoalkyl substituents. If this rationalisation is correct then attempts to increase the water solubility of these compounds, and hence inhibition against PARP, would be fruitless.

4.1.4 The Preparation of the 3-(Purinealkyloxy)benzamides

These compounds were prepared from their corresponding 3-(bromoalkyloxy)benzamides by stirring them with 6-chloropurine and potassium carbonate in DMF. The reactions were followed by TLC and work up consisted of removing the solvent under vacuum, followed by flash chromatography to give a mixture of the *N*7 and *N*9 isomers of the chloropurine. This mixture was converted to the corresponding adenine mixture by reaction with ammonia (high pressure, 50°C, overnight). This procedure produced a mixture of isomers that was separable by flash chromatography.

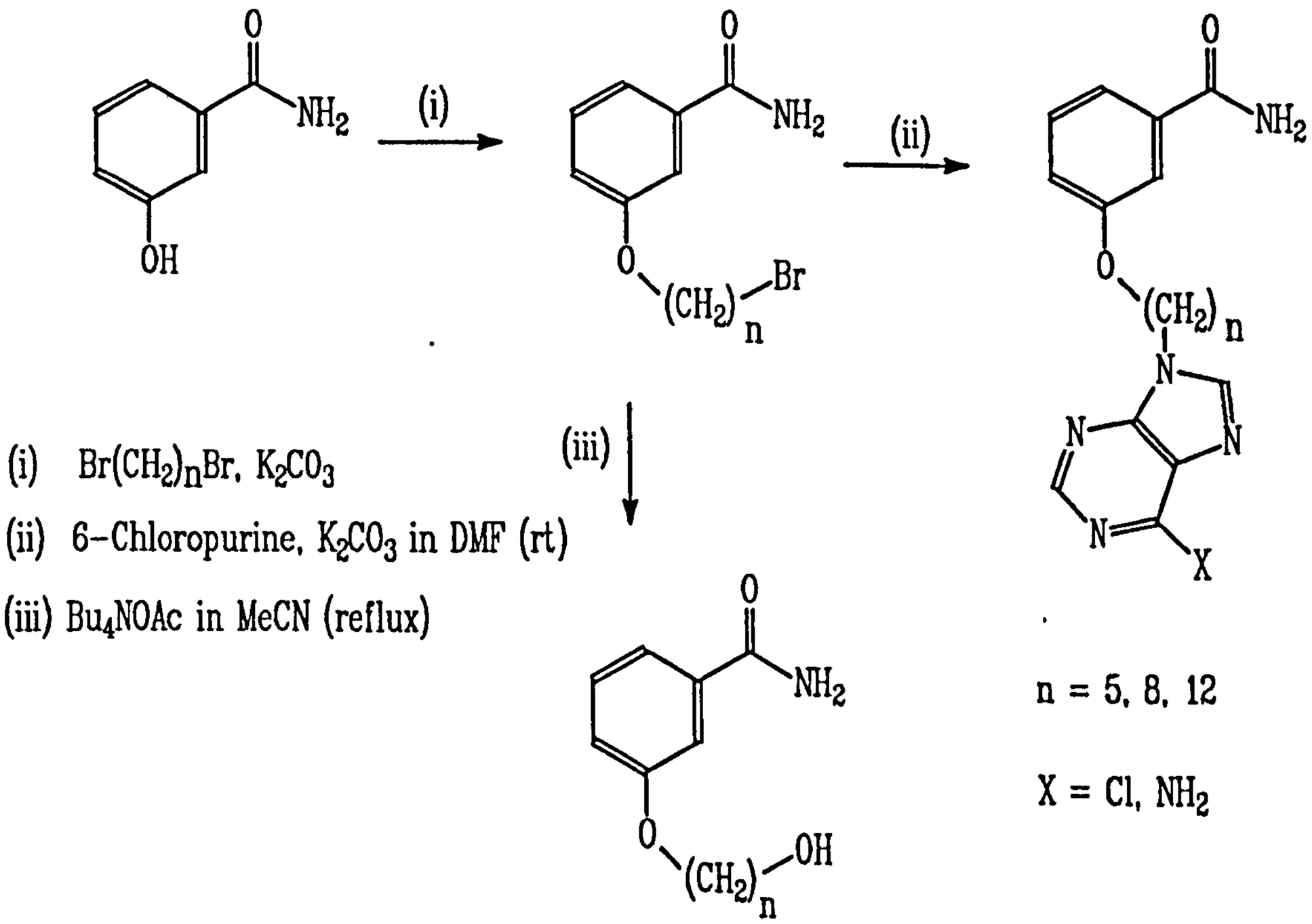

The Preparation of 3-(Purinealkyloxy)benzamides

Scheme 6

The ^1H NMR spectra of these two classes of compounds were very similar to the spectra of the 3-(bromoalkoxy)benzamides (see earlier). The slight differences were the presence of the purine signals appearing in the downfield region of the spectra (further downfield than the aromatic benzene protons) and a slight downfield shift of the two triplets which represent the methylene protons α to the aromatic oxygen and nitrogen atoms at the ends of the alkyl chains.

4.1.4.1 Potency of the 3-(Purine-9-alkyloxy)benzamides

Of this class of six compounds, three show some inhibition against PARP: 3-(5-(6-chloropurin-9-yl)pentyloxy)benzamide (38), 3-(5-(6-aminopurin-9-yl)pentyloxy)

Compound No	Chain Length n	10 μM	% Inhibition 30 μM	100 μM
38	5	16	38, 45	68, 71, 74
39	8	26, 31, 32	Insoluble	Insoluble
40	12	2, 0	5, 20	3

Table 10

Compound No	Chain Length n	10 μM	% Inhibition 30 μM	100 μM
41	5	16	38, 45	65, 69
42	8	41, 29, 20		Insoluble
43	12	14, 37	52, 21, 50	73, 75

Table 11

benzamide (**41**) and 3-(12-(6-aminopurin-9-yl)dodecyloxy)benzamide (**43**). The potency of the pentyloxy compounds (**38** and **41**) against PARP can be rationalised in the same manner that the potency of 3-(5-bromopentyloxy)benzamide (**35**) was rationalised. That is, they bind to PARP in a similar manner to that in which inhibitors such as 3-methoxybenzamide (**4**) bind to PARP. Since they possess some aqueous solubility and their 3-substituent groups are not bulky enough to interfere with this binding: they show some inhibition against PARP.

3-(12-(6-Aminopurin-9-yl)dodecyloxy)benzamide (**43**) was envisioned and synthesised as a direct analogue of NAD^+ and as such was expected to show inhibition against PARP. It is noteworthy that the corresponding 6-chloropurine analogue did not show any inhibition, indicating that there may be an adenine receptor site within PARP. However, further evidence is required to prove this assumption.

4.1.5 The Preparation of the 3-(Hydroxyalkyloxy)benzamides

An attempt was made to synthesise these compounds by the preparation of the acetates from the bromides and hydrolysing the acetates to the alcohols.

It was hoped to prepare 3-(8-acetyloctyloxy)benzamide (**44**) from 3-(8-bromooctyloxy)benzamide (**36**) by heating an ethanolic solution of the latter compound under reflux in the presence of sodium acetate. This reaction was followed by TLC but no transformation was detected (five hours). The reaction was repeated in an aprotic solvent with a different reagent (a consequence of solubility problems). Therefore, a solution of 3-(8-bromooctyloxy)benzamide (**36**) in acetonitrile was heated under reflux in the presence of *n*-tetrabutylammonium acetate and the reaction was followed by TLC. After eight hours the presence of a product,

with a similar R_f to the starting material, was observed. Upon work up the reaction mixture produced a white solid which, based upon ^1H NMR evidence, was thought to be a mixture of starting material, reagent and product. The spectrum had signals in the downfield region which were in similar positions and had similar splitting patterns to those found in the similar region of the spectra of the 3-(bromoalkyloxy)benzamides (see Section 4.1.3) which were indicative of a 1,3-disubstituted benzene. Two, almost superimposed, triplets appear at δ 4.10 which were thought to represent the protons α to the oxygen atom connected to the aromatic ring and the protons α to the oxygen atom connected to the acetyl group. Another triplet (at δ 3.62) had a much smaller integral than the previous signal. This signal was assigned to the methylene protons α to the bromine atom of the starting material (**36**) which usually appear at δ 6.64 ppm (see Section 4.1.3). The methylene protons α to the quaternary nitrogen of the reagent (*n*-tetrabutylammonium acetate) appear as a multiplet at δ 3.29. The acetate methyl protons of both the reagent and the product appear as a singlet (δ 2.10) whilst the remaining methylene protons appear as a series of multiplets between δ 2.00 and δ 1.25. Lastly a triplet (at δ 1.11) is seen which represents the methyl protons of the reagent.

Analysis of the integrals within this spectrum indicate the ratio of product to the starting material is 3 to 1 and the ratio of the product to the reagent is 2.4 to 1.

Since the R_f's of the starting material and the product were so similar the acetate within the reaction mixture was hydrolysed to the alcohol, since the alcohol was expected to have a lower R_f than the acetate, it was hoped that the alcohol could be won from the reaction mixture chromatographically. The transformation was effected by stirring the reaction mixture in a methanolic aqueous ammonia solution overnight. A TLC of the reaction mixture showed a mixture of two compounds of widely differing R_f's. These compounds were then separated chromatographically and a ^1H NMR spectrum obtained of the slower running compound. This spectrum indicated

that this fraction contained 3-(8-hydroxyoctyloxy)benzamide (**45**) with the salient features being two triplets which were thought to the oxygen atom connected to the aromatic ring (δ 4.49) and the methylene protons α to the hydroxyl group (δ 4.10). Unfortunately this spectrum also showed that the reagent was present in this chromatographic fraction. In conclusion, it is possible to effect the transformation of the bromide to the alcohol *via* the acetate but the reaction requires further optimisation.

4.2.1 *cis/trans*-3-Methoxycyclohexanecarboxylic acid (46)

Inhibitors were designed that were not dependent upon NAD^+ as a template but were based upon the rationalisation of literature inhibitors. One of these rationalisations was that for the molecule to be active some conjugation was necessary within a six membered ring that was substituted at the three position and contained an amide functionality at the one position. If this hypothesis is correct then the saturated 3-methoxycyclohexane carboxamide should not be an inhibitor. This compound was synthesised to test this hypothesis. The title compound was obtained commercially and consisted of a mixture of four compounds, *ie* two pairs of enantiomers. The *cis*-pair were the (*R*,*S*)- and (*S*,*R*)-3-methoxycyclohexanecarboxylic acids (**46a** and **46b**); whilst the *trans*-pair consisted of (*R*,*R*)- and (*S*,*S*)-3-methoxycyclohexanecarboxylic acids (**46c** and **46d**, see Figure 16). Since the carboxamides produced from these compounds were not expected to show any inhibitory properties it was considered expedient - since this starting material was readily available - to submit the resultant carboxamides in this form for evaluation.

If this mixture was found to show inhibition of PARP then separation into (firstly) the two pairs of enantiomers would be required. Since the pairs of enantiomers were diastereomeric toward each other, separation by HPLC was envisaged. The purity of

cis *trans*

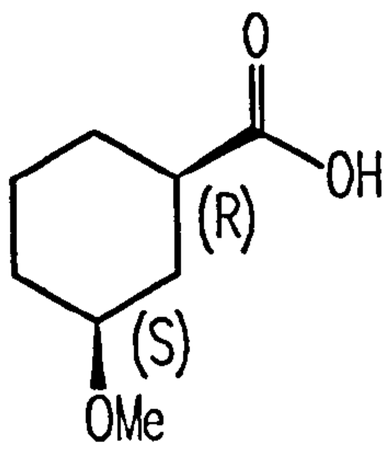

46a

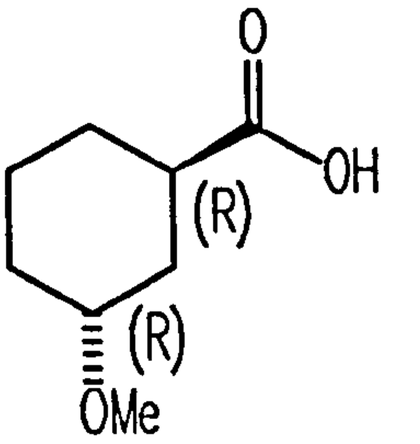

46c

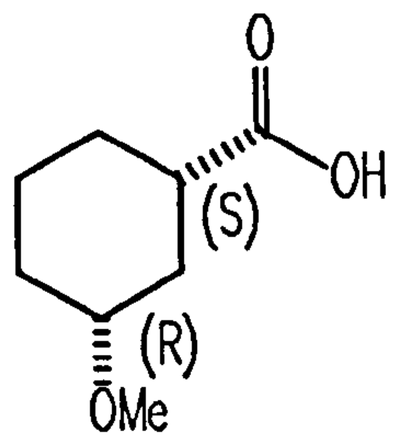

46b

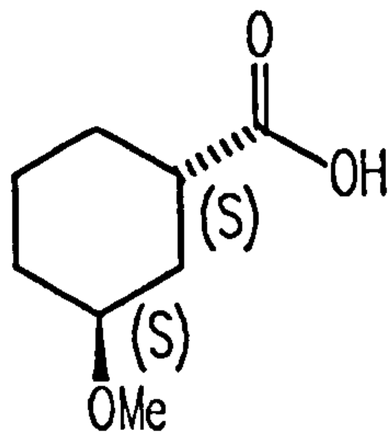

46d

The Isomers of *cis* / *trans*-3-methoxycyclohexanecarboxylic Acid

Figure 16

the two pairs could be checked by ^{1}H NMR spectroscopy. It was for this reason that the ^{1}H NMR spectrum of the diastereomeric *cis*/ *trans* 3-methoxycyclohexanecarboxylic acid was determined.

4.2.1.1 Determination of the *cis* to *trans* ratio of 3-methoxycyclohexanecarboxylic acid (46) by ^{1}H NMR spectroscopy

A 500 MHz ^{1}H NMR spectrum of *cis*/ *trans*-3-methoxycyclohexanecarboxylic acid (46) shows two different NMR signals for (amongst others) the proton at the 3

The ^{1}H NMR Spectrum of *cis/trans*-

3-Methoxycyclohexanecarboxylic Acid

Spectrum 6

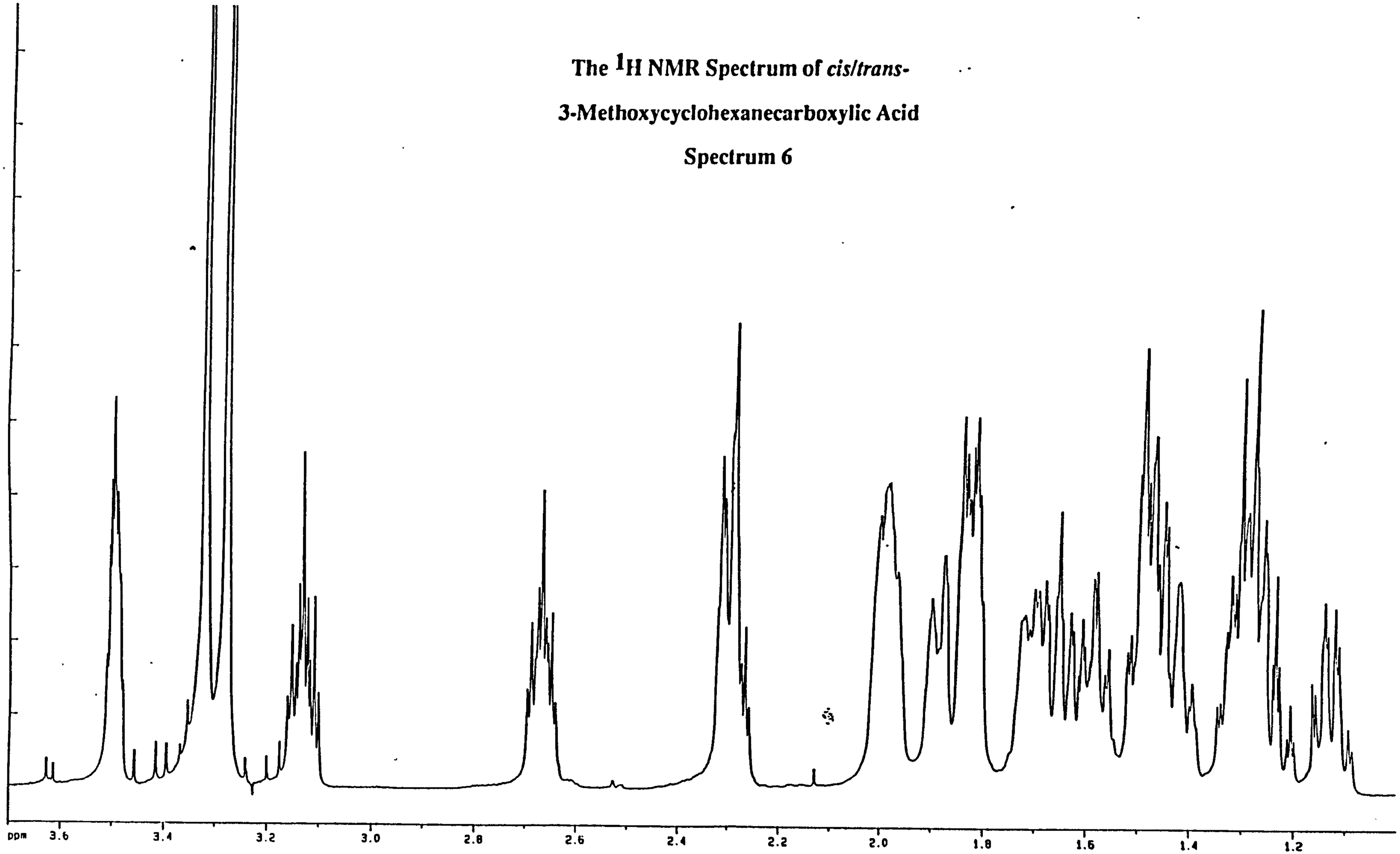

cis

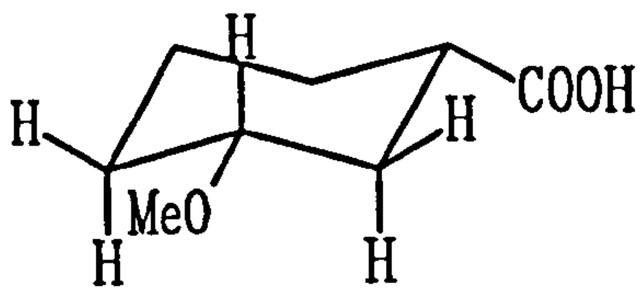

trans

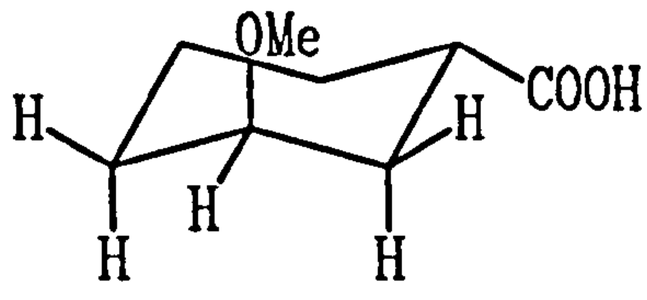

cis/trans-3-Methoxycyclohexanecarboxylic Acid

Figure 17

position. These two signals differ both in chemical shift and broadness of signal. It was from the broadness of the signal that these two peaks were assigned to their constituent molecule. In the *cis* compound (where 3H is axial) the 3H signal is broad due to two axial axial splittings with two equatorial equatorial splittings. The *trans* compound (3H equatorial) has a narrower 3H signal since this proton has no axial axial splittings, only axial equatorial and equatorial equatorial splittings (see Figure 17). The integrals of the two signals showed that the ratio of the *cis* to *trans* compounds was 1.2 to 1 (see Spectrum 6).

4.2.2 *cis/ trans* 3-Methoxycyclohexylcarboxamide (47)

This compound was prepared from 3-methoxycyclohexanecarboxylic (46) acid by treatment with thionyl chloride followed by aqueous ammonia. The product was recrystallized from ethyl acetate to give *cis/ trans*-3-methoxycyclohexanecarboxamide (47). A 100 μM solution of this mixture gave 9, 15 and 3 % inhibition of PARP.

4.2.3 Attempted Synthesis of 3-Methoxy-1,4-Dihydrobenzamide (48)

The next class of inhibitors to be assessed was those with partial saturation of the aromatic ring. 3-Methoxy-1,4-dihydrobenzamide (**48**) was expected to be formed either by reduction of 3-methoxybenzoic acid (**49**) and functional group transformation of the acid to the amide, or by reduction of 3-methoxybenzamide (**4**). Upon further reduction a number of tetrahydrobenzamides could be envisioned. This latter class of compounds would tell us about the extent of unsaturation necessary for inhibition and also where it was most effective.

4.2.4 The Birch Reduction[52]

Birch reductions are carried out in liquid ammonia with a dissolving metal (usually sodium) and an alcohol as a proton source. The effect of this reaction is to reduce aromatic systems to their dihydro, tetrahydro and fully reduced states. The mechanism involves a single electron transfer process. Sodium donates an electron to the aromatic system to form a radical anion (**50**). The radical anion, **50**, is then protonated to leave a radical (**51**) which receives another electron from sodium to form an anion (**52**). The anion (**52**) thus formed is protonated to form the dihydro product (**53**) shown in Scheme 7.

4.2.4.1 Regioselectivity of the Birch Reduction[53]

Regioselectivity - which bonds will be reduced - is seen within the Birch reduction. This phenomenon has been explained by molecular orbital theory. Thus, benzene is known to form 1,4-cyclohexadiene (**53**) rather than 1,3-cyclohexadiene (**54**). Molecular orbital treatment of the precursor cyclohexadiene anion shows that there is a larger electron density at the 3-position (rather than the equivalent 2- or 4-positions)

and hence protonation at this position gives the 1,4-cyclohexadiene product. The regioselectivity that is of relevance to the research described in this thesis occurs when the aromatic starting materials are substituted. Again molecular orbital theory has been used to explain the empirical substitution patterns observed for these compounds.[54] A compound with an electron donating group (*eg* -OMe) will direct an incoming electron away from the carbon to which it is attached. A compound with an electron withdrawing group will attract an electron toward the carbon to which it is attached.

If 3-methoxybenzoic acid were reduced under Birch conditions then the predicted product would be the 1,4-dihydro acid. The electron withdrawing substituent - the

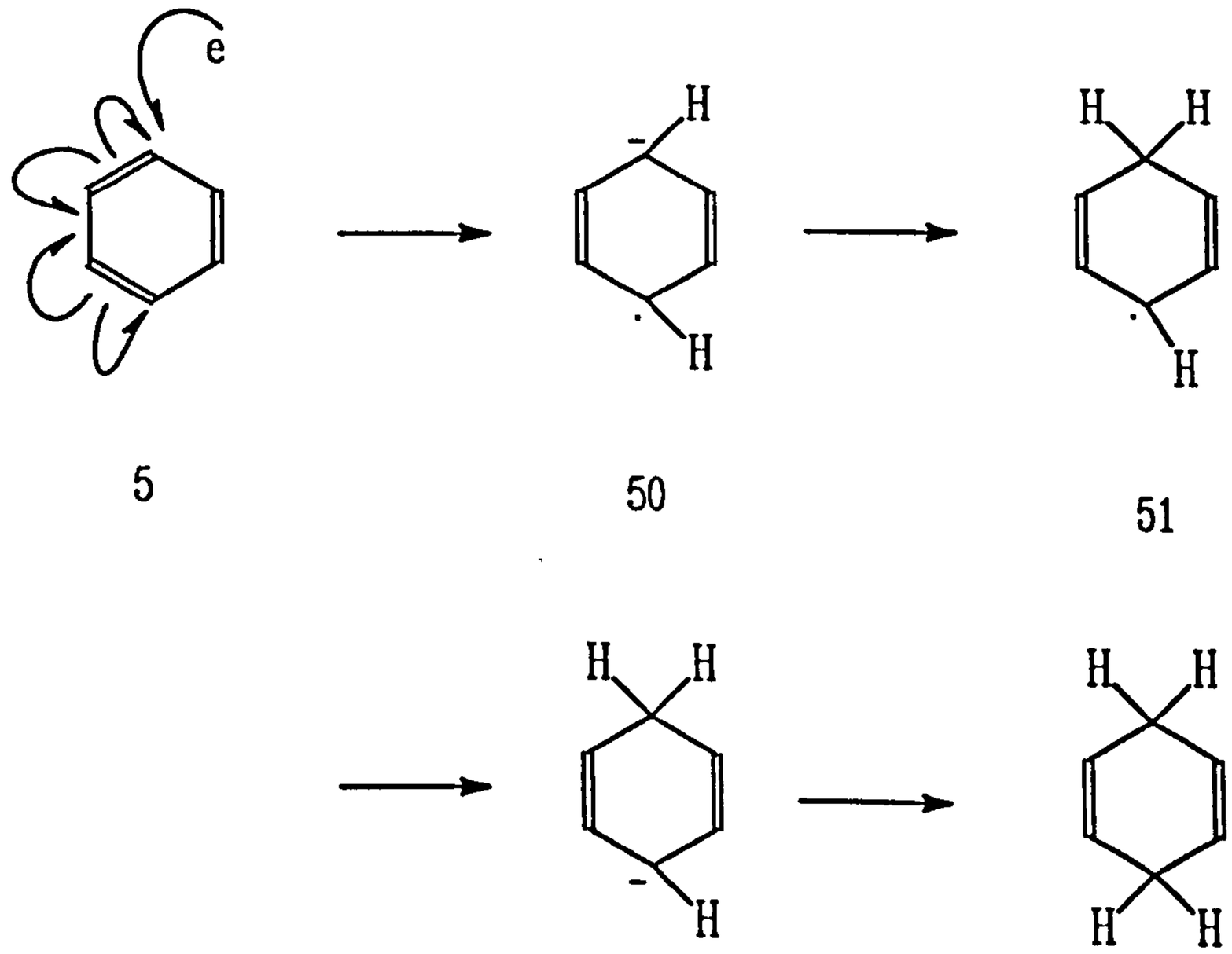

5 50 51

52 53

The Birch Reduction of Benzene

Scheme 7

carboxylic acid - would attract an incoming electron and stabilise the negative charge produced, whilst the electron donating methoxy group would repel any incoming electrons: both these effects work in conjunction to give the product.

4.2.4.2 Synthesis of 3-Methoxy-1,4-dihydrobenzoic acid (55)

The title compound (**55**), prepared from 3-methoxybenzoic acid (**49**) by the Birch reduction, was an oil that could not be crystallized and began to decompose upon prolonged manipulation. However, a ^{1}H NMR spectrum of the compound was consistent with the proposed structure and also with the literature.[52] The H1 proton of this compound appeared as a broad multiplet (δ 3.51) which was coupled to the H2 doublet (δ 4.68). The two vinyl protons H5 and H6 formed a multiplet (δ 5.75), as did the H4'and H4" protons (δ). The ^{13}C NMR spectrum of this compound was not reported by the earlier workers but our determination was consistent with the structure of the acid. Due to the compounds instability no other characterization was attempted.

The dihydro acid (**55**) was reacted with ethyl chloroformate and liquid ammonia but no 3-methoxy-1,4-dihydrobenzamide (**48**) was isolated.

4.2.4.3 The Birch Reduction of 3-Methoxybenzamide (4)

It was supposed that 3-methoxy-1,4-dihydrobenzamide (**48**) could not be prepared from 3-methoxybenzoic acid (**49**) because the manipulation of the unstable intermediate, 3-methoxy-1,4-dihydrobenzoic acid (**55**), caused it's decomposition. Not only was the reoxidation back to the starting material envisioned but also migrations about the ring were possible.

If 3-methoxybenzamide (**4**) could be directly converted to 3-methoxy-1,4-dihydrobenzamide (**48**) the manipulation and functional group interconversion of an unstable intermediate would be avoided.

3-Methoxybenzamide (**4**) was prepared by treating 3-methoxybenzoic acid (**49**) with thionyl chloride to give the intermediate acid chloride (**56**). Quenching this with aqueous ammonia gave the desired product (**4**, see Scheme 8).

3-Methoxybenzamide (**4**) was reduced under Birch conditions but did not give 3-methoxy-1,4-dihydrobenzamide (**48**), instead 3-methoxy-1,4,5,6-tetrahydrobenzamide (**57**) was produced. The structure of this compound was supported by its ^1H NMR spectrum. This contained a multiplet (δ 1.71) of four protons, the 5',5" and 6',6" protons. The H1 proton appeared as a broad multiplet (δ 3.01) whilst the methoxy protons gave a narrow singlet (δ 3.52). Further, the

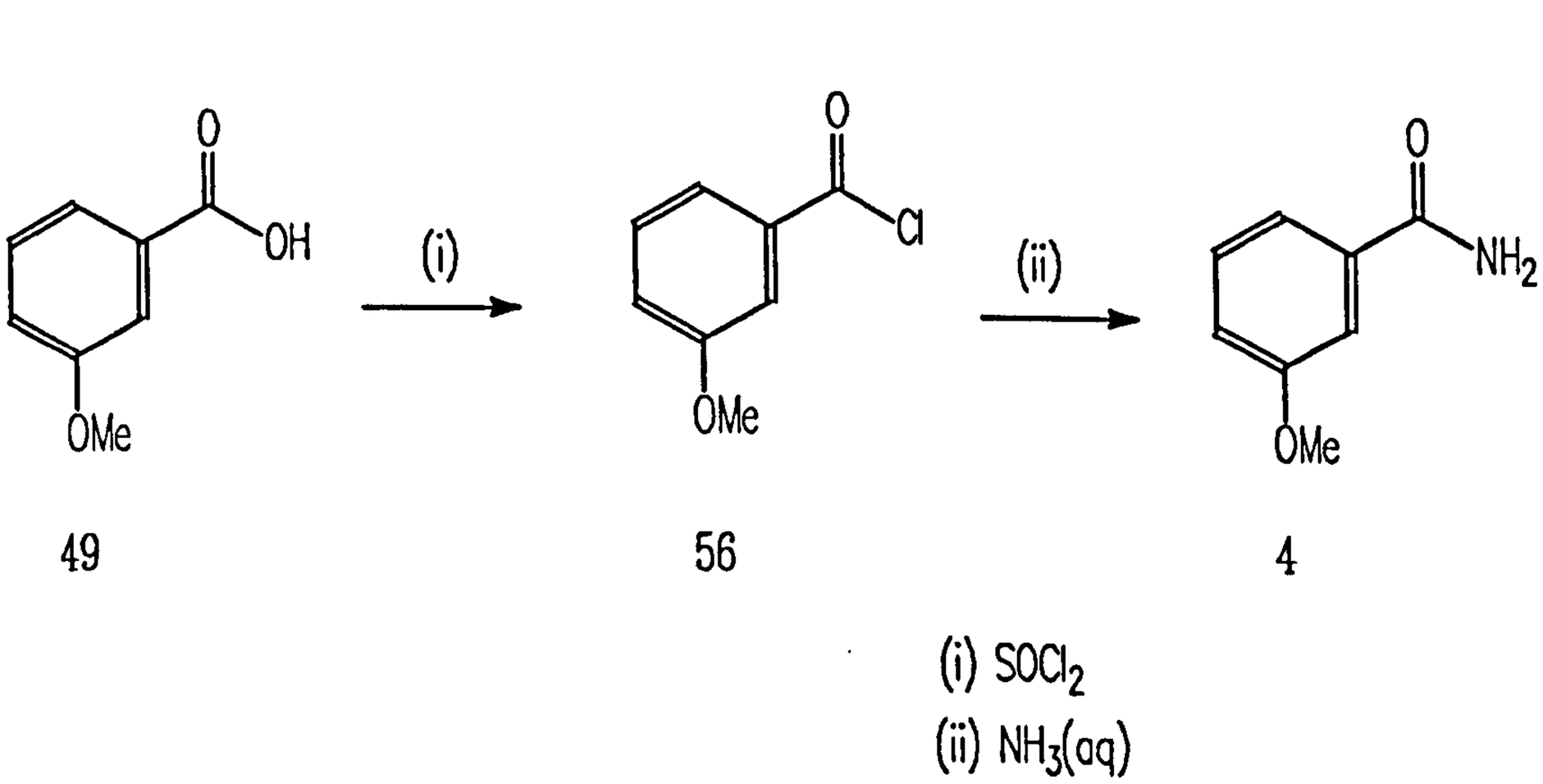

The Preparation of 3-Methoxybenzamide

Scheme 8

vinylic proton appeared as a doublet (δ 4.61) in the expected place for an enol ether and the amide protons were downfield and separate (δ 5.86 and δ 6.01).

This result can be rationalized by supposing that initially 3-methoxy-1,4-dihydrobenzamide (48) was formed but underwent a bond migration. The bond migration formed the conjugated 3-methoxy-4,5-dihydrobenzamide (58) which was susceptible to further reduction under the reaction conditions. The initial bond migration is a consequence of proton extraction at the 1 position, which in turn, is a consequence of the basicity of the alkoxide present. This phenomenon has been

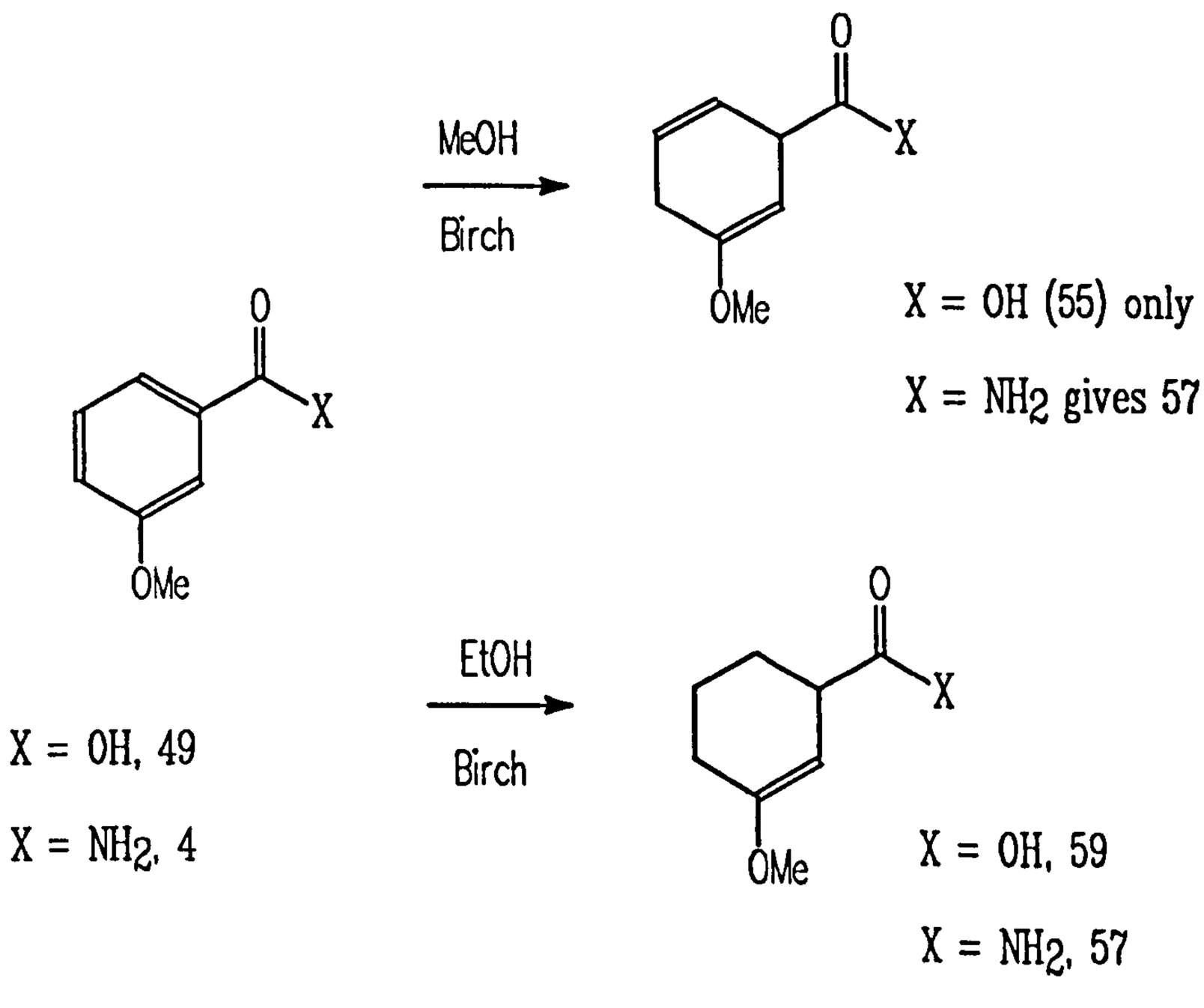

The Birch Reductions of 3-Methoxybenzoic Acid and 3-Methoxybenzamide

Scheme 9

studied in the case of 3-methoxybenzoic acid (**49**). When methanol was used as the proton source 3-methoxy-1,4-dihydrobenzoic acid (**55**) was formed, but when ethanol was used 3-methoxy-1,4,5,6-tetrahydrobenzoic acid (**59**) was formed.[55] The increased basicity of the ethoxide anion, over the methoxide anion, causes the necessary bond migration that allows further reduction of the benzene ring.

The Birch reduction of 3-methoxybenzamide (**4**) was carried out with both ethanol and methanol as proton sources and for each case the tetrahydro product was obtained. The proton at the 1 position was more labile in the dihydro amide (**48**) than the dihydro acid (**55**). This is because, under the conditions of the reaction, the dihydro acid (**55**) exists as an anion, hence further deprotonation (to form a dianion) is difficult. However, the dihydro amide (**48**) does not exist as an anion and is therefore susceptible to deprotonation at the 1 position (and hence bond migration *etc*, see Scheme 9).

4.3 *N*-Alkylnicotinamides

These compounds were simple NAD^+ analogues. They were synthesised both to determine their inhibitory activity and as precursors to the *N*-alkyl dihydronicotinamides.

The compounds prepared were the *N*- methyl (60), ethyl (61) and benzyl (62) nicotinamides as their iodides - with the exception of benzyl which was the chloride (see Figure 18). They were simply prepared by heating under reflux nicotinamide with the alkyl halide in ethanol. All were prepared in good yield and were easily purified by recrystallisation.[53,54]

4.3.1 Spectroscopic Properties of *N*-Alkylnicotinamides

The ^1H NMR spectra of this class of compounds can be analysed by considering three aspects of the molecules: the alkyl substituent, the amide group and the heterocyclic ring system.

So, considering the alkyl substituent, the protons α to the positively charged nitrogen appear at about δ 5. Thus, the methyl protons of *N*-methylnicotinamide iodide (60) are represented by a singlet at δ 4.5 while the methylene protons of *N*-ethylnicotinamide iodide (61) are represented by a signal at δ 4.8. The protons of the methyl part of the latter compound (61) produce a signal at δ 1.7. The spectrum of the benzyl compound (62) was obtained by dissolving the compound (62) in D_2O rather than d_6-DMSO and so the chemical shifts of the benzyl spectrum can only be cautiously compared to those of the methyl (60) and ethyl (61) compounds. The spectrum of the benzyl compound (62) is further complicated by the presence of an HOD peak which integrated for approximately two protons. The spectrum thus has

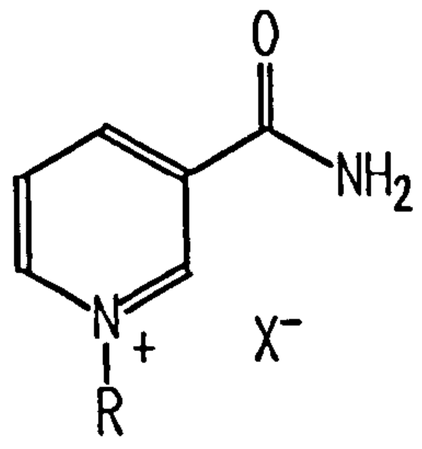

R = Me, X^- = I^- 60

= Et, = I^- 61

= Bn, = Cl^- 62

The Alkylnicotinamide Salts

Figure 18

two singlets at δ 4.9 and δ 6.0 (internal standard: sodium salt of trimethylsilylpropanesulphonic acid). The heterocyclic signals within the spectrum correlate closely with the chemical shifts of the heterocyclic signals of the methyl (**60**) and ethyl (**61**) compounds and so upon this basis the methylene signal was assigned to δ 6.0 and the HOD peak to δ 4.9. The aromatic signals of the benzyl group appeared in the usual place (*ca* δ 7.6) as a narrow multiplet.

The amide group has two characteristic signals which occur because of the partial double bond nature between the carbon and nitrogen atoms. The magnetically inequivalent protons appear close to δ 8 and δ 8.5. These signals are not present within the spectrum of the benzyl compound (**62**) because of proton deuterium exchange.

The heterocyclic ring protons have similar chemical shifts and splitting patterns within this series of compounds (**60, 61** and **62**). The signal furthest upfield, a double doublet, is the H5 proton (δ 8.3 - 8.4). The H5 signal from the benzyl compound (**62**) appears as a triplet rather than a double doublet; this is a consequnece of the solution properties of the different solvents. The H4 proton appears as a doublet at

approximately the same position within all the spectra (δ 9). Next the H6 proton appears as a double doublet (*ca* δ 9.4) and lastly the H2 proton appears as a singlet (δ 9.5).

4.3.1.1 Potency of the N-Alkylnicotinamides

These compounds displayed little inhibition against PARP. This was thought to be a consequence of of an electron deficient aromatic ring and hence a diminished carbonyl electron donor capacity. Although these compounds were similar to NAD^+ in terms of nicotinamide electronic structure they were dissimilar in that they obviously lack the sugars, phosphates and adenine. This result supports the tentative rationale used to explain the potency of 3-(12-(6-aminopurin-yl)dodecyoxy) benzamide (**43**, see Section 4.1.4.1).

Compound No	Alkyl Substituent	% Inhibition (100 μM)
60	Me	0, 5
61	Et	0, 10
62	Bn	0, 0

Table 12

4.3.2 *N*-Alkyl-dihydronicotinamides

These compounds were NADH analogues and were different in two respects from the NAD^+ analogues: the heterocyclic ring was not aromatic and the amide oxygen was more electron rich. The latter point arises because the nitrogen is no longer positively charged and also the nitrogen is conjugated to the oxygen.

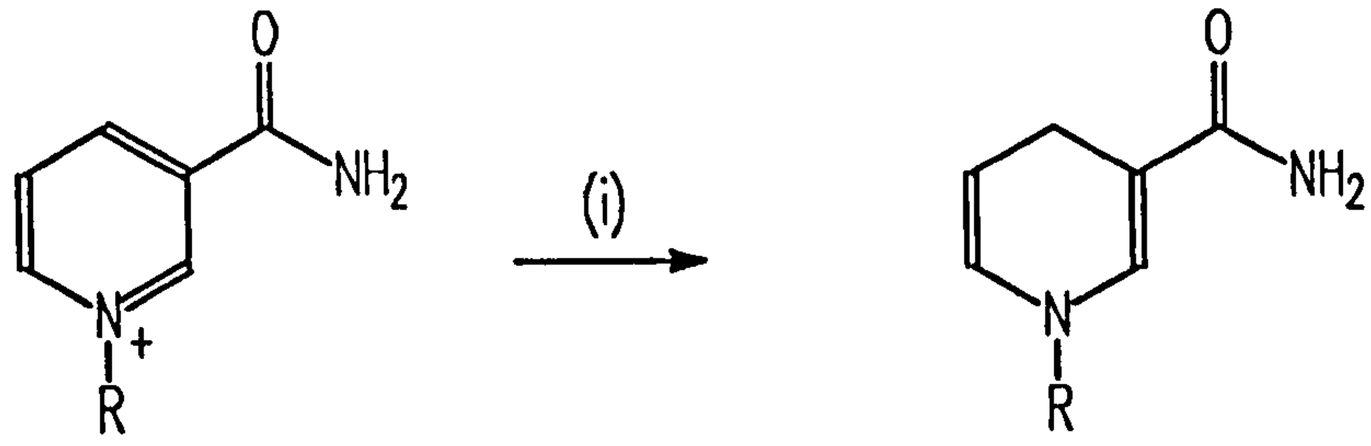

(i) aqueous Na_2CO_3
$Na_2S_2O_4$
under $N_2(g)$

The Reduction of the *N*-Alkylnicotinamide Salts

Scheme 10

The compounds in this class were all prepared by the reduction of the corresponding *N*-alkylnicotinamide salts with sodium hydrosulphite (see Scheme 10).[56,57] As expected these compounds were unstable, being susceptible to atmospheric oxidation. The benzyl compound (**63**) was the easiest to prepare and gave a reasonable yield upon recrystallisation. The methyl and ethyl compounds (**64** and **65**) were less stable; the methyl compound (**64**) was prepared as an oil and could not be recrystallised. It was, however, pure by TLC - a single blue fluorescent spot - and ^{1}H NMR spectroscopy (see spectrum 7). The ethyl compound (**65**) was recrystallised with difficulty using low temperature (-30°C to 0°C) recrystallisation techniques to give pure yellow crystals (see experimental for more details).

The mechanism of this reaction is of interest: it was initially thought to be a single electron transfer (SET) process, as depicted in Scheme 11; however, there is literature evidence[58] suggesting that an intermediate (**16**, in scheme 12) occurs along the reaction coordinate which then breaks down into the products.

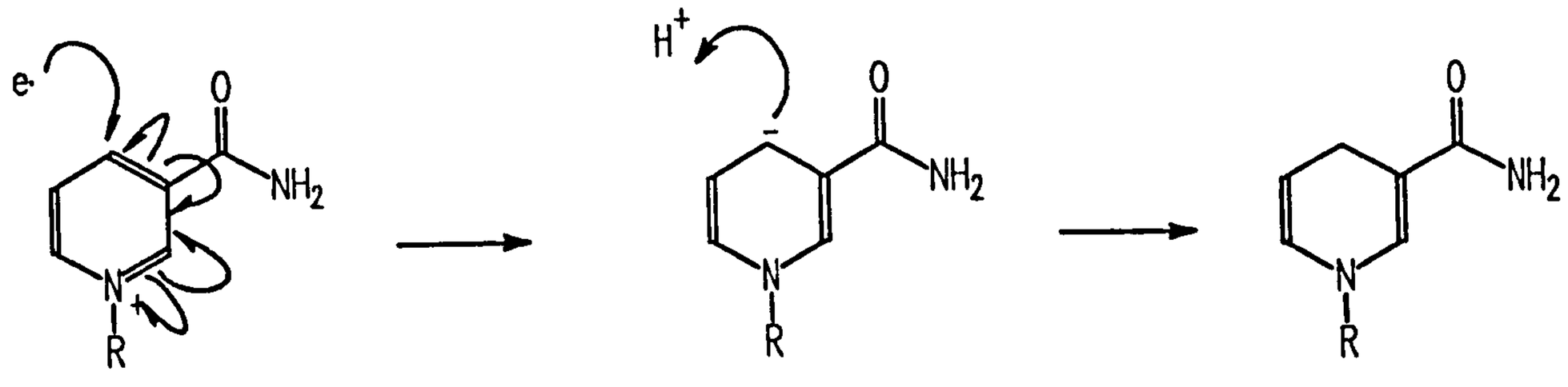

The SET Mechanism of the Reduction of *N*-Alkylnicotinamide Salts

Scheme 11

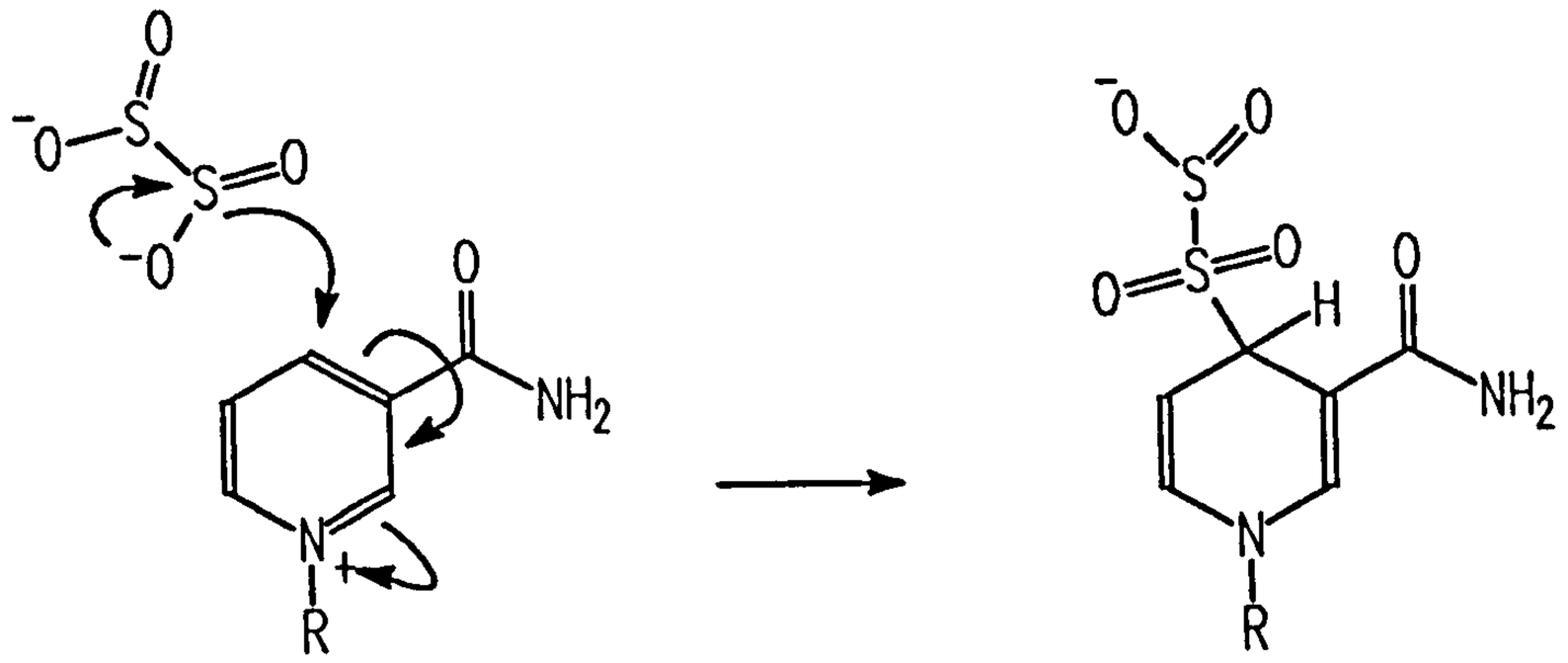

The Non-SET Mechanism of the Reduction of *N*-Alkylnicotinamide Salts

Scheme 12

4.3.3 Spectroscopic Properties of *N*-Alkyl-1,4-dihydronicotinamides

The ^{1}H NMR spectra of this class of compounds corroborate their structures and like the *N*-alkylnicotinamide salts (see Section 4.3.1), they can be analysed by considering three aspects of their molecular structure: the amide functional group, the alkyl substituent and the ring system. The simplest member of this class of compounds is *N*-methyl-1,4-dihydronicotinamide (64). Its spectrum will be analysed and

The ^{1}H NMR Spectrum of N-Methyl-1,4-Dihydronicotinamide

Spectrum 7

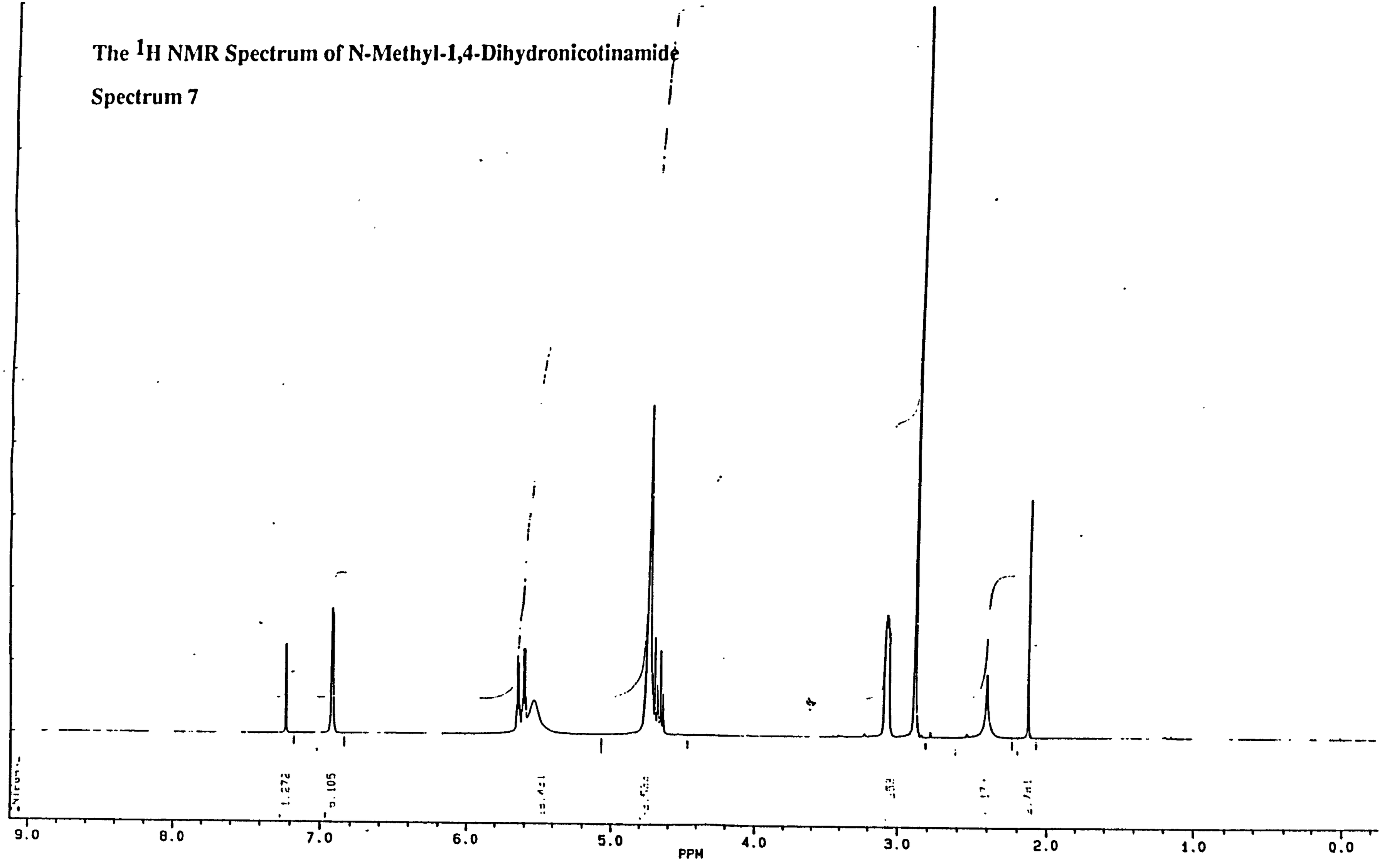

comparisons will be drawn between other members of its class and the *N*-alkylnicotinamide salts.

4.3.1.1 ^{1}H NMR Spectrum of *N*-Methyl-1,4-dihydro nicotinamide (64)

The *N*-methyl signal, which is α to the ring nitrogen, appears as a singlet near δ 3 rather than δ 5 as in the case of the *N*-alkylnicotinamide salts. This is a consequence of the lack of positive charge upon the nitrogen. Since the ring has been reduced it contains an alkyl methylene group at the four position. The signal for this group appears (δ 3.06) as a double triplet covering a very narrow range of the spectrum (δ 3.05 to δ 3.07). These protons are coupled to the alkene protons H5 (J = 3), H6 (J = 1.6) and H2 (J =1.6) forming the multiplet described. The other ring protons appear further downfield. The proton H5, appears at δ 4.66 which is further upfield than expected for a 1,4-dihydrocyclic ring system (*eg* the vinylic protons of 5,8-dimethyl-1,4-dihydronaphthalene appear at δ 5.78).[51] The H5 proton in this compound is pushed upfield by the electron donating capacity of the nitrogen atom in the manner

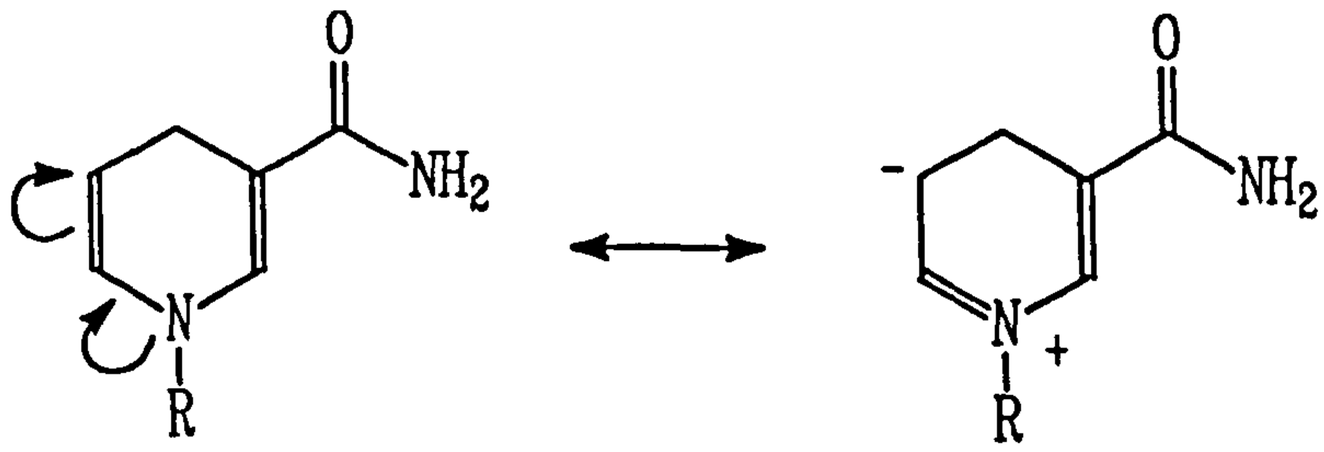

Electron Density Donation within an

N-Alkyl-1,4-dihydronicotinamide Ring

Figure 19

shown (Figure 19). The multiplicity of this signal (H5) is a double triplet. It is coupled to the H6 proton (J = 7.5) and the methylene (H4',4") protons (J = 3). The coupling to the two methylene protons forms the triplet which is further split by the H6 proton. No long range coupling from H2 is seen. The next ring signal downfield is produced by the H6 proton which is next to the nitrogen atom. This signal appears as a double triple doublet. It is coupled to H5 (J = 8), the ring methylene protons (H4',4"; J = 3) and the H2 proton (J = 1.6). Lastly, the proton between the amide function and the nitrogen, H2, appears as a doublet (J = 1.6). This proton is coupled to the H6 proton whilst no coupling to the methylene protons (H4',4") is seen (see Spectrum 7).

The ^{1}H NMR spectrum of *N*-ethyl-1,4-dihydronicotinamide (**65**) is similar to that of *N*-methyl-1,4-dihydronicotinamide (**64**). The methylene signal of the *N*-ethyl group overlaps with the ring methylene group and complicates the spectrum whilst the methyl group appears as a triplet at δ 1.11, the expected position for an alkyl group.

The ^{1}H NMR spectrum of *N*-benzyl-1,4-dihydronicotinamide (**63**) is essentially the same as the earlier examples. The benzyl methylene protons appear as a singlet (δ 4.25) whilst the phenyl protons appear as a complex multiplet (δ 7.28).

4.3.2 Potency of the *N*-Alkyl-1,4-dihydronicotinamides

Only the *N*-ethyl and *N*-benzyl compounds (**65** and **63**) could be prepared pure enough to be assayed. The assay found that both of these compounds showed some inhibition against PARP which supported the idea that electron carbonyl donor capacity was important for inhibition (Table 13).

Compound No	Alkyl Substituent	10 μM	% Inhibtion 30 μM	100 μM
65	Et		0	0, 48, 37
63	Bn	10	11, 30, 20	28, 54, 42

Table 13

4.4 Benzoxazole-4-carboxamides

It was known from earlier work that a fixed amide orientation and an electron rich *meta* substituent were necessary for inhibition of PARP.[26] The benzoxazole-4-carboxamides were synthesized with a view to exploit the entirely new and novel idea

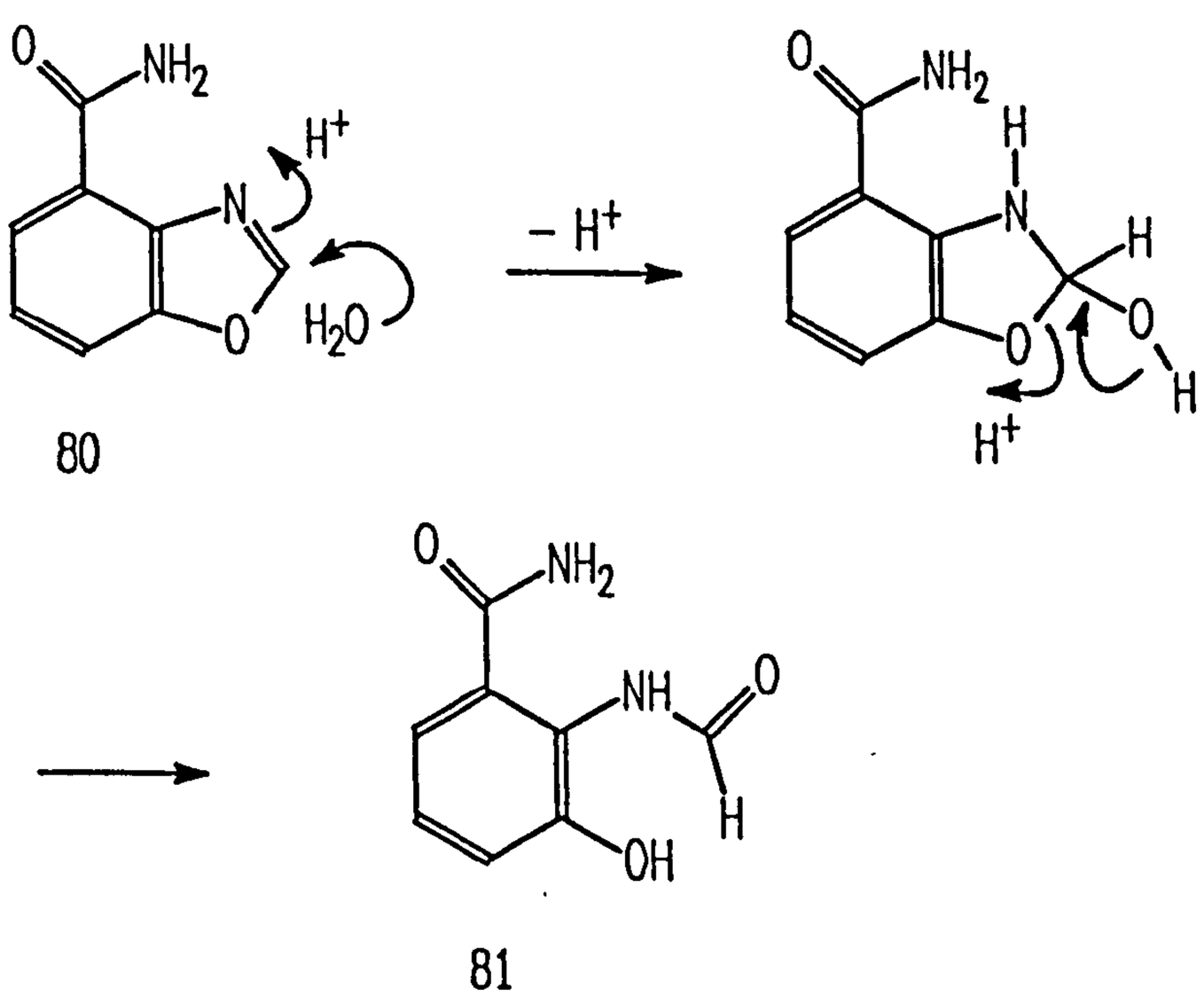

81

Electrophillicity of Benzoxazole-4-carboxamide

Scheme 13

of fixing the amide orientation by a 'hydrogen bond'. That is, the 'hydrogen bond' between the amide proton and the benzoxazole ring nitrogen. These molecules also possess an electron rich *meta* substituent, the oxygen atom of the benzoxazole molecule.

4.4.1 2-Alkylbenzoxazole-4-carboxamides

A 2-alkylbenzoxazole-4-carboxamide was chosen for synthesis before the simpler homologue, benzoxazole-4-carboxamide (80), because the two position of the latter compound has been shown to be electrophilic.[60] Thus, if water behaved as an adventitious nucleophile it may attack the benzoxazole at the two position and ring open to the formamide (**81**, see Scheme 13). An alkyl substituent at the two position should donate electron density, by hyperconjugation, and thereby decrease the electrophilicity of the two position.

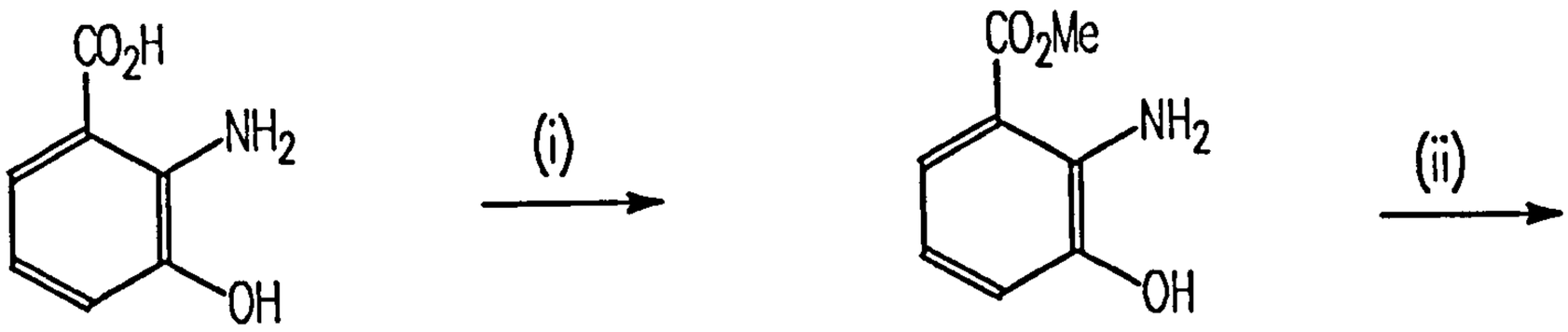

83 84

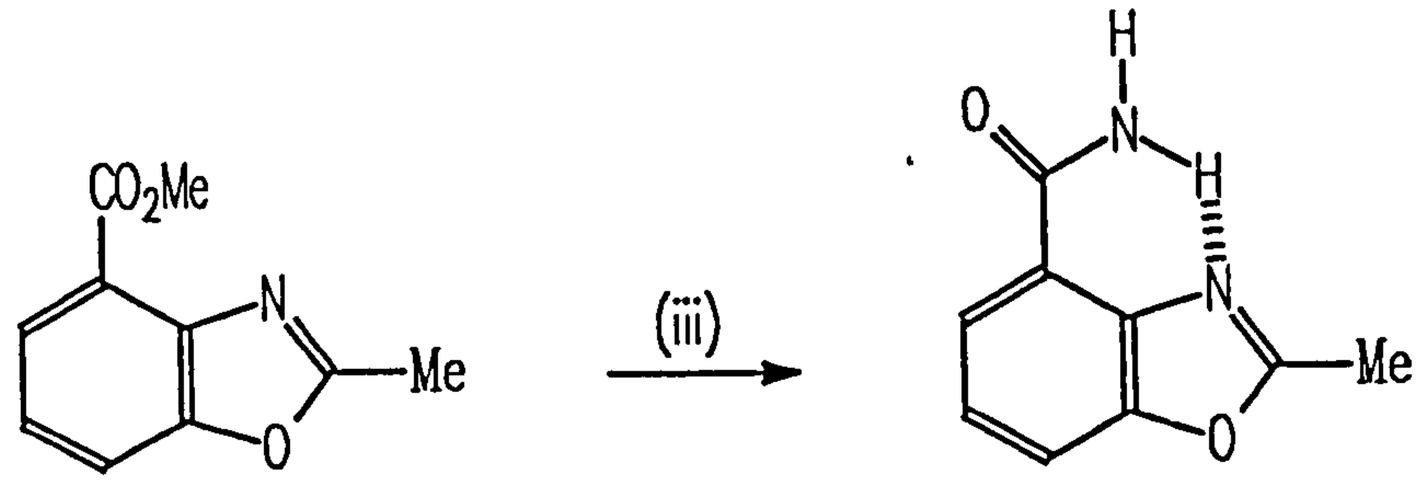

85 82

(i) HCl, MeOH

(ii) xylene, pyridinium p-toluenesulphonic acid and
either: acetyl chloride or triethyl orthoformate

(iii) NH_3 fifty degrees fifteen kilobars

The Preparation of 2-Methylbenzoxazole-4-carboxamide

Scheme 14

4.4.2 2-Methylbenzoxazole-4-carboxamide (82)

The title compound was chosen for synthesis since it was the simplest 2-alkylbenzoxazole-4-carboxamide and it could be prepared from readily available starting materials. It was made from commercially available 3-hydroxyanthranilic acid (2-amino-3-hydroxy-benzoic acid, **83**) by the cyclisation of the ester, methyl 2-amino-3-hydroxybenzoate (**84**). This ester (**84**) was prepared by saturating a suspension of **83** in dry methanol with dry hydrogen chloride gas and heating this

mixture under refluxing conditions. The cyclisation to the benzoxazole was done with acetyl chloride which was heated with the ester (**84**) under refluxing conditions in *m*-xylene. Triethylamine was present to neutralise the hydrogen chloride formed and an acid catalyst (pyridinuium *p*-toluenesulphonic acid) was necessary for the reaction to go to completion. The amide (**80**) was formed by reacting the newly formed benzoxazole ester (**85**) with ammonia under pressure (see Scheme 14).

The benzoxazole ester (**85**) was also prepared by the reaction of the methyl 2-amino-3-hydroxybenzoate (**84**) with methylacetimidate by heating a mixture of the two compounds in methanol under refluxing conditions. This reaction was found to require pyridinium *p*-toluenesulphonic acid (an acid catalyst) for it to go to completion and was not appreciably cleaner than the acetyl chloride reaction.

4.4.3 ^{1}H NMR Spectroscopic Properties of 8 hydroxy-2-Methyl-4(3*H*)-Quinazolinone (82')

Whilst the writing of this thesis was being completed, my successor Louise Pemberton[59] obtained crystals of compound **82** suitable for *X*-ray analysis. The analysis showed to our surprise that the benzoxazole structure was incorrect. The correct structure for **82** is 8-hydroxy-2-methyl-4(*3H*)-quinazolinone (**82'**). It is now clear that subjecting the ester **85** to liquid ammonia at 50 °C/15 kBar causes some kind of molecular rearrangement. One possibility is that **82** is formed, but then suffers nucleophilic attack by ammonia at C-2 leading to cleavage of the oxazole and eventual formation of a pyrimidine ring:

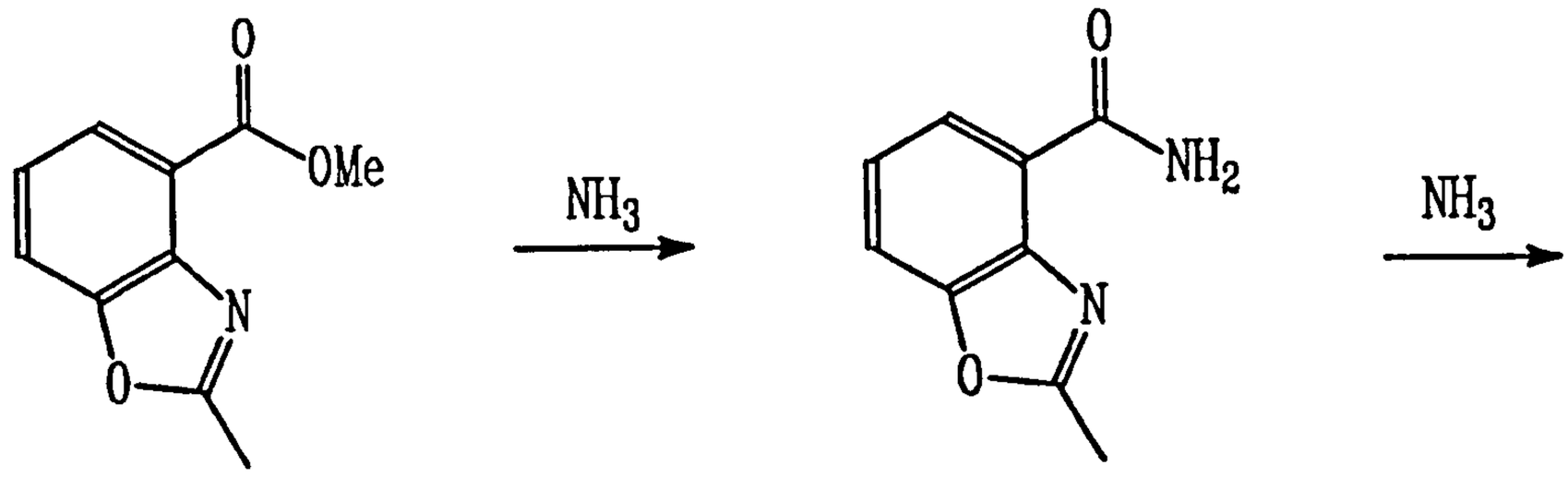

85 82

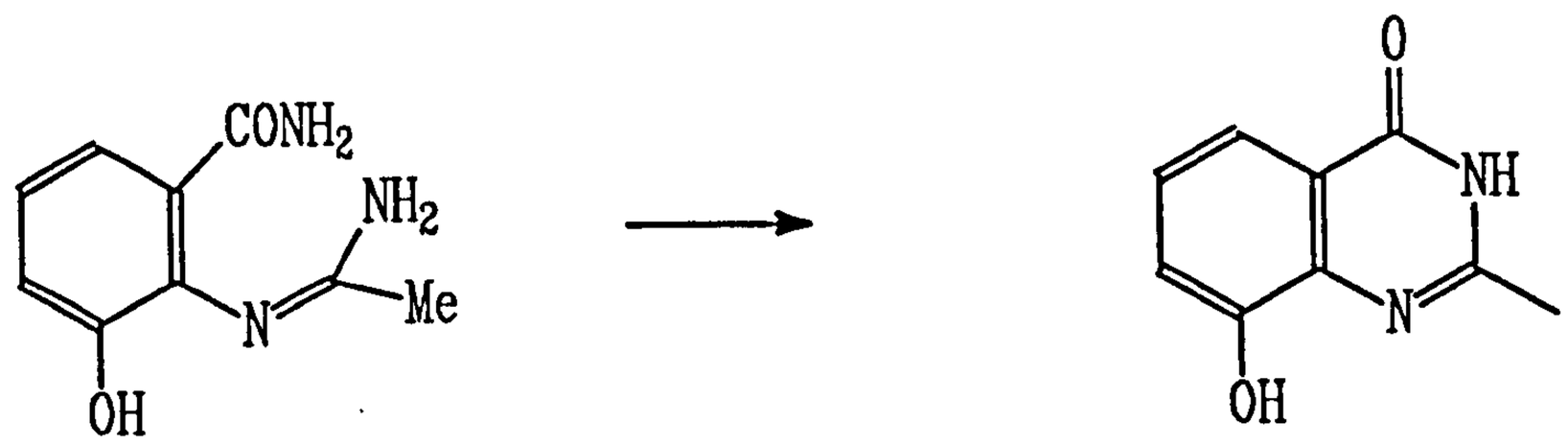

82'

Louise Pemberton has recently prepared the actual benzoxazole **82** (from the corresponding carboxylic acid, which was converted into its acid chloride and treated with aqueous ammonia at room temperature). She has now prepared a series of isomeric benzoxazole and quinazolinone carboxamides. The ^{1}H and ^{13}C NMR of the benzoxazoles show characteristic differences from those of the quinazolinones. By comparing the spectroscopic data for compound **80** with data for authentic benzoxazole and quinazolinone carboxamides, it is concluded that **80** is actually 8-hydroxy-4(*3H*)-quinazolinone (**80'**). Experiments are in progress to determine the precise mechanism of conversion of **84** into **82'**.

A striking feature of the ^{1}H NMR spectrum of the title compound is the difference in chemical shift of the two acidic protons. One appears as a broad hump at δ 11.75 and is thought to be the proton that is at position three, whilst the other proton, the phenolic proton, appears as a narrower hump at δ 8.01. The aromatic protons appear as two double-doublets and a triplet. The furthest downfield of these signals is the H5 double-doublet (δ 7.30) which is proximate to the carbonyl carbon. The triplet (δ 6.94) is H6 which lies next to the other double-doublet, H7 (δ 6.88). Lastly, the

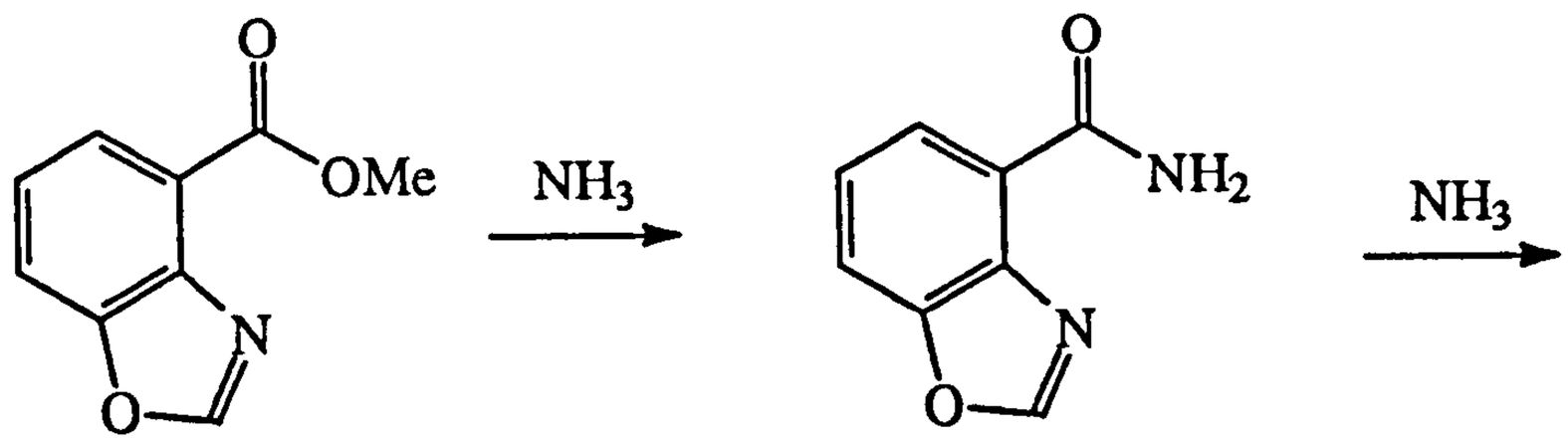

86 80

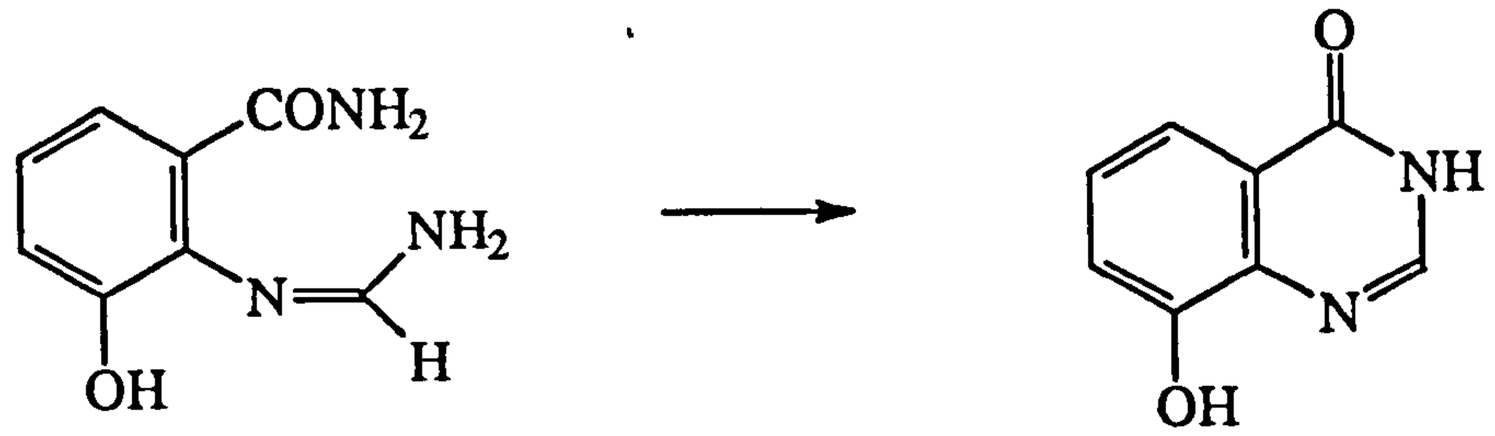

80'

methyl appears as a singlet at δ 2.14.

4.4.4 8-Hydroxy-4(3*H*)-Quinazoline (80')

The title compound was prepared from methyl 2-amino-3-hydroxybenzoate (**84**) by reaction with triethyl orthoformate. The methyl benzoxazole-4-carboxylate (**86**) was transformed into the quinazoline by the reaction with ammonia at high pressure (*cf* Scheme 14 and see above).

This compound has very similar spectroscopic properties to that of the 2-alkyl substituted analogue described earlier.

Table 15 **Potency of the 2-Alkyl and Non-Substituted 8-Hydroxy-4(3*H*)-Quinazolinones**

Compound No	80'	82'
Substituent	H	Me
% Inhibition at: 0.1 μM		17, 18
" 0.5 μM	18	59
" 1.0 μM	36, 39	63, 68
" 2.0 μM	54	
" 10 μM	78	92
" 30 μM	87	92
" 100 μM	95	96

These compounds were the most potent inhibitors against PARP thus far synthesised at Newcastle upon Tyne. As such it was considered worthwhile to obtain their IC_{50}'s (μM) against PARP. The IC_{50} (μM) of 8-hydroxy-2-methyl-4(3*H*)-quinazoline (**82'**) is 0.385 ± 0.039 which compares favourably with the value obtained for the literature inhibitor, 3,4-dihydro-5-methoxy-1(2*H*)-isoquinolinone, of 0.40 ± 0.033.

Chapter 5

5.1 The Nature of the Amide Functional Group

It appears that the amide functional group is essential for the inhibitors of PARP to be potent. This can be rationalized by supposing that a hydrogen type bond is formed within the binding site of the enzyme to the carbonyl oxygen of the amide. A consequence of this is that the strength of this bond will depend upon the amount of electron density upon the oxygen. A large amount of electron density will give a strong bond and hence potency to the inhibitor. Thus, if this supposition is correct, a correlation between potency and the extent of electron donor carbonyl ability will be observed. Organic chemists often predict qualitatively the extent of carbonyl donor ability within molecules, thus an aromatic amide with an electron donating group at the *para* position has a stronger electron donor carbonyl group than the corresponding compound that has an electron withdrawing group at the *para* position. However, in order to determine a correlation between the extent of carbonyl donation and inhibitory potency, a quantitative measure of carbonyl electron donation capacity is required.

5.1.1 The Determination of Charge Distribution About a Molecule

A number of physical properties of a molecule depend upon charge distribution about that molecule. The measurement of these physical properties can thus give an indication of the extent of electron density upon the carbonyl oxygen of an inhibitor of PARP. The techniques used to measure some of these physical properties are:

(i) *X*-ray Analysis

(ii) NMR Spectroscopy

(iii) IR Spectroscopy

(i) *X*-ray Analysis

X-ray analysis is a method that determines the charge distribution or (synonymously) electron density about a molecule. Hence, it is possible to use this technique to determine the electron density about the carbonyl oxygen of a potential inhibitor of PARP.

(ii) NMR Spectroscopy

The chemical shift of a nucleus is dependent upon the electron density about that nucleus. Thus, the less the electron density about the nucleus, the further downfield (the greater ppm) the nucleus' signal will appear within an NMR spectrum. This phenomenon can be applied very simply to the amide carbonyl group by measuring the chemical shift of this carbonyl carbon in the ^{13}C NMR spectrum of the molecule. Thus, the greater the electron density upon the oxygen, the less there is on the carbon and therefore the further downfield the ^{13}C NMR signal will appear. Thus, in ^{13}C NMR spectroscopy there is a quick and convenient method for determining the amount of electron density upon the carbonyl carbon atom. Care must be used when applying this technique. The chemical shift of a nucleus is related to the electron density about that nucleus since an opposing magnetic field is created by the movement of these electrons. It is the strength of this magnetic field that is responsible for the chemical shift of the nucleus. However, the magnetic field caused by the electrons about the measured nucleus is not the only magnetic field within the molecule that can affect the measured nucleus. Fields created by electrons about bonds and nuclei at relatively large distances from the nucleus under inspection may be strong enough to alter the chemical shift of that nucleus. So for this reason, even though this technique is valid, it can only be applied with caution.

(iii) IR Spectroscopy

This technique probes the vibrational properties of the bonds of a molecule. Briefly, a sample is bathed in IR light to produce a spectrum (either by the continuous wave or Fourier transform experiment). The spectrum produced consists of a plot of absorbance against wavenumber (the reciprocal of wavelength); thus an absorbance is seen within the spectrum where the frequency of the IR vibration is equal to the vibrational frequency of a chemical bond within the molecule.

Characteristic vibrational frequencies within IR spectra for the different carbonyl functional groups are seen with aldehydes (1740 - 1720 cm^{-1}), ketones (1725 - 1705 cm^{-1}), carboxylic acids (1725 - 1700 cm^{-1}), esters (1750 - 1735 cm^{-1}) and amides (≈ 1650 cm^{-1} when primary and in solid state).[61,62] The cause of this difference can be ascribed to the proportions of the three forms of the carbonyl group shown in Figure 21. Further, the proportions of these forms 'a', 'b' and 'c', is dependent upon the electronegativities of the substituents X and Y. The greater the electronegativities of X and Y, the greater the proportion of form 'a' within the system. Similarly, the greater the electron donating capacities of X and Y the greater the proportion of form 'c'. Also, it can be seen that the greater the amount of form 'a', the higher the carbonyl stretching frequency (see Table 16).

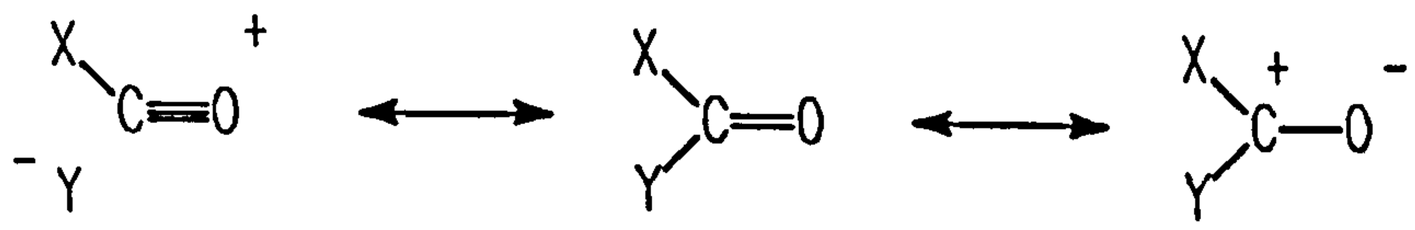

Carbonyl Carbon/Oxygen IR Stretching

Figure 21

Compound	ν(C=O)cm^{-1}
F.CO.F	1928
F.CO.Cl	1868
F.CO.H	1834
Cl.CO.Cl	1827
H.CO.H	1745

Table 16

It follows that the greater the amount of form 'c', the lower the wavenumber of the carbonyl bond.

In this technique there is an excellent probe for the determination of electron density upon the oxygen atom of the carbonyl bond.

5.1.2 The Cephalosporins and Penicillins

A similar situation exists in the cephalosporins and penicillins: a labile lactam functional group. The lability of this group and hence drug activity has been investigated by researchers using a number of different techniques including IR spectroscopy.[63,64,65] It was known from biological work that the penicillins (88) and Δ3 - cephalosporins (89) were active against a number of strains of bacteria whilst Δ2 - cephalosporins (90) were found to be inactive toward the same strains of bacteria (see Figure 22 for structures).

The crystal structures of these classes of compounds show that the lactam nitrogen in

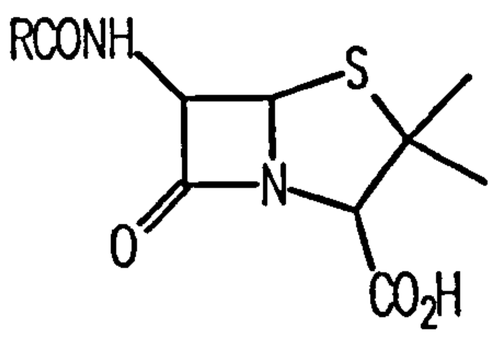

88

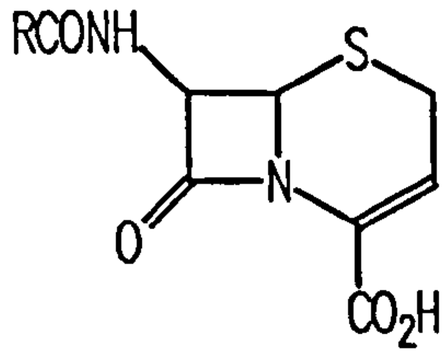

89

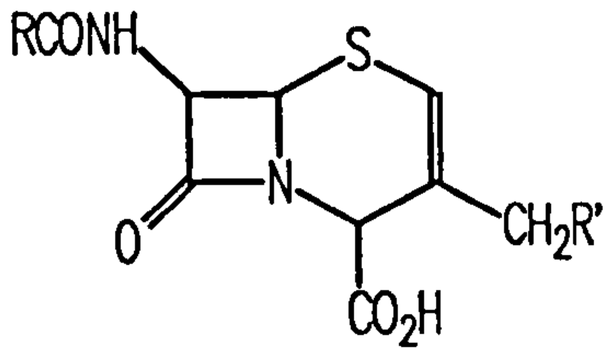

90

Structures of the Cephalosporins and Penicillins

Figure 22

the biologically active comounds (**88** and **89**) is pyramidal whilst the similar nitrogen in the inactive compounds is planar. The biologically inactive compound was also found to have a shorter, carbonyl carbon to nitrogen, bond length. Finally, IR correlation studies showed that the biological activity of the compounds increased as the carbonyl lactam stretching bond increased.

Compound	ν(CO)/cm^{-1}	Active
Penicillins	1780 - 1770	Yes
Δ^3 - cephalosporins	1776 - 1764	Yes
Δ^2 - cephalosporins	1760 - 1756	No

Table 17

The biological activity of these compounds was also seen to increase with ease of basic hydrolysis of the lactam amide bond. All these results can be rationalized by considering the two lactam canonical forms shown in Figure 23.

In structure, **91a**, the nitrogen of the β-lactam is pyramidal, its carbonyl IR stretch is

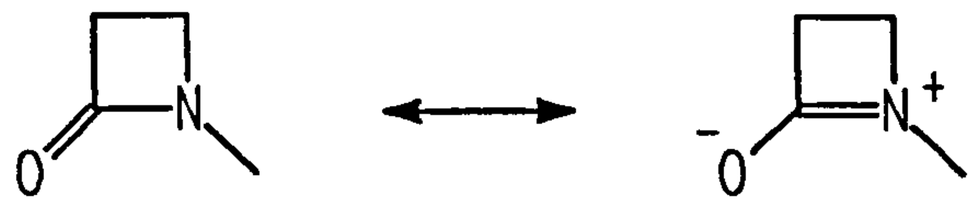

91a 91b

The Canonical Forms of the Beta Lactam Ring

Figure 23

indicative of a short C=O bond and the lactam is susceptible to base hydrolysis. For the structure, **91b**, to occur the ring must be planar, allowing the nitrogen lone pair to overlap with the C=O system. The single bond character of the carbonyl group gives the compound a shorter IR wavenumber value and further, this structure is not the optimum structure for base hydrolysis to occur (since the LUMO of the carbonyl carbon is occupied by the nitrogen lone pair electrons). It is structure **91a**, that is the biologically active form and any compound that has a certain proportion of this canonical structure will have a greater biological activity.

5.1.3 PARP Inhibitors and Activity-Structure Correlations

By making comparisons with literature work it seems entirely probable that a correlation between PARP inhibitory potency and IR carbonyl amide stretch (or ^{13}C chemical shift) will be seen. However, there are a number of reasons why a correlation may not be seen.

In the previous activity-structure correlation study there has only been one parameter (lactam lability) that has been responsible for the compound's activity. In PARP inhibitors the full extent of structural properties other than that of the amide carbonyl is not known and in this way the correlation may be obscured. Thus, although the amide may have the optimum charge distribution it may have an inappropriate

substituent elsewhere within the molecule making the inhibitor inactive. A means of avoiding this problem is to place the inhibitors into classes of similar compounds and only make comparisons within the same class. However, even when inhibitors belong to the same class of compounds correlations between the degree of inhibition of these compounds and their spectroscopic properties are difficult to make. Thus, the 3-(purine-9-alkyloxy)benzamides, as exemplified in tables **18** and **19** show no correlations. For example, 3-(6-chloropurine-5-pentyloxy)benzamide (**38**) shows 16 % inhibition of PARP at 10 μM concentration whilst 3-(6-chloropurine-5-dodecyloxy)benzamide (**40**) shows practically no inhibition at the same concentration (10 μM). Their spectroscopic properties however have a mean deviation of 0.0105 ppm between their ^{13}C chemical shifts and a mean deviation of 2 cm^{-1} between their $IR_{C=O}$ stretching frequencies.

Table 18

Compound Number	δ_C C=O / ppm	$IR_{C=O}$ / cm^{-1}	Inhibition 10 μM	30 μM	100 μM
38	167.925	1680	16	38, 45	68, 71, 74
39	167.927	1686	26, 31, 32	Insol	Insol
40	167.946	1684	2, 0	5, 20	3

Table 19

Compound Number	δ_C C=O / ppm	$IR_{C=O}$ / cm^{-1}	Inhibition 10 μM	30 μM	100 μM
41	167.963	1682	16	38, 45	65, 69
42	167.998	1678	41, 29, 20	NA	Insol
43	167.986	1679	14, 37	52, 51, 50	73, 75

Thus, for the technique of inhibition and spectroscopic property correlation to be tenable the compounds in question should show a large degree of inhibition and share the same mechanism of inhibition.

Chapter 6

6.1 Vinyl Chloride

Vinyl chloride (9), the starting material for the industrial synthesis of the plastic polyvinyl chloride (PVC), is established as a human carcinogen. Exposure to this compound over a period of time can lead to the rare cancer, angiosarcoma of the liver (so rare, that in 1974 there were only 20 to 25 cases per year of this cancer in the USA[66] and only 3 to 4 cases per year in England and Wales[67]). Three of the reported cases of liver angiosarcoma occurred in workers at an American plant manufacturing PVC.[68] Further investigation of the company personnel led to the identification of 2 cases who had died some years previously[69] and to the identification of 2 additional cases among the current workers.[70,71] A British study of 7000 men who were exposed to vinyl chloride in the manufacture of PVC between 1940 and 1974, concluded that vinyl chloride could cause liver cancer in a very few workers exposed to the chemical. There was no evidence that vinyl chloride causes cancers other than those of the liver.[72]

The ultimate carcinogen of vinyl chloride is produced by metabolic activation in the liver. Thus, inhalation of vinyl chloride and liver metabolism lead to the characteristic excretion products found in the host's urine (*eg* *S*-(2-hydroxyethyl)cysteine **92**, *N*-acetyl-*S*-(2-hydroxyethyl)cysteine **93**, *S*-carboxymethylcysteine **94** and thiodiglycolic acid **95**).[73,74,75,76,77] Application of the Ames test to vinyl chloride showed a greater mutagenicity when liver microsomes were present within the reaction medium.[78] Furthermore, liver microsomes were found to catalyse the covalent attachment of vinyl chloride to macromolecules.[79] Other studies have demonstrated liver microsomal uptake of ^{14}C-vinyl chloride and its transformation to protein alkylating metabolites *in vitro*.[80] Lastly, vinyl chloride metabolites have been shown to react with RNA both *in vitro* and *in vivo* to form 1,N^6-ethenoadenosine (**96**)[81] and 3,N^4-ethenocytidine (**97**).[82]

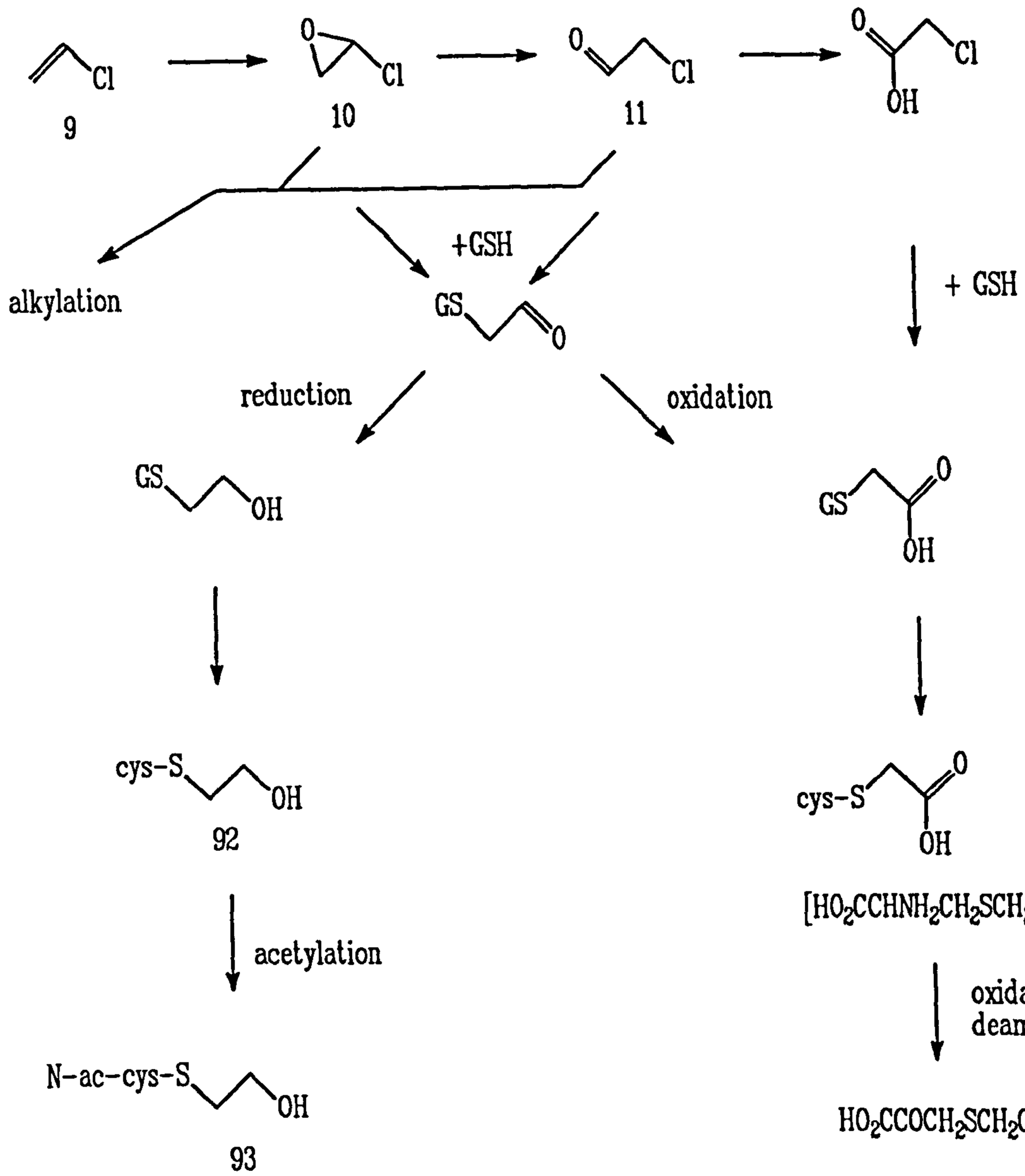

The Metabolic Activation of Vinyl Chloride

Scheme 15

The ultimate carcinogen of vinyl chloride is either chlorooxirane (**10**) or chloroacetaldehyde (**11**). Initially, chlorooxirane (**10**) is formed in the liver in the manner depicted in Scheme 15.[74] This compound (**10**) then rearranges, either spontaneously or by acidic catalysis, to chloroacetaldehyde (**11**). Spontaneous rearrangement (*nb* the half life of chlorooxirane in aqueous solution at physiological pH was found to be 1.6 minutes)[83] occurs when a carbon oxygen bond of the oxirane cleaves to a corresponding zwitterion (**98a** or **98b**), which forms chloroacetaldehyde by either a 1,2-hydride (**98a**) or a 1,2-chloride (**98b**) shift. Acid catalysed rearrangement begins with oxygen protonation, which is followed by carbon oxygen bond cleavage to give the cation **99**. Deprotonation of **99** forms an enol which tautomerises to chloroacetaldehyde (see Scheme 16).

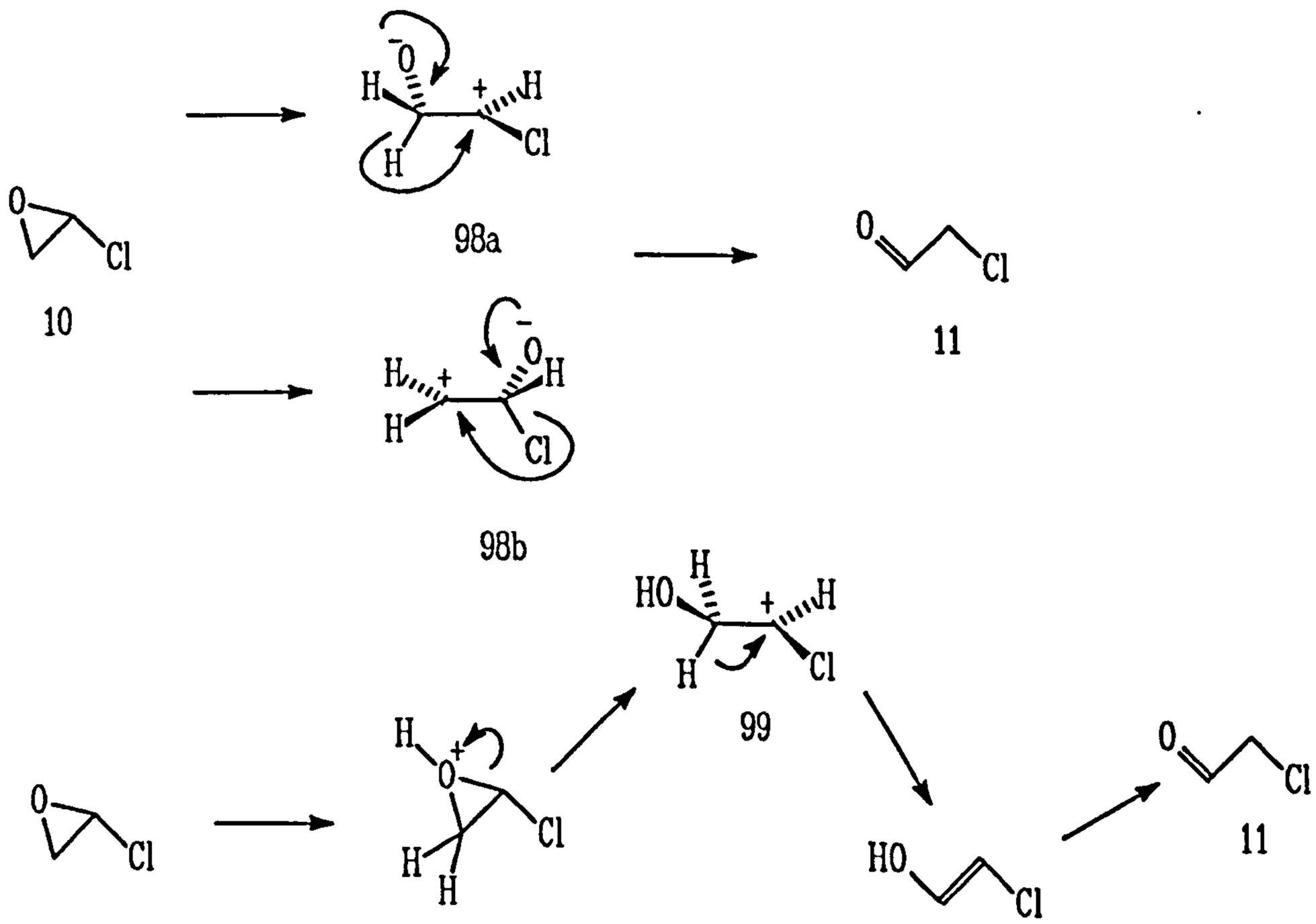

The Rearrangement of Chlorooxirane to Chloroacetaldehyde

Scheme 16

Both chlorooxirane (**10**) and chloroacetaldehyde (**11**) have been shown to be mutagenic,[83] but because chlorooxirane is more reactive than chloroacetaldehyde it has been suggested that the former compound is the ultimate carcinogen of vinyl chloride.[84,85] Even so, further studies have been undertaken to determine the mechanism of the mutagenesis caused by chloroacetaldehyde,[86] since this compound is exposed to DNA for a longer time than chlorooxirane.

6.1.2 The Reaction of Chloroacetaldehyde with Nucleosides

Chemical carcinogenesis occurs when a chemical interacts with the DNA of a cell. In

100 102

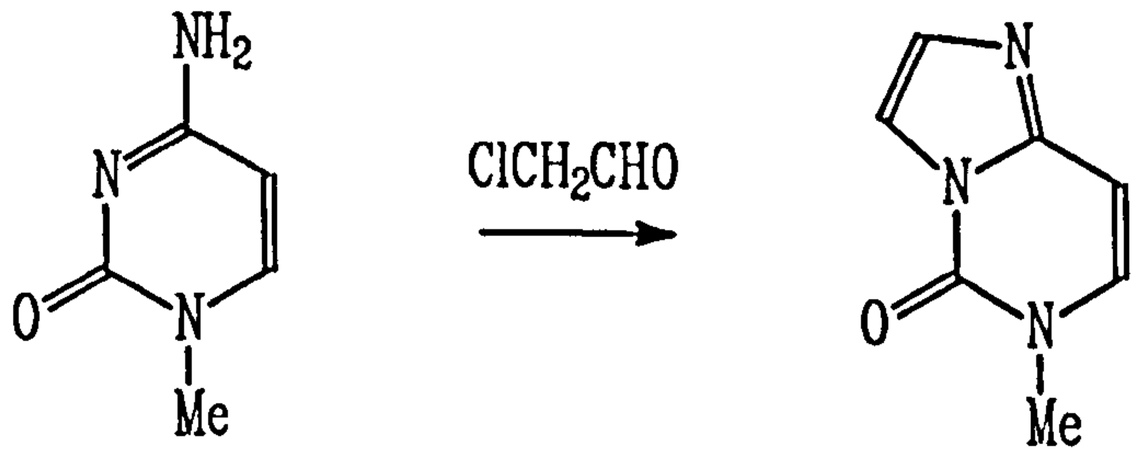

101 103

The Preparation of *N*9-Methylethenoadenine and *N*1Methylethenocytosine

Scheme 17

this process the integrity of the bases of DNA is corrupted and this, if not repaired, can lead to cell mutation. This cell mutation may lead to the formation of a cancerous cell. Therefore, an understanding of the chemistry between carcinogens and nucleosides will lead to a greater understanding of chemical carcinogenesis. Chloroacetaldehyde has been used to modify DNA and RNA with a view to investigating the structural and functional properties of these molecules. The conditions for these reactions were established using N^9-methyladenine (**100**) and N^1-methylcytosine (**101**) as model compounds.[87] It was found that chloroacetaldehyde reacted with N^9-methyladenine in slightly acidic aqueous solution to form N^9-methylethenoadenine (**102**, see Scheme 17). Similarly, the interaction of N^1-methylcytosine with chloroacetaldehyde in acidic aqueous solution gave N^1-methylethenocytosine (**103**, see Scheme 17). The modification of these adenine and cytosine species under such mild conditions led to the investigation of the reaction of chloroacetaldehyde with the four common nucleosides.

Aqueous solutions of ribonucleoside (each 0.01M) were incubated with 1 M chloroacetaldehyde (pH 2.0 - 5.0, 50 °C). Adenosine (**104**) was found to form ethenoadenosine (96, optimum pH = 4.5) while cytidine (**105**) formed ethenocytidine (97, optimum pH = 3.5). However, no reaction was observed with uridine (**106**) or guanosine (**107**). The specificity of chloroacetaldehyde for the adenine and cytidine species was further confirmed by a paper chromatographic study.

The products of the chloroacetaldehyde modification of nucleic acid bases, 1,N^6-ethenoadenosine (**96**) and 3,N^4-ethenocytidine (**97**), are fluorescent.[88] The special spectroscopic properties of these compounds suggest a number of applications *eg* the extended conjugation of 1,N^6-ethenoadenosine shifts its absorption spectrum to longer wavelengths allowing excitation to occur outside the range of the absorption of proteins and nucleic acids. The fluorescence of 1,N^6-ethenoadenosine (λ_{max} 415 nm in buffered aqueous solution at pH = 7.0) has a Stokes shift of 104.5 kJ mol^{-1}, which

is in a favourable position for detection in the presence of protein fluorescence. The quantum yield for this compound was found to be close to 0.6 and it had a fluorescent lifetime of 20 nanoseconds, which meant that if it was bound to molecules as large as 250 kDa, their rotation could still produce appreciable depolarisation of the emitted fluorescence. The biological activity of some of the adenine coenzymes was preserved to a large extent in the corresponding etheno compounds with certain enzymes. Both 'etheno' ATP and ADP were found to be enzymatically active in tests with hexokinase, adenylate kinase, pyruvate kinase, phosphofructokinase, tyrosine-activating enzyme and polynucleotide phosphorolyase.

6.1.3 Reaction Mechanism of Chloroacetaldehyde with either Adenosine or Cytidine

One application of the base modification of nucleic acids by chloroacetaldehyde was the examination of the tertiary structures of tRNA's in solution. When a tRNA is incubated with a buffered chloroacetaldehyde solution[89] any exposed adenine or cytosine moieties form etheno derivatives. For example, this technique was used to study the conformational changes occurring in yeast $tRNA^{Phe}$ after Y-base excision.[90] Before tRNA's were modified with chloroacetaldehyde the reaction at the monomer level was re-investigated.[91,92,93] The optimum pH of the reaction (adenine at pH = 4.5 and cytosine at pH = 3.5) was confirmed, but at higher pH's guanine modification was observed. The specificity of the reaction for adenine and cytosine was therefore maintained by keeping the pH in the region 3 to 4.

The reaction mechanism proposed[93] consisted of alkylation, cyclisation and dehydration. Thus, when the reaction was followed by TLC an intermediate (either the alkylation product or the cyclisation product) was observed. Attempts at isolating this intermediate (by preparative TLC) gave a compound that was contaminated (≈ 5%) by the etheno product. However, analysis of this mixture showed the following:

no covalently bound chlorine was present within the intermediate; the molecular mass was that of the hydrated etheno product; ^{1}H NMR spectroscopy (of the cytosine system) clearly showed the presence of an ABX system. All of these facts led to the conclusion that the intermediate is the cyclic compound that occurs before dehydration to the etheno product. The reaction mechanism can be described by Scheme 18. In the mechanism proposed (Scheme 18), the orientation of attack of chloroacetaldehyde is assumed. There is no direct evidence that the exocyclic nitrogen of the base reacts with the carbonyl carbon of chloroacetaldehyde, whilst the endocyclic nitrogen of the base reacts with the methylene carbon of chloroacetaldehyde. If the exocyclic nitrogen of the base reacts with the methylene carbon of chloroacetaldehyde and the endocyclic nitrogen of the base reacts with the carbonyl carbon, a reaction sequence can be envisaged (see Scheme 19) that is consistent with the data presented above. A hydrated etheno intermediate is formed that has no covalently attached chlorine, has the same molecular mass as the hydrated etheno compound in Scheme 18 and should have an ABX system in its ^{1}H NMR spectrum.

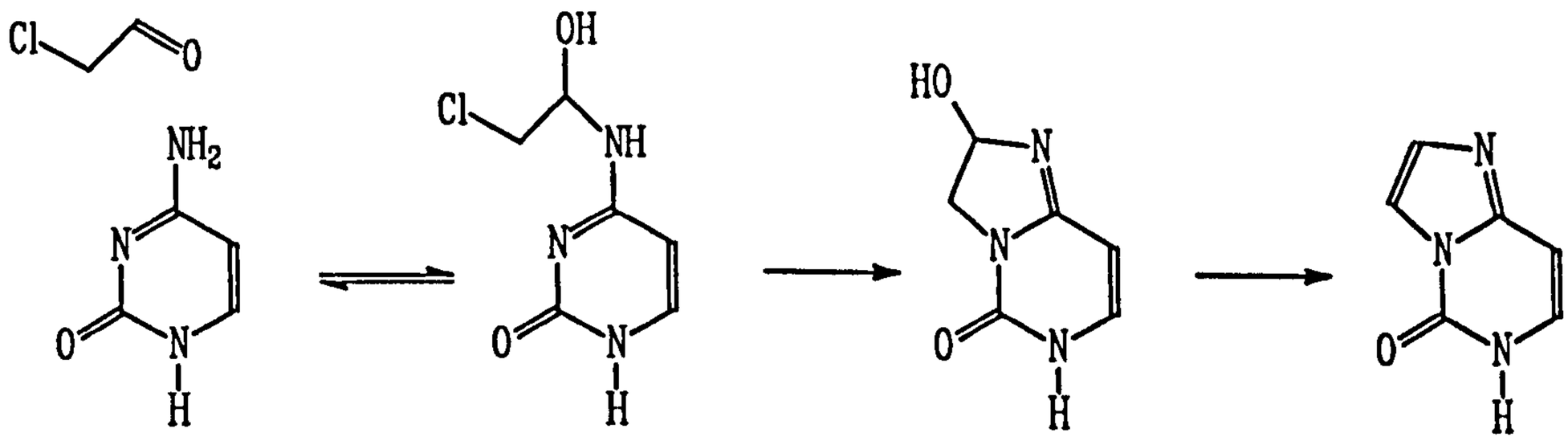

The Proposed Etheno- Forming Reaction Mechanism of Chloroacetaldehyde

Scheme 18

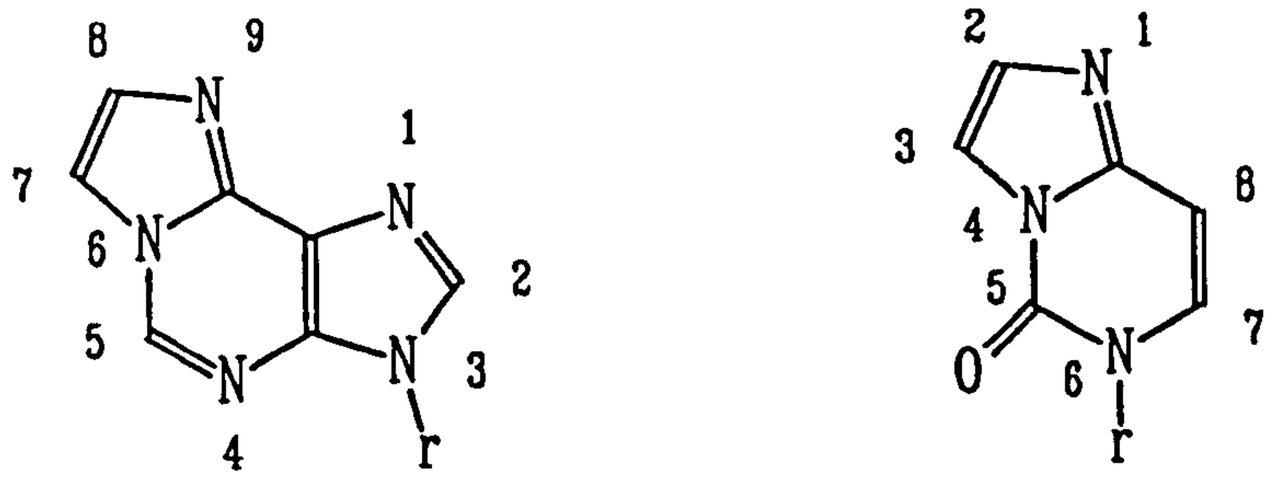

The Systematic Numbering of Ethenoadenosine

and Ethenocytidine

Figure 24

Nomenclature. The compound ethenoadenosine (96) has the systematic name 3-β-D-ribofuranosylimidazo[2,1-i]purine, while ethenocytidine (97) has the systematic name 5,6-dihydro-5-oxo-6-β-D-ribofuranosylimidazo[1,2-c]pyrimidine. The systematic names will be used as a basis for naming any intermediates, while the etheno names will be kept for the end products. The systematic numbering is given in Figure 24.

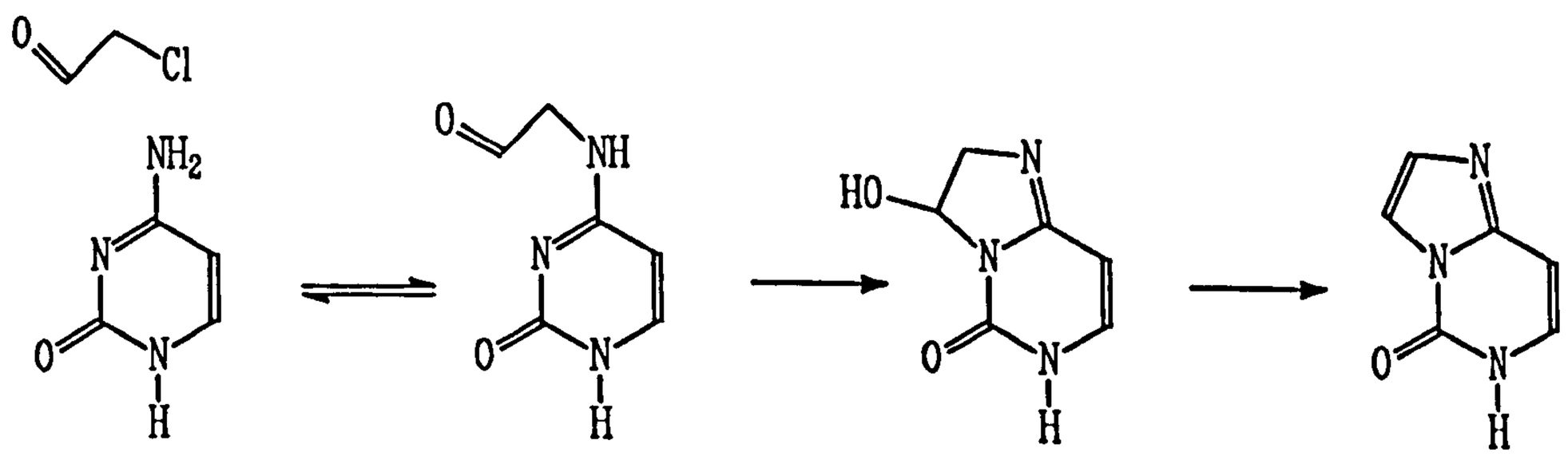

The Alternative Etheno- Forming Reaction Mechanism of Chloroacetaldehyde

Scheme 19

The following work investigates the orientation of attack of chloroacetaldehyde to nucleic acid bases.

The literature suggests that the orientation of attack is such that the exocyclic amine reacts with the carbonyl carbon. This seems to be the case when 2-bromobutanal reacts with adenosine,[94] because the crystal structure of the product shows that it is 7-ethyl-3-β-D-ribofuranosylimidazo[2,1-i]purine (**108**, see Scheme 20).

However, this result does not prove the orientation of attack of chloroacetaldehyde with adenosine.

6.1.3.1 The Carbinolamine Intermediate

The orientation of the attack of chloroacetaldehyde to, for example, adenosine, is reflected in the structure of the carbinolamine intermediate formed. If the carbonyl carbon of chloroacetaldehyde is bonded to the exocyclic nitrogen, ring closure forms 7,8-dihydro-8-hydroxy-3-β-D-ribofuranosylimidazo[2,1-i]purine (**109**), while the opposite chloroacetaldehyde orientation forms 7,8-dihydro-7-hydroxy-3-β-D-

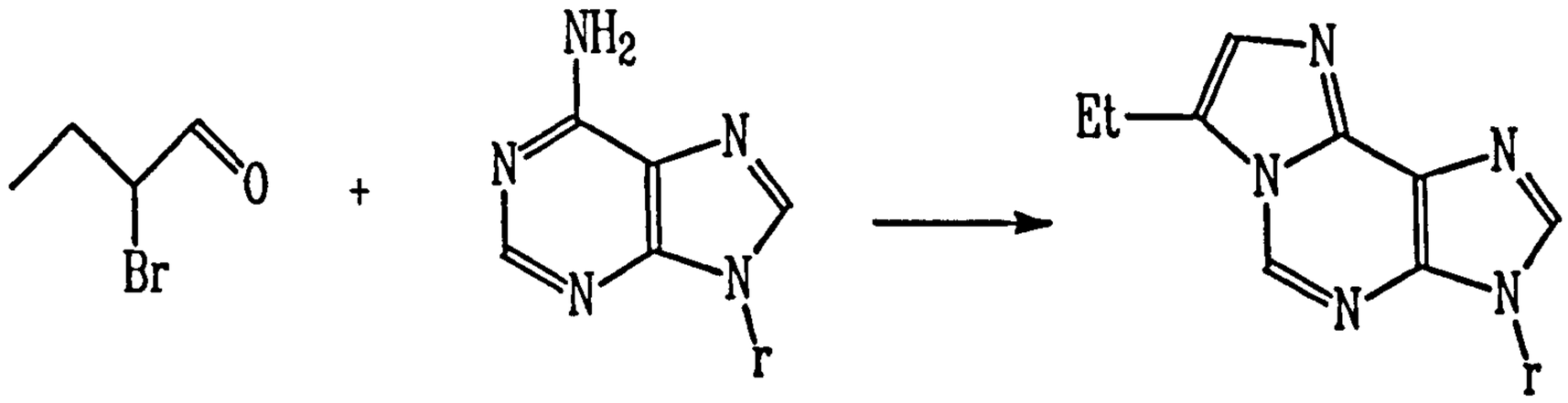

The Reaction of 2-Bromobutanal with Adenosine

Scheme 20

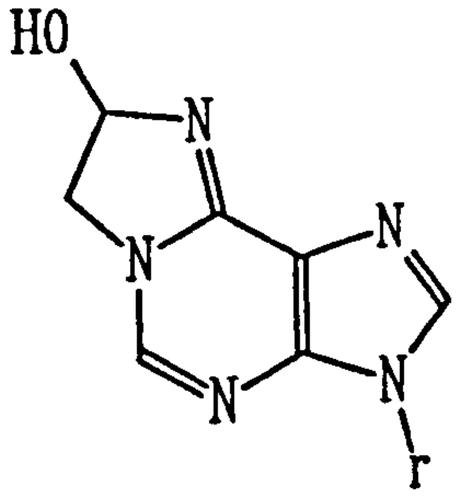

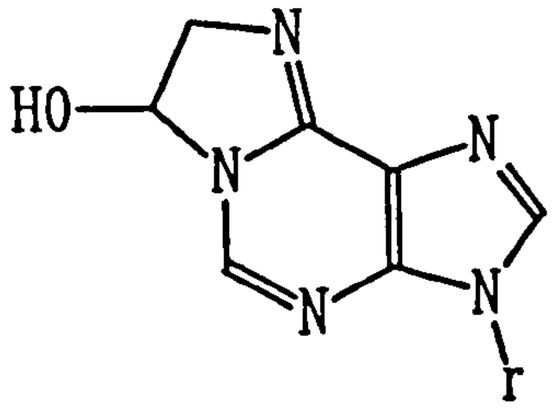

109 110

The Carbinolamine Intermediates of the Chloroacetaldehyde/Adenosine Reaction

Figure 25

ribofuranosylimidazo[2,1-i]purine (**110**, see Figure 25 and Figure 24 for numbering system).

6.1.3.2 Synthesis of N^6-(2,2-Dimethoxyethyl)adenosine (111)

In order to investigate the chloroacetaldehyde/adenosine reaction, N^6-(2,2-dimethoxyethyl)adenosine (**111**) was prepared. The synthesis of this molecule, in terms of the chloroacetaldehyde/adenosine reaction, means that:

(i) the exocyclic nitrogen (N^6) of adenosine has displaced the chloride anion of chloroacetaldehyde (*ie* the orientation of attack of chloroacetaldehyde to adenosine has been unambiguously defined)

(ii) reaction to the cyclic intermediate can be easily effected by mild acid catalysis and thus, the cyclisation (and subsequent dehydration) can be monitored.

The compound (**111**) was prepared by treating 6-chloropurinriboside (**112**) with 2,2-

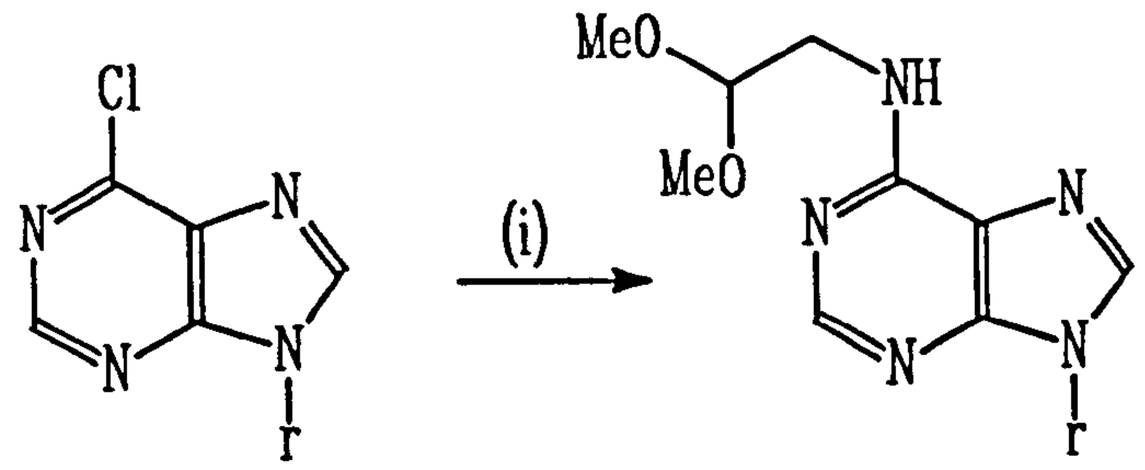

(i) 2,2-Dimethoxyethylamine and triethylamine in DMF

The Preparation of N^6-(2,2-Dimethoxyethyl)adenosine

Scheme 21

dimethoxyethylamine (**113**, see Scheme 21). The ^{1}H NMR spectrum of this compound was similar to that of adenosine.[95] The purine signals appeared in similar positions (H2, δ 8.40 and H8, δ 8.25) with the proton attached to the exocyclic nitrogen (N^6) appearing at δ 7.87. The signals for the protons attached to the ribose part of the molecule appeared in the same position as the corresponding adenosine signals. The ethyl protons were buried within this 'sugar' region. Thus the H2' multiplet had an integral that was consistent with the presence of an extra proton and this signal was assigned to the acetal carbon proton. Similarly, the methylene protons (α to the acetal carbon proton) were found within the H5',5" multiplet. The methoxy protons appeared as a singlet (δ 3.30).

6.1.3.3 The Acid Catalysed Decomposition of N^6-(2,2-Dimethoxyethyl)adenosine

A solution of N^6-(2,2-dimethoxyethyl)adenosine (**111**) was dissolved in d_4-methanol and acidified by the addition of acetyl chloride (1.1 equivalents). By placing this

mixture into the probe of an NMR spectrometer and heating to 60 °C the acid catalysed decomposition of this compound was observed, over a period of 64 hours, by ^{1}H NMR spectroscopy. The decomposition of this compound was found to follow the route depicted in Scheme 22.

The rationale advanced for the acid catalysed decomposition of N^6-(2,2-dimethoxyethyl)adenosine, as depicted in Scheme 22, was elucidated by the consideration of the ^{1}H NMR spectra obtained from the decomposition of this

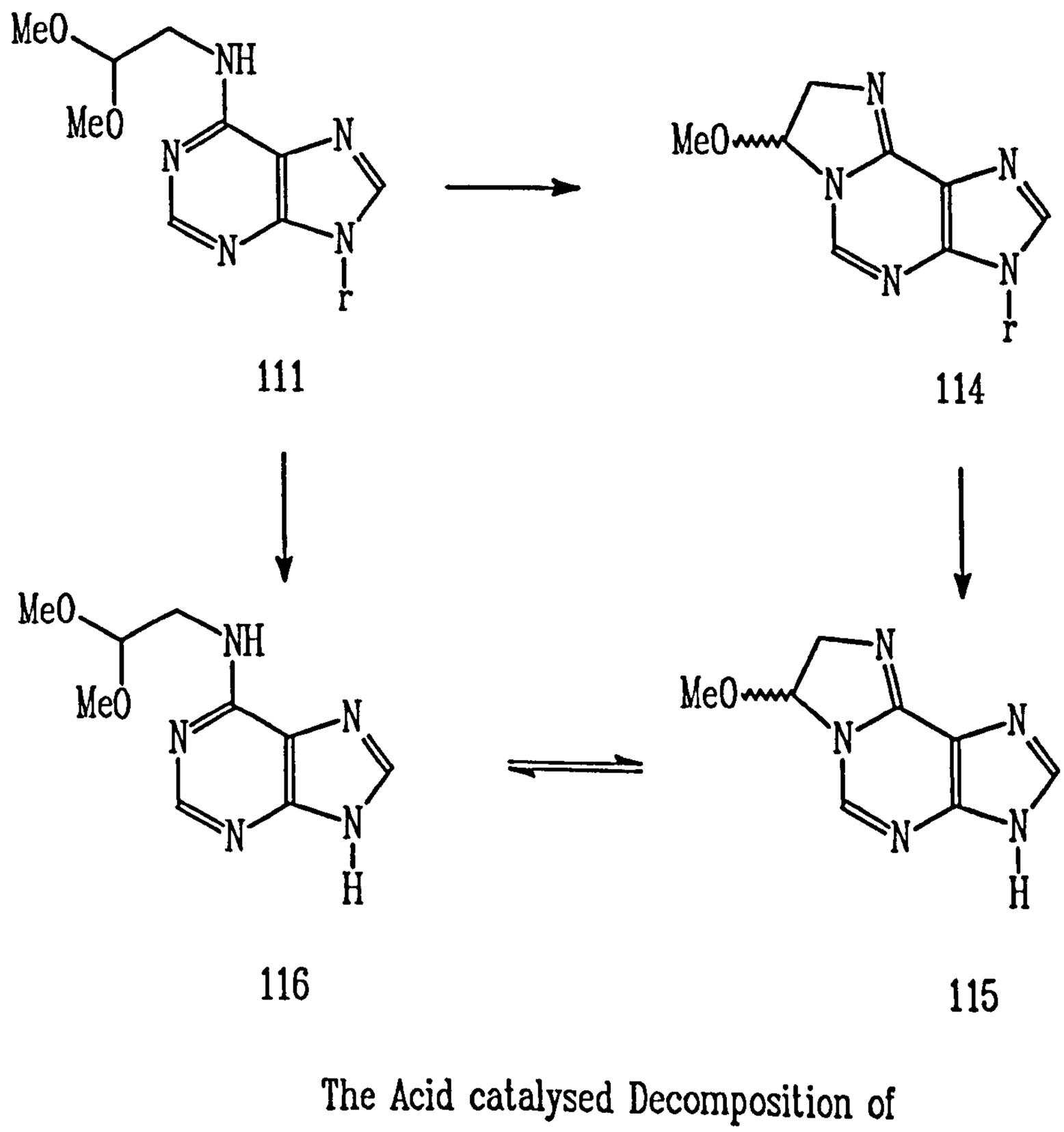

The Acid catalysed Decomposition of

N^6-(2,2-Dimethoxyethyl)adenosine

Scheme 22

compound. This rationale can be illustrated with five ^{1}H NMR spectra taken at time zero (or zero plus the time taken to load the NMR spectrometer and determine a spectrum), 40 min, 2 h, 8 h and 64 h.

At time zero (spectrum 8) all four compounds depicted in Scheme 22 are present within the reaction mixture. The two hemi-acetal/aminals (**114** and **115**) are represented by the protons of the *N*1-*N*6 ethyl bridge. Thus, the proton at position 7 of the two molecules appears as a broad doublet (δ 6.5). This signal is assumed to be made up of two overlapping double-doublets (*cf* spectrum 12, after 64 h). The two protons at the 8 position of one of the hemi-acetal/aminals begins to appear at δ 4.49 but does not appear as a double-doublet since the signal is masked by the H3' nucleoside signal. The two acetals (**111** and **116**) are represented by their 2-ethyl proton which appears as a triplet for each molecule. The depurinated acetal (**116**) has a triplet which appears at δ 4.87 while the analogous proton of the starting material (**111**) lies beneath the nucleoside H2' proton's signal. The methylene signals (1-ethyl) of either acetal were not distinct within this spectrum.

The second spectrum (spectrum 9, 40 min later), shows a relative increase in the amount of the hemi-acetal/aminals present, as represented by the signal at δ 6.5. Another feature of this signal was that it had slightly resolved itself into a double doublet at its apex. This indicated that, of the two hemi-acetal/aminals present, one of them was beginning to predominate (the depurinated 7-methoxy-3,7,8-trihydroimidazo[2,1-i]purine, **115**). Further, the part of the double doublet in view, which represents the methylene group at the 8 position of 7-methoxy-3,7,8-trihydroimidazo[2,1-i]purine (**115**), had increased in size. The acetal triplet of the starting material (δ 4.79) had markedly decreased in size, which was to be expected since this signal was affected by both depurination and cyclisation. The acetal triplet of the depurinated compound (**116**, δ 4.87) appeared slightly more distinct as the H2' nucleoside starting material signal decreased in size.

The Acid Catalysed Decomposition of N^6-(2,2-Dimethoxyethyl)adenosine - 0 h

Spectrum 8

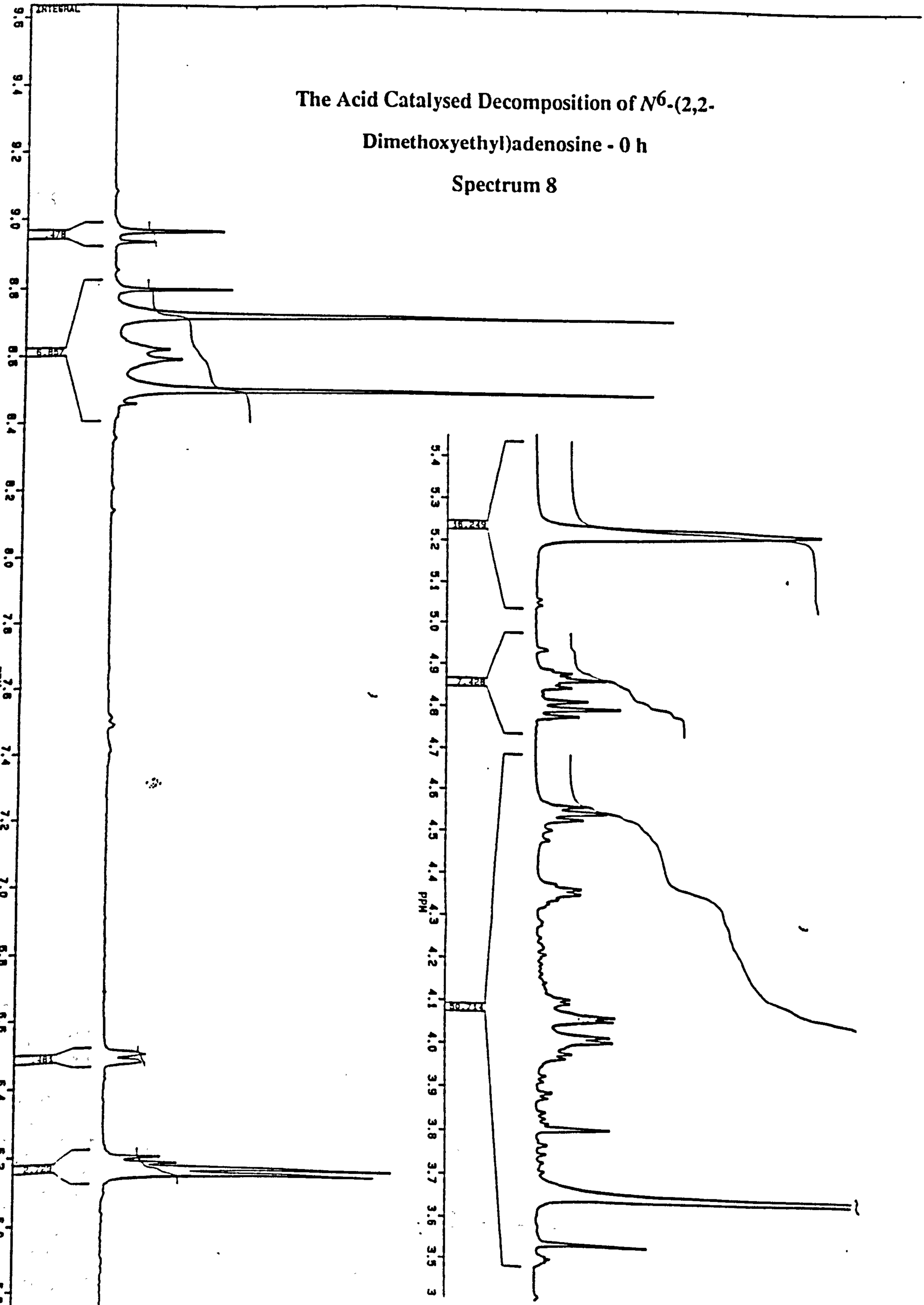

The Acid Catalysed Decomposition of N^6-(2,2-Dimethoxyethyl)adenosine - 40 min

Spectrum 9

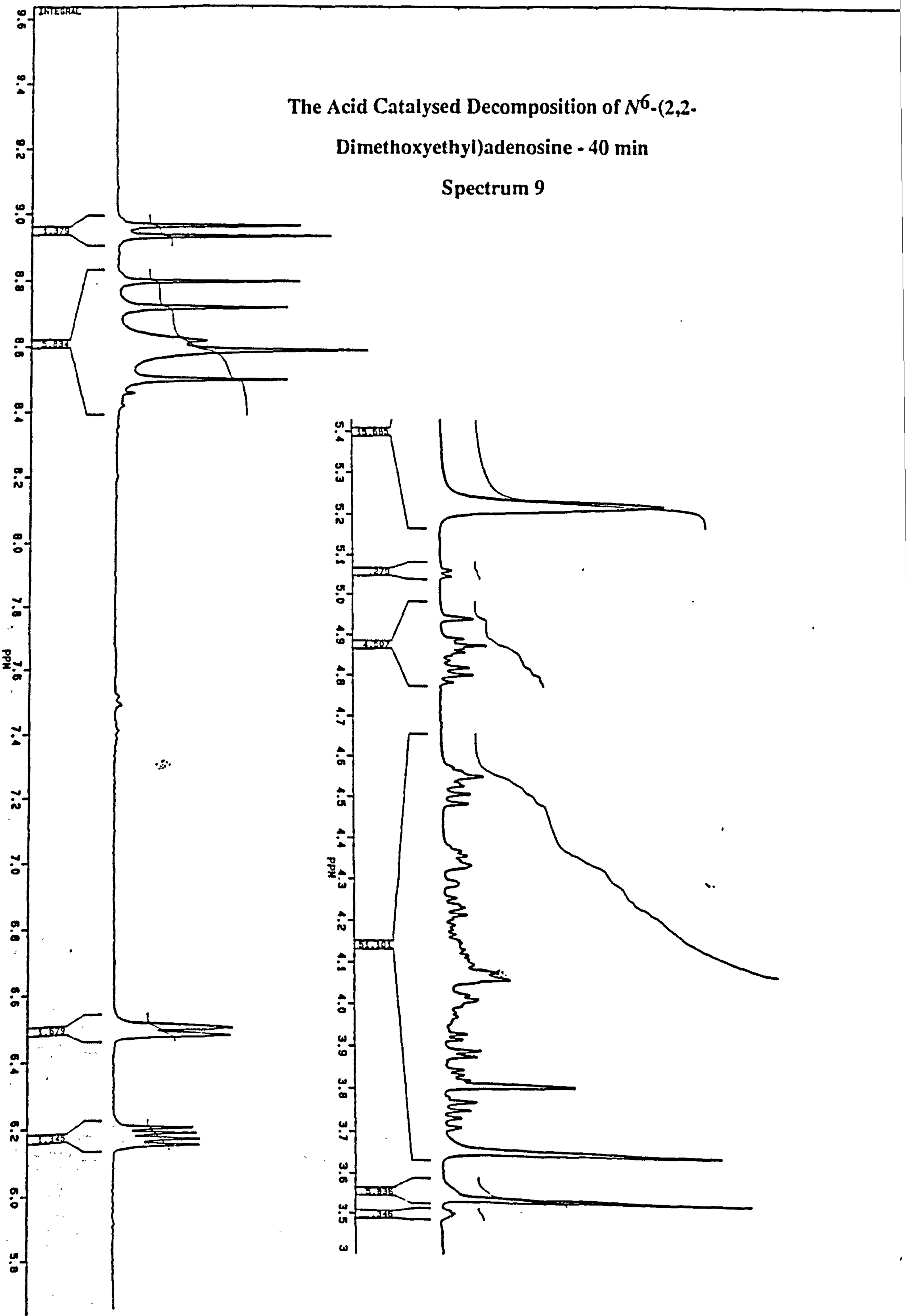

The Acid Catalysed Decomposition of N^6-(2,2-Dimethoxyethyl)adenosine - 2 h

Spectrum 10

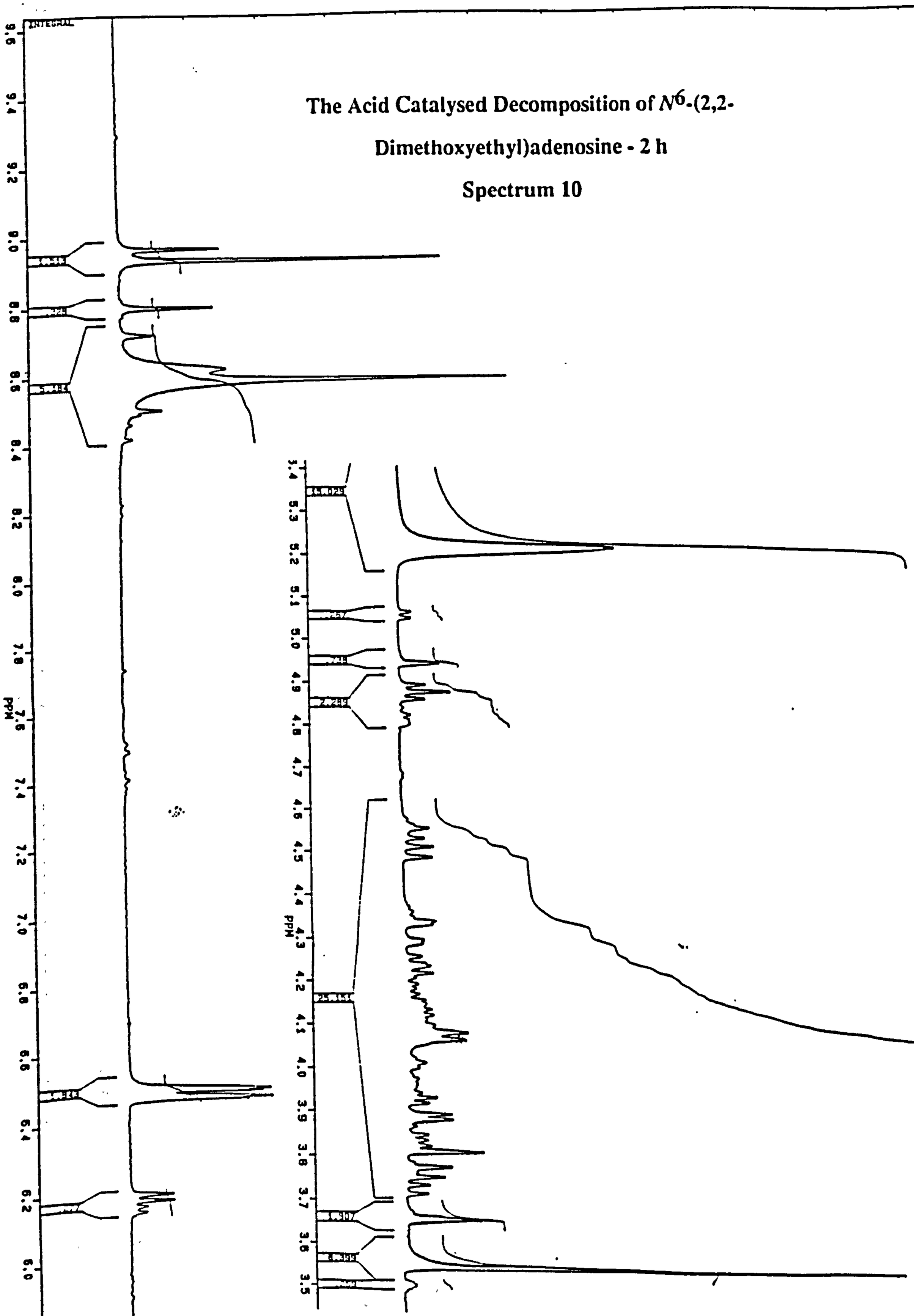

The Acid Catalysed Decomposition of N^6-(2,2-Dimethoxyethyl)adenosine - 8 h

Spectrum 11

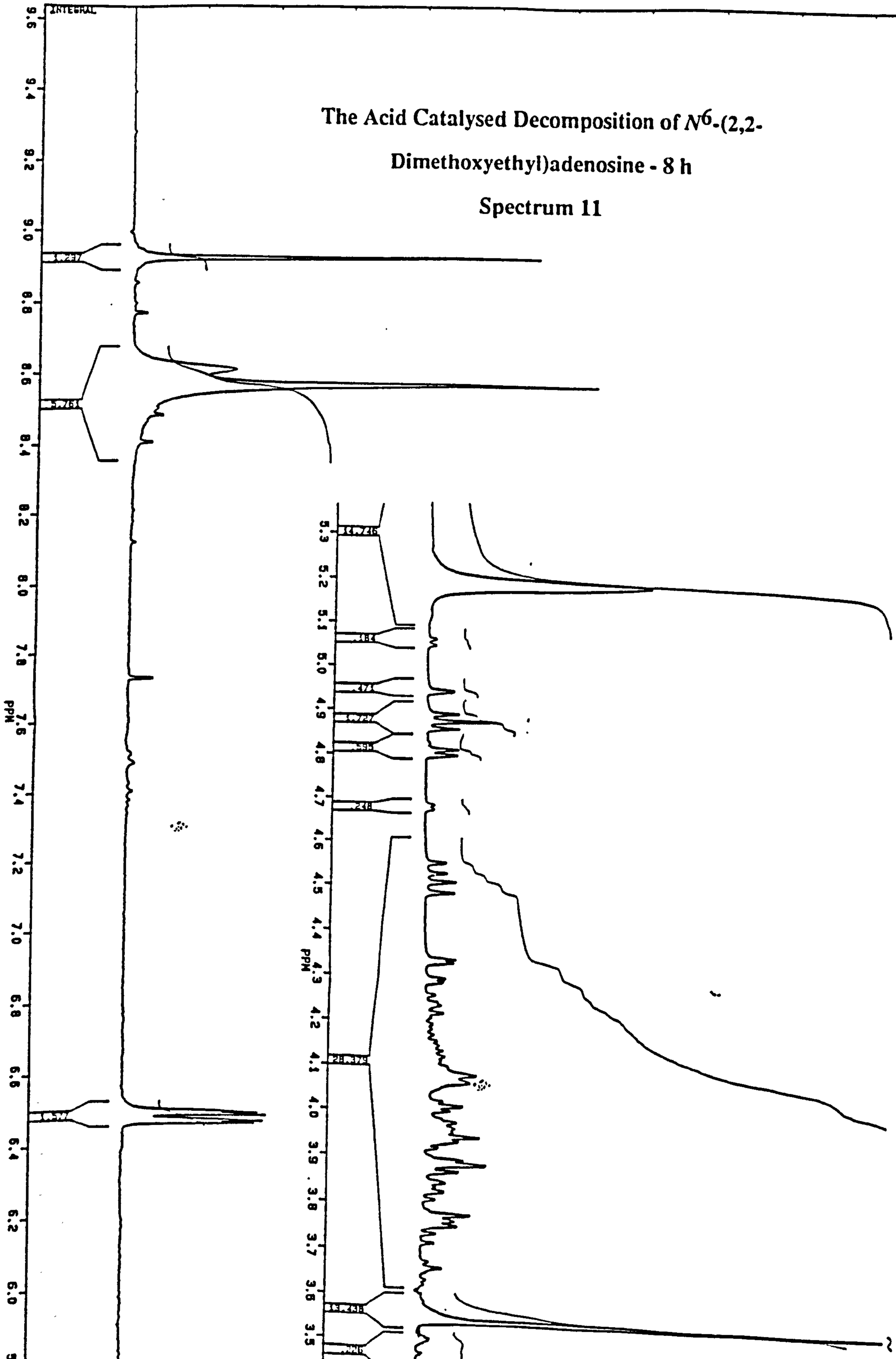

The Acid Catalysed Decomposition of N^6-(2,2-Dimethoxyethyl)adenosine - 64 h

Spectrum 12

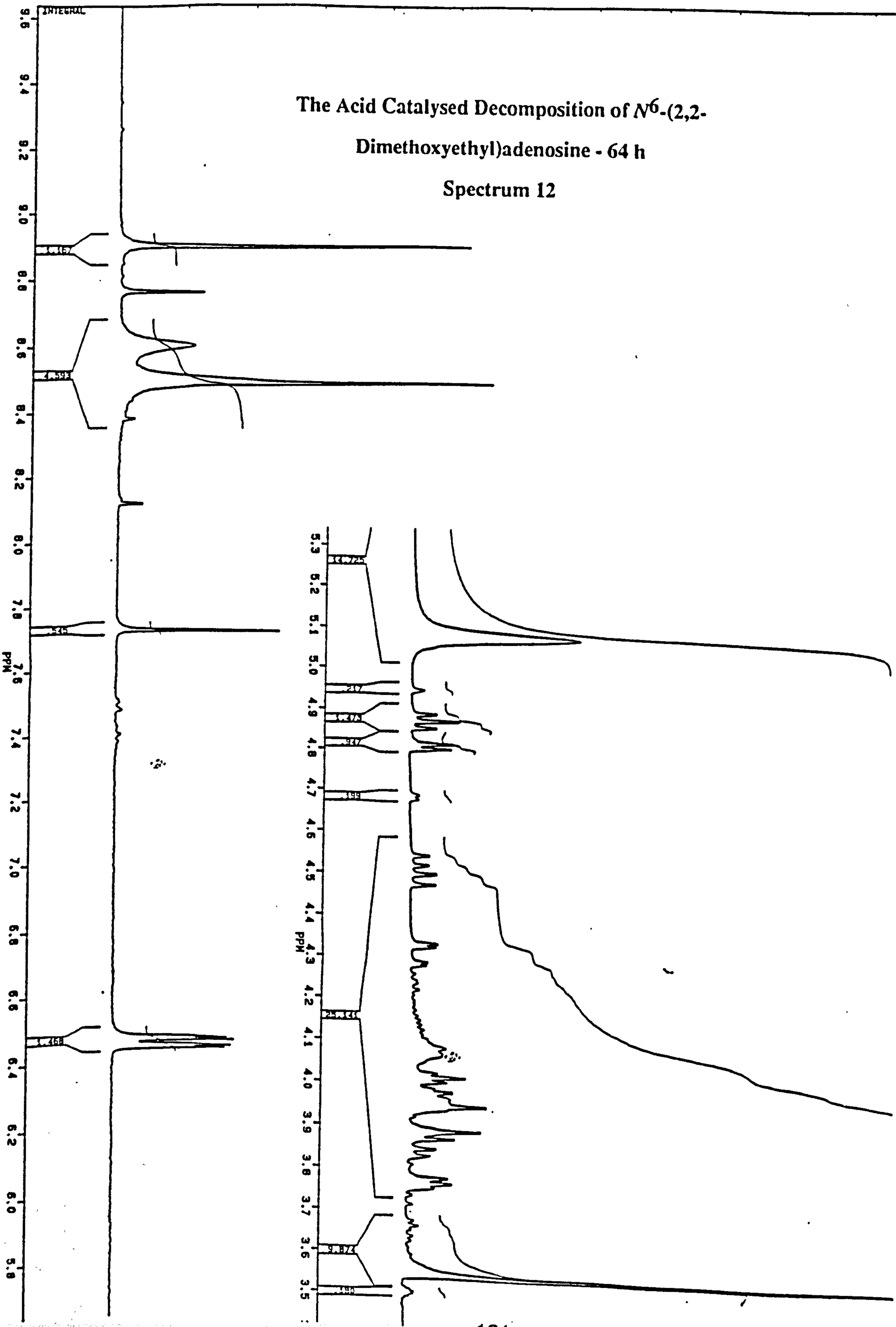

Two hours later (spectrum 10) the presence of the hemi-acetal/aminals had increased, which was indicated by the presence of the double doublet (δ 6.5) representing the proton on carbon 7 of these compounds. The signals produced by the two protons on carbon 8, two double doublets (δ 4.5 and δ 4.3), were increasing in size and clarity. The depurinated acetal, represented by the triplet (δ 4.87) produced by the proton on the acetal carbon, was now very prominent.

After eight hours (spectrum 11) the reaction was essentially complete. The double doublet (δ 6.5) representing the proton at position 7 of 7-methoxy-3,7,8-trihydroimidazo[2,1-i]purine (**115**) was clearly resolved. The double doublets representing the two protons at the 8 position of this compound (**115**) were clearly represented (δ 4.5 and δ 4.3), whilst the acetal proton of the depurinated compound appeared as a distinct triplet at δ 4.89. Finally, this spectrum indicated that the two depurinated compounds were in a proportion of about one to one.

The last spectrum (number 12, sixty four hours) showed no difference from that taken at eight hours.

6.1.3.4 The Depurination of N^6-(2,2-Dimethoxyethyl)adenosine

Throughout the course of the acid catalysed decomposition of N^6-(2,2-dimethoxyethyl)adenosine depurination occurs, *ie* the bond between N^9 of the purine and C1' of the sugar is cleaved. This process for adenosine has been shown to be unimolecular and acid catalysed (A_1),[96] which is what is expected for N^6-(2,2-dimethoxyethyl)adenosine. Under the conditions of the reaction, upon depurination, the sugar initially forms a mixture of α- and β-D-methylribofuranosides (**117** and **118**, see Scheme 23). The two furanosides formed are not stable but exist in a

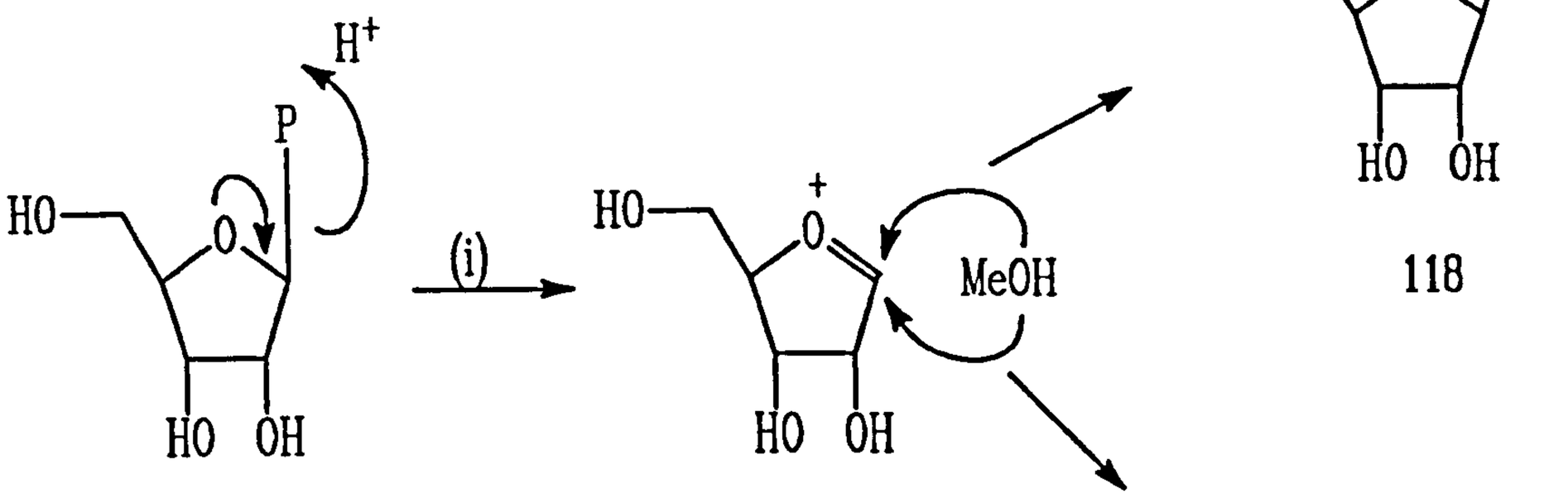

111 122 118

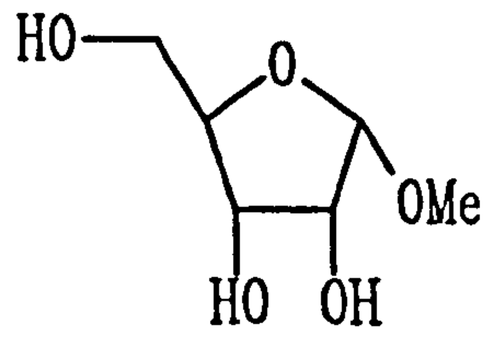

117

P = N^6-(2,2-dimethoxyethyl)adenyl

(i) d_4-MeOH + 1.1 equiv Acetyl Chloride

The Depurination of N^6-(2,2-Dimethoxyethyl)adenosine

Scheme 23

dynamic equilibrium with their corresponding pyranosides (α- and β-D-methylribopyranosides **119** and **120**, respectively). Protonation of the anomeric oxygen of a furanoside and attack by methanol at the anomeric carbon causes the molecule to ring open to a dimethyl acetal (**121**). Ring closure with the 5'-OH group rather than the 4'-OH forms the pyranosides. The pyranosides thus formed can revert to the furanosides in a similar manner and hence an equilibrium mixture of the four molecules is created within the reaction. The α and β anomers may be formed by two routes. The methoxy group of an anomer may be protonated and subsequently depart from the molecule to leave a cation (*eg* **122**, Scheme 23). Attack of this cation by methanol at either face of the anomeric carbon will form either an α or β anomer. The other route is *via* the dimethyl acetal which can ring close in the manner

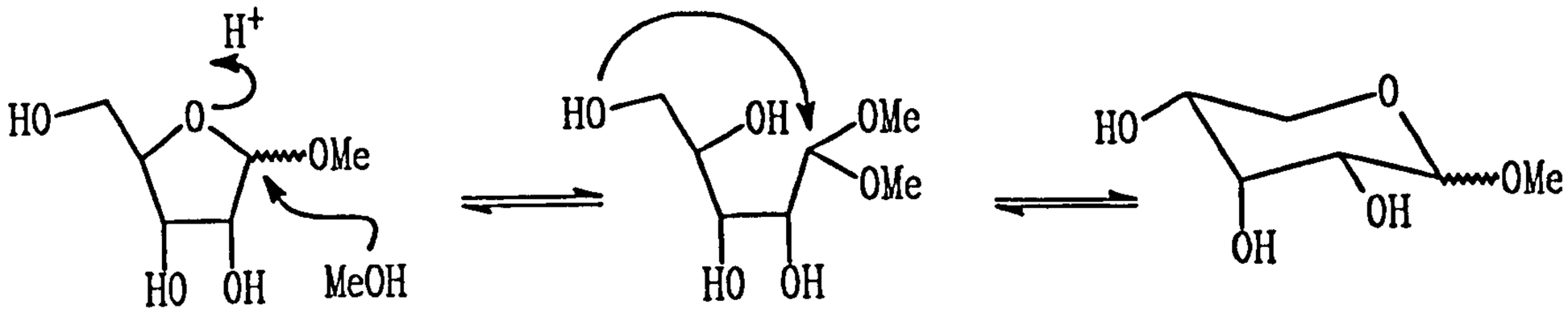

117, 118 121 120

The Mutarotation of Methyl Beta-D-Ribofuranoside

Scheme 24

described above but with attack at either face of the anomeric carbon. (see Scheme 24).

The acid catalysed depurination of N^6-(2,2-dimethoxyethyl)adenosine and subsequent mutarotation of the released D-methylriboside is described below and is presented as further evidence to corroborate the rationale depicted in Scheme 22.

At zero time (spectrum 8) the anomeric proton of the starting nucleoside is predominant and appears as a doublet at δ 6.18. The hemi-acetal/aminal (**114**) anomeric proton appears next to the starting material signal (δ 6.19) as a very small doublet. Further downfield in this spectrum it is possible to see that depurination has begun by the presence of the two furanosides. These two sugars are represented by their anomeric protons: a doublet at δ 5.05 (α-D-methylribofuranoside **117**) and a singlet at δ 4.92 (β-D-methylribofuranoside **118**).

In spectrum 9 (determined forty minutes later) the two anomeric doublets of the nucleosides, **111** and **114**, (δ 6.19 and δ 6.18, respectively) are in equal proportion but have decreased in size. Meanwhile the proportions of the two α- and β-D-methylribofuranosides have increased but it is not possible to determine whether or not any pyranosides are present within the system. This is because a signal from

another part of the molecule occupies the region where these signals are expected to occur (see below).

Two hours later (spectrum 10), the two nucleosides have almost completely disappeared whilst the two furanosides are clearly present with β-D-methylfuranoside (**118**) in predominance. A trace amount of α-D-methylribopyranoside (**119**) is seen at δ 4.65, but as yet it is not possible to say whether or not there is any β-D-methylribopyranoside (**120**) present.

Spectrum 11 (eight hours later) clearly shows the presence of the four mutarotated molecules of D-methylriboside with the β-D-methylribopyranoside (**120**) present in a slightly larger amount than the corresponding β-D-methylribofuranoside (**118**).

Sixty four hours later (spectrum 12) the four sugar molecules appear to be in the same proportion as they were after eight hours. Unfortunately α-D-methylribofuranoside (**117**) is indicated in this spectrum only by the presence of a shoulder on the methanol OH peak.

In order to corroborate the rationale depicted in Scheme 22, the following compounds were synthesised:

(i) N^6-(2,2-dimethoxyethyl)adenine (**116**)

(ii) 7-methoxy-3,7,8-trihydroimidazo[2,1-i]purine (**115**)

(iii) β-D-Methylribofuranoside (**118**)

and their ^{1}H NMR spectroscopic properties determined. Further, the ^{1}H NMR spectroscopic properties of β-D-methylribofuranoside were determined after standing in acidified d_4-methanol overnight and an attempt was made to synthesise 7,8-dihydro-7-methoxy-3-β-D-ribofuranosylimidazo[2,1-i]purine (**114**).

6.1.3.4 (i) The Synthesis of N^6-(2,2-Dimethoxyethyl)adenine (116)

The synthesis of the title compound was attempted by employing the same reaction conditions which were used in the synthesis of N^6-(2,2-dimethoxyethyl)adenosine. A mixture of 6-chloropurine, 2,2-dimethoxyethylamine and triethylamine was stirred together in DMF, but no reaction was observed by TLC. This was thought to be because triethylamine extracted the N^9 proton from 6-chloropurine to form a negatively charged species which repelled any nucleophiles that were present in the system. An attempt was made to overcome this problem by synthesising the protected purine: 6-chloro-*N*9-dimethylsilylthexylpurine. However this reaction proved difficult to follow and the silylated purine was never isolated.

A search of the literature was then made in an attempt to find a model compound, *ie* a compound that was prepared from 6-chloropurine (**124**) and a nitrogen nucleophile. The model compound found was N^6-benzyladenine (**123**) which was prepared by heating a mixture of 6-chloropurine and benzylamine (2.1 equivalents) in 2-methoxyethanol under refluxing conditions. This method was adapted to the preparation of the title compound by replacing benzylamine with 2,2-dimethoxyethylamine. Upon work up of the reaction mixture the title compound was obtained in good yield (see Scheme 25).

The ^{1}H NMR Spectrum of N^6-(2,2-Dimethoxyethyl)adenine (116)

The N^9 proton of the title compound appeared furthest downfield (δ 13.04) as a broad singlet. The two purine peaks, H2 (δ 8.03) and H8 (δ 8.21), appeared next to the N^6 proton's signal (a broad singlet at δ 7.65). The ethyl protons were poorly resolved

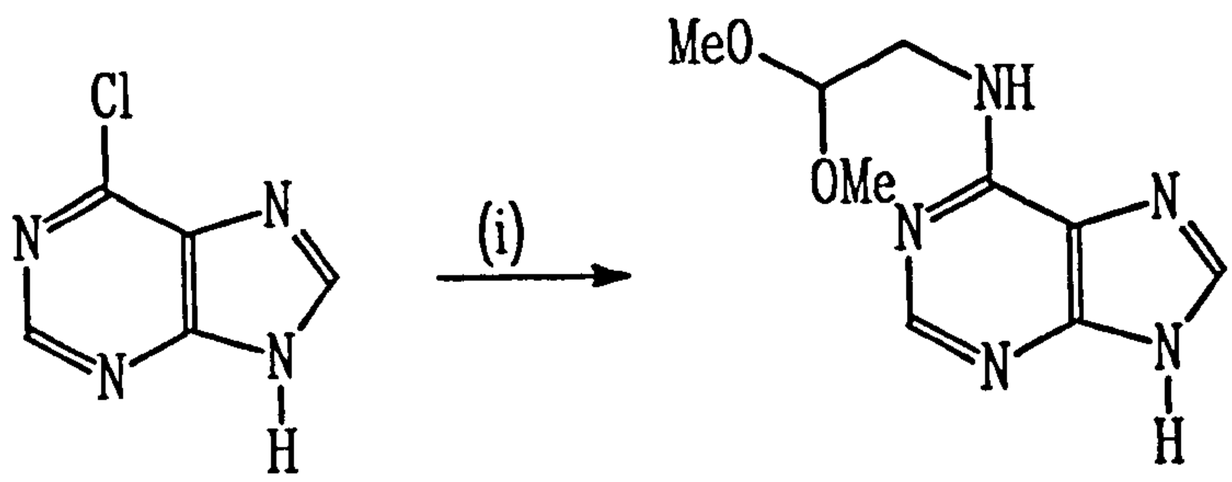

(i) 2,2-dimethoxyethylamine in

2-methoxyethanol.

The Preparation of N^6-(2,2-Dimethoxyethyl)adenine

Scheme 25

with the 2-ethyl proton appearing as a broad singlet (δ 4.74) while the 1-ethyl protons appeared as a broad singlet (δ 3.69). Lastly, the methoxy protons appeared as a singlet at δ 3.38.

6.1.3.4 (ii) The Synthesis of 7-Methoxy-3,7,8-trihydroimidazo [2,1-i]purine (115)

The title compound was prepared by heating a mixture of N^6-(2,2-dimethoxyethyl)adenine (**116**) and D-camphorsulphonic acid (1.1 equivalents) in acetonitrile under refluxing conditions. The apparatus was fitted with a Dean-Stark trap which had its solvent dead volume replaced with fresh solvent on an hourly basis. The reaction was thought to be a reversible reaction. By replacing the solvent, the concentration of the methanol in the system, which is liberated upon cyclisation, was decreased to zero. In this way the reaction was taken to completion (see Scheme 26).

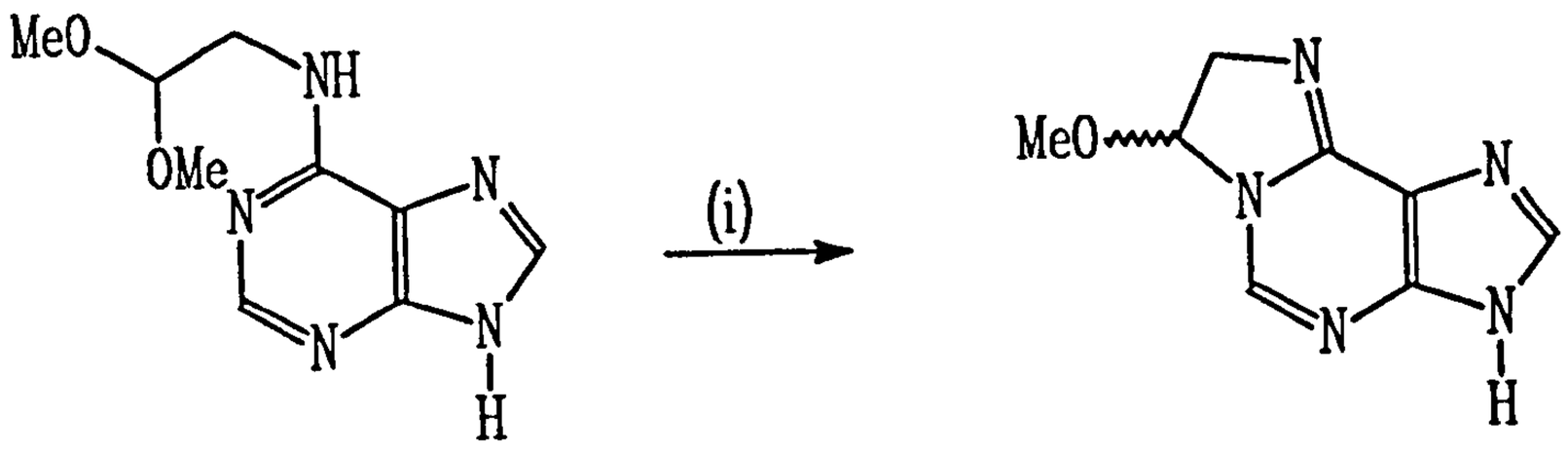

116 115

(i) D-Camphor Sulphonic Acid in

Acetonitrile

The Preparation of 7-Methoxy-3,7,8-trihydroimidazo

[2,1-i]purine

Scheme 26

The ^{1}H NMR Spectrum of 7-Methoxy-3,7,8-trihydroimidazo[2,1-i]purine (115)

The N^3 proton of the title compound appeared at δ 13.09. The purine protons, (H5 and H2) appeared at δ 8.75 and H8 δ 8.35 (respectively). The proton on carbon seven appeared as a double doublet (δ 6.25) coupled to two other double doublets (δ 4.18 and δ 3.98) which are the protons on carbon eight. Lastly, the methoxy protons appear as a singlet at δ 3.50.

6.1.3.4 (iii) The Synthesis of β-D-Methylribofuranose (118)

To a methanolic solution of D-ribose was added a catalytic amount of acetyl chloride; this mixture was then stirred and the reaction followed by TLC. After fifty minutes the starting material had disappeared and the reaction was quenched with sodium carbonate. In this manner the kinetic product β-D-methylribofuranose (**118**) was

obtained after work up and purification. (It was thought that the α anomer (**117**) was also formed but this did not crystallise out in the work up procedure).

The ^{1}H NMR spectrum of the title compound has a distinctive singlet peak at δ 4.92 which represents the anomeric proton H1'. The remaining protons are represented by multiplets appearing between δ 4.40 and δ 3.60, with the methoxy protons appearing as a singlet (δ 3.52).

A solution of β-D-methylriboside was prepared in d_4-methanol and acidified by a catalytic amount of acetyl chloride. This mixture was left to stand overnight and a ^{1}H NMR spectrum of the solution was obtained. This showed four anomeric protons indicating the presence all of the four forms of D-methylriboside. The anomeric protons of the four compounds appeared as follows (ref):

α-D-methylribofuranoside (**117**)	δ 5.09 doublet
β-D-methylribofuranoside (**118**)	δ 4.92 singlet
β-D-methylribopyranoside (**120**)	δ 4.81 doublet
α-D-methylribopyranoside (**119**)	δ 4.71 doublet

Therefore, the ^{1}H NMR evidence presented above supports the rationale of the acid catalysed decomposition of N^6-(2,2-dimethoxyethyl)adensosine depicted in Scheme 22.

6.1.3.5 The Attempted Synthesis of 7,8-dihydro-7-methoxy-3-β-D-ribofuranosylimidazo[2,1-i]purine (114)

In order to substantiate further the rationale of the acid catalysed decomposition of N^6-(2,2-dimethoxyethyl)adenosine (**111**), it was considered necessary to synthesize 7,8-dihydro-7-methoxy-3-β-D-ribofuranosylimidazo[2,1-i]purine (**114**). In principle,

this could be done by attaching a suitably modified ribose to 7-methoxy-3,7,8-trihydroimidazo[2,1-i]purine (**115**), a process known as nucleoside synthesis. Two requisites are necessary to achieve this process: the bond formed must be β and the sugar must react as a furanoside. Both of these requirements are usually satisfied by initial sugar modification. For example, 2-deoxyadenosine[97] (**125**) was formed when 6-chloropurine (**124**) and 1-chloro-2-deoxy-3,5-di-*O*-*p*-toluyl-α-D-erythropentofuranose (**126**) were reacted together and the product modified by methanolic ammonia. In this case the sugar was locked into its furan form by the initial formation of 2-deoxy-methylribofuranoside (**127**). This compound was then converted to the protected chloride (**126**) in the manner shown in Scheme 27.[98] Before adapting this literature procedure to the synthesis of 7,8-dihydro-7-methoxy-3-β-D-ribofuranosylimidazo[2,1-i]purine (**114**) a novel preparation of 2-

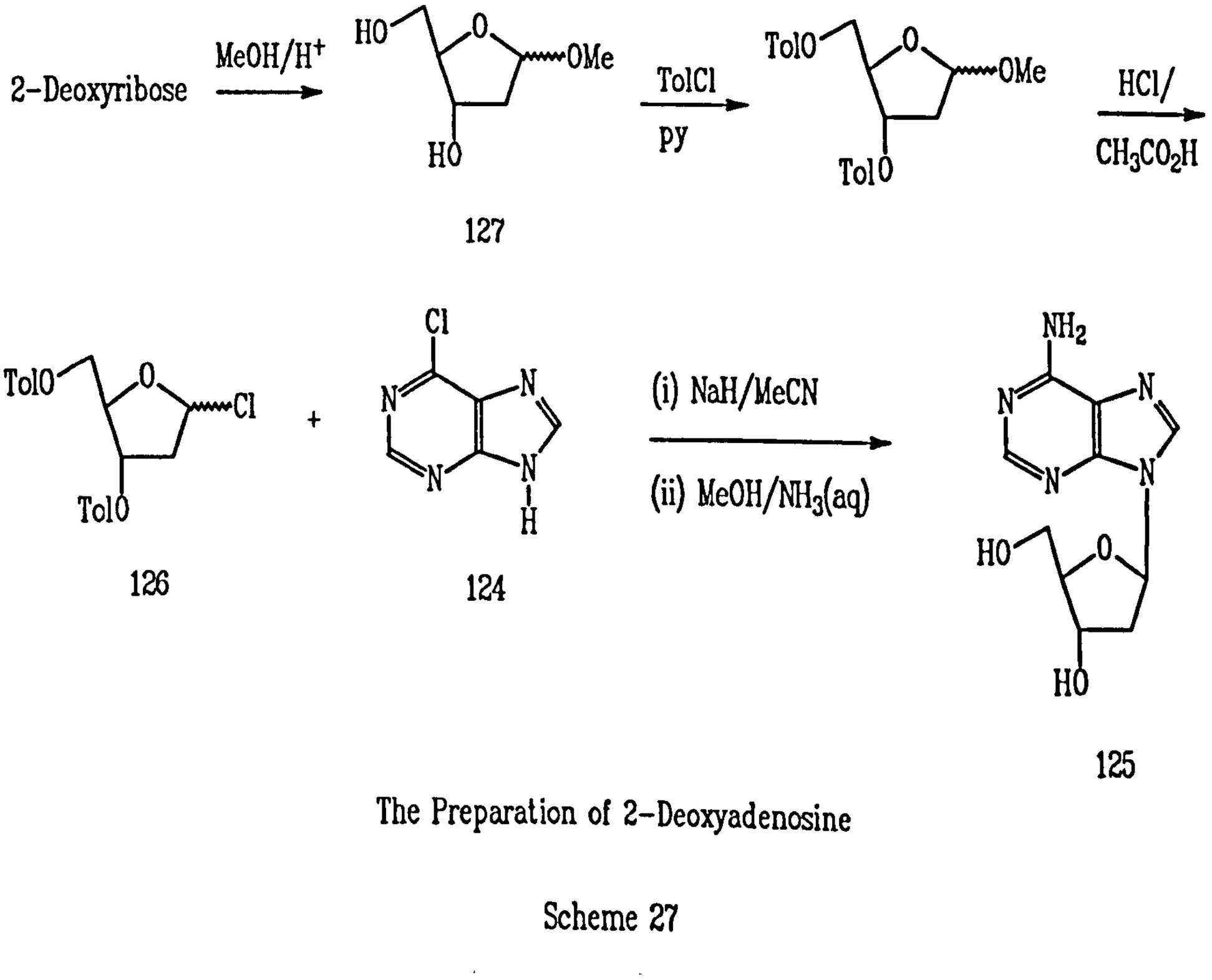

The Preparation of 2-Deoxyadenosine

Scheme 27

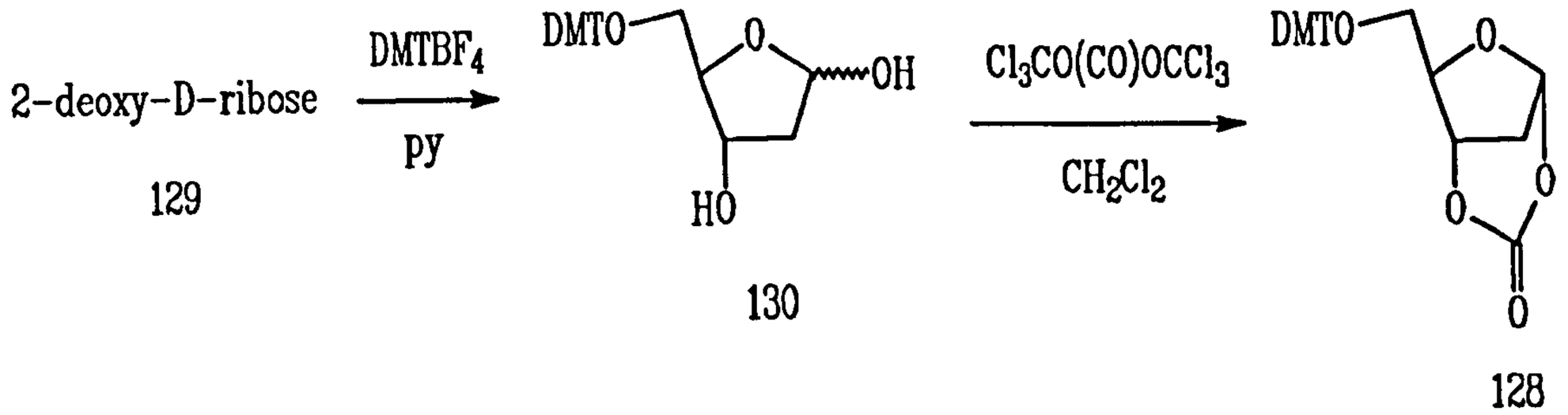

A Proposed 2-Deoxyribose Modification

Scheme 28

deoxynucleosides was explored. This consisted of the reaction of a base with 1,3-(5-(2,2'-dimethoxytrityl))-2-deoxyribofuranose carbonate (**128**) which was prepared by treating 2-deoxy-D-ribose (**129**) with 2,2'-dimethoxytriyltetrafluoroborate to give 5-(2,2'-dimethoxytrityl)-2-deoxyribofuranose[99,100] (**130**). This reaction locked 2-deoxy-D-ribose into its furanose form which was about to be activated by forming the carbonate (**128**, see Scheme 28).

The suitability of triphosgene (which was thought to be safer than phosgene) was tested by reacting it with 1,2-diphenylethanediol (**131**). The reaction yielded the carbonate *cis*-4,5-diphenyl[1,3]dioxalan-2-one (**132**) but unfortunately the reaction conditions were not applied to 5'-(2,2'-dimethoxytrityl)-2'-deoxyribofuranose (**128**).

6.1.3.6 The Dehydration of the Carbinolamine Intermediate

When chloroacetaldehyde reacts with adenosine, ethenoadenosine is formed by dehydration of a carbinolamine intermediate (either **109** or **110**, Figure 25). This dehydration goes *via* one of two carbocations, the nature of which is dependent upon the precursor carbinolamine. Thus, the proposed 7,8-dihyro-8-hydroxy-3-β-D-

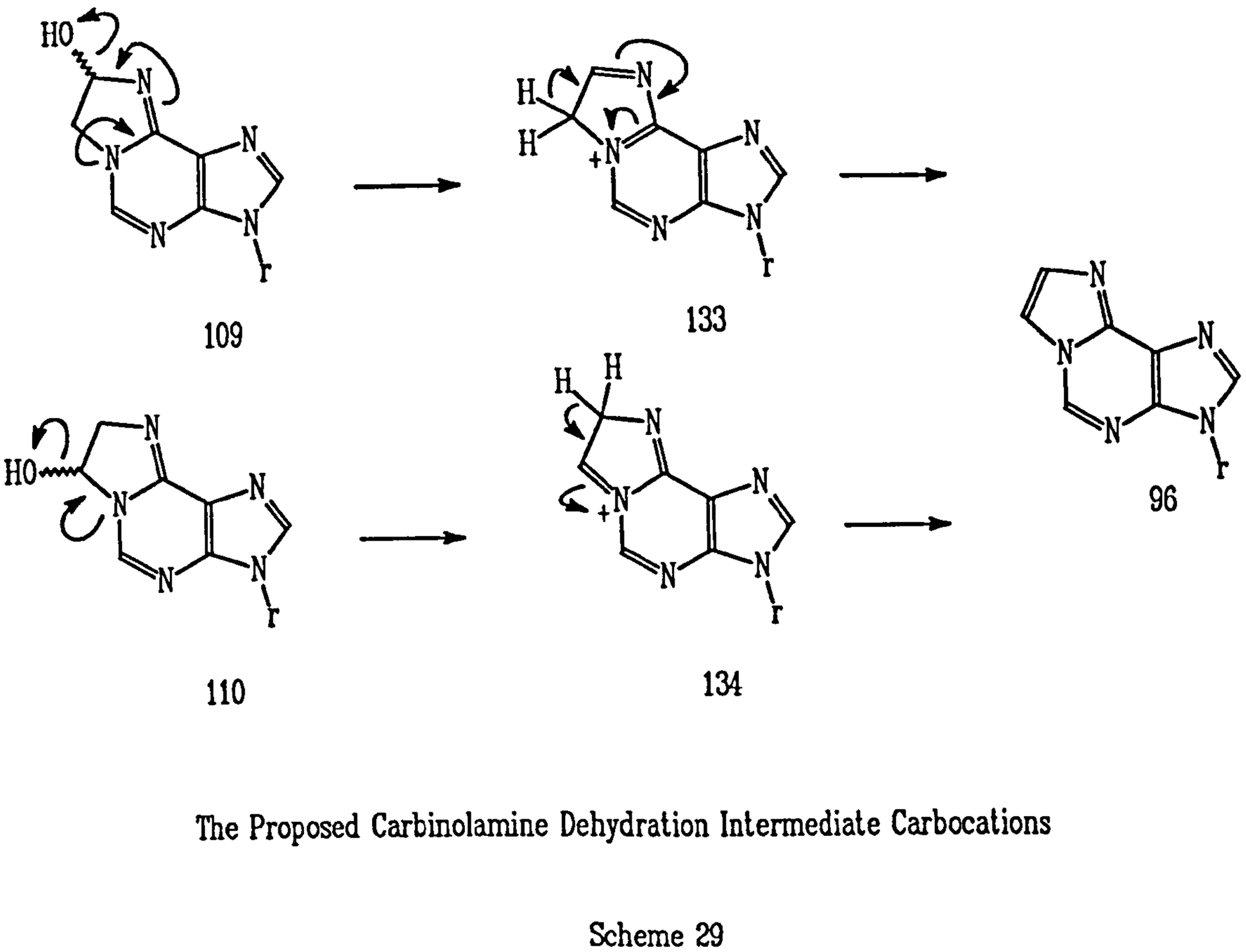

The Proposed Carbinolamine Dehydration Intermediate Carbocations

Scheme 29

ribofuranosylimidazo[2,1-i]purine intermediate (**109**) dehydrates *via* the styreneoidal carbocation **133**, while the proposed 7,8-dihyro-7-hydroxy-3-β-D-ribofuranosylimidazo[2,1-i]purine intermediate (**110**) dehydrates *via* the orthoquinoidal carbocation **110**, as depicted in Scheme 29.

Applying this rationale to the acid catalysed decomposition of N^6-(2,2-dimethoxyethyl)adenosine, loss of methanol can only occur *via* the orthoquinoidal carbocation. No ethenoadenosine was formed under the conditions of the decomposition (1.1 equivalents of acid, 60 °C, 64 hrs) therefore, it appears that (irrespective of the differing leaving group abilities of methanol and water) the orthoquinoidal cation presents a significant energy barrier towards ethenoadenosine.

6.1.3.7 The Deuteriation of Ethenoadenine (133)

Two mechanistic pathways have been described for the conversion of adenosine, by chloroacetaldehyde, to ethenoadenosine. These two postulated pathways are dependent upon the orientation of attack of chloroacetaldehyde to adenosine, with each proposed route forming its particular carbinolamine (Figure 25, **109** or **110**), which dehyrates *via* its particular carbocation (either **134** or **135**, Scheme 29) to ethenoadenosine. If one of the two proposed carbocations presents a lower energy pathway to ethenoadenosine, then the carbinolamine and hence chloroacetaldehyde/adenosine orientation that creates this particular carbocation is the one that occurs. A method of determining which of the two carbocations is the most

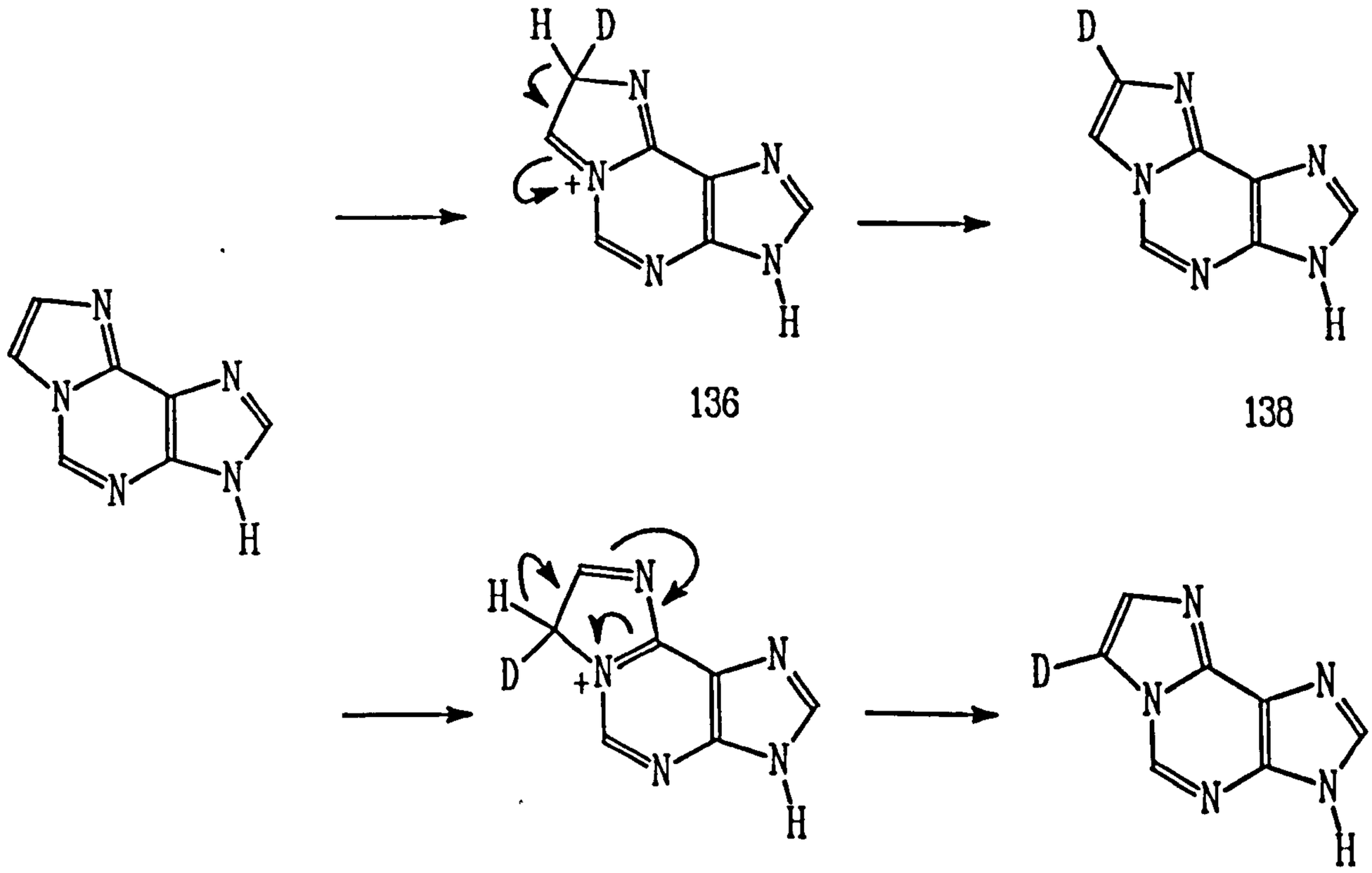

136 138

137 139

The Deuteriation of Ethenoadenine

Scheme 30

accessible is provided by the deuteriation of ethenoadenine. (Ethenoadenine rather than ethenoadenosine was chosen for simplicity). By heating ethenoadenine in acidified d_4-methanol a proton may be exchanged for a deuterium *via* one of the two carbocations shown in Scheme 30. Further, which particular proton is exchanged (H10 or H11: *nb* if ethenoadenine is named 3-hydro-imidazo[2,1-i]purine position 10 becomes position 8 and position 11 becomes 7) will depend upon which mechanistic pathway is followed. Exchange of H10 occurs *via* an orthoquinoidal carbocation **(136)** while H11 exchange occurs *via* a styreneoidal carbocation **(137,** see Scheme 30). Therefore, ^{1}H NMR spectroscopy can determine which proton has been exchanged.

6.1.3.7.1 The ^{1}H NMR Spectrum of Ethenoadenine (133)

The ^{1}H NMR spectrum of the title compound contained four signals which were assigned as follows:

Ethenoadenine	3-Hydro-imidazo[2,1-i] purine	Chemical Shift
H2	H5	δ 9.32
H8	H2	δ 8.43
H10	H8	δ 8.21
H11	H7	δ 7.76

Table 18

The following work is described using the etheno numbering system. A NOESY spectrum of this compound showed that a strong correlation existed between H10 and

H11 and a weak correlation was observed between H11 and H2. No other correlations were observed.

The solution was then acidified (1.1 equivalents of acetyl chloride) causing the ethenoadenine to precipitate. This was redissolved by heating and a 1H NMR spectrum taken at 60 °C. When the spectrum was observed there were three peaks at: δ 8.90, δ 8.27 and δ 7.88. It was not possible, using this evidence, to say which proton had been exchanged.

The reaction mixture was neutralised by passing it through an ion exchange column, the solvent removed and the compound dried under high vacuum. The mixture was then redissolved in d_4-methanol and gave a ^1H NMR spectrum which showed the presence of five peaks. These peaks were all broad singlets, the first appearing at δ 9.38 was assigned to H2; the next peak, which had a smaller integral, was assigned to H8 (δ 8.48); a slightly smaller peak appeared next at δ 8.28 which was thought to be H10. A small peak, that did not integrate, appeared at δ 7.81 which was thought to be the remains of the exchangeable H11 signal. (A relatively large peak was observed at δ 7.55 - thought to be an unknown decomposition product of the reaction).

6.1.3.8 Conclusion

The reaction mechanism of the formation of ethenoadenosine from chloroacetaldehyde and adenosine can be inferred from our experimental results. The acid catalysed decomposition of N^6-(2,2-dimethoxyethyl)adenosine studied by ^1H NMR suggests that the orthoquinoidal pathway is a hindrance, in which case the accessible intermediate is the styrenoidal carbocation (134). This carbocation is derived from 7,8-dihydro-8-hydroxy-3-β-D-ribofuranosylimidazo[2,1-i]purine (109) formed when the carbonyl carbon of chloroacetaldehyde reacts with the exocyclic

(N^6) nitrogen of adenosine and the *N*1 nitrogen reacts with the methylene carbon of chloroacetaldehyde.

The results of the ethenoadenine deuterium exchange reaction also indicate that the mechanistic pathway is *via* the styrenoidal cation.

In conclusion, our results support the initial assumption of the Polish research workers. The reaction intermediate observed during the formation of ethenoadenosine from adenosine by chloroacetaldehyde is 7,8-dihydro-8-hydroxy-3-β -D-ribofuranosylimidazo[2,1-i]purine (**109**).

Future Work

Direct evidence of the mechanism of the reaction of chloroacetaldehyde could be obtained by isotopic labelling studies.

Chapter 7

7.1 Materials and Methods

7.1.1 Chemicals

The major sources of chemicals were the Aldrich Chemical Company, BDH Limited, Janssen Chemicals and the Sigma Chemical Company.

Unless other wise stated, the chemicals were used as supplied without further purification.

7.1.2 Solvents

The solvents used were either Analar grade, which were used directly, or standard laboratory grade purified using the methods outlined in the Newcastle University Department of Chemistry research guide or in Perrin and Armarego.[101]

7.1.3 Methods

Nitrogen was obtained from a standard BOC industrial cylinder. Thin layer chromatography (TLC) was done on aluminium backed Kieselgel 60 F254 plates (Merck catalogue number 5554), 0.2 mm thickness. Flash chromatography[102] was done with C60-H (40 - 60 μm) silica gel from Rhone - Poulenc. Thin layer chromatograms were taken in the usual way except when an acid chloride was being detected. In this instance a small amount of the reaction mixture was added to methanol (which contained a catalytic amount of triethylamine). A thin layer chromatogram was determined from this mixture: the amount of ester observed was thought to represent the amount of acid chloride present in the reaction mixture.

7.1.4 Instrumentation

Elemental Analysis — Combustion analyses were performed using a Carlo Erba 1106 CHN analyser.

Infra - Red Spectrometry

Infra-red spectra were recorded on a Nicolet 20-PC Fourier Transform IR spectrophotometer.

Mass Spectroscopy — Mass spectra were recorded on a Kratos MS80 RF spectrophotometer.

Melting Points — Melting points were determined using a Kofler Block Hot Stage apparatus and are uncorrected.

Nuclear Magnetic Resonance Spectroscopy

^{1}H, ^{13}C and ^{31}P NMR spectra were recorded on either a Hitachi Perkin Elmer R24B (60 MHz), a Bruker WP-200 (200 MHz), or a Bruker WM-300WB (300 MHz) NMR spectrometer.

Ultra violet Spectroscopy

UV spectra were recorded on a Kontron UVIKON-810 spectrophotometer.

7.1.4 PARP Assay

This assay was carried out by Dr B Durkacz at:

The North of England Cancer Research Unit, The Royal Victoria Infirmary, Victoria Road, Newcastle upon Tyne.

NMR Parameters for NAD^+/NADH Determination

Proton and ^{13}C NMR spectra were recorded on a Bruker AMX500 spectrometer at measuring frequencies of 500.13 and 125.76 MHz respectively using samples dissolved in D_2O in 5mm od soda glass tubes. For the proton spectra the residual HOD resonance was suppressed by pre-saturation and typically 64 transients were acquired into 32768 data points. A sine-bell weighting function was applied to the FID which was then zero filled prior to Fourier transformation into 65536 data points over a spectral width of 16 ppm. Proton chemical shifts were determined relative to internal dioxane at δ 3.74 ppm. For the ^{13}C spectra 2048 transients were acquired under proton decoupling by the waltz-16 sequence into 65536 data points and transformed after application of a 0.5 Hz exponential weighting function into 65536 data points over a spectral range of 160 ppm. ^{13}C chemical shifts are relative to TMS at δ 0 ppm.

Two dimensional proton double quantum filtered COSY spectra were obtained using a 90°-t_1-90° 90° - acquire pulse sequence with appropriate phase cycling. The HOD resonance was suppressed by pre-saturation and typically 8 transients were acquired for each value of t_1 to yield a 512 x512 data matrix which was subject to a sine-bell multiplication and zero-filling in each dimension prior to Fourier transformation into a 1024 x 1024 data matrix. Base-line smoothing routines were used in each dimension, and some artifacts were removed by symmetrization. Two dimensional rotating frame nuclear Overhauser effect (ROESY) spectra were obtained similarly using a $90°_x$-t_1-$(\text{spin-lock})_y$ - acquire pulse sequence with a typical spin-lock time of 350 ms and spin-field of *ca* 12000 Hz.

Two dimensional $^{13}C/^1H$ correlation spectra were acquired by ^{13}C observation using sequences due to Bax[103,104] which for one-bond correlations included a binary rotation pulse to remove homonuclear coupling in the proton (t_1) dimension and with

proton decoupling during acquisition. Normally ca 96 transients were acquired into 2048 data points for each 512 values of t_1 and the resulting data matrix was transformed into 2048 x 1024 data points after zero-filling in the t_1 dimension and multiplication by sine-bell weighting functions in each dimension. Inverse $^{1}H/^{13}C$ correlation spectra with broadband (GARP) ^{13}C decoupling were acquired into a 512 x 1024 data matrix with 16 transients for each of the 1024 values of t^1 again using a sequence due to Bax.[105]

Experimental

3-Methoxybenzamide (4)

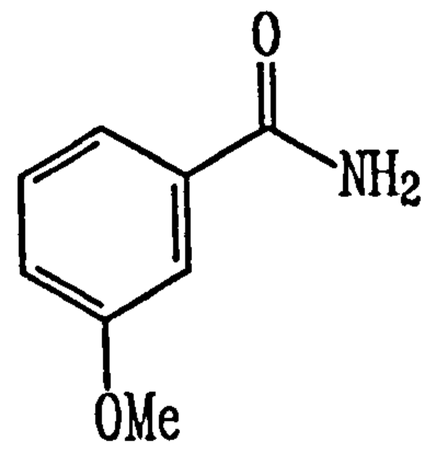

4

3-Methoxybenzoic acid (2.0 g, 13.2 mmol) and thionyl chloride (16.3 g, 137.1 mmol) were heated together under refluxing conditions (1 hr), afterwhich the thionyl chloride was distilled away under reduced pressure (12 mmHg) to leave a brown liquid. This liquid was dissolved in THF (5 ml) to form a pale brown solution which was slowly added to a 35 % aqueous ammonia solution (15 ml). Upon cooling (ice/water bath) a white/yellow solid was formed which was collected by filtration. The solid was recrystallised from ethyl acetate (charcoalation) to give white crystals (1.3 g, 8.6 mmol, 65.2 % yield). mp 124 - 125 °C (literature[106] 134 °C), (Found: C, 63.16; H, 5.89; N, 9.13. $C_8H_9NO_2$ requires C, 63.58; H, 5.96; N, 9.27 %); δH (200 MHz, $CDCl_3$) 3.47(1H, s, *H2*), 3.90 (3H, s, O*Me*), 7.18 (1H, m, *H6*), 7.4 - 7.5 (3H, m, *H4,5*,N*H*), 8.09 (1H, s, N*H*).

3-Hydroxybenzamide (29)

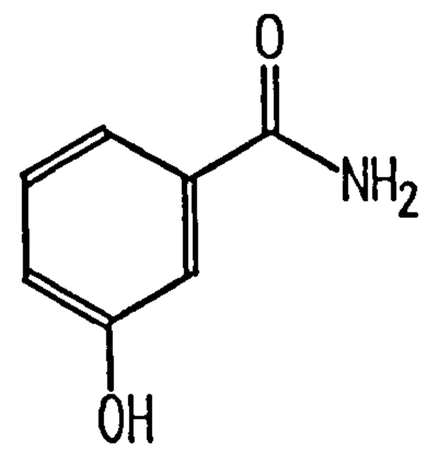

3-Acetoxybenzoic acid (**29**, 1 g, 5.56 mmol) was heated under refluxing conditions (2.5 h) in thionyl chloride (3 ml, 4.89 g, 41.1 mmol) or until the reaction was complete by TLC, afterwhich the excess thionyl chloride was distilled away under reduced pressure (12 mmHg) to leave a yellow tinged oil (*ca* 0.5 ml). The oil was carefully pipetted into a cooled (ice) 35 % aqueous ammonia solution and left to stir (*ca* 0.25 h). This mixture was boiled to reduce its volume (*ca* 10 ml) and left to cool, crystals formed which were recrystallised from water to give white crystals (0.5 g, 65 % yield) mp 136 - 137 °C (literature[107] 169 °C)(Found: C, 61.5; H, 5.1; N, 10.4. $C_7H_7NO_2$ requires C, 61.3; H, 5.1; N, 10.2 %); ν_{max}(KBr)/cm^{-1} 3403 (Phenol OH), 3245 (NH_2), 1653 and 1615 (Amides I and II), 1451 (benzene), 1258 (OH); δ_H(200 MHz, d_6-DMSO) 9.8 (1H, s, O*H*), 8.0 (1H, s, N*H*), 7.6 - 7.2 (4H, m, N*H*, *H*2,5,6), 7.1 (1H, m, *H*4); δ_C(50.28 MHz, d_6-DMSO) 168 (CO), 157 (C1), 136 (C3), 129 (C2), 118 (C6), 118 (C4), 114 (C5); m/z 137 (M^+), 121 (M^+ - O), 93 (M^+ - $CONH_2$).

3-Acetoxybenzoic acid (33)[49]

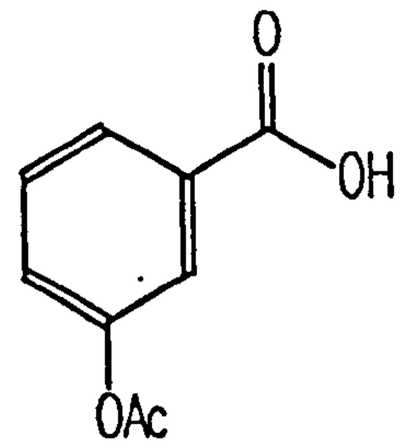

33

Acetic anhydride (0.8 g, 8 mmol) was added to a cooled (ice) aqueous solution (2 ml) of sodium hydroxide (0.6 g, 15 mmol) and 3-hydroxybenzoic acid (1 g, 7.3 mmol) along with some pieces of ice (*ca* 2 g). After stirring (1 h), the mixture was acidified with 6M hydrochloric acid (3 ml, 18 mmols) whereupon a milky white precipitate was formed. The mixture was extracted with dichloromethane (3 x 30 ml), the resulting solution was dried (magnesium sulphate) and the solvent was removed by rotary evaporation to give a white solid (1.21 g, 92 % yield). Recrystallisation gave white crystals (115 mg, 88 % yield) mp 129 - 131 °C (from water, literature[108] 133 ° C from water) (Found: C, 59.7; H, 4.3. $C_9H_8O_4$ requires C, 60.0; H, 4.5 %); ν_{max}(KBr)/ cm^{-1} 3087 and 3021 (OH), 1761 (OAc), 1678 (CO_2H), 1586 and 1455 (benzene CH), 1204 (CO stretch); δ_H(200 MHz, $CDCl_3$) 7.92 (1H, dt, *J* 7.8, 1.3, *H*6), 7.7 (1H, t, *J* 1.3, *H*2), 7.4 (1H, t, *J* 7.8, *H*5), 7.3 (1H, dt, *J* 7.8, 1.3, *H*4), 2.23 (3H, s, $OCOCH_3$); δ_C (50.28 MHz, $CDCl_3$) 171 (CO_2H), 169 ($O\underline{C}OCH_3$), 150 (C1), 131 (C3), 129 (C2), 127 (C6), 127 (C4), 123 (C5), 21 ($OCO\underline{C}H_3$); m/z 180 (M^+), 163 (M^+ - OH), 121 (M^+ - OH - ketene).

3-(Bromoalkyloxy)benzamides

General Procedure A

A solution of 3-hydroxybenzamide, potassium carbonate and a dibromoalkane in acetonitrile was heated under refluxing conditions until the reaction was complete by TLC (*ca* 2h). The solvent was removed by rotary evaporation to give a white sticky solid which was purified by flash chromatography and recrystallisation.

3-(5-Bromopentyloxy)benzamide (35)

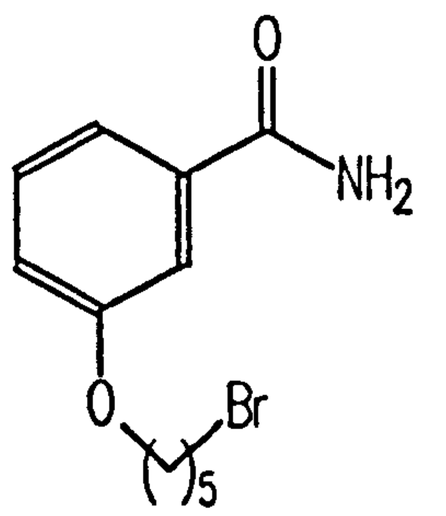

35

The title compound was prepared from a solution of 3-hydroxybenzamide (0.50 g, 3.65 mmols), potassium carbonate (0.50 g, 3.65 mmol) and 1,5-dibromopentane (1.8 g, 7.30 mmol) in acetonitrile (18 ml) by the general procedure A. Recrystallisation gave 35 as white flaky crystals (0.74 g, 70 % yield) mp 98 - 99 °C (from petrol/ethyl acetate), (Found: C, 50.7, H, 5.4, N, 4.95. $C_{15}H_{22}NO_2Br$ requires C, 50.4, H, 5.6, N, 4.9 %); ν_{max}(KBr)/cm^{-1} 3345 and 3160 (NH), 2932 (CH_2), 1665 and 1632 (Amides I and II), 1601 and 1586 (benzene CH), 1451 (CH_2), 1252 (CO stretch); δ_H(200 MHz, d_6-DMSO) 8.09 (1H, s, N*H*), 7.49 (4H, m, *H*2,5,6 and N*H*), 7.1 (1H, d, *J* 7.99, *H*4), 4.11 (2H, t, *J* 6.2, CH_2O), 3.67 (2H, t, *J* 6.6, CH_2Br), 1.90 (4H, m,

$CH_2CH_2CH_2$), 1.62 (2H, m, $CH_2CH_2CH_2$); δ_C(50.28 MHz, d_6-DMSO) 168 (CO), 158.85 (C3), 129.63 (C2), 120 (C4), 117.79 (C6), 113.53 (C5), 67.73 (OCH_2), 35.36 (CH_2Br), 32.30 ($\underline{C}H_2CH_2O$), 28.12 ($\underline{C}H_2CH_2Br$), 24.63 ($OCH_2CH_2\underline{C}H_2$); m/z 285/287 ($M^+$).

3-(8-Bromooctyloxy)benzamide (36)

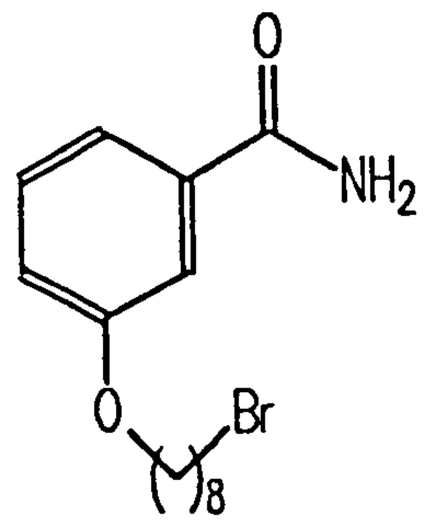

36

The title compound was prepared from a solution of 3-hydroxybenzamide (0.50 g, 3.65 mmol), potassium carbonate (0.50 g, 3.65 mmol) and 1,8-dibromooctane (2.0 g, 7.3 mmol) in acetonitrile (18 ml) by the general procedure A. Recrystallisation gave 36 as white crystals (0.78 g, 65 % yield) mp 111 - 112 °C (from ethyl acetate), (Found: C, 54.9; H, 6.7; N, 4.3. $C_{15}H_{22}NO_2Br$ requires C, 54.9; H, 6.8; N, 4.3 %); ν_{max}(KBr)/cm^{-1} 3366 and 3173 (amide NH stretch), 2938 and 2923 (aliphatic CH stretch), 2857 (ether CH stretch), 1659 (amide I CO stretch), 1626 (amide II - NH bending), 1603 and 1584 (benzene ring); δ_H(200 MHz, d_6-DMSO) 8.07 (1H, s, N*H*), 7.52 (4H, m, N*H* and aromatic *H*2,5,6), 7.18 (1H, m, *H*4), 4.09 (2H, t, *J* 8, OCH_2), 3.62 (2H, t, *J* 8, $BrCH_2$), 1.87 (4H, m), 1.44 (8H, s, alkyl envelope); δ_C (50.28 MHz, d_6-DMSO) 167.96 (CO), 158.89 (C3), 135.99 (C1), 129.59 (C5), 119.93 (C6), 117.79 (C4), 113.49 (C2), 67.86 (OCH_2), 35.44 ($\underline{C}H_2CH_2Br$), 32.57 ($CH_2\underline{C}H_2Br$), 28.96 ($OCH_2\underline{C}H_2CH_2\underline{C}H_2$), 28.42 ($\underline{C}H_2CH_2CH_2CH_2Br$), 27.82 ($\underline{C}H_2CH_2CH_2Br$), 25.764 ($OCH_2CH_2\underline{C}H_2$); m/z 327/329 ($M^+$).

3-(12-Bromododecyloxy)benzamide (37)

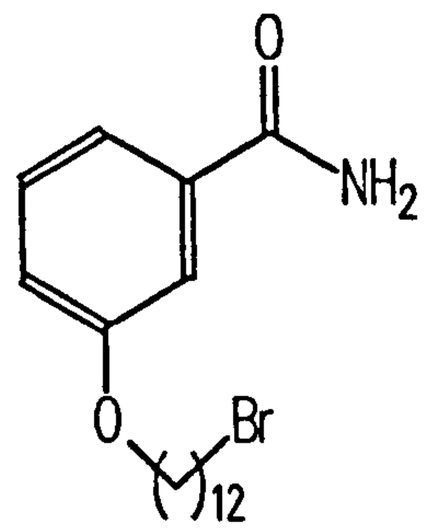

37

The title compound was prepared from a solution of 3-hydroxybenzamide (0.50 g, 3.65 mmol), potassium carbonate (0.50 g, 3.65 mmol) and 1,12-dibromododecane (2.48 g, 7.56 mmol) in acetonitrile (18 ml) by the general procedure A. Recrystallisation gave 37 as white flaky crystals (0.94 g, 68 % yield) mp 117 - 118°C (from petrol/ethyl acetate), (Found: C, 59.4; H, 7.9; N, 3.5. $C_{19}H_{30}NO_2Br$ requires C, 59.4; H, 7.9; N, 3.6 %); ν_{max}(KBr)/cm $^{-1}$ 3370 and 3175 (NH), 2938 and 2921 (CH_2), 2853 (OCH_2), 1659 and 1626 (Amides I and II), 1603 and 1584 (benzene CH), 1449 (CH_2), 1252 (CO stretch); δ_H(200 MHz, d_6-DMSO) 8.08 (1H, s, N*H*). 7.46 (4H, m, N*H* and aromatic *H*2, 5, 6), 7.15 (1H, d, *J* 8, *H*4), 4.09 (2H, t, *J* 6, O*CH*$_2$), 3.61 (2H, t, *J* 6, *CH*$_2$Br), 1.85 (4H, m), 1.36 (16H, m); δ_C(50.28 MHz, d_6-DMSO) 167.93 (CO), 158.89 (C3), 135.99 (C1), 129.56 (C5), 119.93 (C6), 117.76 (C4), 113.49 (C2), 67.87 (OCH_2), 35.43 - 25.87 (alkyl chain); m/z 383/385 (M^+).

3-(5-(6-Chloropurin-9-yl)pentyloxy)benzamide (38)

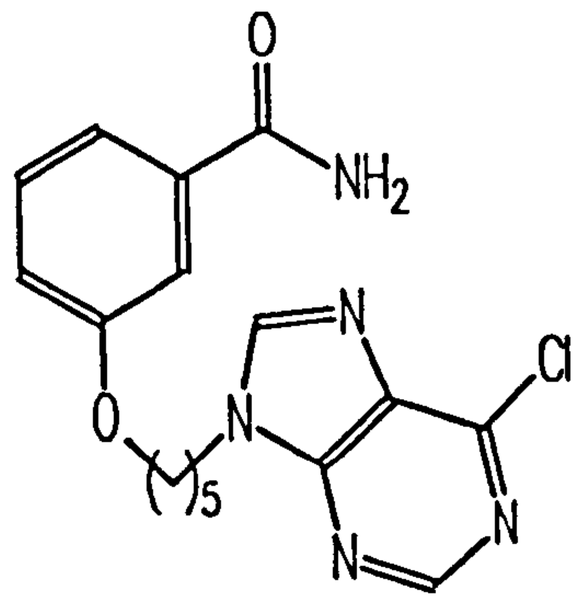

38

A solution of 3-(5-bromopentyloxy)benzamide (500 mg, 1.7 mmol), 6-chloropurine (270 mg, 1.7 mmol) and potassium carbonate (240 mg, 1.7 mmol) in DMF (7.5 ml) was stirred for two days (rt). The solvent was then removed under vacuum (0.001 mmHg) and the remaining white solid (of *N*7 and *N*9 isomers) was chromatographed (silica, 10 % MeOH/ CH_2Cl_2) to give a single product (*N*9 isomer) as a glass. This was triturated with ether (≈ 5 ml) to give a white solid which was recrystallised to give the product (38, 120.3 mg, , 20 % yield) mp 132 - 133°C (from ethyl acetate), (Found: C, 56.7, H, 4.3, N, 19.4. $C_{17}H_{18}N_5O_2Cl$ requires C, 56.57, H, 5.0, N, 19.5 %); ν_{max} (KBr)/cm^{-1} 3376 and 3173 (amide NH_2), 2951, 2928 and 2851 (CH_2), 1680 and 1624 (amide I and II), 1593 and 1584 (benzene ring); δ_H(200 MHz, d_6-DMSO) 8.88 (1H, s, purine *H*8), 8.85 (1H, s, purine *H*2) 8.05 (1H, s, CON*H*). 7.56 (4H, m, N*H* and aromatic *H*2,5,6), 7.15 - 7.10 (1H, m, *H*4), 4.44 (2H, t, *J* 7, OCH_2), 4.08 (2H, t, *J* 6.3, CH_2N), 2.12 - 1.98 (2H, m, OCH_2CH_2), 1.94 - 1.80 (2H, m, NCH_2CH_2), 1.59 - 1.43 (2H, m, $CH_2CH_2CH_2$); δ_C(50.28 MHz, d_6-DMSO) 167.93 (CO), 158.77 (C3), 152.31 (*p*C4), 151.76 (*p*C8), 149.29 (*p*C5), 147.86 (*p*C2), 136.02 (C1), 131.18 (*p*C6), 129.60 (C5), 119.96 (C6),117.80 (C4), 113.46 (C2), 67.59 (OCH_2), 44.03 (NCH_2), 29.07 ($OCH_2\underline{C}H_2$), 28.337 ($\underline{C}H_2CH_2N$), 22.890 ($CH_2\underline{C}H_2CH_2$); m/z 359/361 (M^+). (nb p = purine)

3-(8-(6-Chloropurin-9-yl)octyloxy)benzamide (39)

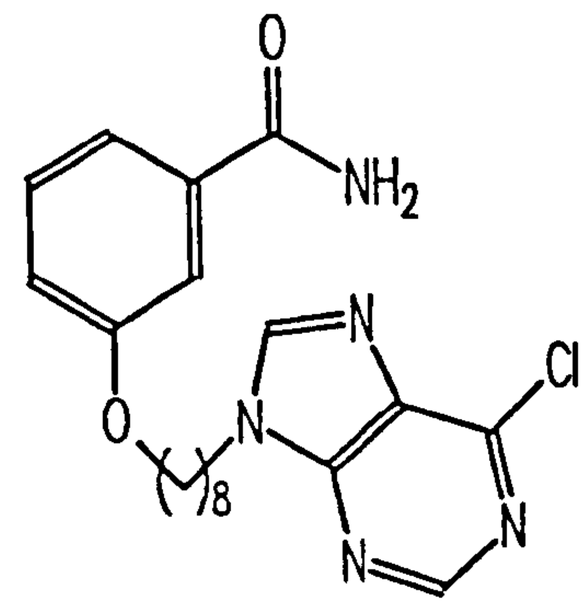

39

A solution of 3-(8-bromooctyloxy)benzamide (500 mg, 1.5 mmol), 6-chloropurine (236 mg, 1.5 mmol) and potassium carbonate (210 mg, 1.5 mmol) in DMF (7.5 ml) was stirred for two days (rt). The solvent was removed under vacuum (0.001 mmHg) and the white solid (of *N*7 and *N*9 isomers) was chromatographed (silica gel, 5 % petrol/THF) to give a single product (*N*9 isomer) a white solid (74 mg) which was recrystallised (2x) to give (39, 58.7 mg, 10 % yield) mp 116 - 117°C (ethanol) (Found: C, 59.2, H, 6.1, N, 16.9. $C_{20}H_{24}N_5O_2Cl$ requires C, 59.8, H, 6.0, N, 17.4 %); ν_{max}(KBr)/cm^{-1} 3382 and 3189 (amide NH_2), 2938 and 2857 (CH2), 1686 and 1611 (amides I and II), 1597 and 1586 (benzene ring); δ_H(200 MHz, d_6-DMSO) 8.87 (1H, s, purine *H*8), 8.83 (1H, s, purine *H*2), 8.05 (1H, s, CON*H*). 7.54 - 7.38 (4H, m, CON*H* and aromatic *H*2, 5, 6), 7.16 - 7.12 (1H, m, *H*4), 4.38 (2H, t, *J* 7, OCH_2), 4.06 (2H, t, *J* 6.3, CH_2N), 1.99 - 1.74 (4H, m, OCH_2CH_2 and CH_2CH_2N), 1.39 (8H, m, alkyl env); δ_C(50.28 MHz, d_6-DMSO) 167.93 (CO), 158.85 (C3), 151.74 (*p*C8) 151.66 (*p*C2), 135.99 (C1), 129.60 (C5), 119.90 (C6), 117.79 (C4), 113.46 (C2), 67.82 (OCH_2), 44.11 (NCH_2), 29.29 (OCH_2CH_2), 28.87 ($OCH_2CH_2CH_2$ and NCH_2CH_2), 25.69 ($NCH_2CH_2CH_2CH_2$); m/z 401/403 (M^+).

3-(8-(6-Chloropurin-9-yl)dodecyloxy)benzamide (40)

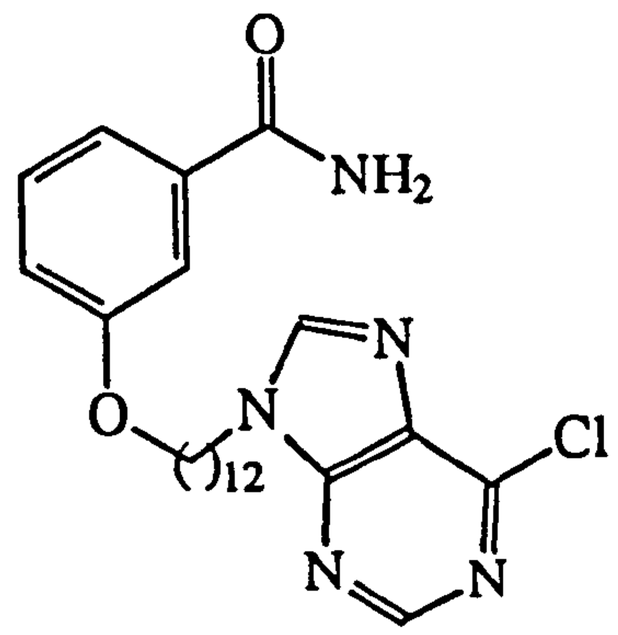

40

A mixture of 3-(12-bromododecyloxy)benzamide (500 mg, 1.3 mmol), 6-chloropurine (201.3 mg, 1.3 mmol) and potassium carbonate (180.0 mg, 1.3 mmol) in DMF (6.5 ml) was stirred for three days (rt). The solvent was removed under vacuum (0.001 mmHg) and the white solid (of *N*7 and *N*9 isomers) was chromatographed (silica gel, 5 % petrol/THF) to give a single product (*N*9 isomer) a white solid (204 mg) which was recrystallised to give (204.1 mg, 34.3 % yield) mp 135 - 137°C (DMSO and water) (Found: C, 63.0, H, 6.9, N, 15.4. $C_{20}H_{24}N_5O_2Cl$ requires C, 62.95, H, 7.0, N, 15.3 %); ν_{max}(KBr)/cm^{-1} 3306 and 3205 (amide NH_2), 2906 and 2845 (CH_2), 1690 and 1622 (amides I and II), 1586 (benzene ring); δ_H(200 MHz, d_6-DMSO) 8.84 (1H, s, purine *H*8), 8.81 (1H, s, purine *H*2), 8.10 (1H, s, CON*H*). 7.5 - 7.4 (4H, m, CON*H* and aromatic *H*2, 5, 6), 7.2 - 7.15 (1H, m, *H*4), 4.34 (2H, t, *J* 7, OCH_2), 4.10 (2H, t, *J* 6.3, CH_2N), 1.91 - 1.72 (4H, m, OCH_2CH_2 and CH_2CH_2N), 1.37 (16H, m, alkyl env); δ_C(50.28 MHz, d_6-DMSO) 169.33 (CO), 159.13 (C3), 151.83 (*p*C8) 151.77 (*p*C2), 134.31 (C1), 127.66 (C5), 120.11 (C6), 117.05 (C4), 115.34 (C2), 71.25 (OCH_2), 44.19 (NCH_2), 29.89 (OCH_2CH_2), 27.62 ($OCH_2CH_2CH_2$ and NCH_2CH_2), 24.11 ($NCH_2CH_2CH_2CH_2$); m/z 457/459 (M^+).

3-(5-(6-Aminopurin-9-yl)penyloxy)benzamide (41)

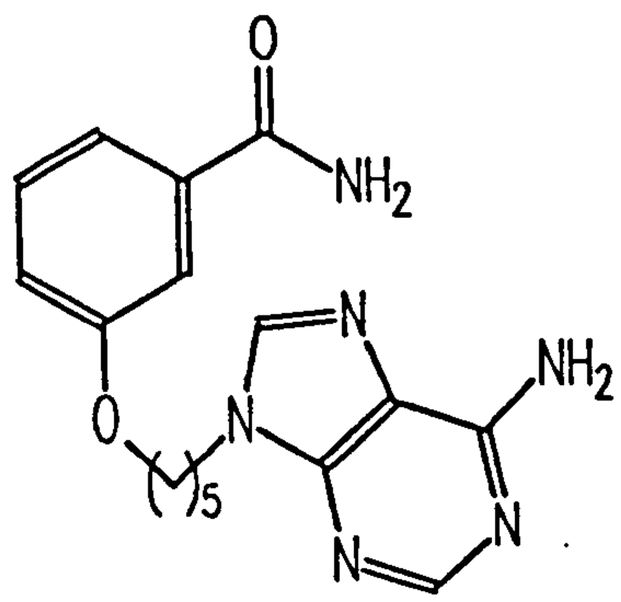

A bomb was charged with a mixture (392 mg, 1.1 mmol) of 3-(6-chloro-7-(5-pentyloxy)purine)benzamide, 3-(6-chloro-9-(5-pentyloxy)purine)benzamide and liquid ammonia (60 ml) and heated under pressure (66 °C, 30 bar, 16 h). The ammonia was evaporated away to leave a yellow solid which was chromatographed (silica gel, 10 % methanol/dichloromethane) to give a pale yellow solid which was recrystallised to give the title compound (204 mg, 54 % yield) mp 148 - 149 °C (from water), (Found: C, 60.4; H, 6.0; N, 25.0. $C_{17}H_{20}N_6O_2$ requires C, 60.0; H, 5.9; N, 24.7 %); δ_H(200 MHz, d_6-DMSO) 8.25 (2H, m, purine *H*8,2), 8.06 (1H, s, CON*H*). 7.61 - 7.38 (4H, m, CON*H* and aromatic *H*2,5,6), 7.31 (2H, s, NH_2) 7.15 - 7.11 (1H, m, *H*4), 4.27 (2H, t, *J* 7, OCH_2), 4.07 (2H, t, *J* 6.3, CH_2N), 2.05 - 1.78 (4H, m, $OCH_2CH_2CH_2CH_2CH_2N$), 1.56 - 1.41 (2H, m, NCH_2CH_2), 1.59 - 1.43 (2H, m, $CH_2CH_2CH_2$); δ_C(50.28 MHz, d6-DMSO) 167.96 (CO), 158.81 (C3), 156.28 (pC2), 152.70 (pC8), 149.11 (pC5), 141.18 (pC4), 135.99 (C1), 129.60 (C5), 119.97 (C6), 119.09 (C4), 117.80 (C2), 87.68 (CH_2O), 50.43 (CH_2N), 29.45 (CH_2CH_2O), 28.41 (CH_2CH_2N), 22.95 ($CH_2CH_2CH_2$); m/z 340 (M^+).

3-(8-(6-Aminopurin-9-yl)octyloxy)benzamide (42)

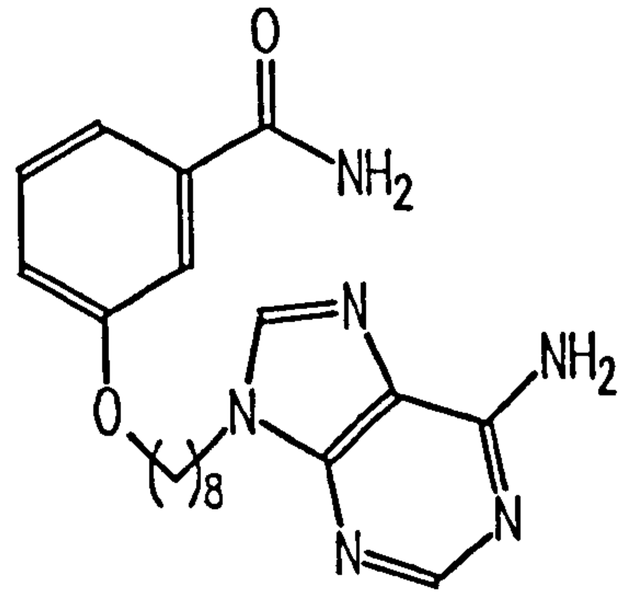

A bomb was charged with a mixture (110 mg, 0.27 mmol) of 3-(8-*N*7-(6-chloropurine)octyloxy)benzamide, 3-(8-*N*9-(6-chloropurine)octyloxy) benzamide and liquid ammonia (60 ml) and heated under pressure (64 °C, 30 bar, 16 H). The ammonia was evaporated away to leave a yellow solid which was chromatographed (silica gel, 15 % methanol/dichloromethane) to give a pale yellow solid which was recrystallised to give the title compound (56 mg, 62 % yield) mp 199 - 199.5°C (from methanol) (Found: C, 62.4, H, 6.5, N, 21.9 $C_{20}H_{26}N_6O_2$ requires C, 62.8, H, 6.9, N, 22.0 %); vmax(KBr)/cm^{-1} 3445 (NH_2), 3297 and 3108 (amide NH_2), 2936 and 2921 (CH_2), 1678 and 1601 (amides I and II), 1512 (benzene); δ_H(200 MHz, d_6-DMSO) 8.24 (1H, s, purine *H*8), 8.23 (1H, s, purine *H*2), 8.06 (1H, s, CONH). 7.55 - 7.39 (4H, m, CON*H* and aromatic *H*2,5,6), 7.30 (2H, s, NH_2), 7.17 - 7.13 (1H, m, aromatic *H*4), 4.23 (2H, t, *J* 7, OCH_2), 4.07 (2H, t, *J* 6.3, CH_2N), 1.94 - 1.76 (4H, m, OCH_2CH_2 and CH_2CH_2N), 1.40 (8H, m, alkyl env); δ_C(50.28 MHz, d_6-DMSO) 167.998 (CO), 158.85 (C3), 152.71 (*p*C8), 141.21 (*p*C2), 136.05 (C1), 129.67 (C5), 119.97 (C6), 117.87 (C4), 113.59 (C2), 67.90 (OCH_2), 43.22 (NCH_2), 29.698 (OCH_2CH_2), 28.96 ($OCH_2CH_2CH_2$ and NCH_2CH_2), 26.31 ($OCH_2CH_2CH_2CH_2$), 25.76 ($NCH_2CH_2CH_2CH_2$); m/z 338 (M^+ - $CONH_2$).

3-(8-(6-Aminopurin-9-yl)dodecyloxy)benzamide (43)

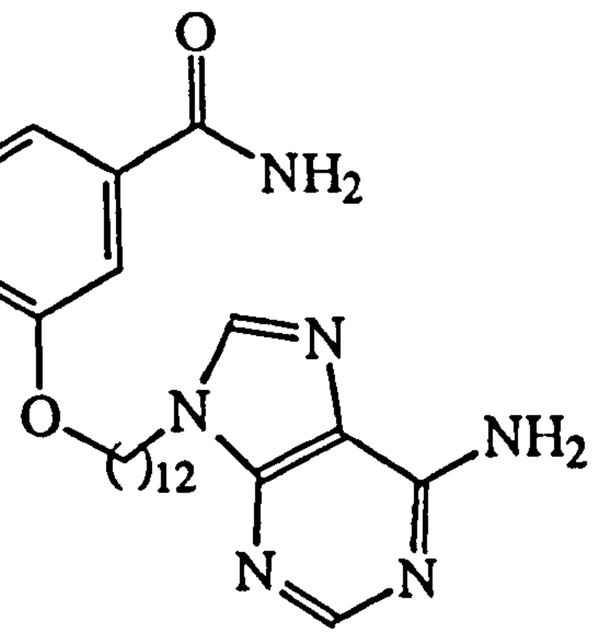

43

A bomb was charged with a mixture (436.3 mg, 0.954 mmol) of 3-(8-*N*7-(6-chloropurine)dodecyloxy)benzamide, 3-(8-*N*9-(6-chloropurine)dodecyloxy) benzamide and liquid ammonia (60 ml) and heated under pressure (64 °C, 30 bar, 16 H). The ammonia was evaporated away to leave a yellow solid (359.6 mg) which was chromatographed (silica gel, 15 % methanol/dichloromethane) to give a pale yellow solid which was recrystallised to give the title compound (32 mg, 7.7 % yield) mp 205 - 206°C (decomposition, from methanol) (Found: C, 65.8, H, 7.65, N, 19.21 $C_{24}H_{34}N_6O_2$ requires C, 65.75, H, 7.76, N, 19.18 %); νmax(KBr)/cm^{-1} 3455 (NH_2), 3293 and 3100 (amide NH_2), 2941 and 2928 (CH_2), 1676 and 1601 (amides I and II), 1515 (benzene); δ_H(200 MHz, d_6-DMSO) 8.23 (1H, s, purine *H*8), 8.21 (1H, s, purine *H*2), 8.10 (1H, s, CONH). 7.6 - 7.4 (4H, m, CON*H* and aromatic *H*2,5,6), 7.28 (2H, s, NH_2), 7.19 (1H, m, aromatic *H*4), 4.25 (2H, t, *J* 7, OCH_2), 4.11 (2H, t, *J* 6.3, CH_2N), 2.04 - 1.75 (4H, m, OCH_2CH_2 and CH_2CH_2N), 1.40 (16H, m, alkyl env); δ_C(50.28 MHz, d_6-DMSO) 168.017 (CO), 159.58 (C3), 152.01 (*p*C8), 141.81 (*p*C2), 136.53 (C1), 129.36 (C5), 119.89 (C6), 118.84 (C4), 112.09 (C2), 69.94 (OCH_2), 42.32 (NCH_2), 31.23 ($OCH_2\underline{C}H_2$), 30.06 ($OCH_2CH_2\underline{C}H_2$ and $NCH_2\underline{C}H_2$), 25.81 ($OCH_2CH_2CH_2\underline{C}H_2$), 25.64 ($NCH_2CH_2CH_2\underline{C}H_2$); m/z 438 ($M^+$ - $CONH_2$).

cis/trans-3-Methoxycyclohexanecarboxamide (47)

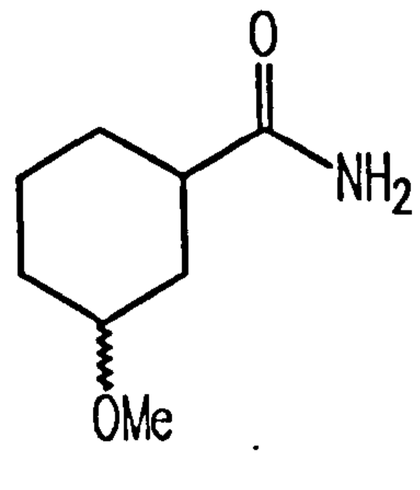

47

To a solution of *cis/trans*-3-methoxycyclohexanecarboxylic acid (0.5 g, 3.1 mmol) in THF (3 ml) was added thionyl chloride (0.41 g, 3.5 mmol) dropwise over 5 minutes with stirring. The resulting solution was stirred at 22 °C (24 h) until the reaction was complete as indicated by TLC. The reaction mixture was then carefully pipetted into 35% aqueous ammonia (10 ml), afterwhich excess ammonia and THF were removed at the water pump. The resulting solution was extracted with dichloromethane (5 × 10 ml), then dried ($MgSO_4$) and the solvent removed by rotary evaporation to leave an off white solid. The crude product was recrystallisation from ethyl acetate to give shiny white crystals (0.41 g, 84 % yield), mp 117 - 118 °C (from ethyl acetate), (Found C, 61.4; H, 9.7; N, 8.9. $C_8H_{15}NO_2$ requires C, 61.1; H, 9.6; N, 8.9 %); ν_{max}(KBr)/cm^{-1} 3349 and 3173 (NH), 2936 (CH_2), 2859 and 2820 (OCH_3), 1663 and 1632 (Amides I and II), 1429 (CH_3), 1100 and 1088 (CO); δ_H(500 MHz, $CDCl_3$) 10.81 (4H, brs, $NH_{2\ cis\ +\ trans}$), 3.49 (1H, tt, *J* 2.8, 4.8, $H3_{trans}$), 3.32 (3H, s, OCH_{3cis}), 3.28 (3H, s, OCH_{3trans}), 3.13 (1H, tt, *J* 4.0, 10.8, $H3_{cis}$), 2.67 (1H, tt, *J* 3.8, 10.2, $H1_{trans}$), 2.28 (1H, tt, *J* 3.7, 12.0, $H1_{cis}$), 2.26 - 1.0 (16H, m, $(H2',2'',4',4'',5',5'',6',6'')_{cis\ +\ trans}$); m/z 157 ($M^+$), 142 ($M^+ - CH_3$), 125 ($M^+ - CH_3OH$), 113 ($M^+ - CONH_2$).

3-Methoxy-1,4-dihydrobenzoic Acid (55)

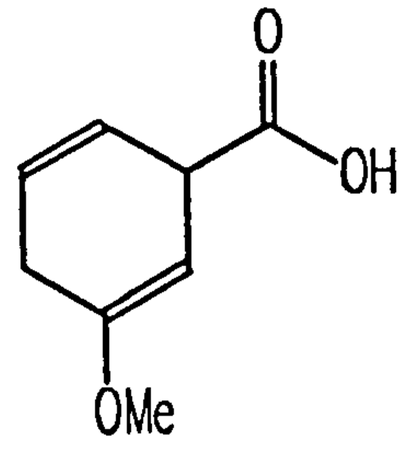

Ammonia (110 ml) was condensed into a stirred solution of 3-methoxybenzoic acid (5.0 g, 33 mmol) in dry methanol (45 ml). Sodium (3.6 g, 327 mmol) was added to this mixture which was left to stir until the blue colour dissipated. The reaction was then quenched with excess ammonium chloride (20.0 g, 374 mmol) and the ammonia allowed to evaporate from the mixture (0.5 h). The residual ammonia was then removed under vacuum (12 mmHg) keeping the reaction flask below 0 °C.

Hydrochloric acid was then carefully added to the mixture until the pH = 4.5 all the time the flask temperature was kept below 0 °C. The reaction mixture was then extracted with dichloromethane (5 × 100 ml), dried ($MgSO_4$) and the solvent removed by rotary evaporation to give a pale yellow oil (3.73 g, 74 % yield), δ_H(200 MHz, $CDCl_3$) 2.65 (2H, m, *H*4',4"), 3.51 (3H, s, OCH_3), 3.84 (1H, m, *H*1), 4.68 (1H, d, *J* 4, *H*2), 5.75 (2H, m, *H*5,6), 10.59 (1H, brs, CO_2H); δ_C(50.28 MHz, $CDCl_3$) 28.41 (C4), 42.98 (OMe), 53.96 (C1), 89.20 (C2), 121.78 (C3), 125.63 (C6), 154.70 (C5), 179.48 (CO); m/z 154 (M^+).

3-Methoxy-1,4,5,6-tetrahydrobenzamide (57)

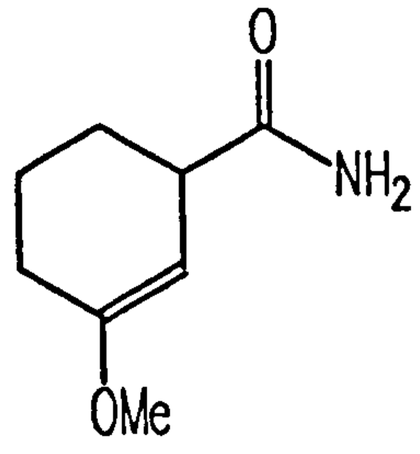

57

Ammonia (20 ml) was condensed into a stirred solution of 3-methoxybenzamide (1.0 g, 6.6 mmol) in dry methanol (9 ml). Sodium (0.84 g, 76.4 mmol) was added to the reaction mixture, after the blue colour dissipated (5 mins) the reaction was quenched with ammonium chloride (8.0 g, 149.5 mmol). The liquid ammonia was left to evaporate under a stream of nitrogen gas (2.5 h), afterwhich water (30 ml) was added forming a white milky precipitate which was filtered off. The filtrate was extracted with dichloromethane (5 × 50 ml), dried ($MgSO_4$) and the solvent removed by rotary evaporation to leave an oil. This was triturated with ether to give a solid which gave the title compound upon recrystallisation (25.0 mg, 2.4 % yield) mp 122 - 123 °C (from petrol/ethyl acetate), (Found: C, 62.1; H, 8.5; N, 9.2. $C_8H_{13}NO_2$ requires C, 61.9; H, 8.4; N, 9.0 %); ν_{max}(KBr)/cm^{-1} 3350 and 3169 (NH), 1658 and 1634 (amides I and II); δ_H(500 MHz, $CDCl_3$) 1.71 (4H, m, *H*5',5",6',6"), 2.06 (2H, m, *H*4',4"), 3.01 (1H, m, *H*1), 3.52 (3H, s, OCH_3), 4.61 (1H, d, *J* 2.1, *H*2), 5.86 (1H, brs, N*H*), 6.01 (1H, brs, N*H*); m/z 155 (M^+), 111 (M^+ - $CONH_2$).

N-Alkylnicotinamide Salts

General Procedure B

A stirred solution of nicotinamide and alkylhalide in ethanol was heated under refluxing conditions overnight. The solvent and excess alkylhalide were carefully removed by distillation to leave a solid which was purified by recrystallisation.

N-Methylnicotinamide Iodide (60)

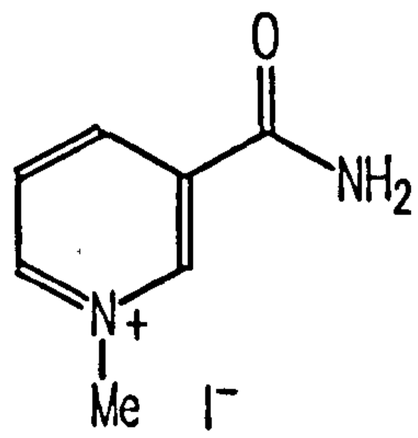

60

The title compound was prepared from a solution of nicotinamide (5.00 g, 41 mmol) and methyl iodide (6.84 g, 48 mmol) in ethanol (50 ml) using the general procedure B. Recrystallisation gave 60 as yellow crystals (9.5 g, 88 % yield) mp 203-204°C (from water), (Found: C, 31.9; H, 3.3; N, 10.5. $C_7H_9N_2OI$ requires C, 31.8; H, 3.4; N, 10.6 %); ν_{max}(KBr)/cm^{-1} 3326 and 3156 (NH), 2955 (CH_3), 1686 and 1642 (Amides I and II), 1584 and 1507 (Pyridine), 1462 (CH_3), 1393 (CH_3); δ_H(200 MHz, d_6-DMSO) 4.51 (3H, s, CH_3), 8.19 (1H, s, N*H*), 8.35 (1H, dd, *J* 8, 6, *H*5), 8.55 (1H, s, N*H*), 8.98 (1H, d, *J* 8, *H*4), 9.23 (1H, d, *J* 6, *H*6), 9.56 (1H, s, *H*2); δ_C(50.28 MHz, d_6-DMSO) 48.93 (CH_3), 127.83 (C5), 133.34 (C4), 143.34 (C6), 145.83 (C2), 147.46 (C1), 163.22 (CO); m/z 137 (M^+), 93 (M^+ - $CONH_2$).

N-Ethylnicotinamide Iodide (61)

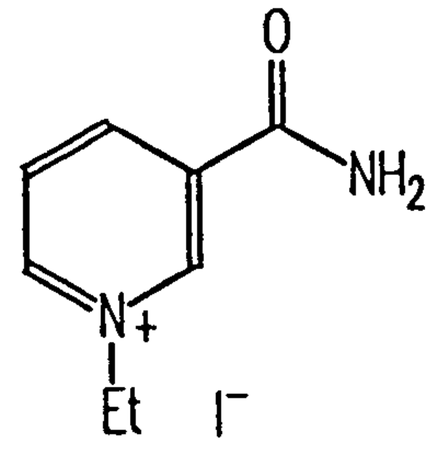

61

The title compound was prepared from a solution of nicotinamide (5.00 g, 41 mmols) and ethyl iodide (8.70 g, 56 mmol) in ethanol (50 ml) using the general procedure B. Recrystallisation gave 61 as yellow crystals (8.7 g, 76 % yield) mp = 196 - 198°C (from water methanol and ether literature[54] 198 °C) (Found: C, 34.5; H, 4.0; N, 10.0. $C_8H_{11}N_2OI$ requires C, 34.55; H, 4.0; N, 10.1 %); ν_{max}(KBr)/cm^{-1} 3337 and 3168 (NH), 2942 (CH_2CH_3), 1676 and 1634 (amides I and II), 1609 and 1504 (pyridine), 1385 (CH_3); δ_H(200 MHz, d_6-DMSO) 1.64 (3H, t, *J* 7.3, C*H*$_3$), 4.82 (2H, q, *J* 7.3, C*H*$_2$), 8.20 (1H, s, N*H*), 8.37 (1H, dd, *J* 8,6, *H*5), 8.57 (1H, s, N*H*), 8.99 (1H, d, *J* 8, *H*4), 9.38 (1H, d, *J* 6, *H*6), 9.63 (1H, s, *H*2); δ_C(50.28 MHz, d_6-DMSO) 16.57 (CH_3), 57.22 (CH_2), 128.30 (C5), 133.90 (C4), 143.74 (C6), 144.70 (C2), 146.50 (C3), 163.22 (CO); m/z 151 (M^+, 100 %), 136 (M^+ - NH_2), 123 (M^+ - Et), 108 (M^+ - $CONH_2$).

N-Benzylnicotinamide Chloride (62)

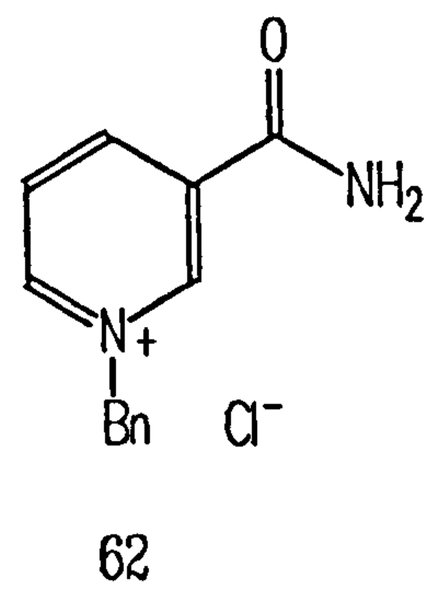

62

The title compound was prepared from a solution of nicotinamide (5.0 g, 41 mmol) and benzylchloride (7.8 g, 62 mmol) in ethanol (41 ml) using general procedure B. Recrystallisation gave **62** as white crystals (8.6 g, 84 % yield) mp 221-222°C (from methanol, literature [54] 236 °C with decomposition) (Found: C, 62.5; H, 5.5; N, 11.5. $C_{13}H_{13}N_2OCl$ requires C, 62.8; H, 5.3; N, 11.3 %); υ_{max} (KBr)/cm^{-1} 3382 and 3130 (NH), 2940 (CH_2), 1701 and 1651 (amides I and II), 1588 and 1512 (pyridine), 1439 (CH_2); δ_H(200 MHz, D_2O internal standard sodium 3-trimethylsilylpropanesulphonoate) 6.0 (2H, s, C*H*$_2$Ph), 7.53 - 7.61 (5H, m, Ph), 8.30 (1H, t, *J* 6, *H*5), 8.99 (1H, d, *J* 8, *H*4), 9.21 (1H, d, *J* 6, *H*6), 9.49 (1H, s, *H*2); δ_C(50.28 MHz, D_2O internal standard sodium 3-trimethylsilylpropanesulphonoate) 169 (CO), 147.98 (C3), 145.76 (C2), 135.43 (C6), 133.74 (C4), 133.62 (C5), 131.62 (*i*Bn), 131.14 (*m*Bn), 130.73 (*o*Bn), 130.12 (*p*Bn), 66.59 (CH_2Ph); m/z 213 (M^+), 170 (M^+ - $CONH_2$), 122 (M^+ - Bn), 91 (Bn).

N-Benzyl-1,4-dihydronicotinamide (63)

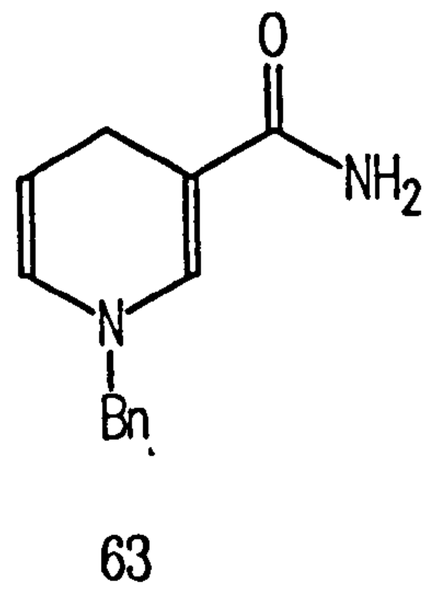

63

Into an aqueous solution of *N*-benzylnicotinamide chloride (1.0 g, 4.0 mmol) and sodium carbonate (1.5 g, 14 mmol) at 60 °C was added sodium dithionite (2.8 g, 16.1 mmol). This solution was left to stir (45 mins) as a pale yellow precipitate was formed which was filtered off and recrystallised to give pale yellow crystals (0.52 g, 61 % yield) mp 121 - 122 °C (from ethyl acetate, literature[54] 123 °C) (Found: C, 72.7; H, 6.4; N, 13.4. $C_{13}H_{14}N_2O$ requires C, 72.9; H, 6.6; N, 13.7 %); ν_{max}(KBr)/cm^{-1} 3357 and 3171 (NH), 2818 (CH_2), 1684 and 1645 (amides I and II), 1563 (C=C); δ_H(200 MHz, $CDCl_3$) 3.13 (2H, dd, *J* 3, 1.6, *H*4',4"), 4.25 (2H, s, C*H*$_2$Ph), 4.71 (1H, ddd, *J* 8, 3, 1.6, *H*5), 5.51 (2H, brs, N*H*$_2$), 5.70 (1H, m, *H*6), 7.11 (1H, d, *J* = 1.6 *H*2); δ_C(50.28 MHz, $CDCl_3$) 22.93 (CH_2Ph), 57.50 (C4), 98.09 (C3), 103.31 (C5), 127.28 (*p*Ph), 127.90 (*o*Ph), 128.93 (C6 and *m*Ph), 129.10 (*i*Ph), 140.04 (C2), 171.23 (CO); m/z 214 (M^+), 123 (M^+ - Bn), 91 (Bn).

N-Methyl-1,4-dihydronicotinamide (64)

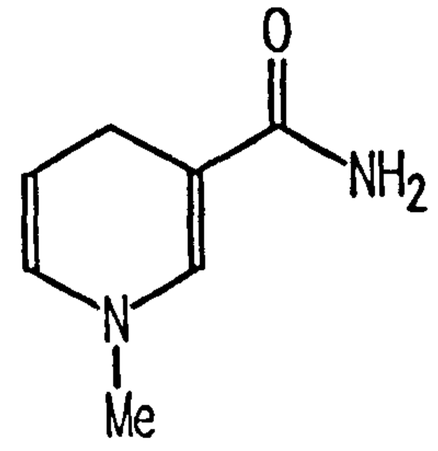

64

Into a stirred aqueous solution (10 ml) of *N*-methylnicotinamide iodide (1.0 g, 3.8 mmol) and sodium carbonate (3.0 g, 28.3 mmol), purged with nitrogen, was added sodium hydrosulphite (2.8 g, 16.1 mmol) and the solution left to stir (2h). The yellow solution was extracted with peroxide free ether (10 × 20 ml) dried ($MgSO_4$) and left to stand in the refrigerator (-25°C, 16h). The mother liquor was decanted from the small crystals that were formed whilst the remaining ether was blown off by nitrogen (all these operations were done at -20 °C). The crystals were then put under high vacuum and allowed to warm to room temperature, whereupon they formed a yellow oil (0.27 g, 52 % yield); δ_H(200 MHz, $CDCl_3$) 2.87 (3H, s, C*H*$_3$), 3.05 (2H, dt, *J* 3, 1.6, 1.6, *H*4',4"), 4.66 (1H, dt, *J* 8, 3, 3, *H*5), 5.53 (2H, brs, N*H*$_2$), 5.61 (1H, ddd, *J* 8, 3, 1.6, *H*6), 6.92 (1H, d, *J* 1.6, *H*2); δ_C(50.28 MHz, $CDCl_3$) 22.53 (CH_3), 40.70 (C4), 98.02 (C3), 102.84 (C5), 129.85 (C6), 140.44 (C2), 170.64 (CO); m/z 138 (M^+), 123 (M^+ - CH_3), 94 (M^+ - $CONH_2$).

N-Ethyl-1,4-dihydronicotinamide (65)

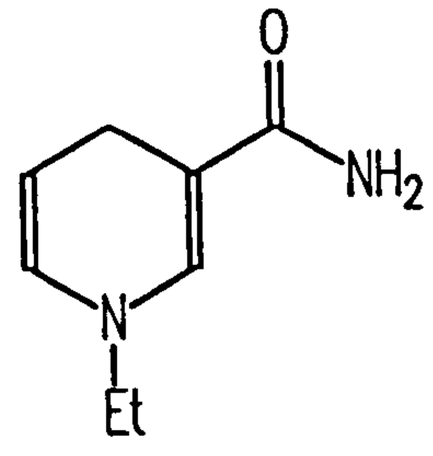

An aqueous solution (20 ml) of sodium carbonate (3.6 g, 34 mmol) and *N*-ethylnicotinamide iodide (1.0 g, 3.6 mmol) was purged with nitrogen (0.5 H). Sodium disulphite (3 g, 17.2 mmol) was added and the solution was left to stir (40 mins). Upon addition of the disulphite the solution changed colour from orange and formed a yellow precipitate, the solution was extracted with ether (10 x 10 ml), the ether extracts were then dried (sodium sulphate) and the ether removed under vacuum to give a yellow transparent oil (0.47 g, 85 % yield). (TLC 10 % MeOH in CH_2Cl_2 $R_f = 0.35$, blue fluorescent spot).

The oil was partially dissolved in ethyl acetate to give a yellow supernatant liquid over a thin yellow tar. The solution was transferred to another round bottomed flask and cooled (0 °C). Petrol was added dropwise to the solution until the cloud point was almost reached. The flask was stoppered and placed in the freezer (-25 °C) overnight. Bright yellow crystals formed. The temperature of the flask was kept between minus thirty and minus forty degrees whilst the mother liquor was pipetted away and the crystals washed with cold petrol. The petrol was then pipetted away to leave yellow crystals which were dried under high vacuum (0.05 mmHg, rt, dark). (First crop 104 mg, 19 % yield, second crop 66 mg, 12 % yield) mp 88 - 89 °C (from petrol/ethyl acetate) (Found: C, 63.3; H, 7.9; N, 18.3. $C_8H_{12}N_2O$ requires C, 63.1; H, 7.95; N, 18.4 %); ν_{max}(KBr)/cm^{-1} 3382 and 3206 (NH), 2978 (CH_3), 2807

(CH_2N), 1684 and 1645 (amides I and II), 1563 (C=C); δ_H(200 MHz $CDCl_3$) 1.09 (3H, t, *J* 7.2, C*H*$_3$), 3.10 (4H, q, *J* 7.2, CH_3CH_2, m, C*H*$_2$), 4.69 (1H, dt, *J* 3.5, 8.0, C*H*=CHN), 5.43 (2H, brs, N*H*$_2$), 5.68 (1H, ddd, *J* 1.62, 3.33, 8, CH=C*H*N), 7.01 (1H, d, *J* 1.61, NC*H*=C); δ_C(50.28 MHz, $CDCl_3$) 15.18 (CH_3), 22.93 (CH_2), 48.59 (NCH_2), 98.12 (C=<u>C</u>CO), 102.92 (C=<u>C</u>CH_2), 128.64 (<u>C</u>=CCH_2), 139.41 (<u>C</u>=CCO), 170 (C=O); m/z 152 (M^+), 151 (M^+ - H), 136 (M^+ - NH_2), 123 (M^+ - Et), 106 (M^+ - $CONH_2$).

8-Hydroxy-4(3*H*)-Quinazolinone (80')

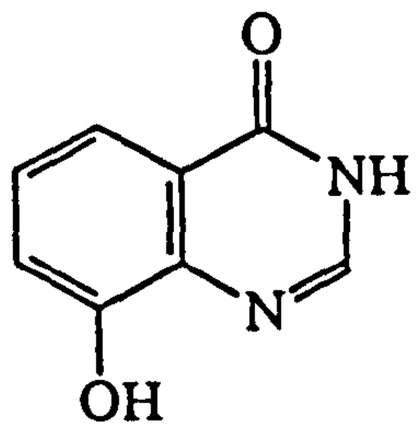

80'

A mixture of methyl 4-benzoxazolecarboxylate (275 mg, 1.56 mmol) and liquid ammonia (60 ml) was placed into an autoclave and heated (55 °C, 15 KBar) until the reaction was complete (18 H). The ammonia was evaporated from the product to leave a brown solid which was purified by sublimation (140 °C, 0.001 mmHg) to give a pale yellow solid (13 mg, 5 % yield) mp 233 - 234 °C (Found: C, 59.9; H, 3.9; N, 17.6. $C_8H_6N_2O_2$ requires C, 59.6; H, 3.7; N, 17.3 %); ν_{max}(KBr)/cm^{-1} 3319 (NH), 1695 and 1674 (amides I and II); δ_H(200 MHz; d_6-DMSO); 8.13 (1H, s, *H*2), 7.62 (1H, d, *J* 8, *H*5), 7.41 (1H, t, *J* 8, *H*6), 7.28 (1H, d, *J* 8, *H*7), 5.83 (4H, brs, N*H* + O*H* + *H*OD); m/z 162 (M^+ 61 %).

8-Hydroxy-2-Methyl-4-(3*H*)-Quinazolinone (82')

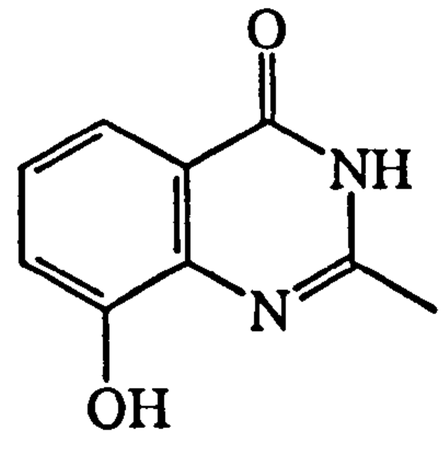

82'

A mixture of methyl 2-methyl-4-benzoxazolecarboxylate (218 mg, 1.1 mmol) and liquid ammonia (60 ml) were placed into an autoclave and heated (55 °C, 15 KBar) until the reaction was complete (16 h). The ammonia was evaporated from the product to leave an orange solid which was sublimed (160 °C, 0.001 mmHg) to give 2-methyl-4-benzoxazolecarboxamide as a yellow solid (58 mg, 30 % yield) mp 249 - 250 °C, (Found: C, 61.4; H, 4.4; N, 15.9. $C_9H_8N_2O_2$ requires C, 61.4; H, 4.6; N, 15.9 %); ν_{max}(KBr)/cm^{-1} 1672 (amide I), 1627 (amide II); δ_H(200 MHz; $CDCl_3$ and d_6-DMSO) 2.14 (3H, s, C*H*$_3$), 6.87 (1H, dd, *J* 7.5, 2, *H*7), 6.94 (1H, t, *J* 8, *H*6), 7.29 (1H, dd, *J* 7.5, 2, *H*5); δ_C(50.28 MHz; $CDCl_3$) 162.05 (CO), 152.86 (C8), 152.60 (C9), 132.27 (C2), 126.54 (C5), 121.76 (C7), 118.45 (C6), 115.77 (C4), 21.72 (CH_3); m/z 176 (M^+ 100 %), 107 (M^+ - 69).

Methyl 2-Amino-3-Hydroxybenzoate (84)

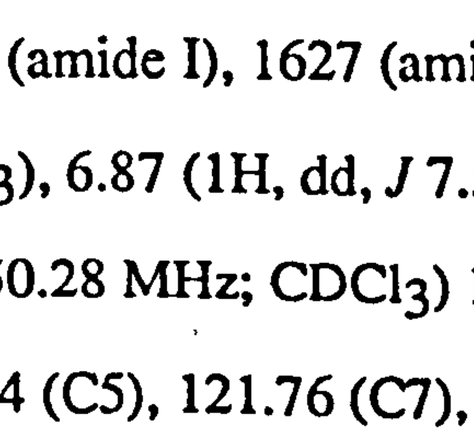

84

To a suspension of 2-amino-3-hydroxybenzoic acid (1.0 g, 6.54 mmol) in dry methanol (30 ml) was added dry hydrogen chloride until saturation. The reaction mixture was heated under refluxing conditions (17 h) and the solvent removed by rotary evaporation to leave a brown solid. The solid was dissolved in water (20 ml) and neutralised with sodium bicarbonate until effervescence stopped. Sodium chloride (*ca* 3 g) was added to the aqueous solution and the product was extracted with ethyl acetate (5 x 20 ml). The pooled aliquots were dried (magnesium sulphate) and the solvent removed by rotary evaporation to give a malty brown solid which was recrystallised to give the title compound (815 mg, 75 % yield) mp 95 - 96 °C (lit[109] 97 - 98 °C), (Found: C, 57.8; H, 5.8; N, 8.6. $C_8H_9NO_3$ requires C, 57.5; H, 5.4; N, 8.4 %); ν_{max} (KBr)/cm^{-1} 3410 (OH), 3327 (NH), 3024 (ArH), 1705 (CO); δ_H(200 MHz; $CDCl_3$) 3.86 (3H, s, Me), 5.74 (3H, br s, OH and NH_2), 6.48 (1H, t, *J* 7, *H*5), 6.80 (1H, d, *J* 7, *H*4), 7.45 (1H, d, *J* 7, *H*6); δ_C(50.28 MHz; $CDCl_3$) 51 (Me), 111 (C1), 115 (C5), 118 (C4), 123 (C6), 140 (C2), 143 (C3), 169 (CO); m/z 167 (M^+, 88 %), 135 (M^+ - 32), 107 (M^+ - 60).

Methyl 2-Methyl-4-Benzoxazolecarboxylate (85)

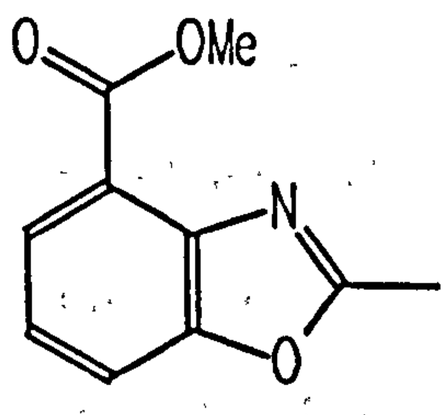

85

To a solution of methyl 2-amino-3-hydroxybenzoate (0.50 g, 3 mmol) in *m*-xylene (50 ml) were placed: acetyl chloride (0.28 g, 3.6 mmol), triethylamine (0.36 g, 3.6 mmol) and pyridinium *p*-toluenesulphonate (0.20 g, 0.80 mmol). This mixture was refluxed (18 h), then the solvent was removed by rotary evaporation to give a brown

oil, which was column chromatographed (10% MeOH in CH_2Cl_2 on silica) to give a yellow solid which was recrystallised to give the title compound (504 mg, 88 % yield) mp = 74 - 75 °C (petrol); (lit[57] 77 - 79 °C); (Found: C, 63.1; H, 4.5; N, 2.4. $C_{10}H_9NO_3$ requires C, 62.8; H, 4.75; N, 2.1 %); ν_{max}(KBr)/cm^{-1} 3088 (aromatic H), 1724 (CO), 1607 (C=C), 1566 (C=C), 1487 (C=C); δ_H(200 MHz; $CDCl_3$) 2.69 (3H, s, CCH_3), 3.99 (3H, s, OCH_3), 7.33 (1H, t, *J* 8, *H*6), 7.63 (1H, dd, *J* 8, 1, *H*7), 7.94 (1H, dd, *J* 8, 1, *H*5); δ_C(50.28 MHz; $CDCl_3$) 165.93 (CO), 151.64 (C8), 141.06 (C9), 126.65 (C5), 123.93 (C7), 121.66 (C4), 114.60 (C6), 52.52 (OCH_3), 14.81 (CH_3); m/z 191 (M^+ 38 %), 160 (M^+ - OCH_3), 133 (M^+ - CO_2CH_3)

Methyl 4-Benzoxazolecarboxylate (86)

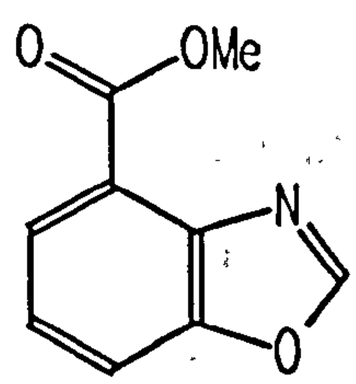

A mixture of methyl 2-amino-3-hydroxybenzoate (0.50 g, 3 mmol) and triethylorthoformate (1.46 g, 9.8 mmol) was refluxed (16 h) in *m*-xylene (100 ml). The solvent was then removed to give a brown oil which was column chromatographed (1% to 5% MeOH in CH_2Cl_2 on silica) to give the product as a sticky brown solid which was recrystallised (ethyl acetate) to give the title compound (273 mg, 51 % yield) mp (Found: C, 60.8; H, 3.9; N, 8.3. $C_9H_7NO_3$ requires C, 61.0; H, 4.0; N, 7.9 %); ν_{max}(KBr)/cm^{-1}; δ_H(200 MHz; $CDCl_3$) 4.08 (3H, s, OCH_3), 7.50 (1H, t, *J* 8, *H*6), 7.82 (1H, d, *J* 8, *H*7), 8.10 (1H, d, *J* 7.5, *H*5), 8.28 (1H, s, *H*2); m/z 177 (M^+ 65 %), 146 (M^+ - OMe), 118 (M^+ - CO_2Me).

N^6-(2,2-Dimethoxyethyl)adenosine (111)

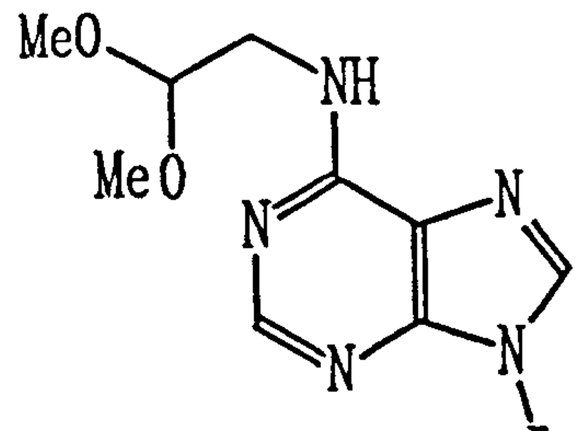

111

A solution in DMF (10 ml) of 6-chloropurine riboside (1 g,3.48 mmol), 2,2-dimethoxyethanamine (0.73 g, 7 mmol), and triethylamine (1.05 g, 10.4 mmol) was left to stir (64 h, RT) until the reaction was complete (by TLC). The precipitate formed (triethylammonium chloride) was filtered off (aided by DMF) and the solvent was removed under vacuum (0.01 mmHg) to leave a viscous oil, which was recrystallised (methanol) to give white shiny crystals (1.063 g, 86% yield).
mp 177 - 178 °C (methanol), (Found: C, 47.3, H, 5.9, N, 19.7. $C_{14}H_{21}N_5O_6$ requires C, 46.7, H, 5.9, N, 19.5, %); ν_{max}(KBr)/cm^{-1} 3400 (OH), 1620 (C=N-conjugated, cyclic), 1100 (C-O); δ_H(200 MHz; d_6-DMSO) 8.38 (1H, s, *H*2), 8.23 (1H, s, *H*8), 7.82 (1H, brs, N*H*), 5.89 (1H, d, *J* 6.16, *H*1'), 5.45 (2H, m, OH-5', OH-3'), 5.36 (1H, d, *J* 4.60, OH-2'), 4.60 (2H, m; *H*2', $(CH_3O)_2CH$), 4.14 (1H, m, *H*3'), 3.96 (1H, m, *H*4'), 3.60 (4H, br m, *H*5',5", CH_2NH_2), 3.28 (6H, s, $(CH_3O)_2$); δ_C (50.28 MHz; d_6-DMSO) 154.86 (C6), 152.62 (C2),149 (C4), 140.26 (C8), 120 (C5), 101.77 ($(CH_3O)_2\underline{C}$), 88.21 (C1'), 86.15 (C4'), 73.70 (C2'), 70.85 (C3'), 61.68 (C5'), 53.25 ($\underline{C}H_2NH_2$). m/z 356 (M^+), 324 (M^+ - CH_3OH), 224 (depurination), 192, (depurination and loss of methanol).

7-Methoxy-3,7,8-trihydroimidazo[2,1-i]purine (115)

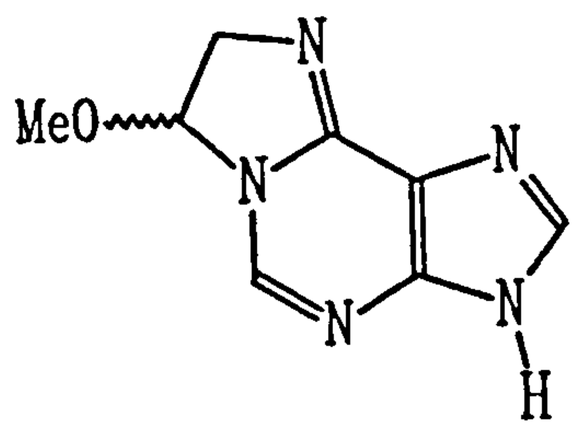

A flask was charged with N^6-(2,2-dimethoxyethyl)adenine (100 mg, 0.45 mmol), D-(-)-camphor sulphonic acid (115 mg, 0.5 mmol), and acetonitrile (25 ml). This was fitted with a Dean-Stark trap (dead volume of 14.5 ml) and set to reflux, with the trap being drained and replenished every hour for eight hours. The solvent was then removed by rotary evaporation to leave a pinkly tinged glass. An aqueous solution of this glass was then passed through an ion exchange column (Amberlite IRA-67 free base, 1 g). The aqueous solution of the free base was then freeze dried to leave a pale yellow fluffy solid (101 mg) which was recrystallised to give a white solid (76 mg, 88 % yield). mp 188 °C (dec) (methanol) δ_H(200 MHz; d_6-DMSO) 8.31 (1H, s, *H*8), 7.95 (1H, s, *H*2), 5.88 (1H, dd, *J* 2.0, 6.7, *H*11), 3.93 (1H, dd, *J* 6.7, 14.9, *H*10'), 3.75 (1H, dd, *J* 2.0, 14.9, *H*10"); δ_C(50.28 MHz, d_6-DMSO) 164 (C4), 160.76 (C6), 157.33 (C5), 149 (C2), 148 (C8), 97.96 (C11), 62.16 (C10), 61.21 (CH_3O); m/z 191 (M^+).

N^6-(2,2-Dimethoxyethan)adenine (116)

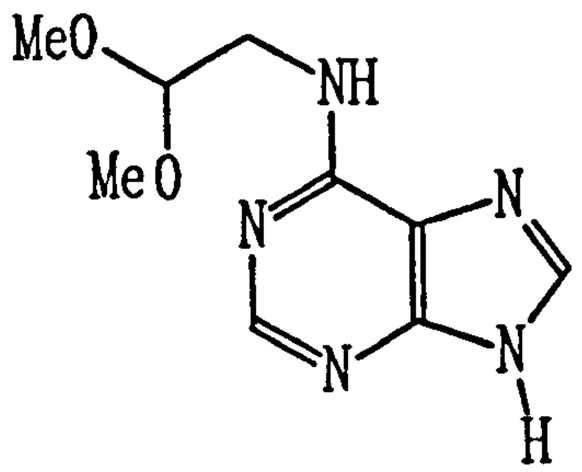

A 2-methoxyethanol (1 ml) solution of 6-chloropurine (200 mg, 1.3 mmol) and 2,2-dimethoxyethanamine (287 mg, 2.73 mmol) was heated under reflux (125 °C, 1.5 H) until the reaction was complete (by TLC). The solvent was removed under vacuum (0.001 mmHg), to leave a mixture of white and brown solids which were triturated with water to give a pink solid within a brown solution. The solid was collected by filtration and washed with water. The pink solid was then decolourised with charcoal and recrystallised to give white flaky crystals (198 mg, 68% yield). mp 228 -229 °C (ethanol), (Found C, 48.3, H, 5.8, N, 31.2. $C_9H_{13}N_5O_2$ requires C, 48.4, H, 5.8, N, 31.4); ν_{max}(KBr)/cm^{-1} 2834 (OMe, C-H stretch), 1626 (purine ring), 1597 (purine ring), 1539 (NH); δ_H(200 MHz; d_6-DMSO) 12.96 (1H, brs, *H*9), 8.21 (1H, s, *H*8), 8.13 (1H, s, *H*2), 7.53 (1H, brs, N^6*H*), 4.65 (1H, t, *J* 5.4, $(CH_3O)_2CH$), 3.64 (2H, brs, CH_2NH), 3.29 (6H, s, $(CH_3O)_2$); δ_C(50.28 MHz; d_6-DMSO) 154.48 (C6), 152.60 (C2), 139.31 (C8), 102.04 ($\underline{C}(OCH_3)_2$), 53.31 ($\underline{C}H_2NH$). m/z 224 (M^+), 192 (M^+ - CH_3OH).

α,β-Methylribofuranosides (117, 118)[110]

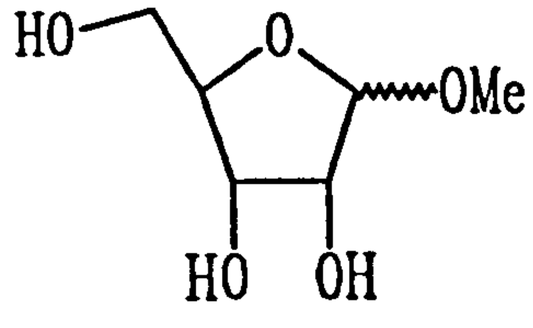

117 and 118

To a methanol solution of D-ribose (0.25 M, 5.2 ml) was added two drops of acetyl chloride from a Pasteur pipette. This mixture was stirred until it was non-reducing (Fehlings solution) and the starting material could not be detected by TLC (50 min, RT). Potassium carbonate was then added to the reaction mixture, the methanolic solution was then decanted from the excess potassium carbonate . Dichloromethane (5 ml) was used to wash the reaction flask , the washings were combined with the methanolic solution and both solvents were removed by rotary evaporation to leave a white oil. This oil was then Kugelrohr distilled (200 °C, 0.01 mmHg) to give a colourless oil (189.6 mg, 89% Yield). (Found C, 43.8; H,7.4. $C_6H_{12}O_5$ requires C, 43.9, H, 7.3 %); ν_{max}(KBr)/cm^{-1} 3377.79 (OH), 2839.58 (OMe); δ_H(200 MHz; D_2O) 4.94 (1H, s, *H*1), 3.92 (1H, dd, *J* 3.31, 11.78, *H5'*), 3.71 (1H, dd, *J* 6.28, 11.76, *H5"*); δ_C(50.28 MHz, D_2O) 110.15, 104.93 (βαC1), 86.77, 85.16 (αβC2), 76.48, 73.45 (αβC3), 72.99, 71.63 (βαC4), 65.31, 63.60 (βαC5), 55.70, 55.71 (αβOMe); m/z 164.089.

N^6-Benzyladenine (123)[111]

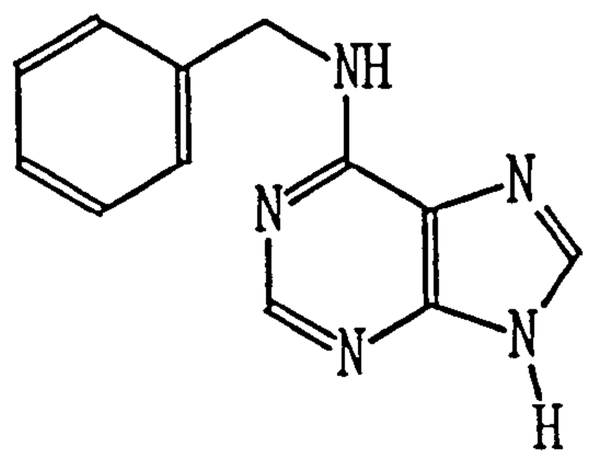

123

A 2-methoxyethanol (1 ml) solution of 6-chloropurine (200 mg, 1.3 mmol) and benzylamine (293 mg, 2.73 mmol) was refluxed (0.5 H) until the reaction was complete (by TLC). The excess benzylamine and the solvent were then removed under vacuum (0.05 mmHg) to leave a yellow solid. This solid was triturated with water to form an off-white solid which was recrystallised from a 1:1 mixture of ethanol and water to give
beige rod shaped crystals (182 mg, 62% yield) mp 226 - 228 °C (ethanol and water (1:1)), (Found: C, 64.2; H, 5.1; N, 31.1. $C_{12}H_{11}N_5$ requires C, 64.0, H, 4.9, N, 31.1 %), δ_H(200 MHz; d_6-DMSO) 8.32 (1H, s, *H*8), 8.26 (1H, s, *H*2), 7.30 (5H, m, Ph), 4.82 (2H, s, PhCH_2). δ_C(50.28 MHz; d_6-DMSO) 152.70 (C2),140.54 (C8), 139.48 (Ph, C1), 128.49 (*o*Ph), 127.53 (*m*Ph),126.91 (*p*Ph), 43.31 ($\underline{C}H_2$Ph); m/z 225 (M^+), 148 (M^+ - Ph), 135 (adenine), 120 (protonated purine), 106 (BnNH).

cis-4,5-Diphenyl[1,3]dioxalan-2-one (132)[102]

132

To a dry (under nitrogen), cooled (ice/salt) dichloromethane (4 ml) solution of hydroxybenzoin (1.07g, 5 mmol) and triethylamine (1 ml) was added triphosgene (49 mg, 17 mmol). The temperature of this mixture was slowly allowed to rise (RT) until the reaction was complete (0.5 H, by TLC). Water (10 ml) was then added to the reaction mixture and the product extracted with dichloromethane (3 x 20 ml), the extracts were pooled, dried ($MgSO_4$) and the solvent removed by rotary evaporation to leave a white solid (93 mg) which was recrystallised from aqueous ethanol to give white needles (59.4 mg, 61% yield) mp 127 °C (Found C, 74.8; H, 5.12; CHO requires C, 75.0; H, 5.0 %); ν_{max}(KBr)/cm^{-1} 1788.24 (CO), 1653.21 (Ph), 1452.58 (Ph); δ_H(200 MHz, $CDCl_3$) 7.2 - 6.8 (10H, m, 2 x Ph), 5.91 (2H s, C*H*); δ_C(50.28 MHz, $CDCl_3$) 82.19 (Ph<u>C</u>), 126.19 (C2), 128.31 (C4), 128.87 (C3), 132.91 (C1), 155.00 (C=O); m/z 241 (M^+), 197 (M^+ - CO_2), 179 (PhCHPhC).

References

1 L Stryer, Biochemistry, 3rd ed,W H Freeman, New York, 1988.

2 T Boulikas, *Anticancer Res*, 1991, **11**, 489.

3 H Hilz and P Stone, *Rev Physiol Biochem Pharmacol*, 1976, **76**, 1.

4 O Hayaishi and K Ueda, *Ann Rev Biochem*, 1977, **46**, 95.

5 P Chambon, P Mandel and J D Weill, *Biochem Biophys Res Commun*, 1963, **11**, 638.

6 P Chambon, J Doly, P Mandel, M T Strosser and J D Weill, *Biochem Biophys Res Commun*, 1966, **25**, 638.

7 A Klug and D Rhodes, *Trends in Biochemical Sciences*, 1987, **12**, 464.

8 J M Berg, *Nature*, 1986, **319**, 264.

9 G Gradwohl, J M de Murcia, M Molinette, F Simonin, M Koken, J H J Hoeijmalers and G de Murcia, *Proc Natl Acad Sci USA*, 1990, **87**, 2990.

10 Y Shizuta, S Ito, K Nakata and O Hayaishi, *Methods in Enzymology*, 1980, **66**, 159.

11 H J Burtscher, B Auer, H Klocker, M Schweiger and M Hirsch-Kaufmann, *Anal Biochem*, 1986, **152**, 285.

12 H Giner, F Simonin, G de Murcia and J Menissier-de Murcia, *Gene*, 1992, **114**, 279.

13 A L Harris and D Dickson, in Molecular Mechanisms in Bioorganic Processes, eds C Bleasdale and B T Golding, The Royal Society of Chemistry, Cambridge, 1990, p 83.

14 C Bleasdale, B T Golding, G Kennedy, J O MacGregor and W P Watson, *Chem Res Toxicol*, 1993, **6**, 407.

15 F P Guengerich and D H Kim, *Chem Res Toxicol*, 1991, **4**, 413.

16 M T Leithauser, A Liem, B C Stewart, E C Miller and J A Miller, *Carcinogenesis*, 1990, **11**, 463.

17 F I Lee and D S Harry, *Lancet*, 1974, 1316.

18 M Fox and D Scott, *Mutat Res*, 1980, **75**, 131.

19 D Rhodes, MPhil Thesis, University of Newcastle upon Tyne, 1990.

20 B G Katzung, Basic and Clinical Pharmacology, 2nd edition, Lange Medical Publications, Los Altos, California, 1982.

21 B W Durkacz, O Omidiji, D A Gray and S Shall, *Nature*, 1980, **283**, 593.

22 N Nduka, C J Skidmore and S Shall, *Eur J Biochem*, 1980, **105**, 525.

23 J M Lunn and A L Harris, *Br J Cancer*, 1988, **57**, 54.

24 J Huet and F Laval, *Cancer Res*, 1985, **45**, 987.

25 M R Purnell and W J D Whish, *Biochem J*, 1980, **185**, 775.

26 M J Suto, W R Turner, C M Arundel-Suto, L M Werbel and J Sebolt-Leopold, *Anti-Cancer Drug Design*, 1991, **7**, 107.

27 M Banasik, H Komura, M Shimoyama and K Ueda, *J Biol Chem*, 1992, **267**, 1569.

28 H Halldorsson, D A Gray and S Shall, *FEBS letters*, 1978, **85**, 349.

29 N A Berger and S J Petzold, *Biochem*, 1985, **24**, 4352.

30 K Grube, J-H Kupper and A Burkle, *Anal Biochem*, 1991, **193**, 236.

31 B S Reddy, W Saenger, K Muhlegger and G Weimann, *J Am Chem Soc*, 1981, **103**, 907.

32 J March, Advanced Organic Chemistry, 3rd edition, 1985, J Wiley and Sons, New York, p 22.

33 B Pullman and A Saran, *Prog Nucl Acid Res Mol Biol*, 1976, **18**, 216.

34 R H Sarma and N O Kaplan, *Biochemistry*, 1970, **9**, 539.

35 J Jacobus, *Biochemistry*, 1971, **10**, 161.

36 W van Gerresheim, C Kruk and J W Verhoeven, *Tetrahedron Lett*, 1982, **23**, 565.

37 G Ah-Kow, F Terrier, M-J Pouet and M-P Simonnin, *J Org Chem*, 1980, **45**, 4399.

38 M Blumstein and M A Rafferty, *Biochem*, 1973, **12**, 3585.

39 D E Dorman and J D Roberts, *Proc Nat Acad Sci USA*, 1970, **65**, 19.

40 H H Mantsch and I C P Smith, *Biochem Biophys Comm*, 1972, **46**, 808.

41 R D Lapper, H Mantsch and I C P Smith, *J Am Chem Soc*, 1972, **94**, 6243.

42 R D Lapper, H Mantsch and I C P Smith, *J Am Chem Soc*, 1973, **95**, 2878.

43 R D Lapper and I C P Smith, *J Am Chem Soc*, 1973, **95**, 2880.

44 D B Davies and H Sadikot, *Organic Magnetic Resonance*, 1982, **20**, 180.

45 A Glasfeld, P Zbinden, M Dobler, S A Benner and J D Dunitz, *J Am Chem Soc*, 1988, **110**,5152.

46 J A Pople, W G Schneider, and H A Bernstein, High Resolution Nuclear Magnetic Resonance, McGraw Hill, New York, 1959, Chapter 6.

47 J Smith, personal communication.

48 M Matzner, R P Kurkjy and R J Cotter, *Chem Rev*, 1964, **64**, 645.

49 S L Kitson, Personal Communication.

50 K-K Park, Y-J Surh, B C Stewart and J A Miller, *Biochem Biophys Res Commun*, 1990, **169**, 1094.

51 F D Chattaway, *J Chem Soc*, 1931, 2495.

52 A J Birch, *Quart Rev Chem Soc*, 1950, **4**, 69.

53 P W Rabideau and D L Huser, *J Org Chem*, 1983, **48**, 4266.

54 H E Zimmerman and P A Wang, *J Am Chem Soc*, 1990, **112**, 1280.

55 M E C Biffin, A G Moritz and D B Paul, *Aust J Chem*, 1972, **25**, 1329.

56 P Karrer, *Helv Chim Acta*, 1936, **19**, 811.

57 P Karrer and F J Stare, *Helv Chim Acta*, 1937, **20**, 418.

58 D H Williams and I Fleming, Spectroscopic methods in Organic Chemistry, 4th edition, McGraw-Hill Book Company (UK) Limited, 1989.

59 L Pemberton, personal communication.

60 S W Goldstein and P J Dambek, *J Heterocyclic Chem*, 1990, **27**, 335.

61 J I Braum and V W Laurie, *Tetrahedron*, 1968, **24**, 2595.

62 R E Kagarise, *J Am Chem Soc*, 1955, **77**, 1377.

63 R M Sweet and L F Dahl, *J Am Chem Soc*, 1970, **92**, 5489.

64 D B Boyd, *J Med Chem*, 1973, **16**, 1195.

65 D B Boyd, R B Hermann, D E Preist and M M Marsh, *J Med Chem*,

1975,18, 408.

66 British Medical Journal Editorial, *British Medical Journal*, 1974, 1, 590.

67 P J Baxter and A Fox, *Lancet*, 1975, 1, 27.

68 J L Creech and M N Johnson, *J Occup Med*, 1974, 16, 150.

69 J B Block, *Journal of the American Medical Association*, 1974, 229, 53.

70 L Makk, J L Creech, J G Whelan and M N Johnson, *Journal of the American Medical Association*, 1974, 230, 64.

71 H Falk, J L Creech, C W Heath, M N Johnson and M Key, *Journal of the American Medical Association*, 1974, 230, 64.

72 A J Fox and P F Collier, *Br J Ind Med*, 1977, 34, 1.

73 T Green and D E Hathway, *Chem Biol Interact*, 1975, 11, 545.

74 T Green and D E Hathway, *Chem Biol Interact*, 1977, 17, 137.

75 P G Watanabe, G R McGowan and P J Gehring, *Toxicol Appl Pharmacol*, 1976, 36, 49.

76 P G Watanabe, G R McGowan, E O Madrid and P J Gehring, *Toxicol Appl Pharmacol*,, 1976, 37, 49.

77 G Müller, K Norpoth and R Eckhard, *Int Arch Occup Environ Health*, 1976, 38, 69.

78 H Bartsch and R Montesano, *Mutation Research*, 1975, 32, 93.

79 H Kappus, H M Bolt, A Buchter and W Bolt, *Nature*, 1975, 257, 134.

80 H Kappus, H M Bolt, A Buchter and W Bolt, *Toxicol Appl Pharmacol*, 1976, 37, 461.

81 R J Laib and H M Bolt, *Toxicology*, 1977, 8, 185.

82 R J Laib and H M Bolt, *Arch Toxicol*, 1978, 39, 135.

83 H Malaveille, H Bartsch, A Barbin, A Camus, R Montesano, A Croisy and P Jacquignon, *Biochem Biophys Res Commun*, 1975, 63, 363.

84 A Barbin, H Bresil, A Croisy, P Jacquignon, C Mallaveille, R Montesano and H Bartsch, *Biochem Biophys Res Commun*, 1975, 67, 596.

85 G Bonse and H Henschlrer, *CRC Crit Rev Toxicol*, 1976, 5, 395.

86 J S Jacobsen and M Z Humayun, *Biochem*, 1990, **29**, 496.

87 N K Kochetkov, V N Shibaev, A A Kost and N D Zelinsky, *Tetrahedron Lett*, 1971, **22**, 1993.

88 J A Secrist III, J R Barrio, N J Leonard and G Weber, *Biochem*, 1972, **11**, 3499.

89 W J Krzyzosiak, J Biernat, J Ciesiolka, K Gulewicz and M Wiewiorowski, *Nucleic Acids Res*, 1981, **9**, 2841.

90 W J Krzyzosiak, and J Ciesiolka, *Nucleic Acids Res*, 1983, **11**, 6913.

91 J Biernat, J Ciesiolka, P Gornicki, R W Adamiak, W J Krzyzosiak and M Wiewiorowski, *Nucleic Acids Res*, 1978, **5**, 789.

92 J Biernat, J Ciesiolka, P Gornicki, W J Krzyzosiak and M Wiewiorowski, *Nucleic Acids Res Special Publication*, 1978, **4**, 203.

93 W J Krzyzosiak, J Biernat, J Ciesiolka, P Gornicki and M Wiewiorowski, *Polish J Chem*, 1979, **53**, 243.

94 A H-J Wang, L G Dammann, J R Barrio and I C Paul, *J Am Chem Soc*, 1974, **96**, 1205.

95 F Hansske, D Madej and M J Robins, *Tetrahedron*, 1984, **40**,125.

96 J L York, *J Org Chem*, 1981, **46**, 2171.

97 Z Kazimierzuk, H B Cottam, G R Revankar and R K Robins, *J Am Chem Soc*, 1984, **106**, 6379.

98 M Hoffer, *Chem Ber*, 1960, **93**, 2777.

99 K Groebke and C Leumann, *Helv Chim Acta*, 1990, **73**, 608.

100 C Bleasdale, S B Ellwood and B T Golding, *J Chem Soc Perkin Trans 1*, 1990, 803.

101 D D Perrin, W L F Armarego and D R Perrin, Purification of Laboratory Reagents, 2nd edition, Pergamon Press, Oxford, 1980.

102 W Clarke Still, M Kahn and A Mitra, *J Org Chem*, 1978, **43**, 2923.

103 A Bax, *J Magn Reson*, 1983, **53**, 517.

104 A Bax, *J Magn Reson*, 1983, **53**, 149.

105 A Bax, R H Griffey and B L Hawkins, *J Magn Reson*, 1985, **55**, 301.

106 O L Brady and F P Dun, *J Chem Soc*, 1923, 1783.

107 R H Sarma and C L Woronick, *Biochem*, 1972, **11**,170.

108 E Tommila and C N Hinshelwood, *J Chem Soc*, 1938, 1801.

109 J Gripenberg, *Acta Chem Scand*, 1959, **13**, 1305.

110 L J Haynes, N A Hughes, G W Kenner and A Todd, *J Chem Soc*, 1957, 27.

111 M W Bullock, J J Hand and L R Stockstad, *J Am Chem Soc*, 1956, 78, 3693.

112 J Sarel, *J Org Chem*, 1959, **24**, 1873.